



— BUREAU OF —
RECLAMATION

Additive Manufacturing Investigation and Demonstration for Hydropower Applications – Case Studies

**Research and Development Office
Science and Technology Program
Final Report No. ST-2021-19085-5, TM-8540-2021-019**



REPORT DOCUMENTATION PAGE			Form Approved OMB No. 0704-0188	
The public reporting burden for this collection of information is estimated to average 1 hour per response, including the time for reviewing instructions, searching existing data sources, gathering and maintaining the data needed, and completing and reviewing the collection of information. Send comments regarding this burden estimate or any other aspect of this collection of information, including suggestions for reducing the burden, to Department of Defense, Washington Headquarters Services, Directorate for Information Operations and Reports (0704-0188), 1215 Jefferson Davis Highway, Suite 1204, Arlington, VA 22202-4302. Respondents should be aware that notwithstanding any other provision of law, no person shall be subject to any penalty for failing to comply with a collection of information if it does not display a currently valid OMB control number. PLEASE DO NOT RETURN YOUR FORM TO THE ABOVE ADDRESS.				
1. REPORT DATE (DD-MM-YYYY) July 2023		2. REPORT TYPE Research, Final Report		3. DATES COVERED (From - To) October 2019–September 2023
4. TITLE AND SUBTITLE Additive Manufacturing Investigation and Demonstration for Hydropower Applications – Case Studies			5a. CONTRACT NUMBER XXXR4524KS RR4888FARD1901801	
			5b. GRANT NUMBER	
			5c. PROGRAM ELEMENT NUMBER 1541 (S&T)	
6. AUTHOR(S) David Tordonato dtordonato@usbr.gov Stephanie Prochaska Matthew Jermyn mjermyn@usbr.gov Grace Weber gweber@usbr.gov			5d. PROJECT NUMBER Final Report No. ST-2021-19085-5	
			5e. TASK NUMBER	
			5f. WORK UNIT NUMBER 86-68540	
7. PERFORMING ORGANIZATION NAME(S) AND ADDRESS(ES) David Tordonato Materials and Corrosion Laboratory Technical Service Center Bureau of Reclamation U.S. Department of the Interior PO Box 25077, Denver Federal Center Denver CO 80225-0007			8. PERFORMING ORGANIZATION REPORT NUMBER 8540-2021-019	
9. SPONSORING/MONITORING AGENCY NAME(S) AND ADDRESS(ES) Science and Technology Program Research and Development Office Bureau of Reclamation U.S. Department of the Interior PO Box 25007, Denver Federal Center Denver CO 80225-0007			10. SPONSOR/MONITOR'S ACRONYM(S) R&D: Research and Development Office Reclamation: Bureau of Reclamation DOI: U.S. Department of the Interior	
			11. SPONSOR/MONITOR'S REPORT NUMBER(S) Final Report ST-2021-19085-5	
12. DISTRIBUTION/AVAILABILITY STATEMENT Final Report may be downloaded from https://www.usbr.gov/research/projects/index.html				
13. SUPPLEMENTARY NOTES				
14. ABSTRACT This project undertook a collaboration with Oak Ridge National Laboratory to determine the feasibility and cost and to demonstrate the efficacy of additively manufactured replacements for selected hydropower facility components. Reclamation's Technical Service Center partnered with several regional and area offices to identify opportunities where additive manufacturing could be deployed. Three parts were selected and pursued as case studies: governor parts for Glen Canyon Dam, log boom anchors for Nimbus Dam, and generator exciter bearing slinger rings for Grand Coulee Dam. For each case study, researchers selected one or more additive manufacturing processes that seemed most feasible to replicate or improve upon the conventional part. Researchers worked with manufacturers to produce the additively manufactured components. To evaluate efficacy, the parts underwent material properties testing (density, tensile, bend, hardness, fatigue), metallography and fractography, three-dimensional scanning, and cost-benefit analysis.				
15. SUBJECT TERMS Additive manufacturing, 3D printing, aging infrastructure, governor valve, log boom anchor, slinger ring, fabrication, powder bed fusion, stainless steel, aluminum bronze, polylactic acid				
16. SECURITY CLASSIFICATION OF:			17. LIMITATION OF ABSTRACT	18. NUMBER OF PAGES 258
a. REPORT U	b. ABSTRACT U	THIS PAGE U		
				19b. TELEPHONE NUMBER (Include area code) 303-445-2394

Additive Manufacturing Investigation and Demonstration for Hydropower Applications – Case Studies

prepared by

**Technical Service Center
Materials and Corrosion Laboratory Group
David Tordonato, Materials Engineer
Stephanie Prochaska, Materials Engineer
Matthew Jermyn, Materials Engineer
Grace Weber, Materials Engineer**

Cover Photograph: A photograph showing additively manufactured case study parts, including an aluminum bronze slinger ring half, stainless steel and aluminum bronze governor parts, and an aluminum log boom anchor (David Tordonato, Reclamation).

Mission Statements

The U.S. Department of the Interior protects and manages the Nation's natural resources and cultural heritage; provides scientific and other information about those resources; and honors its trust responsibilities or special commitments to American Indians, Alaska Natives, and affiliated Island Communities.

The mission of the Bureau of Reclamation is to manage, develop, and protect water and related resources in an environmentally and economically sound manner in the interest of the American public.

Disclaimer

Information in this report may not be used for advertising or promotional purposes. The data and findings should not be construed as an endorsement of any product or firm by the Bureau of Reclamation, U.S. Department of Interior, or Federal Government. The products evaluated in the report were evaluated for purposes specific to the Bureau of Reclamation mission. Reclamation gives no warranties or guarantees, expressed or implied, for the products evaluated in this report, including merchantability or fitness for a particular purpose.

Acknowledgements

The Science and Technology Program, Bureau of Reclamation, sponsored this research.

Peer Review

**Bureau of Reclamation
Technical Service Center
Materials and Corrosion Laboratory Group**

Technical Memorandum No. 8540-2021-019

Additive Manufacturing Investigation and Demonstration for Hydropower Applications – Case Studies

MATTHEW JERMYN Digitally signed by MATTHEW
JERMYN
Date: 2023.09.27 07:40:16 -06'00'

Prepared by: **Matthew Jermyn**
Materials Engineer, Materials and Corrosion Laboratory, 86-68540

GRACE WEBER Digitally signed by GRACE WEBER
Date: 2023.09.26 14:03:36 -06'00'

Checked by: **Grace Weber**
Materials Engineer, Materials and Corrosion Laboratory, 86-68540

DAVID TORDONATO Digitally signed by DAVID
TORDONATO
Date: 2023.09.26 13:27:47 -06'00'

Technical Approval by: **David (Dave) Tordonato**
Materials Engineer, Materials and Corrosion Laboratory, 86-68540

MEREDITH HEILIG Digitally signed by MEREDITH
HEILIG
Date: 2023.09.27 15:16:54 -06'00'

Peer Review by: **Meredith Heilig**
Materials Engineer, Materials and Corrosion Laboratory, 86-68540

“This information is distributed solely for the purpose of pre-dissemination peer review under applicable information quality guidelines. It has not been formally disseminated by the Bureau of Reclamation. It does not represent and should not be construed to represent Reclamation’s determination or policy.”

Acronyms and Abbreviations

ASTM	American Society for Testing and Materials
CAD	computer-aided design
d	diameter
DED	direct (or directed) energy deposition
DMLM	direct metal laser melting
Elong.	elongation
HRB	Rockwell Hardness B
ICP	inductively coupled plasma
ICP-MS	inductively coupled plasma-mass spectroscopy
ID	inner diameter
IN718	Inconel 718
Leco	Leco combustion analysis
Lit.	literature
L-PBF	laser powder bed fusion
MDF	Manufacturing Demonstration Facility
Min.	minimum
No.	number
OD	outer diameter
ORNL	Oak Ridge National Laboratory
PBF	powder bed fusion
PLA	polylactic acid
Ra	roughness average
Reclamation	Bureau of Reclamation
SLA	stereolithography
SLM	selective laser melting
SS	stainless steel
Std.	standard
U.S.	United States
USACE	U.S. Army Corps of Engineers
USD	United States dollar

Symbols and Measurements

%	percent
±	plus or minus
°C	degree Celsius

°F	degree Fahrenheit
μm	micrometers
Al	aluminum
cm	centimeters
cSt	centistokes
F	face
ft-lb	foot-pound(s)
g/cm ³	gram(s) per centimeter cubed
GPa	gigapascals
H	horizontal
HF	horizontal face specimen
HX	horizontal cross-section specimen
in ²	square inch(es)
J	joules
lb	pound(s)
lb/in ²	pound(s) per square inch
lb/in ³	pound(s) per cubic inch
Mg	magnesium
mm	millimeter(s)
mm ³	cubic millimeter(s)
MPa	megapascals
NaOH	sodium hydroxide
tpi	threads per inch
Si	silicon
V	vertical
VF	vertical face specimen
VX	vertical cross-section specimen
X	cross-section

Contents

	<i>page</i>
1 Introduction.....	3
1.1 Project Background.....	3
1.2 Case Selection	3
2 Case Study A: Governor Valves.....	5
2.1 Component Selection.....	5
2.2 Component Functionality	5
2.2.1 Pilot Valve.....	6
2.2.2 Gate Limit Valve.....	6
2.3 Conventional (Baseline) Components.....	6
2.3.1 Conventional Materials and Manufacturing Processes.....	6
2.3.2 Conventional Cost Estimates.....	6
2.4 Additive Cost and Feasibility Estimates and Selections	7
2.4.1 Stainless Steel Parts.....	7
2.4.2 Naval Brass Parts	8
2.5 Stainless Steel Governor Parts Results.....	10
2.5.1 Printing Process.....	10
2.5.2 Machining.....	13
2.6 Aluminum Bronze Governor Parts Results	16
2.6.1 Printing Process.....	16
2.6.2 Machining.....	17
2.7 Stainless Steel Laboratory Test Sample Results	20
2.7.1 Tensile Testing	22
2.7.2 Bend Testing.....	23
2.7.3 Hardness Testing.....	23
2.7.4 Metallography	24
2.8 Aluminum Bronze Laboratory Test Sample Results.....	27
2.8.1 Tensile Testing	28
2.8.2 Bend Testing.....	29
2.8.3 Hardness Testing.....	30
2.8.4 Fatigue Testing	32
2.8.5 Metallography	34
2.9 Governor Part Field Results Summary	35
2.9.1 Cost-Benefit Analysis of Additive Manufacturing	36
2.9.2 Manufacturing Challenges and Notes.....	36
3 Case Study B: Forebay Log Boom Anchor.....	37
3.1 Conventional (Baseline) Component Designs, Fabrication, Costs, and Service.....	37
3.1.1 Design and Fabrication	37
3.2 Additive Manufacturing Alternatives.....	38
3.2.1 Redesign for Additive Manufacturing.....	38
3.2.2 Cost and Feasibility Estimates and Selections	39
3.2.3 Additive Manufacturing Process.....	40

3.3	Laboratory Test Results.....	43
3.3.1	Mechanical Testing	43
3.3.2	Metallography	48
3.3.3	Fractography.....	50
3.3.4	Density.....	51
3.3.5	Field Results.....	51
3.3.6	Cost-Benefit Analysis of Additive Manufacturing	51
4	Case Study C: Slinger Rings	53
4.1	Component Selection.....	53
4.2	Component Functionality	54
4.3	Conventional (Baseline) Components.....	54
4.3.1	Conventional Design and Fabrication	54
4.3.2	Conventional Costs.....	55
4.4	Additive Manufacturing Results	55
4.4.1	Printed Aluminum Bronze Slinger Ring Parts.....	55
4.4.2	Cast Slinger Ring Parts With Printed Polylactic Acid Pattern.....	59
4.4.3	Laboratory and Field Test Results.....	64
4.5	Additive Manufacturing Cost Estimates	65
4.5.1	Printed Aluminum Bronze Slinger Ring Parts.....	65
4.5.2	Printed Polylactic Acid Slinger Ring Patterns.....	65
4.5.3	Cast Slinger Ring Parts	65
4.6	Cost-Benefit Analysis of Additive Manufacturing.....	66
5	Summary of Hydropower Component Additive Manufacturing Case Studies.....	67
5.1	Lessons Learned and Recommendations for Process Improvement.....	67
5.2	Priorities for Future Efforts.....	68
5.2.1	Hybrid Additive Manufacturing Technology and In Situ Repairs.....	68
5.2.2	Printing More Advanced Parts Including a Turbine Runner or Pump Impellor ...	68
5.2.3	Embedded Sensors and Smart Design.....	68
5.2.4	Corrosion Susceptibility of Additively Manufactured Parts	69
5.2.5	Using Additive Manufacturing to Create Parts With Enhanced Properties.....	69
5.3	Implications for the Entire Reclamation Hydropower Fleet.....	69
6	References.....	71
6.1	Additional References—ASTM Standards	72
7	Supporting Datasets	73

Tables

	<i>page</i>
1.—Estimated Cost of Governor Parts Using Conventional Fabrication Methods.....	7
2.—Material Property Comparison for Possible Naval Brass Substitutes	9
3.—Exact Powder Chemical Composition for Stainless Steel Parts	13
4.—Exact Powder Size for Stainless Steel Parts	13
5.—Stainless Steel Tensile and Bend Sample Orientation, Quantity, Dimensions, and Notes	21

6.—Tensile Test Results from 316L Stainless Steel Test Bars and Published Literature Data for 3D Printed and Wrought Stainless Steel.....	22
7.—Bend Test Results for Stainless Steel PBF Governor Parts Test Wall.....	23
8.—Aluminum Bronze Test Samples Printed by Elementum 3D	28
9.—Tensile Test Results from Aluminum Bronze Test Bars and Published Literature Data for Annealed Aluminum Bronze and H01 Tempered Naval Brass	28
10.—Bend Test Results for Aluminum Bronze Test Samples.....	29
11.—Aluminum Bronze Fatigue Testing Results.....	33
12.—Cost of Log Boom Anchor Blocks Produced from Additively Manufactured AlSi10Mg After Stress Relief and Without Overhead.....	40
13.—Tensile Test Results from Test Bars and Published Literature Data for 3D Printed Material (As-Printed) and Cast Aluminum Alloy AlSi10Mg.....	45
14.—Charpy Impact Testing Results	45
15.—PBF AlSi10Mg Vertical and Horizontal Specimen Density Results.....	51
16.—Dimensional Analysis of Slinger Ring Test Castings	62
17.—Lot Pricing for Slinger Ring Castings.....	65

Figures

	<i>page</i>
1.—Pin (H_41365_C), linking bar and sleeve (H_41365_A) of pilot valve (left). Piston (H_41365_D) and sleeve (H_41365_B) of gate limit valve (right).....	5
2.—Schematic showing the two approaches for adding material to the 3D models for printing of the stainless steel governor parts: (a) gate limit valve piston; (b) pilot valve pin; (c) pilot valve linking bar.....	8
3.—Additional material (shown in red) added to the 3D models of the aluminum bronze pilot valve sleeve (top) and gate limit valve (bottom).....	10
4.—3D-printed linking bars. Left: Parts had material added to selected surfaces. Right: Parts had material added to all surfaces.....	11
5.—3D-printed piston of gate limit valve. Left: Parts had material added to selected surfaces. Right: Parts had material added to all surfaces.....	11
6.—3D-printed pin of pilot valve. Left: Parts had material added to selected surfaces. Right: Parts had material added to all surfaces.....	12
7.—All stainless steel governor parts on the build plate.....	12
8.—Example 3D scan results of stainless steel governor part components, as-printed. The greatest value on the color scale (red) is +0.020 inches (+0.50 mm). The lowest value (blue) is -0.020 inches (-0.50 mm).....	14
9.—Example 3D scan result of stainless steel gate limit valve piston after machining. The greatest value on the color scale (red) is +0.0200 inches. The lowest value (pink) is -0.0200 inches.....	15
10.—Additively manufactured and machined pilot valve (Left) compared to original part (Right)....	16

11.—Example 3D scan results of aluminum bronze governor part components, as-printed. The greatest value on the color scale (red) is +0.0130 inches. The lowest value (pink) is -0.0160 inches.	17
12.—Difference in hole alignment between printed pilot valve (left) and original (right).....	18
13.—Machined aluminum bronze additively manufactured parts compared to original parts removed from service. Left: Gate limit valve (additively manufactured part on right). Right: Section control valve (additively manufactured part on left).....	19
14.—Example 3D scan of as-machined pilot valve sleeve assembly. The greatest value on the color scale (red) is +0.0200 inches. The lowest value (pink) is -0.0200 inches.....	20
15.—Left: Schematic of sample orientation for the stainless steel tensile bars (labeled “H” and “V”) and bend samples (labeled “1” and “2”); samples were machined from one printed wall piece; the arrow indicates the “Z” printing direction. Right: Photograph of physical bend samples after removal from test wall.....	21
16.—Photographs of bend test samples after testing. Left: Sample 1 (parallel to Z-axis). Right: Sample 2 (perpendicular to Z-axis).....	23
17.—Hardness traverse test results for the stainless steel PBF governor parts test wall. The traverse was taken along the X-axis build direction.....	24
18.—Naming designation of metallography orientation on tensile bar specimens.	25
19.—Microstructures from sample orientation HF (face of the sample parallel to Z print direction).	26
20.—Microstructures from sample orientation HX (cross section of the sample parallel to Z print direction).	26
21.—Microstructures from sample orientation VF (face of the sample perpendicular to the print direction).	26
22.—Microstructures from sample orientation VX (cross section face of the sample perpendicular to the print direction).	27
23.—Photograph from above of as-printed aluminum bronze samples on build plate.....	27
24.—Photographs of aluminum bronze bend test samples after testing. Left: Sample 1 (parallel to Z-axis). Right: Sample 2 (perpendicular to Z-axis).	30
25.—Hardness traverse results for horizontal aluminum bronze test sample, as-printed (XY orientation).	31
26.—Hardness traverse results for vertical aluminum bronze test sample, as-printed (Z orientation).	31
27.—As-printed aluminum bronze fatigue samples.	32
28.—Left: Fracture surfaces of specimen 12, run at 85% stress level. Right: Fracture surfaces of specimen 22, run at 95% stress level.....	33
29.—Sample “H” cross section of sample oriented perpendicular to the Z / print direction. Micrographs taken at: (a) 250X, (b) 500X, and (c) 1000X.....	34
30.—Sample “V” cross section of sample oriented in the Z / print direction. Micrographs taken at: (a) 250X, (b) 500X, and (c) 1000X.....	35

31.—Microstructural features of aluminum bronze samples. Left: (a) “H” cross section of sample oriented perpendicular to the Z /print direction. Right: (b) “V” cross section of sample oriented parallel to the Z / print direction. Both “H” and “V” samples showed intergranular and intragranular precipitates, spatter, gas porosity, and voids.	35
32.—Left: Photograph showing log boom at Nimbus Dam. Right: Photograph showing old and new conventionally manufactured pier anchors.	37
33.—Components of a conventionally manufactured log boom anchor.	38
34.—Redesigned anchor block optimized for additive manufacturing.	39
35.—Redesigned anchor parts and wall produced by additive manufacturing in as-printed state.	41
36.—Redesigned anchor parts and wall produced by additive manufacturing after post-processing.	42
37.—Side and top view of the finished anchor blocks with the Delrin rails attached and the stainless steel insert pressed into the top shackle.	42
38.—Deviation between design and actual dimensions obtained through a 3D scan of the log boom anchor.	43
39.—Left: Schematic of tensile bar orientation machined from one wall piece. Right: Photograph of a representative machined tensile test bar.	44
40.—Orientation of Charpy v-notch specimens machined from one wall piece.	44
41.—Hardness test results for Horizontal and Vertical specimens showing that for both orientations, hardness increases from bar ends to the centers. Both orientations had similar average hardness values.	46
42.—Test configuration for log boom anchors.	47
43.—Frame capture of anchor piece 2 during testing at 106 lb and 16,882 lb load with no visible deformation.	48
44.—250X micrographs of the HX (left) and VX (right) specimens. Melt pool boundaries are indicated with arrows. Specimens were stain etched with NaOH for 10 minutes (VX) and 5 minutes (HX).	49
45.—100X micrograph of HX showing an aluminum matrix (light) with regions of Si eutectic (dark).	50
46.—The "H" specimens (left) and "V" specimens (right) both exhibited cup-and-cone fracture modes, with the H specimens showing more complete cup-and-cone fracture and the less ductile “V” specimens showing partial cup-and-cone with brittle fracture in the center of the fracture surface.	50
47.—Pair of slinger rings on a bearing.	53
48.—Spare slinger ring received from Grand Coulee.	55
49.—Slinger ring part model. Top: Wireframe of original part model. Bottom: Final part model for printing with added material colored red.	56
50.—Six slinger ring halves as-received from Elementum3D. The ring ID numbers are based on IDs that were inscribed on the parts by Elementum 3D.	56
51.—Example of one control view from the 3D scan report of ring half A2229 showing the OD being under dimension. The greatest value on the color scale (red) is +0.1900 inches. The lowest value (pink) is -0.1600 inches.	57

52.—Representative photograph of the joint between two direct-printed slinger ring halves. Warpage and dimensions being out of tolerance cause the halves to not meet correctly. The left side of the photograph shows the top (based on print orientation) of ring half A2527 and the right side shows the bottom of ring half A2240.....	58
53.—Photograph of ring half A2902, as-received condition.	58
54.—Example of one control view from the 3D scan report of ring half A2902 showing warpage in the Z-plane. The greatest value on the color scale (red) is +0.0300 inches. The lowest value (pink) is -0.0325 inches.	59
55.—Printed PLA ring halves to test the resolution for use as investment casting patterns.	60
56.—Left: Printed PLA ring half pattern with gating system. Right: Small voids in the printed PLA ring surface due to incorrect print settings.	60
57.—Naval brass test castings prior to sand blasting to achieve final surface finish. Left: Two successful test castings. Right: Closeup view of surface texture on test casting.....	61
58.—Labeling of critical slinger ring dimensions with bubbles numbered 1–9 for cast slinger ring dimensional analysis.....	62
59.—Test castings in as-received condition. Warping causes the two halves to not line up properly and affects circularity, as represented by the overlaid red dashed circle.....	63
60.—Additional PLA test patterns printed by ORNL with 100% infill to address the void issue in the original PLA test patterns.	64

Appendices

A—Colorado Metallurgical Services Mechanical Property Data of Service Parts
B—3D Scan Results of Stainless Steel Governor Parts As-Printed
C—3D Scan Results of Stainless Steel Governor Parts As-Machined
D—Aluminum Bronze L-PBF Development Report
E—3D Scan Results of Aluminum Bronze Governor Parts As-Printed
F—3D Scan Results of Aluminum Bronze Governor Parts As-Machined
G—Colorado Metallurgical Services Mechanical Property Data of Printed Stainless Steel
H—Mechanical Property Data of Printed Aluminum Bronze Samples
I—3D Scan Results of Aluminum Log Boom Anchor As-Printed
J—Mechanical Property Data of Printed Aluminum
K—Density Measurement Procedure
L—3D Scan Results of Aluminum Bronze Slinger Rings As-Printed
M—Screenshots of Polylactic Acid Setup

Executive Summary

The Bureau of Reclamation (Reclamation) is faced with maintaining an aging asset portfolio which includes some legacy parts that are no longer in production. This project undertook a collaboration with Oak Ridge National Laboratory to determine the feasibility and cost, and to demonstrate the efficacy of additively manufactured replacements for selected hydropower facility components.

Reclamation's Technical Service Center partnered with several regional and area offices to identify opportunities where additive manufacturing could be deployed. Three parts were selected and pursued as case studies: governor parts for Glen Canyon Dam, log boom anchors for Nimbus Dam, and generator exciter bearing slinger rings for Grand Coulee Dam. For each case study, researchers selected one or more additive manufacturing processes that seemed most feasible to replicate or improve upon the conventional part. Researchers worked with manufacturers to produce the additively manufactured components. To evaluate efficacy, the parts underwent material properties testing (density, tensile, bend, hardness, fatigue), metallography and fractography, three-dimensional scanning, and cost-benefit analysis.

The governor parts were the most challenging case study undertaken due to the material of parts, the parts' complexities and the precision tolerances and final machining requirements. After multiple iterations, the parts were delivered to Reclamation for testing and processing. The laboratory testing showed that additive manufacturing is a viable process for producing parts with satisfactory mechanical properties. However final machining and inspection revealed some dimensional non-conformities that likely originated during reverse engineering, model development, and/or the final machining process. Unfortunately, the operational risk of the non-conformities was deemed too high to proceed with field testing.

The log boom anchor case study succeeded in producing a part that was redesigned and optimized for additive manufacturing, using finite element analysis software to reduce mass by approximately 50 percent. The part was produced by a selective laser melting process with AlSi10Mg, a spherical aluminum alloy powder. The additive manufacturing material had a refined microstructure, due to the high solidification rate, resulting in higher yield and tensile strengths than the cast version. Field testing of the log boom anchor was not possible during the project due to time constraints and is recommended as future work.

The slinger ring case study was unsuccessful in replicating the conventional ring. Two production processes were chosen, one using a printed polymer ring to create a pattern for investment casting of naval brass, and one using powder bed fusion to print aluminum bronze. Both processes resulted in warpage that affected the ring's circularity, which is critical to its function. Further development of the aluminum bronze printing process could reduce warpage, but the technology is not currently ready for use in producing additively manufactured wear rings.

There may be opportunities for additive manufacturing to be deployed selectively within Reclamation's aging infrastructure, but careful consideration must be made for the amount of post-processing required for parts. Additive manufacturing is a viable alternative for components that can be updated, changed, or optimized for strength, weight (or material reduction), or for printing. Another prerequisite for use of additive manufacturing is that the design must allow for materials with established print parameters to be used.

1 Introduction

1.1 Project Background

The Bureau of Reclamation (Reclamation) is faced with maintaining an aging asset portfolio which includes some legacy parts that are no longer in production. The successful implementation of additive manufacturing in applications such as flight-critical components in aerospace applications and 3D printing the wind blade mold for wind turbines bodes well for its use in hydropower.

This project aims to collaborate with Oak Ridge National Laboratory's (ORNL) Water Power Program and Manufacturing Demonstration Facility (MDF) to determine the feasibility and cost, and to demonstrate the efficacy of additively manufactured replacements for hydropower facility components in which:

- There are no longer replacements available from commercial providers,
- no design documentation (drawings) exists,
- additive processes can add value by substantially reducing material waste and/or energy requirements during production,
- or additive manufacturing can allow for an optimized design that enhances strength or other performance characteristics.

Reclamation seeks outcomes that increase the service life of equipment, keep equipment operational while replacements are planned, reduce outage time, or increase the reliability of generating assets. One of the goals of this research project was to gain experience with metal 3D printing to ensure that parts can be produced reliably. Familiarization with the fabrication processes available and their limitations was a second goal.

1.2 Case Selection

Reclamation's Technical Service Center partnered with representatives at several regional and area offices to identify opportunities where additive manufacturing could be deployed to satisfy one or more of the criteria listed above. A list of potential parts was generated and three were ultimately selected and pursued as case studies: governor parts for Glen Canyon Dam, log boom anchors for Nimbus Dam, and generator exciter bearing slinger rings for Grand Coulee Dam.

2 Case Study A: Governor Valves

2.1 Component Selection

A pilot valve and gate limit valve in a hydroelectric governor at Glen Canyon Dam were selected as the candidates for additive manufacturing. These governor parts were identified during the team's initial consultations with research partners in area and project offices. These parts are currently ordered as custom replacements and undergo a manual machining process to meet the functional requirements of the design. 3D printing still requires a final machining process for these parts but printing a near net shape can reduce the amount of machining required.

2.2 Component Functionality

The primary purpose of a governor in a hydroelectric unit is to control the speed and loading of the unit. It accomplishes this by sensing the turbine speed, and then adjusting the wicket gates to control the flow. The main parts in mechanical governors are a speed sensing system, hydraulic power system, distributing valve assembly, servomotor, pilot valve, gate limit valve, and operating controls. In Case Study A of this project, parts of the pilot valve and gate limit valve were selected for additive manufacturing (see Figure 1).

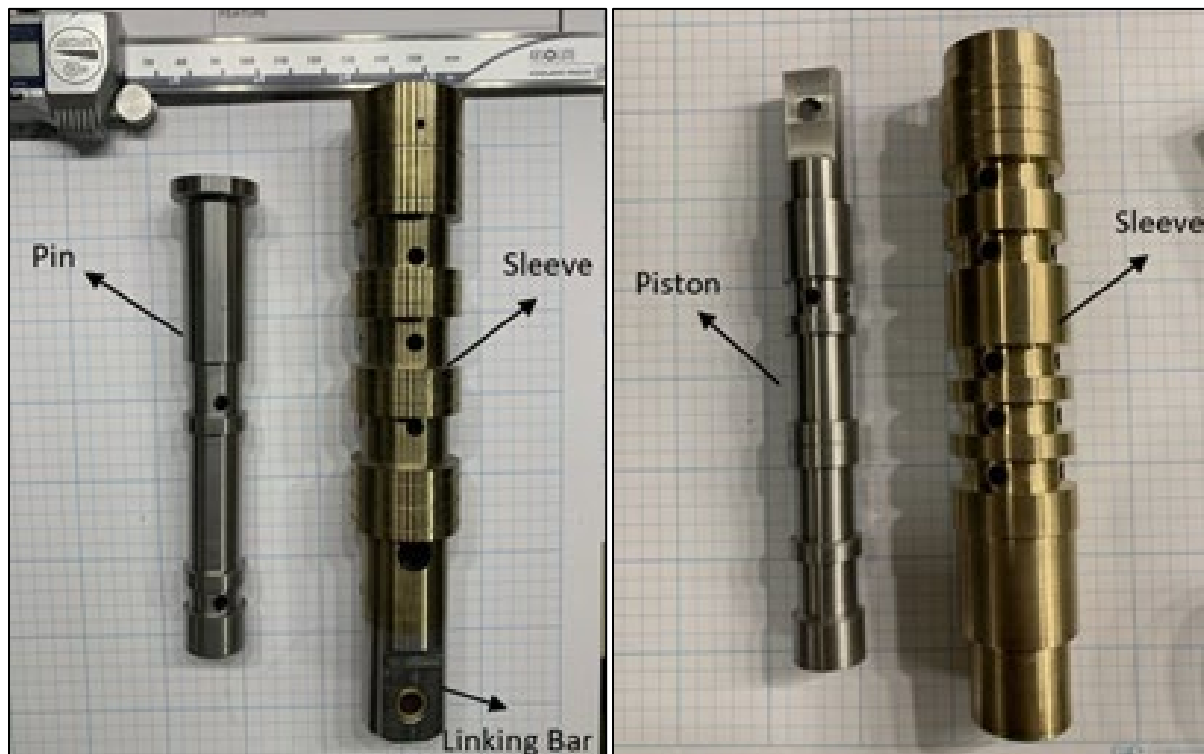


Figure 1.—Pin (H_41365_C), linking bar and sleeve (H_41365_A) of pilot valve (left). Piston (H_41365_D) and sleeve (H_41365_B) of gate limit valve (right).

2.2.1 Pilot Valve

The pilot valve is designed to be sensitive to the forces that result from changes in unit speed. The pilot valve works to maintain direction of the relay valve. The pilot valve is usually designed with a moveable bushing. The plunger of the pilot valve is connected, through a floating lever, to the ball head, and the bushing is connected to the main valve. Whenever the pilot valve moves off center, oil is routed to the main valve servo, causing the main valve to move. The pilot valve bushing is moved off center by the main valve movement, blocking the port of the pilot valve, stopping further main valve movement. The restoring lever between the main valve and the pilot valve bushing is usually adjustable so that the ratio of pilot valve movement to main valve movement is adjustable. In short, this assembly consists of multiple components linked together and requires precise dimensions and tight tolerances to function correctly.

2.2.2 Gate Limit Valve

The gate limit valve provides the operating limit for the wicket gates that control water flow into the turbine unit. When the gate limit setting is above the gate position, the gate limit valve allows unobstructed flow between the pilot valve and the main valve. When the gate position matches the gate limit setting, the gate limit valve blocks all oil flow from the pilot valve. If the gate limit is moved below the gate position, the gate limit valve over-rides the pilot valve and routes oil to close the gates.

2.3 Conventional (Baseline) Components

2.3.1 Conventional Materials and Manufacturing Processes

The pilot valve and gate limit valve are each composed of two parts: sleeve and pin. Third party chemical analysis testing determined that the sleeve was machined from naval brass (UNS C46400) and that the pin was machined from stainless steel (UNS S30300). Results from the analyses are included as Appendix A.

2.3.2 Conventional Cost Estimates

The valves are traditionally fabricated on a lathe. The estimation of conventional cost of these components were provided by ORNL and are listed in Table 1. Alternatively, Glen Canyon Dam staff reported that components can be purchased for roughly \$4,200 in 2022 United States dollars (2022 USD).

Table 1.—Estimated Cost of Governor Parts Using Conventional Fabrication Methods*

Part No.	Prescribed Material	No. of Units	Conventional Material	Std. Cost (USD)	Std. Lead Time (days)	Expedited Cost (USD)	Expedited Lead Time (days)
H_41365_A (pilot valve sleeve)	UNS C46400 (<i>naval brass</i>)	1	C360	892.46	13	1343.83	6
H_41365_B (gate limit valve sleeve)	UNS C46400 (<i>naval brass</i>)	1	C360	945.78	13	1424.29	6
H_41365_C (pilot valve pin)	UNS S30300 (<i>303 SS</i>)	1	303SS	706	12	991.24	7
H_41365_D (gate limit valve pin)	UNS S30300 (<i>303 SS</i>)	1	303SS	604.68	12	849.25	7

Note: No. = number, Std. = standard, USD = U.S. dollars (2021), SS = stainless steel. Cost estimates obtained from Xometry.com, CNC Machining Service.

2.4 Additive Cost and Feasibility Estimates and Selections

Reclamation and ORNL MDF staff discussed the additive manufacturing techniques and corresponding materials for the stainless steel parts and naval brass parts.

2.4.1 Stainless Steel Parts

The stainless steel pins in the pilot valve and gate limit valve can be additively manufactured using selective laser melting (SLM). A cost estimate was not readily available for these parts. In general, costs for SLM printing includes technician labor, material costs, and machine time to print. For the stainless steel parts, the required labor was 10.5 hours to set up the files and machine, print and remove the part, and perform post-printing cleanup. At \$20 per hour, that equates to \$210. The material cost for virgin powder is roughly \$130 per kilogram; however, significantly more material would be required to fill the build volume, which can vary based on part orientation and machine. It is not clear what portion (if any) of these costs can be recouped by reusing or recycling powder in a production environment. Finally, print time was estimated at approximately 23 hours (actual print time was 30 hours, 20 minutes).

Three stainless steel parts were selected for 3D printing at ORNL MDF using an M2 Direct Metal Laser Melting (DMLM) machine from GE Additive. These parts were: the pilot valve pin, the pilot valve linking bar, and the gate limit valve piston. The original parts were 303 stainless steel; however, 316L stainless steel was selected due to material availability and acceptable material properties.

Reclamation mechanical engineers created drawings of the components based on physical measurements of the existing components. These drawings were reviewed by field office partners. From the drawings, researchers generated 3D models for printing. Since each part needed machining after printing, two variations were printed and delivered to Reclamation for machining and testing. The first approach included additional material on all surfaces. The second approach included additional material only on selected surfaces that would require machining.

Figure 2 shows the schematics of the gate limit valve piston, the pilot valve pin, and pilot valve linking bar. In the figure, the thickness of the extra material is 0.040 inches. Note that the parts contain small holes which need to be machined after printing to achieve the desired surface finish and dimensional tolerances. There is no perceived advantage to printing the holes due to the machining requirement, so they were omitted from the print design.

The stainless steel parts were printed vertically, with the left side of each part on the build plate as shown in Figure 2.

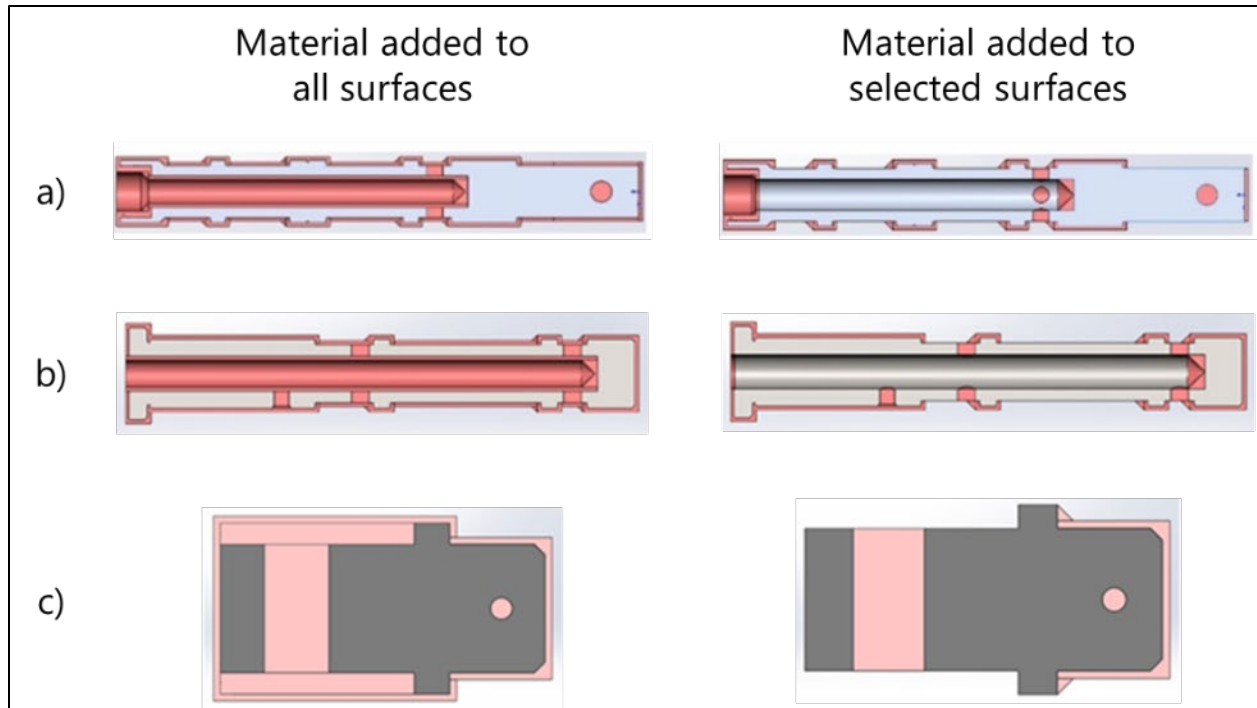


Figure 2.—Schematic showing the two approaches for adding material to the 3D models for printing of the stainless steel governor parts: (a) gate limit valve piston; (b) pilot valve pin; (c) pilot valve linking bar.

2.4.2 Naval Brass Parts

There is currently no mature technology to directly print qualified brass components. Binder jetting techniques can 3D print stainless steel with brass, but the resulting material is a majority stainless steel with some brass infiltrate. Due to the inability to print naval brass, Reclamation and ORNL investigated and discussed possible substitute materials. Table 2 shows several materials property comparisons.

Table 2.—Material Property Comparison for Possible Naval Brass Substitutes

	Naval Brass (H01 Temper) ¹	Al Bronze (UNS:C95300) ²	304 SS ¹	316 SS ¹	Nickel Alloy 625 ¹	Nickel Alloy 718 ¹	Pure Ti ¹	Ti (6Al-4V) ¹	6061 Al-T6 ¹
Density (lb/in ³)	0.304	0.272	0.289	0.289	0.305	0.296	0.163	0.160	0.098
Tensile Strength (lb/in ²)	69,000	80,000–85,000	93,000	80,000	133,000	162,000	32,000	138,000	45,000
Yield Strength (lb/in ²)	46,000	42,000	34,000	35,000	70,000	120,000	20,000	128,000	40,000
Elongation at Break (%)	27	12–15	27	60	46	31	54	14	17
Reduction in Area (%)	50	—	54	65	—	—	—	25-36	—
Hardness (Rockwell B)	78	81	82	80	97	100	—	109	60
Impact (ft-lb)	—	—	240	77	—	—	—	13	—
Modulus of Elasticity (lb/in ²)	1.45 x 10 ⁷	1.6 x 10 ⁷	2.8 x 10 ⁷	2.8 x 10 ⁷	3.0 x 10 ⁷	3.0 x 10 ⁷	1.7 x 10 ⁷	1.7 x 10 ⁷	1.0 x 10 ⁷
Shear Modulus (lb/in ²)	5.66 x 10 ⁶	—	1.1 x 10 ⁷	—	—	1.2 x 10 ⁷	6.2 x 10 ⁶	6.4 x 10 ⁶	26
Poisson Ratio	0.28	—	0.29	—	—	0.284	0.34	0.342	0.33

Note: Al = aluminum, SS = stainless steel, Ti = titanium, lb/in³ = pound(s) per cubic inch, lb/in² = pound(s) per square inch, % = percent, and ft-lb = foot-pound(s).

¹ <https://www.matweb.com/>.

² "Copper Casting Alloys," Copper Development Association (https://www.copper.org/publications/pub_list/pdf/7014.pdf).

Based on the loading conditions of these parts in service, it was determined that yield strength did not need to be equivalent to the originally specified naval brass. Typical loading conditions are far below the yield strength of the naval brass alloy and encasement of the components within the governor assembly does not permit elastic deformation. Wear resistance, however, is a primary consideration of the materials for the valve sleeve, so it was necessary to select a material with similar hardness. For a more exact comparison, the original parts received from service were sent for hardness testing by a third-party laboratory, with results included in Appendix A.

Aluminum bronze, UNS C95300, was the only material identified with properties close enough to naval brass that could feasibly be printed without extensive research and development work. Aluminum bronze printing required some development of the printing parameters and was outsourced to a company that specializes in 3D printing of novel materials.

As with the stainless steel parts, drawings were again created based on the existing components, and were reviewed by field office partners. From the drawings, 3D models were generated for printing, and additional material was added to all surfaces of the aluminum bronze components. Two sets of

printed parts were requested for each component. Note that the parts contain small holes which need to be machined after printing to achieve the desired surface finish and dimensional tolerances. There is no perceived advantage to printing the holes due to the machining requirement, so they were omitted from the print design.

Figure 3 shows cross-sections of the 3D models for each of the aluminum bronze printed sleeves with the additional 0.040 inches of extra material added.

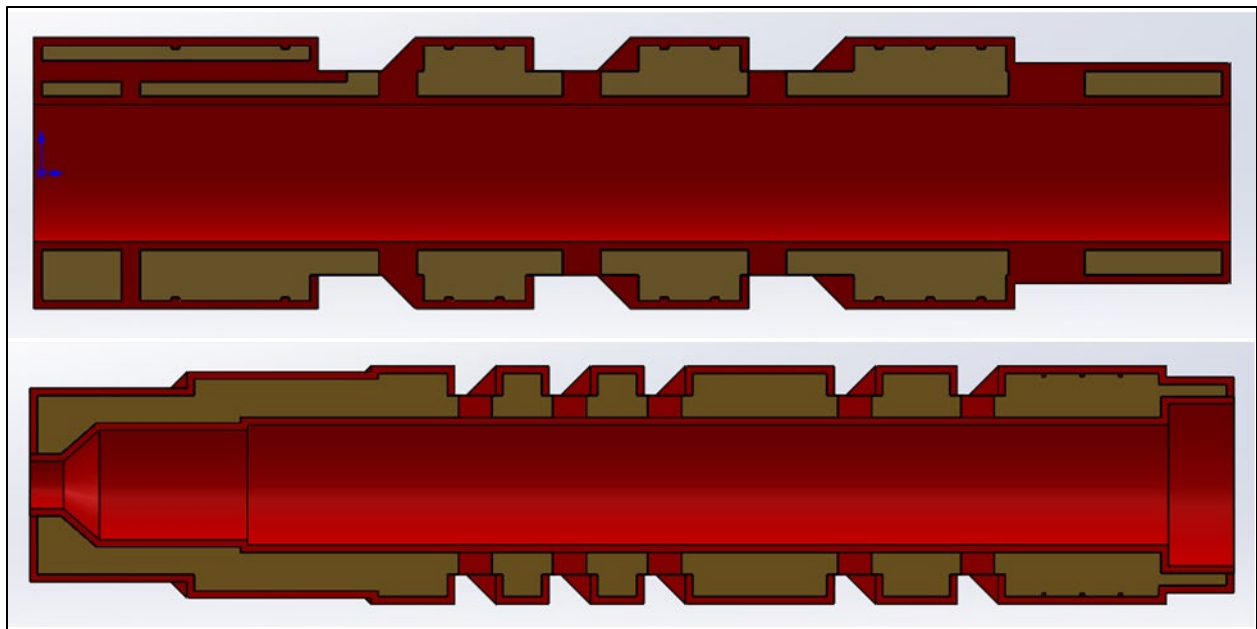


Figure 3.—Additional material (shown in red) added to the 3D models of the aluminum bronze pilot valve sleeve (top) and gate limit valve (bottom).

2.5 Stainless Steel Governor Parts Results

2.5.1 Printing Process

The stainless steel parts were printed using a GE Additive M2 machine at ORNL's MDF. Figure 4, Figure 5, and Figure 6 show the 3D printed parts. Figure 7 shows the parts on the build plate and the vertically printed wall. The technician spent 10.5 hours setting up the models, printing, cleaning up, and completing other associated tasks. The powder information for the starting material can be found in Table 3 and Table 4. The parts were heat treated after printing. The stress relief cycle consisted of an 18-degree Fahrenheit (°F) (10 degrees Celsius [°C]) per minute ramp to 1202 °F (650 °C) with a hold time dependent on mass of the base plate and printed parts. The hold time was followed by a 3.6 °F (2 °C) to 12.6 °F (7 °C) per minute cooldown.



Figure 4.—3D-printed linking bars. Left: Parts had material added to selected surfaces. Right: Parts had material added to all surfaces.



Figure 5.—3D-printed piston of gate limit valve. Left: Parts had material added to selected surfaces. Right: Parts had material added to all surfaces.



Figure 6.—3D-printed pin of pilot valve. Left: Parts had material added to selected surfaces. Right: Parts had material added to all surfaces.

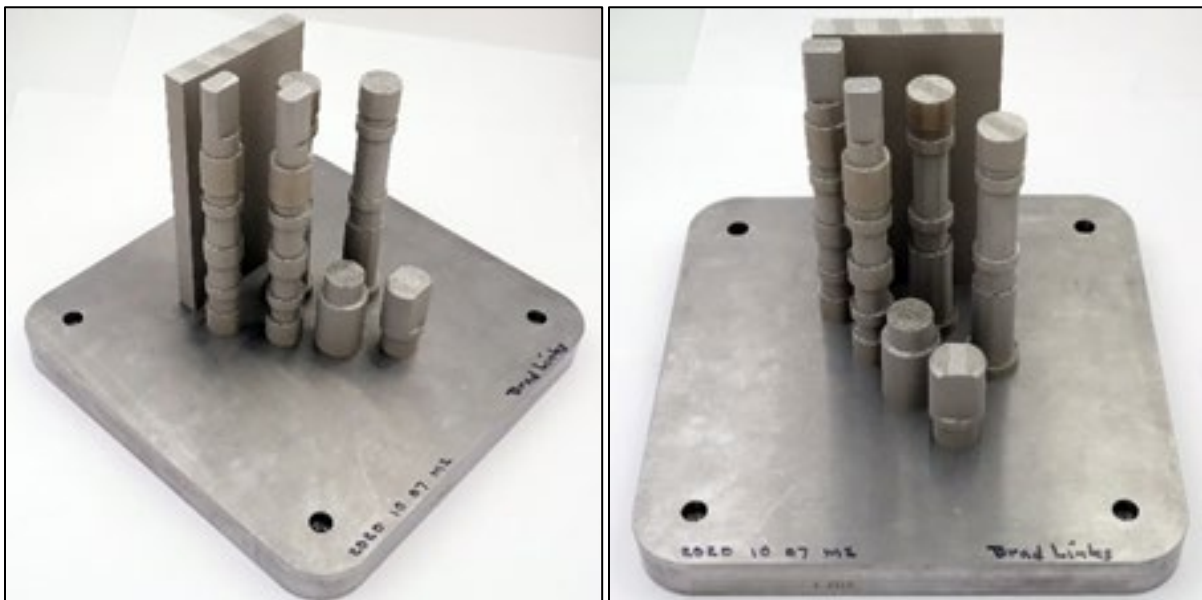


Figure 7.—All stainless steel governor parts on the build plate.

Table 3.—Exact Powder Chemical Composition for Stainless Steel Parts

	Test Method	Minimum (Mass %)	Maximum (Mass %)	Result (Mass %)
Carbon (total)	Leco	—	—	<0.001
Cobalt	ICP-MS	—	—	0.08
Chromium	ICP	16.00	18.00	16.93
Copper	ICP-MS	—	0.75	0.00
Iron	—	—	—	Balance
Manganese	ICP	—	2.00	0.99
Molybdenum	ICP	2.00	3.00	2.46
Nitrogen	Leco	—	0.10	0.01
Nickel	ICP	10.00	14.00	12.22
Oxygen	Leco	—	0.10	0.05
Phosphorus	ICP-MS	—	0.040	<0.005
Sulfur	Leco	—	0.030	0.004
Silicon	ICP-MS	—	1.00	0.36
Total All Other	ICP-MS	—	0.50	<0.10

Note: Leco = Leco combustion analysis, ICP = inductively coupled plasma, and MS = mass spectroscopy.

Table 4.—Exact Powder Size for Stainless Steel Parts

Particle Diameter ¹	Test Method	Minimum (Mass %)	Maximum (Mass %)	Result (Mass %)
d < -16	ASTM B822	—	5	3
10 μm < d < 50 μm	ASTM B822	15	25	19
50 μm < d < 90 μm	ASTM B822	25	35	31
d > 90 μm	ASTM B822	40.0	60	44.5

Note: μm = micrometers.

¹ Microtrac per ASTM B822.

2.5.2 Machining

All stainless steel parts were 3D-scanned in the as-printed condition at ORNL. The results from the scans are shown in the associated ORNL report included in Appendix B. Example images from the report are shown in Figure 8. For both pilot valve component diameters, the scans showed that the maximum positive and negative deviation from the computer-aided design (CAD) model was +0.011-inch (+0.28 millimeters [mm]) and -0.017-inch (-0.42 mm), respectively. This deviation is within the design tolerance. For the gate limit valve components, the maximum positive and negative deviation from the CAD model was +0.009-inch (0.23 mm) and -0.007-inch (-0.18 mm), respectively. This is also within the design tolerance.

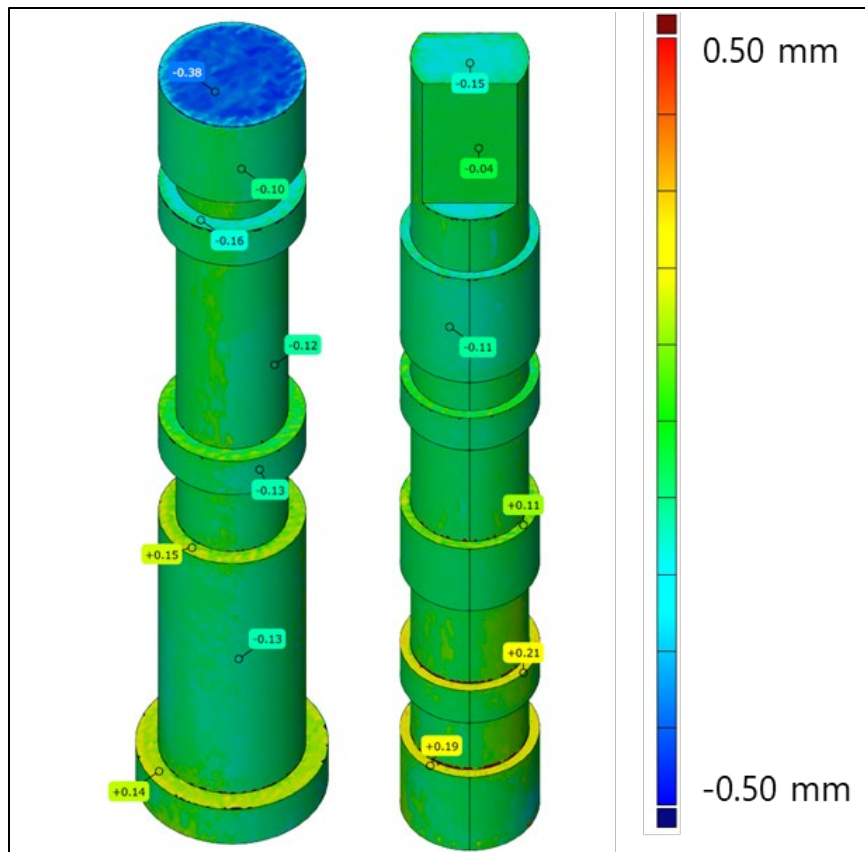


Figure 8.—Example 3D scan results of stainless steel governor part components, as-printed. The greatest value on the color scale (red) is +0.020 inches (+0.50 mm). The lowest value (blue) is -0.020 inches (-0.50 mm).

For all stainless steel components, the 3D-scans indicated the excess material added to the CAD models was sufficient to allow machining to final dimensions and surface finish while remaining within the finished components' design tolerance. Final machining was performed by the Grand Coulee machine shop. The original estimated machining time was 40 hours for two sets of pilot valves and 40 hours for two sets of gate limit valves. Actual machining time was 22 hours per each set of the pilot valves and gate limit valves. The shop provided findings for the research team after machining was performed. These findings are summarized below:

Gate Limit Valve Piston.—The print called for the thread to be left hand at 5 threads per inch (tpi), but the part was right-handed. The part was fabricated with left hand threads at 4.5 tpi to match a spring the shop had on-hand. The shop's spring was provided for use with the part, but the application may require a different spring.

Pilot Valve.—The part was made to the print except for a missing hole where there was a discrepancy between the original part and the drawing. After discussing with the team, the hole was drilled in the location of the original part. The shop also noted that the part was undersized on the relieved areas by 0.020-inch in certain spots. This was not observed prior to machining

and, as a result, the part dimension after machining was 0.615-inch in these areas where the print called for 0.630-inch. In addition, the print was missing the length of the linking bar and the shop observed that the printed linking bar was shorter than the original.

General Notes.—The shop noted that the material did perform like normal, i.e., like rolled stainless steel, during the machining process. The shop advised the team to avoid printing parts with holes because the tooling will follow the holes making any defects difficult to remove. It is also preferred to include additional material to hold onto during the machining process. Figure 10 provides a comparison of the additively manufactured pilot valve after final machining with the original part.

An example of the 3D scans of the as-machined parts can be seen in Figure 9. The complete set of 3D scan results (and color scales) can be found in Appendix C. 3D scanning was not possible on the internal bore of the components due to physical limitations of the scanning probe. Scan results indicate that, overall, the diameters of the machined stainless steel components were within between +0.0038-inch and -0.0153-inch of the dimensions specified by the CAD models provided.

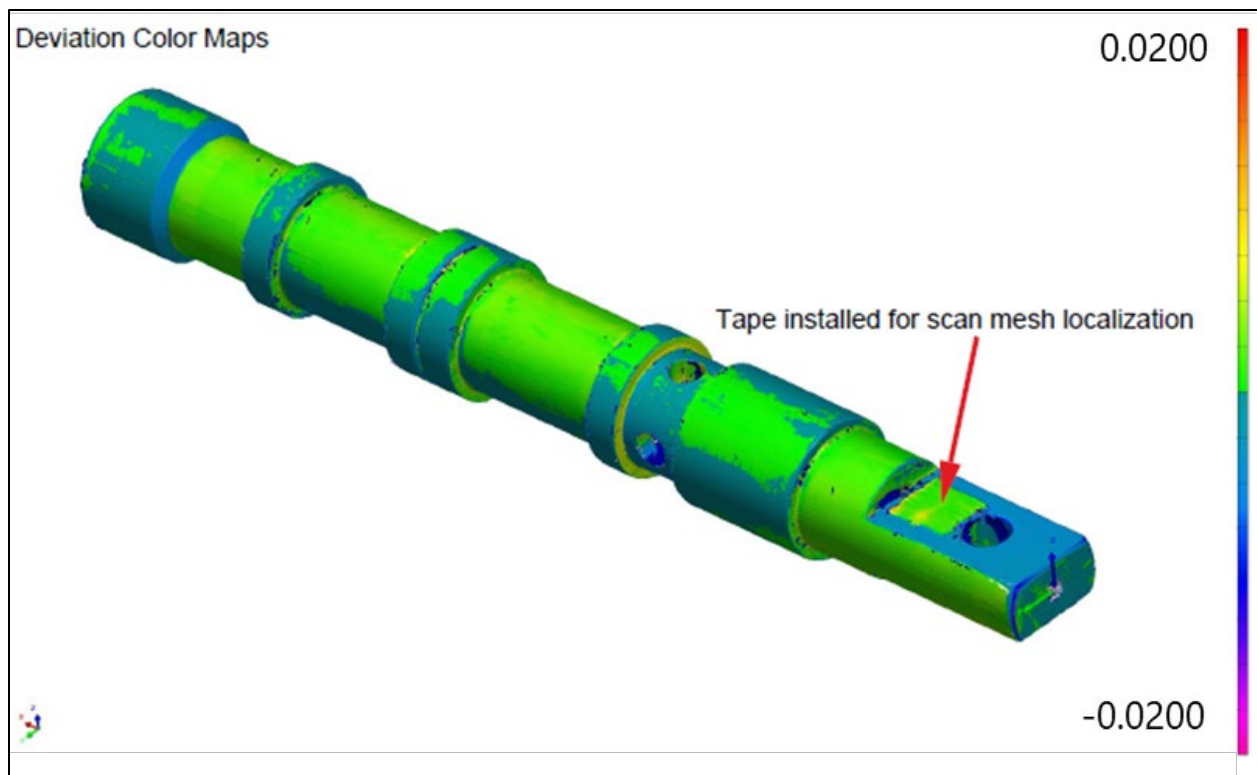


Figure 9.—Example 3D scan result of stainless steel gate limit valve piston after machining. The greatest value on the color scale (red) is +0.0200 inches. The lowest value (pink) is -0.0200 inches.



Figure 10.—Additively manufactured and machined pilot valve (Left) compared to original part (Right).

2.6 Aluminum Bronze Governor Parts Results

2.6.1 Printing Process

Since ORNL did not have the capability to print aluminum bronze, the research team partnered with Elementum 3D to develop printing parameters and a process to heat treat the printed parts to achieve the desired properties. Appendix D details the work performed, issues encountered, and the results for this effort. Elementum 3D developed a Laser Powder Bed Fusion (L-PBF) process and subsequent heat treatment to achieve the target properties (density greater than 99.5% and average hardness of 78 Rockwell Hardness B (HRB)).

2.6.2 Machining

All aluminum bronze parts were 3D-scanned in the as-printed condition at Reclamation. The results from the scans (and color scales) are shown in Appendix E. An example image from the report is shown in Figure 11. For both component diameters, the scans showed that the maximum negative deviation from the CAD model was -0.0045-inch, which was within the design tolerance.

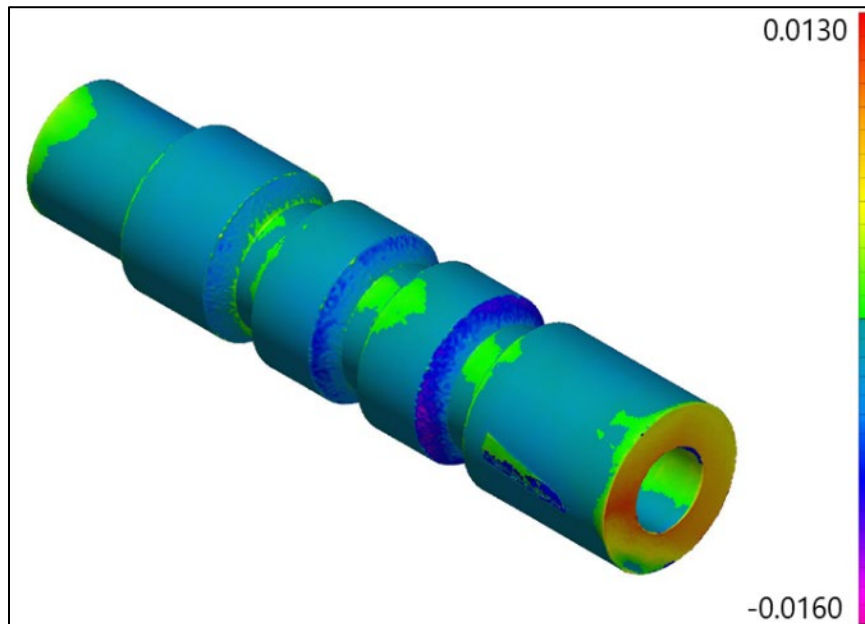


Figure 11.—Example 3D scan results of aluminum bronze governor part components, as-printed. The greatest value on the color scale (red) is +0.0130 inches. The lowest value (pink) is -0.0160 inches.

Due to the geometric complexity of the governor parts, computer-numerical-control (CNC) machining was determined to be the most cost-effective solution to achieve final dimensions and surface finish of the aluminum bronze components. The parts were sent to the Grand Coulee machine shop to make use of the 4-axis machining capabilities at that facility. The shop provided findings for the team after machining was performed. These findings are summarized below:

Gate limit valve sleeve.—The bore in the aluminum bronze sleeve was not straight, meaning internal and external diameters were not concentric. As a result, there was insufficient material in the grooves for machining. From a design standpoint, no groove depth was provided, so the shop used the existing parts as a guide. Tooling issues were encountered where the shop's boring bar was not long enough, so a reamer was used instead. The reamer used was not capable of boring the 0.69-inch internal diameter due to access and tool length limitations; however, an as-printed surface finish was determined to be acceptable for this section of the component.

Section control (pilot) valve sleeve.—Again, the bore in the printed part was not straight. As a result, there was insufficient material in the grooves for machining. In addition, the print was missing the length of the linking bar and shop observed that the printed linking bar was shorter than the original.

General Notes.—Starting the machining process with near-net-shape components posed several challenges for machining that are not usually encountered under traditional circumstances. Typically, solid material is machined down in a subtractive process to achieve final dimensions. In this process, excess solid material provides a means to hold the part while machining. Conversely, it is difficult to hold a part with a near net shape because there is a limited area to grip without damaging the component. For the future, the machine shop would like more material to hold. Similar to the stainless steel components, the shop also advised the team to avoid printing parts with holes.

Another problem that the team observed that was not noted by the machine shop is that there appears to be a difference in the alignment between the holes and the flat faces on the linking bar compared with the original pilot valve, as shown in Figure 12. In the printed and machined components, the holes are aligned with the flat faces; whereas on the original part, it appears the holes are slightly off angle from the flats.



Figure 12.—Difference in hole alignment between printed pilot valve (left) and original (right).

Photographs of machined aluminum bronze additively manufactured parts can be seen alongside parts removed from service in Figure 13. An example of the 3D scans of the as-machined parts (and color scales) is in Figure 14. The complete set of 3D scan results can be found in Appendix F. 3D scanning was not possible on the internal bore of the components due to physical limitations of the scanning probe. Rough areas in the relieved areas can be seen in both figures. As noted in the machinists' notes, this issue arose due to an alignment issue between the bore and the exterior diameter of the as-printed parts. Scan results indicate that overall, the machined aluminum bronze component diameters were within 0.03-inch of the CAD models provided.



Figure 13.—Machined aluminum bronze additively manufactured parts compared to original parts removed from service. Left: Gate limit valve (additively manufactured part on right). Right: Section control valve (additively manufactured part on left).

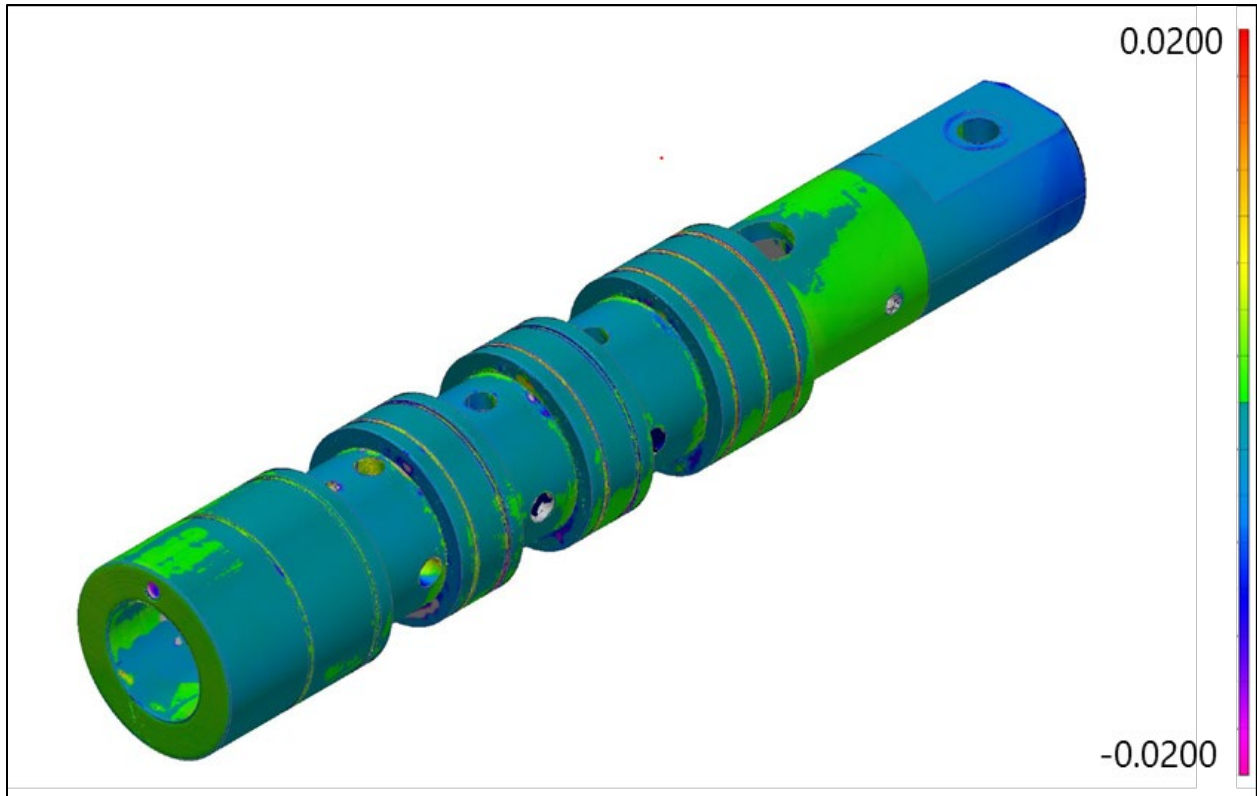


Figure 14.—Example 3D scan of as-machined pilot valve sleeve assembly. The greatest value on the color scale (red) is +0.0200 inches. The lowest value (pink) is -0.0200 inches.

2.7 Stainless Steel Laboratory Test Sample Results

A single wall, approximately 6 inches by 3.5 inches, was printed alongside the stainless steel governor parts. Specimens for mechanical testing were machined from the printed walls. Figure 15 shows the location and orientation of the tensile and bend test specimens that were cut from the wall piece. Round tensile samples with a gauge length four times the diameter were machined in accordance with ASTM E8, (“FIG. 8, Specimen 3.”).

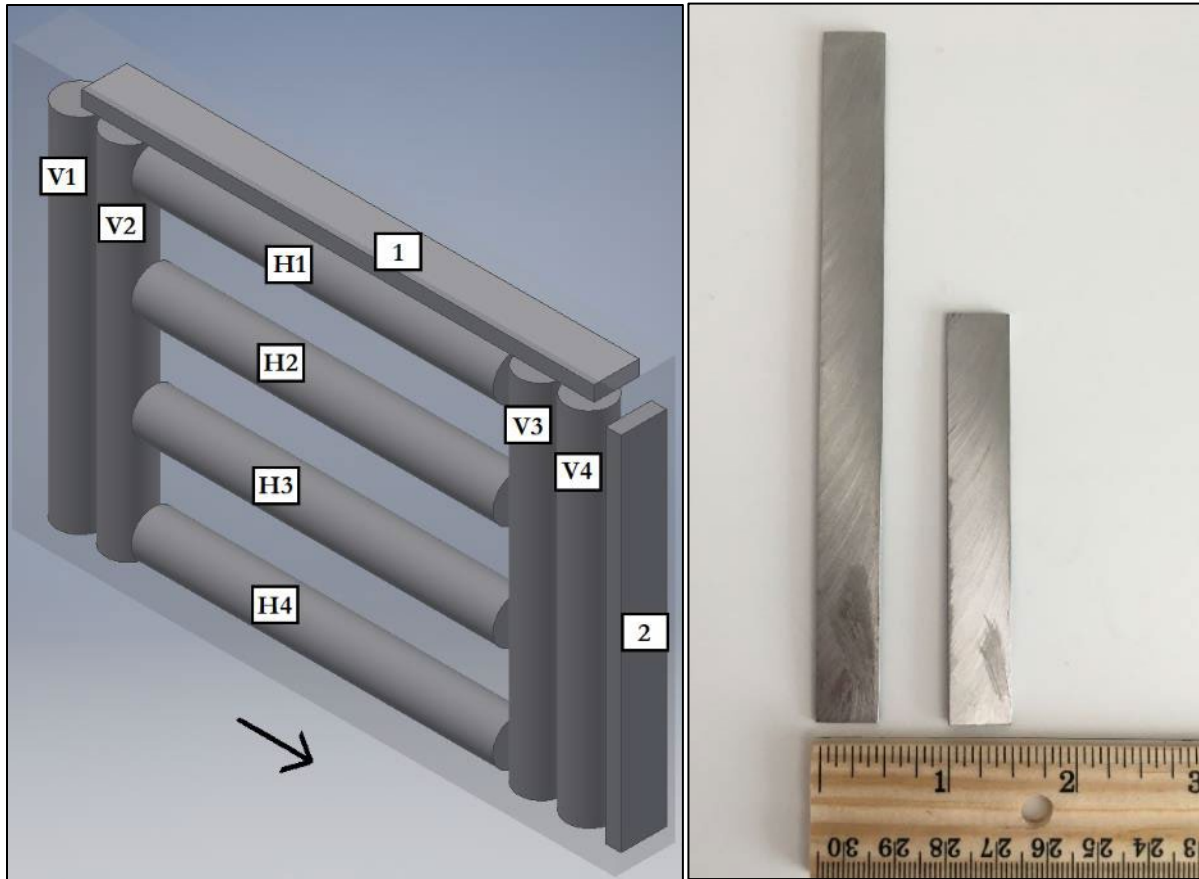


Figure 15.—Left: Schematic of sample orientation for the stainless steel tensile bars (labeled “H” and “V”) and bend samples (labeled “1” and “2”); samples were machined from one printed wall piece; the arrow indicates the “Z” printing direction. Right: Photograph of physical bend samples after removal from test wall.

Note that the wall was printed in the vertical direction as shown in Figure 7. Details of the sample dimensions are provided in Table 5.

Table 5.—Stainless Steel Tensile and Bend Sample Orientation, Quantity, Dimensions, and Notes

Sample Description	Orientation	Quantity	Overall Sample Dimensions (inches [mm])	Notes
V(1-4)	XY	4	0.5 (12.7) diameter, 3.0 (77) long	ASTM E8/E8M – Round Specimen, “Figure 8, Specimen 3”
H(1-4)	Z	4	0.5 (12.7) diameter, 3.0 (77) long	ASTM E8/E8M – Round Specimen, “Figure 8, Specimen 3”
Bend 1	Z	1	Machined to 0.5 x 0.0625 x 3.25	ASTM E290
Bend 2	XY	1	Machined to 0.5 x 0.0625 x 5.5	ASTM E290

2.7.1 Tensile Testing

Tensile testing was conducted by a third-party laboratory (see Appendix G). Tensile testing results can be seen in Table 6, along with literature tensile values of similar material for comparison.

Table 6.—Tensile Test Results from 316L Stainless Steel Test Bars and Published Literature Data for 3D Printed and Wrought Stainless Steel

Specimen	Yield Load (lb)	Yield Strength (lb/in ²)	Tensile Load (lb)	Tensile Strength (lb/in ²)	Elong. (in)	% Elong. (%)	Diameter Reduction (in)	% Area Reduction (%)
H1	2,681	55,000	4,069	83,500	1.52	52	0.1455	66
H2	2,630	54,000	4,061	83,500	1.55	55	0.1420	68
H3	2,573	53,000	4,134	85,000	1.60	60	0.1490	64
H4	2,657	55,000	4,027	83,500	1.53	53	0.1440	66
“H” Specimen Average	2,635	54,250	4,073	83,875	1.55	55	0.1451	66
V1	2,735	56,000	4,209	86,500	1.50	50	0.1320	72
V2	2,767	57,000	4,236	87,000	1.49	49	0.1400	68
V3	2,876	59,000	4,281	88,000	1.47	47	0.1380	69
V4	2,889	59,500	4,249	87,000	1.46	46	0.1430	67
“V” Specimen Average	2,817	57,875	4,244	87,125	1.48	48	0.1383	69
UNS S31603 Lit. Min. Value ¹ (XY direction)	—	30,000	—	75,000	—	30	—	40
UNS S31603 Lit. Min. Value ¹ (Z direction)	—	30,000	—	75,000	—	30	—	40
Annealed UNS S30300 Lit. Min. Value ²	—	30,000	—	75,000	—	40	—	50

Note: Lit. = literature, min. = minimum, and elong. = elongation.

¹ ASTM F3184-16.

² ASM Metals Handbook Vol 1 [1].

The average yield strength for the test bars was 57,875 pounds per square inch (lb/in²) and 54,250 lb/in² for the XY orientation (“V” samples) and Z orientation (“H” samples), respectively. Those values are higher than the minimum required yield strengths stated in ASTM F3184-16, *Standard Specification for Additive Manufacturing Stainless Steel Alloy (UNS S31603) with Powder Bed Fusion*. The “V” and “H” orientation tensile samples had average tensile strengths of 87,125 lb/in² and 83,875 lb/in², respectively, exceeding the minimum required tensile strengths stated in ASTM F3184-16. The “H” tensile samples had a higher average elongation of 55 percent (%), compared to the 48% elongation of the “V” tensile samples. Both measured elongation values were higher than the 30% minimum required by ASTM F3184-16 for XY and Z orientations, and also higher than the 40% requirement for annealed material. Conversely, the “H” samples had a lower average reduction in area of 66% compared to 69% for the “V” samples. These values also exceed the minimum required by ASTM F3184-16.

2.7.2 Bend Testing

Bend testing was completed by a third-party laboratory. The bend was completed in two steps, as per the ASTM E290-14 requirements of a bend and flatten test. In the first step (Type-1) of the test, the sample is bent 180 degrees. In the second step (flattening), a clamping force is applied until both legs of the sample come into contact at the bend. The bend sample dimensions are listed in section 2.7 in Table 5, the bend test results are listed below in Table 7, and photographs of post-tested samples can be seen in Figure 16.

Table 7.—Bend Test Results for Stainless Steel PBF Governor Parts Test Wall

Sample ID	Orientation Related to Z-Axis	Bend 1 (Type-1)	Bend 2 (Flattening)
1	Parallel	No Defects	Many Visible Cracks
2	Perpendicular	No Defects	One Small Crack



Figure 16.—Photographs of bend test samples after testing. Left: Sample 1 (parallel to Z-axis). Right: Sample 2 (perpendicular to Z-axis).

No defects were observed in either sample at the Type -1 bend step of the test. Cracking was observed in both samples after the flattening step of the test. Cracking was more severe in Sample 1 (parallel to Z-axis) than Sample 2 (perpendicular to Z-axis). In accordance with ASTM E290, both samples failed this flattening test. In sample 1, the tensile stresses generated by the test were aligned with the Z-axis print direction. The cracking observed was perpendicular to this axis, correlating with inter-layer cracking. In sample 2, the tensile stresses generated by the test were aligned perpendicular to the Z-axis print direction, and with minimal cracking observed. Consistent with the tensile area reduction results, less overall ductility was qualitatively observed in the z-axis of both samples.

2.7.3 Hardness Testing

A hardness traverse was completed in-house by Reclamation. The results from the test can be seen in Figure 17. Hardness values were recorded at 0.15-inch increments along the 3.5-inch length of the test wall.

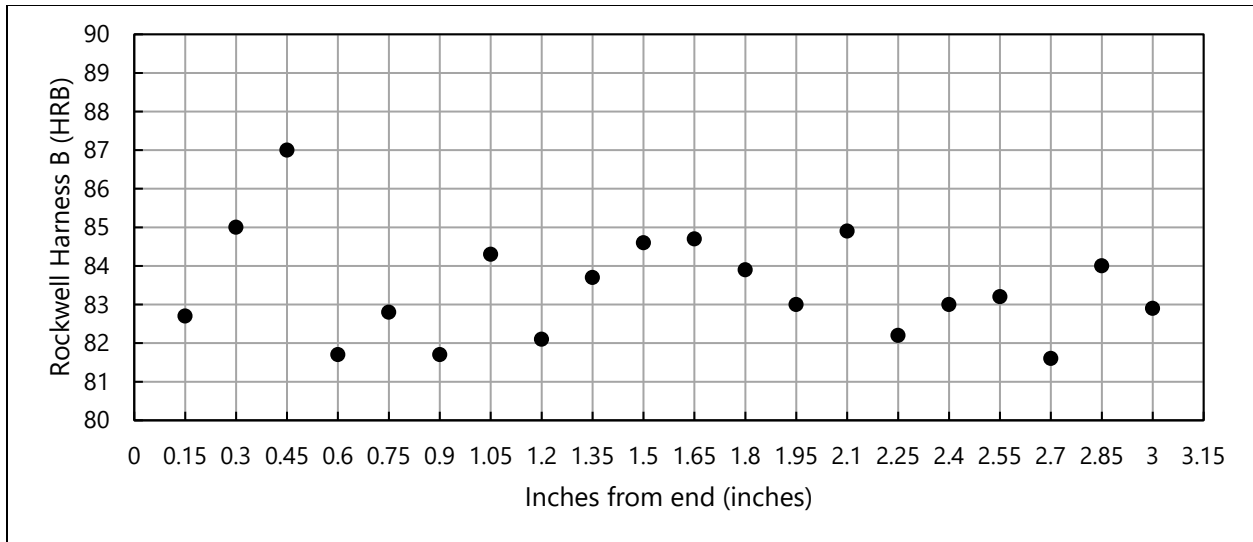


Figure 17.—Hardness traverse test results for the stainless steel PBF governor parts test wall. The traverse was taken along the X-axis build direction.

Hardness ranged between 81 and 85 HRB with exception to one location, 0.45 in (11.43 mm) from the end of the sample, where hardness of 87 HRB was recorded. The average hardness was 83.45 HRB with a standard deviation of 1.3 HRB. The hardness traverse was located along the X-axis build direction and provides an indication of the consistency in print performance along that axis. This average hardness was slightly below the measured hardness of the original part (87 HRB); however, still considered satisfactory for the intended use.

2.7.4 Metallography

Samples for metallographic analysis were taken from the grip portions of tested tensile samples. The nomenclature identifying the samples indicates the orientation of the tensile sample used and the plane being viewed. See Figure 18 for details on sample nomenclature. Samples were prepared with the following procedure:

1. Section metallographic samples from the tested tensile samples using an abrasive metallography saw. Specimens were taken from a horizontal (H) specimen and a vertical (V) specimen (See Figure 15). The face (F) and cross section (X) of each specimen were analyzed for a total of four specimens: HF, HX, VF, and VX, as shown in Figure 18.
2. Cold mount in epoxy and cure for a minimum of 24 hours.
3. Grind from coarser to finer grits:
 - a. 180 grit for 1 minute
 - b. 320 for 1 minute
 - c. 400 for 3 minutes
 - d. 600 for 5 minutes

4. Polish to a mirror finish:
 - a. 6-micron diamond for 5 minutes
 - b. 1-micron diamond for 5 minutes
5. Etch with glyceresia (1:2:3 ratio of nitric acid, glycerol, and hydrochloric acid) for 80 seconds.
6. Image at the following magnifications using an optical microscope:
 - a. 200X, 500X, and 1000X

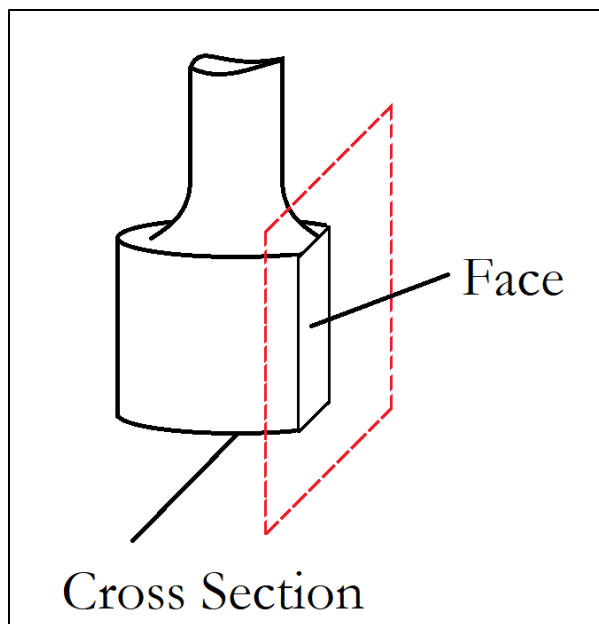


Figure 18.—Naming designation of metallography orientation on tensile bar specimens.

Example images of the microstructures from each sample orientation can be seen in Figure 19 through Figure 22. All samples display a characteristic columnar grain structure within the weld beads. Metals in their solid form are usually polycrystalline, and grains are the individual crystals within that solid, which have a uniform structure. Grain size is consistent throughout the samples and the shape of the grains are elongated parallel to the print direction (XY plane), as seen in the HX and VF section samples. Frequently, researchers observed that grains maintained the same orientation to the grains within adjacent weld beads.

Small circular dark spots and irregular dark spots at grain boundaries indicate the presence of porosity and voids respectively, though these were found in relatively small area fractions of micrographs taken. The porosity and voids are a result of the laser power parameters used. Porosity has been shown to decrease with increased laser power [2, 3]. Impurities are not readily seen in any of the micrographs, indicating purity of the starting powder.

Overall, the melt parameters used to produce these parts resulted in a grain size/shape consistent with the literature on PBF-produced 316 stainless steel [3].

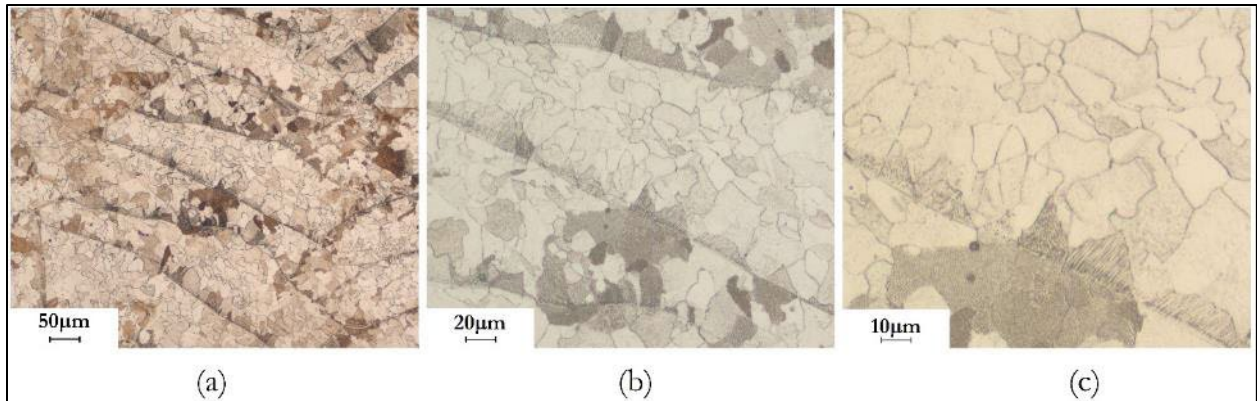


Figure 19.—Microstructures from sample orientation HF (face of the sample parallel to Z print direction).

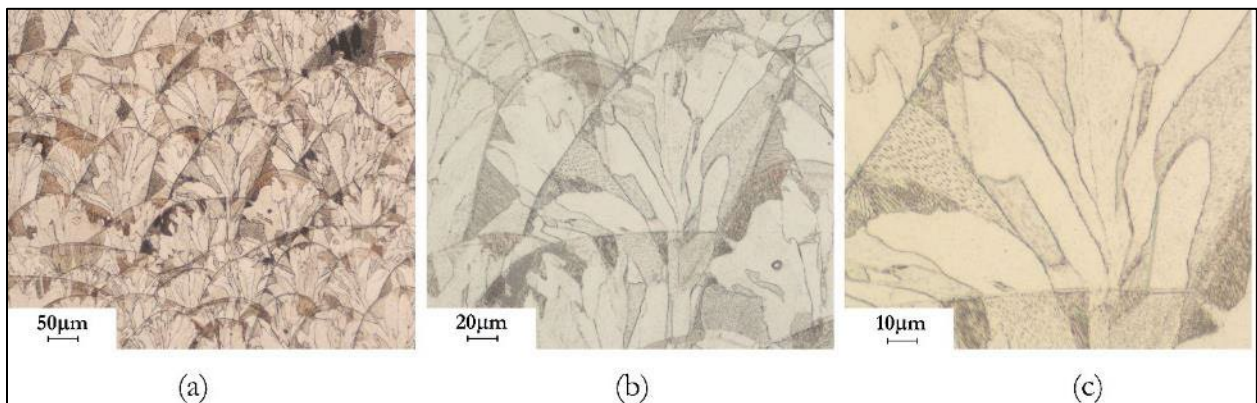


Figure 20.—Microstructures from sample orientation HX (cross section of the sample parallel to Z print direction).

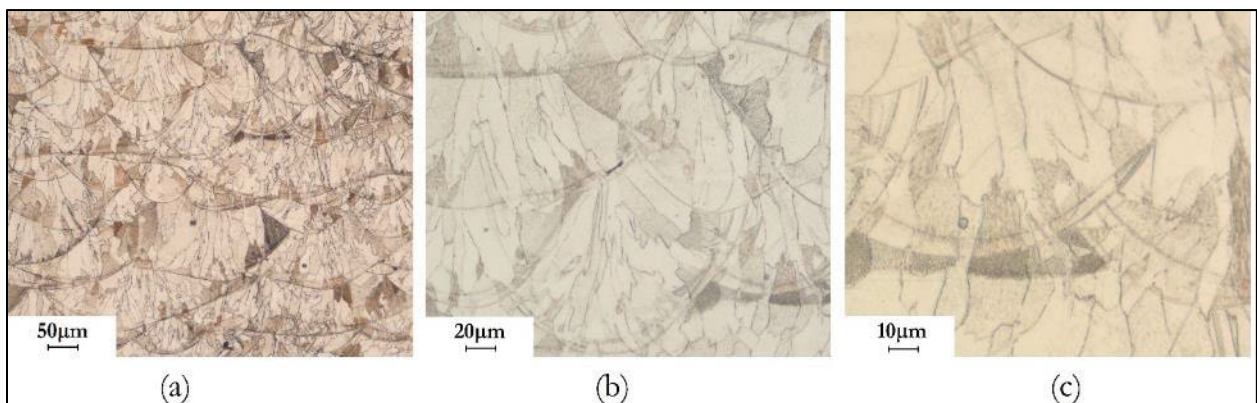


Figure 21.—Microstructures from sample orientation VF (face of the sample perpendicular to the print direction).

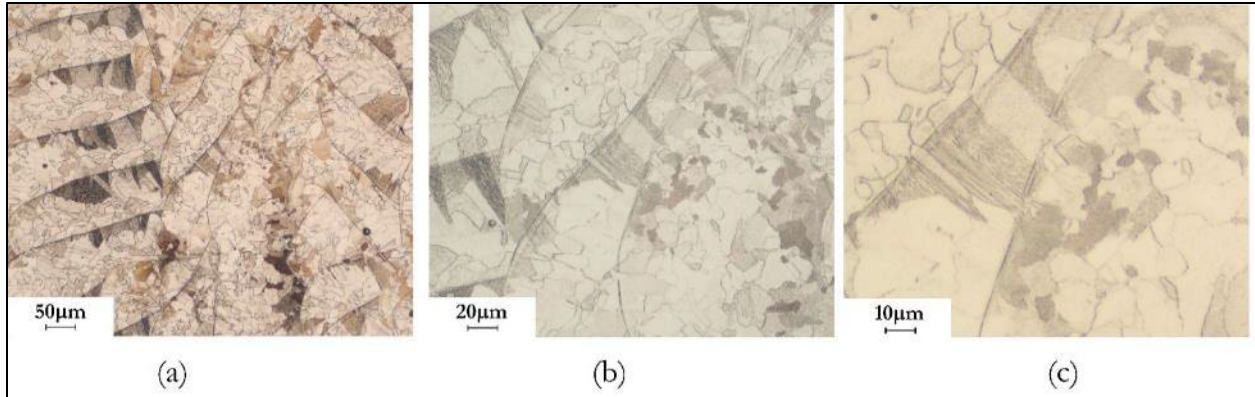


Figure 22.—Microstructures from sample orientation VX (cross section face of the sample perpendicular to the print direction).

2.8 Aluminum Bronze Laboratory Test Sample Results

The aluminum bronze printed components experienced repeated issues with build plate adhesion and warpage. To address these issues, the test samples were printed individually instead of as part of a test wall, as was done with the stainless steel samples. The tensile and fatigue samples were printed as simple cylinders, and then machining was performed prior to testing. Note that these test samples were delivered later as part of a second build in July 2022 whereas the first build produced test samples for the governor parts and slinger ring halves and was delivered in April 2022. The test samples are shown in Figure 23. Table 8 lists all aluminum bronze samples that were printed by Elementum 3D for laboratory testing and analysis.

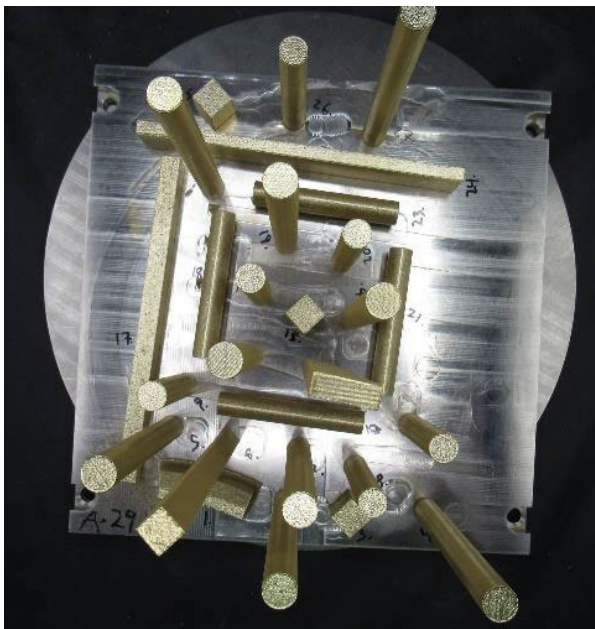


Figure 23.—Photograph from above of as-printed aluminum bronze samples on build plate.

Table 8.—Aluminum Bronze Test Samples Printed by Elementum 3D

Sample Description	Orientation	Qty.	Printed Dimensions (inches [mm])	Notes
Horizontal Tensile	XY	3	0.5 (12.7) diameter, 3 (77) long	ASTM E8/E8M – Round Specimen, “Figure 8, Specimen 3”
Vertical Tensile	Z	3	0.5 (12.7) diameter, 3 (77) long	ASTM E8/E8M – Round Specimen, “Figure 8, Specimen 3”
Horizontal Bend	XZ plane (Bend around Z axis)	1	0.79 x 0.28 x 6.7 (20 x 7 x 170)	ASTM E290. Tested as-printed.
Vertical Bend	ZX plane (Bend around X axis)	1	0.79 x 0.28 x 6.7 (20 x 7 x 170)	ASTM E290. Tested as-printed.
Horizontal Hardness	XY	1	0.39 x 0.39 x 6.7 (10 x 10 x 170)	—
Vertical Hardness	Z	1	0.39 x 0.39 x 6.7 (10 x 10 x 170)	—
Fatigue	Z	9	0.5 (12.7) diameter, 5 (127) long	ASTM E466

Note: Qty. = quantity.

2.8.1 Tensile Testing

Tensile testing was conducted by a third-party laboratory (See Appendix H) in accordance with ASTM E8/E8M. Tensile testing results can be seen in Table 9, along with literature tensile values of similar material for comparison.

Table 9.—Tensile Test Results from Aluminum Bronze Test Bars and Published Literature Data for Annealed Aluminum Bronze and H01 Tempered Naval Brass

Specimen	Yield Load (lb)	Yield Strength (lb/in ²)	Tensile Load (lb)	Tensile Strength (lb/in ²)	Elong. (inches)	Elong. (%)	Diameter Reduction (inches)	Area Reduction (%)
006-H1	1,944	38,800	4,015	80,000	1.29	29	0.2225	22
006-H2	2,059	40,900	4,216	84,000	1.29	29	0.2060	34
006-H3	1,907	38,200	4,055	81,500	1.30	30	0.2240	21
“H” Specimen Average	1,970	39,300	4,095	81,800	1.29	29	0.2175	26
006-V1	1,905	37,600	3,819	75,500	1.36	36	0.2065	34
006-V2	1,868	37,100	3,800	75,500	1.36	36	0.1995	38
006-V3	1,907	37,300	3,850	75,500	1.38	38	0.2005	38
“V” Specimen Average	1,893	37,300	3,823	75,500	1.37	37	0.2022	37
TQ50 Quench Hardened and Temper Annealed UNS C95300 Lit. Value ¹	—	42,000	—	80,000-85,000	—	12-15	—	—
UNS C46400 (Naval Brass H01 Temper) Lit. Value ²	—	46,000	—	69,000	—	27	—	—

Note: Elong. = elongation and lit. = literature.

¹ “Copper Casting Alloys” Copper Development Association (www.copper.org/publications/pub_list/pdf/7014.pdf).

² Copper Development Association (<https://alloys.copper.org/alloy/C46400?referrer=facetedsearch>).

The average yield strength for the test bars was 37,300 lb/in² and 39,300 lb/in² for the Z orientation (“V” samples) and XY orientation (“H” samples), respectively. Those values are lower than comparable materials produced by traditional manufacturing methods. However, the average tensile strength of both orientations was comparable to annealed UNS C95300 (aluminum bronze) material and higher than the H01 tempered UNS C46400 (naval brass) material originally specified for use in the governor parts and slinger rings of this study. The samples in both orientations displayed exceptional ductility, exceeding the literature values for similar materials.

The “H” tensile samples had a lower average elongation of 29%, compared to the 37% elongation of the “V” tensile samples. Similarly, the “H” samples also had a lower average reduction in area of 26% compared to 37% for the “V” samples. While literature on the observed anisotropy in mechanical properties is limited for the additively manufactured aluminum bronze alloy of this study, similar studies of additively manufactured stainless steel have concluded that the anisotropy can arise from crystallographic texture and the size and shape of grain boundary distributions that result from directional solidification ([4] [5] [6]). The lower yield strength of the material was evaluated and determined to still be acceptable for use in the intended applications of this study; the loading on the parts is significantly lower than the yield strength of the material.

2.8.2 Bend Testing

Bend testing was completed by a third-party laboratory. The bend was completed in two steps per the ASTM E290-14 requirements of a bend and flatten test. In the first step (Type-1) of the test, the sample is bent 180 degrees. In the second step (flattening), clamping force is applied until both legs of the sample come into contact at the bend. Bend test results can be found in Table 10 and photographs of post-tested samples seen in Figure 24. The aluminum bronze bend test samples were tested in the as-printed condition, having a thickness of roughly 0.25-inch, as opposed to the stainless steel bend test samples that were machined down to 0.0625-inch.

Unlike the stainless steel samples, both of the aluminum bronze samples exhibited poor ductility. Sample 1 (parallel to Z-axis) failed during the flattening step while sample 2 (perpendicular to Z-axis) failed during the Type 1 bend. Researchers concluded that these results were dominated by the condition of the samples being tested, in the as-printed condition and at full thickness—without machining, the surface roughness of the as-printed parts provides ample crack initiation sites, and the increased thickness of the samples results in much higher tensile forces being generated during the testing. Because of this difference in sample condition, results of the printed aluminum bronze test samples cannot be directly compared with the stainless steel counterparts.

Table 10.—Bend Test Results for Aluminum Bronze Test Samples

Sample ID	Orientation Related to Z-Axis	Bend 1 (Type-1)	Bend 2 (Flattening)
1 (Vertical Bend)	Parallel	No Defects	Large Crack
2 (Horizontal Bend)	Perpendicular	Large Crack	N/A

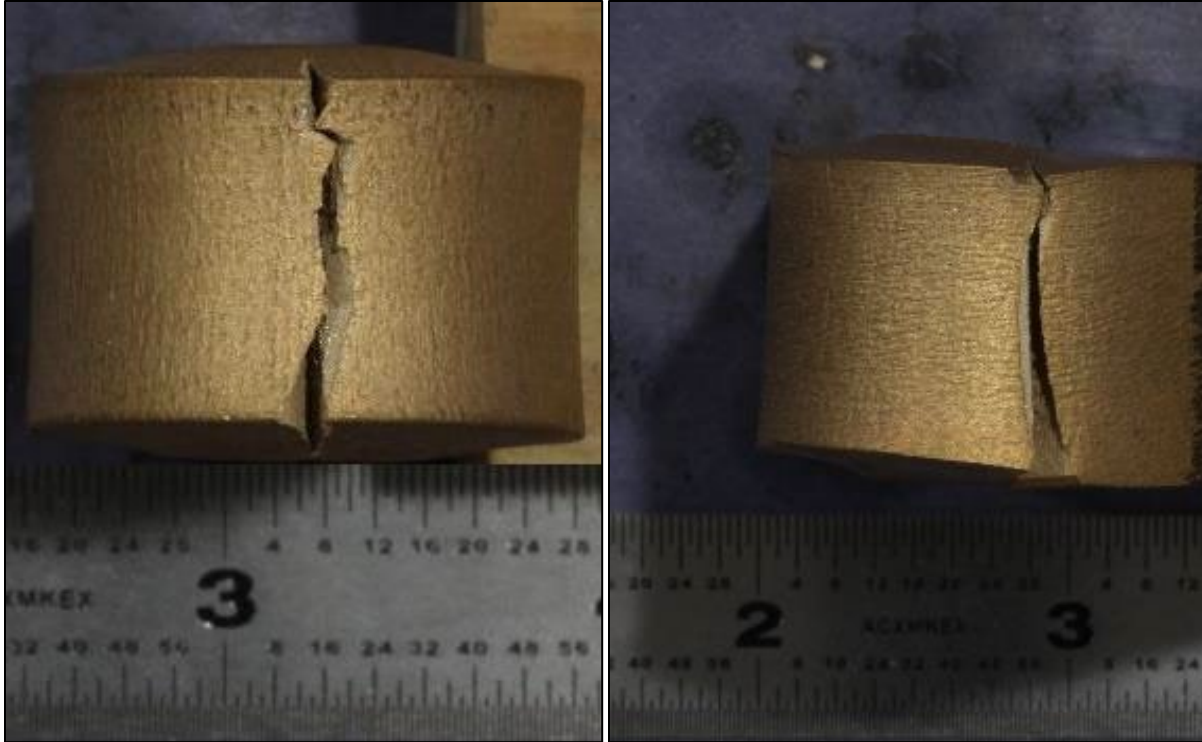


Figure 24.—Photographs of aluminum bronze bend test samples after testing. Left: Sample 1 (parallel to Z-axis). Right: Sample 2 (perpendicular to Z-axis).

2.8.3 Hardness Testing

Hardness traverses on the as-printed aluminum bronze surfaces were completed in-house by Reclamation. The results are shown in Figure 25 and Figure 26. Hardness values were recorded at 0.25-inch increments along specially printed 6.5-inch-long rectangular cuboid test samples. The hardness traverses were located along the X/Y-axis and Z-axis build directions of those test samples, providing an indication of the consistency in performance along those axes. Hardness ranged between 58 and 79 HRB for the X/Y-axis of the horizontally printed sample and between 67 and 78 HRB for the Z-axis of the vertically printed sample. The overall average hardness was 71.8 HRB for both samples; however, the standard deviation in the X-axis build direction was 4.2 HRB, while the standard deviation in the Z-axis build direction was 1.9 HRB. These results represent a decrease in measured hardness from the initial target of 78 HRB and from results achieved by Elementum during development (Appendix D) but still considered acceptable for the intended application.

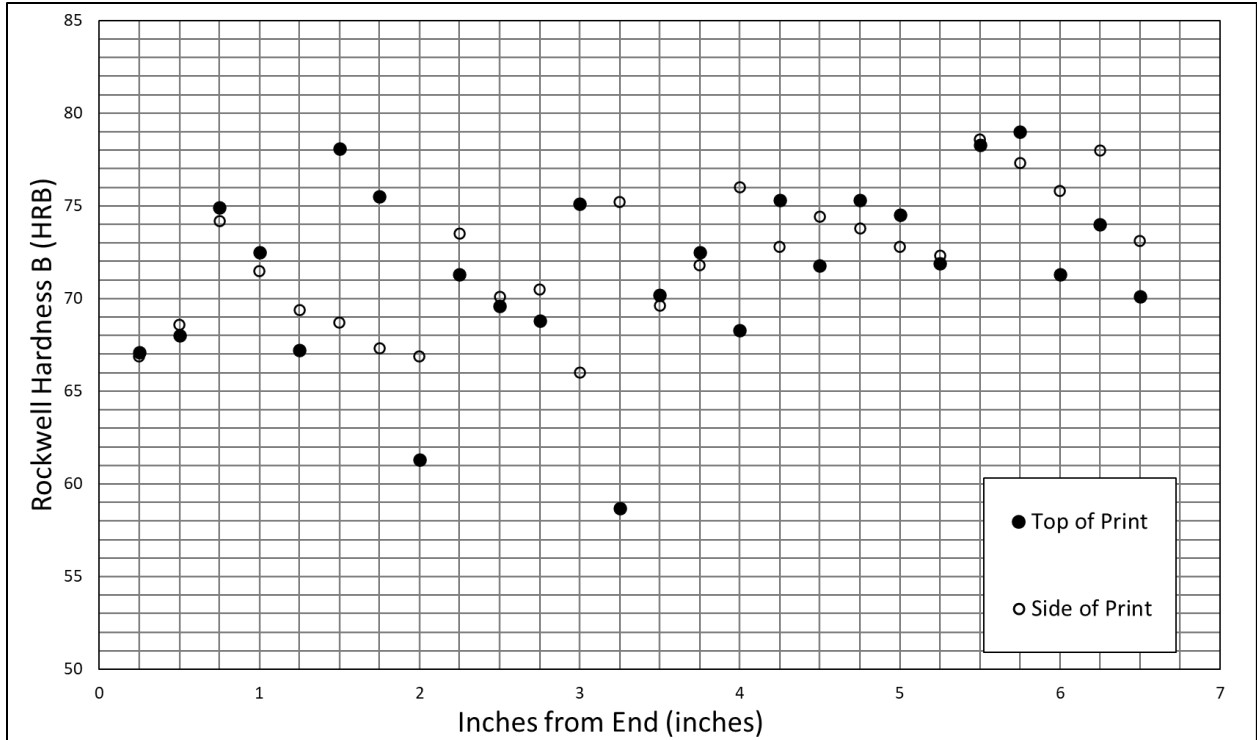


Figure 25.—Hardness traverse results for horizontal aluminum bronze test sample, as-printed (XY orientation).

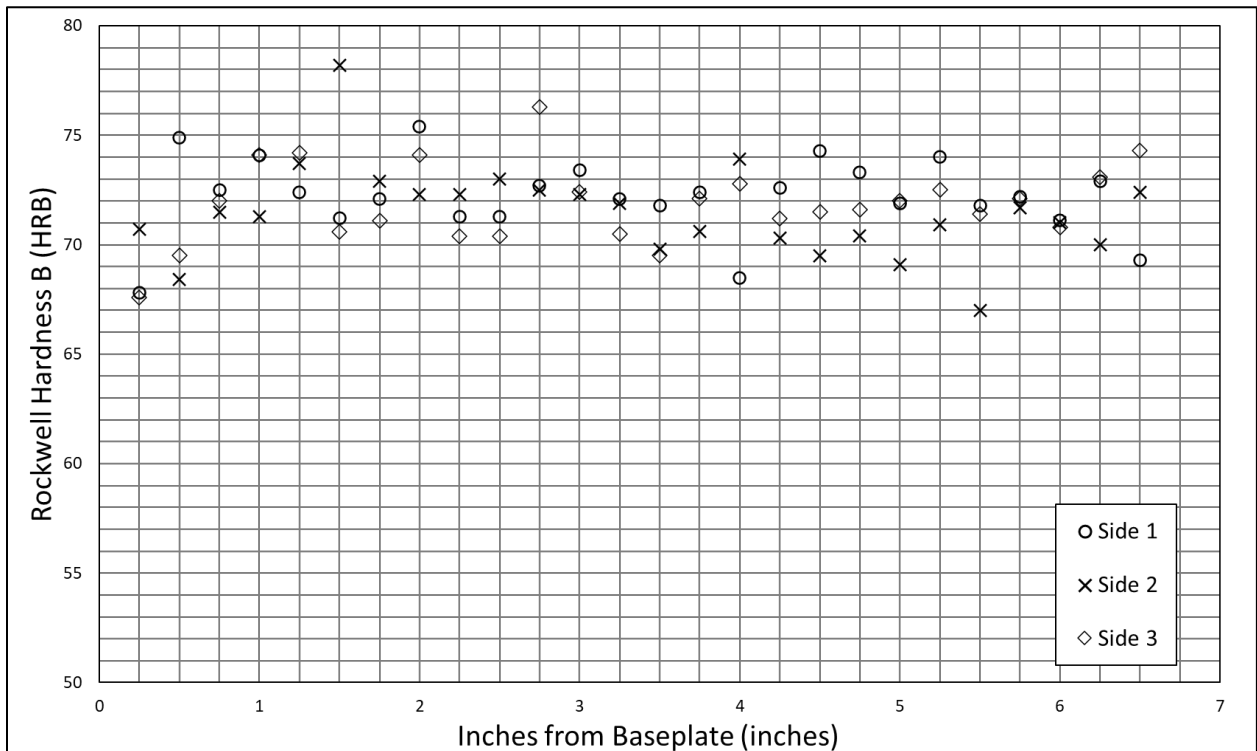


Figure 26.—Hardness traverse results for vertical aluminum bronze test sample, as-printed (Z orientation).

2.8.4 Fatigue Testing

Nine fatigue samples were printed by Elementum 3D. Sample dimensions are listed in section 2.8, Table 8. Pictures of the as-printed samples can be seen in Figure 27. The samples were printed in the vertical orientation using the aluminum bronze printing process and parameters developed by Elementum 3D for this study.



Figure 27.—As-printed aluminum bronze fatigue samples.

The fatigue samples were sent to ORNL for machining and fatigue testing in accordance with ASTM E466-15. The samples were tested in the axial direction with fully reversed ($R=-1.0$) strain cycling at a rate of 20 hertz. The applied cyclical stress levels were chosen based on the average yield stress achieved in the vertical direction, 37,300 lb/in². Three samples were tested at each stress level. Beginning with 75% of the average yield stress, each subsequent stress level was increased by 10%. Fatigue testing results can be seen in Table 11.

Table 11.—Aluminum Bronze Fatigue Testing Results

Test No.	Specimen Bar Designation	Test stress (lb/in ²), R=-1.0	Percent of Yield Stress (%)	Cycles to Failure (#)	Comments
1	02	27,975	75	Runout	—
2	04	27,975	75	Runout	—
3	05	27,975	75	Runout	—
4	07	31,705	85	Runout	—
5	12	31,705	85	2,193,802	Surface crack initiation
6	16	31,705	85	Runout	—
7	19	35,435	95	Runout	—
8	22	35,435	95	7,691,533	Surface and internal crack initiation
9	27	35,435	95	Runout	—

Note: No. = number. Test stresses were selected based on the average yield stress achieved in the vertical direction, 37,300 lb/in². Runout was 10 million cycles.

Most fatigue samples achieved the runout condition of 10 million cycles without failing; at this point, testing was halted and the samples were removed. Two samples failed prior to runout, one at the 85% stress level (specimen 12), and one at the 95% stress level (specimen 22). Fractography results of each failed sample's surfaces can be seen in Figure 28.



Figure 28.—Left: Fracture surfaces of specimen 12, run at 85% stress level. Right: Fracture surfaces of specimen 22, run at 95% stress level.

The fracture surface of specimen 12 exhibited a flat fracture surface, while specimen 22 exhibited a large step in the fracture surface. The difference can be attributed to the number and location of crack initiation sites. Specimen 22 had two crack initiation sites on different planes, one internal and one external. The step observed is at the location where the two cracks approached an overlapping condition as they propagated outward and toward the center of the sample. Fatigue cracks typically initiate on the surface of samples—at locations where cracks, notches, or other discontinuities exist—or internally if voids, second phase particles, or other defects exist [7]. The number of samples that achieved the runout condition is a good indication that after machining, the material was relatively free of any surface and internal imperfections that can accelerate crack initiation and reduce fatigue performance. Overall, the fatigue performance of the aluminum bronze material compared favorably with literature results for similar materials produced by traditional manufacturing methods [8]. The published fatigue strength for UNS95300 is 27,000 lb/in² [9]. For the selected applications, the fatigue performance of this material was considered acceptable for use. It is noted that a more extensive analysis with larger sample counts would be required to obtain the necessary statistics to determine acceptability for a wider range of applications.

2.8.5 Metallography

Metallographic samples were sectioned from the grip section of a horizontally and vertically oriented tensile test specimen and mounted to show the cross section. These are respectively noted as “H” and “V” samples below. After preparation, the samples were etched with Anaconda’s etchant (a mix of sodium chloride, potassium dichromate, and sulfuric acid in deionized water) and imaged with light optical microscopy using magnifications from 250X to 1000X.

Microstructures from the “H” and “V” samples are shown in Figure 29 and Figure 30, respectively. Each sample is primarily composed of consistently sized copper-based primary alpha grains (lightest gray areas), inclined to the build direction. Small, barely visible intragranular iron-aluminum precipitates appear as fine gray dots. At higher magnifications, larger iron-aluminum precipitates can be distinguished as slate-gray shapes dispersed in the intergranular regions. The darkest areas are porosity (round edges) from gas trapped during solidification or voids (rough edges) caused by incomplete melting, both of which were observed in relatively small area fractions within the samples. Areas of laser-induced melt spatter appear as circular gray-blue areas. Microstructural features are noted with arrows in Figure 31 below.

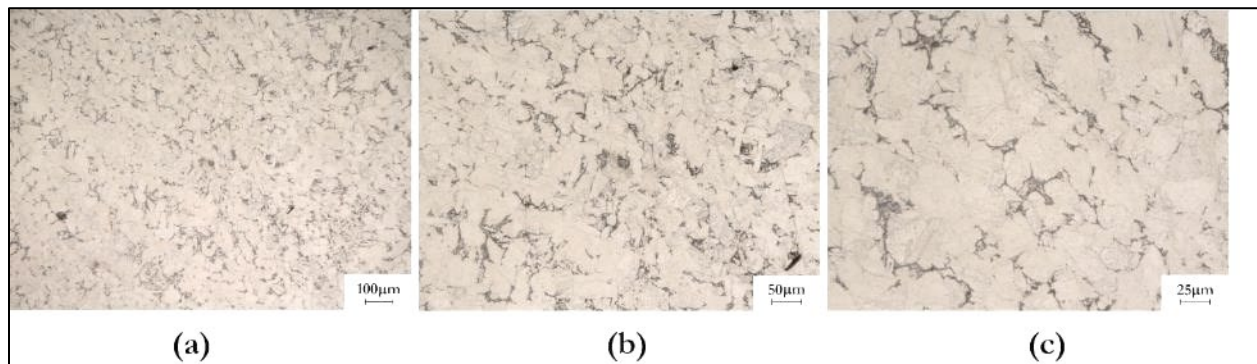


Figure 29.—Sample “H” cross section of sample oriented perpendicular to the Z / print direction. Micrographs taken at: (a) 250X, (b) 500X, and (c) 1000X.

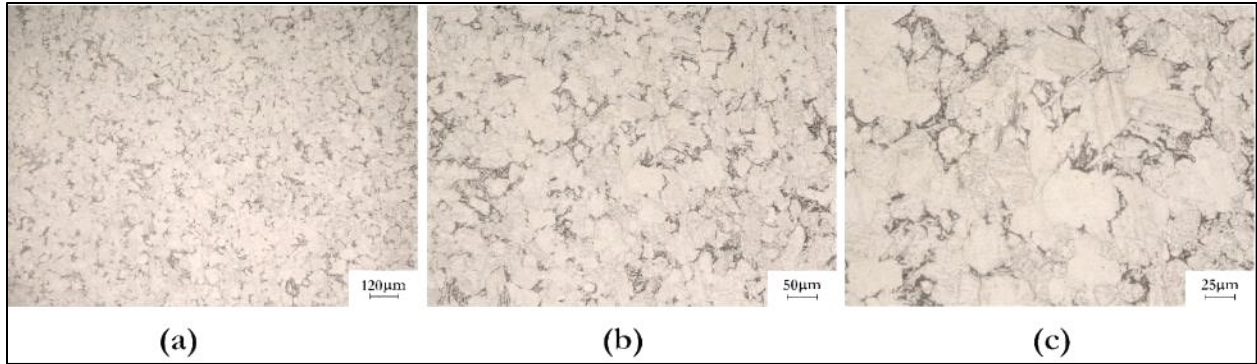


Figure 30.—Sample “V” cross section of sample oriented in the Z / print direction. Micrographs taken at: (a) 250X, (b) 500X, and (c) 1000X.

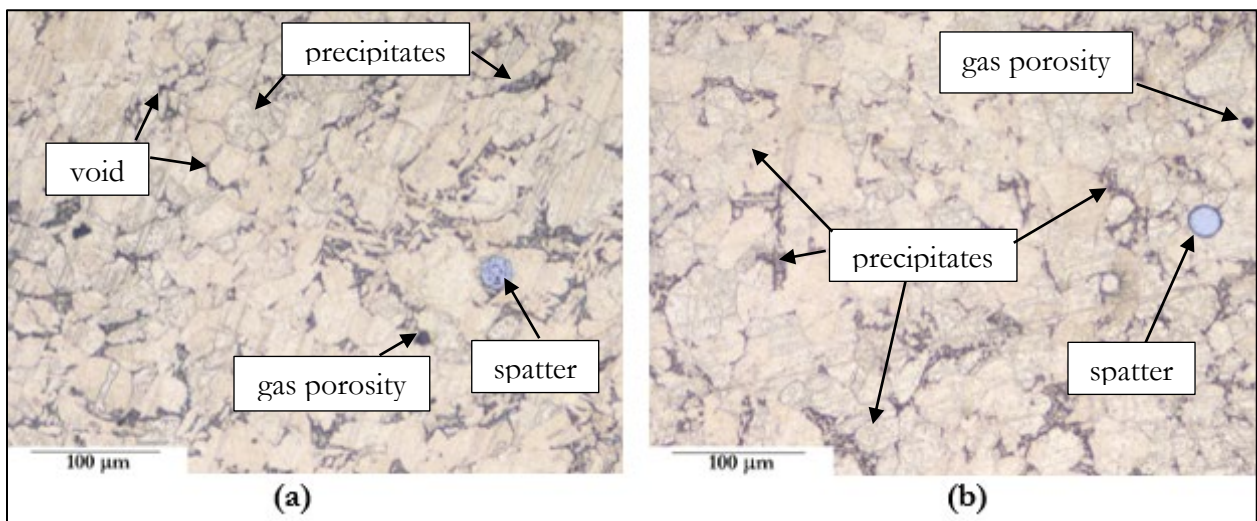


Figure 31.—Microstructural features of aluminum bronze samples. Left: (a) “H” cross section of sample oriented perpendicular to the Z /print direction. Right: (b) “V” cross section of sample oriented parallel to the Z / print direction. Both “H” and “V” samples showed intergranular and intragranular precipitates, spatter, gas porosity, and voids.

2.9 Governor Part Field Results Summary

After discussing with Glen Canyon Dam staff, the research team determined that the parts were unsuitable for field testing due to the dimensional nonconformities identified in the final machining process. The decision factored in the precise tolerance requirements of the governor parts, as well as the consequences of failure if the part did not function as designed and intended. Factoring in both of these perspectives, the nonconformities posed an unacceptable risk to the facility.

2.9.1 Cost-Benefit Analysis of Additive Manufacturing

At this time, additive manufacturing is not a cost-effective alternative for producing intricate parts with tight tolerances since final machining is necessary. The cost of the final machining process for the additively manufactured components likely exceeded the labor cost for traditional machining from stock material.

2.9.2 Manufacturing Challenges and Notes

The governor parts selected for this study were a challenging application for additive manufacturing due to the precise dimensional requirements and surface finish of the parts. There were additional steps required to produce a functional part, each of which proved critical to achieving a satisfactory result. These steps included:

- reverse engineering complex components to determine the correct dimensions and hole placement,
- modifying the design to be suitable for additive manufacturing by adding machine stock to selected surfaces,
- determining (and developing) print parameters and heat treatment protocols,
- printing and quality control,
- final machining of each component and associated quality control, and
- final assembly.

Future part selection for additive manufacturing efforts should consider the additional processes that will be required to produce a functional part.

Another manufacturing complication was the need to print with a material, aluminum bronze, that had little literature available to inform build process settings. This resulted in an enhanced likelihood of warping or fracture in the build, or premature separation of the part from the build plate. For example, the issue of plate separation was encountered when trying to print the aluminum bronze test wall. For future additive manufacturing efforts that will use similarly uncommon print materials, researchers should consider the additional time required to develop and troubleshoot build process settings.

3 Case Study B: Forebay Log Boom Anchor

A log boom/pier anchor at Nimbus Dam was selected as a second case study to demonstrate additive manufacturing. A floating log boom prevents floating debris from entering the Nimbus Powerplant unit intakes. The log boom anchor serves as a termination point for the log boom and is fixed to a vertically oriented rail which allows the boom to move vertically as the reservoir surface elevation fluctuates. Figure 32 (left) shows a picture of Nimbus Dam with the log boom visible as a diagonal line stretching from the right bank (top side) to the dam. Figure 32 (right) shows the log boom anchors; the anchor on the left is old with corrosion and wear after several years in service; on the right is the new anchor which was produced using conventional fabrication methods.

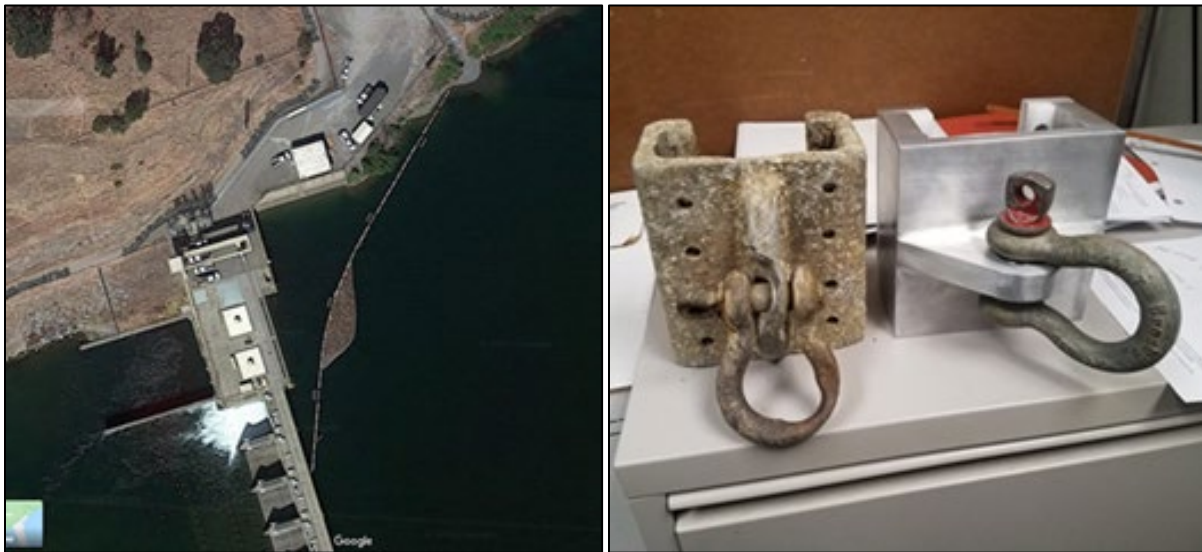


Figure 32.—Left: Photograph showing log boom at Nimbus Dam. Right: Photograph showing old and new conventionally manufactured pier anchors.

3.1 Conventional (Baseline) Component Designs, Fabrication, Costs, and Service

3.1.1 Design and Fabrication

The original log boom anchor is made up of six pieces (shown in Figure 33): one main aluminum body, two aluminum rail bars, two plastic slide bars, and one steel sleeve. The assembled part slides onto a vertical hardened steel “T” rail on the upstream side of the dam pier between spillway gates. The “T” rail is like a vertically oriented train rail. The primary direction of log boom tension is 30 to 45 degrees off the dam face; the anchor eye projects orthogonally from the rail and dam face. Note that the eye was redesigned to be vertically oriented which allows the shackle to rotate laterally to accommodate log boom movement. The maximum expected force applied in that direction is estimated to be 4,500 pounds (lb).

The conventional fabrication of each piece is as described below:

- The main aluminum body is milled and drilled out of one 6061 aluminum billet. The eye is drilled and reamed to a specific dimension. The holes in the rail bars are threaded.
- The aluminum rail bars are milled, drilled, and are bolted to the main body using tapered Allen drive screws. The drill holes for mounting to the body are countersunk. There are also threaded through-holes to accept the plastic slide bars.
- The plastic slide bars are milled, drilled, and counter-sunk to fit tapered Allen drive screws.
- The steel sleeve for the main eye is machined on a lathe for a 0.000 to 0.001-inch interference fit with the aluminum. Its inside dimension should allow for a close tolerance fit with a 0.75-inch steel marine shackle (nut and pin). The hardened steel shackle pin engaged an aluminum bore in the original design. The steel sleeve is a modification of the original design to reduce the wear rate of the shackle's side pull (torque) into the bore.

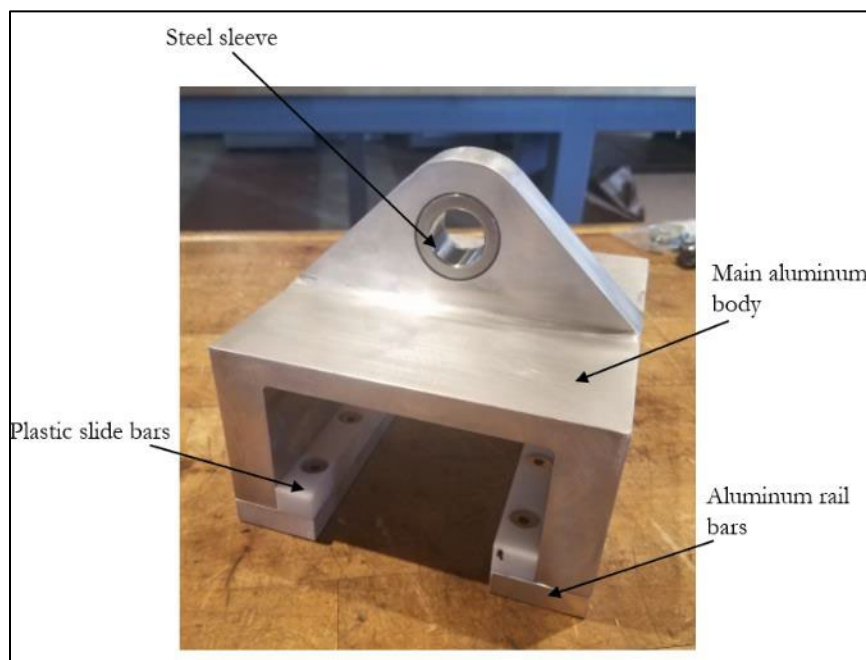


Figure 33.—Components of a conventionally manufactured log boom anchor.

3.2 Additive Manufacturing Alternatives

3.2.1 Redesign for Additive Manufacturing

Since additive manufacturing techniques can be used to manufacture more complex and unique geometries than conventional manufacturing techniques, it is possible to redesign the component geometry to optimize for the available materials, additive manufacturing techniques, reduction in the mass of the part, and reduction in the cost of material.

The geometry of the anchor block was optimized for additive manufacturing by the Reclamation research team using finite element analysis software. The optimized geometry of the anchor part provides a novel design based on stress analysis and reduces the part's mass by approximately 50%. The new design of anchor blocks is shown in Figure 34.

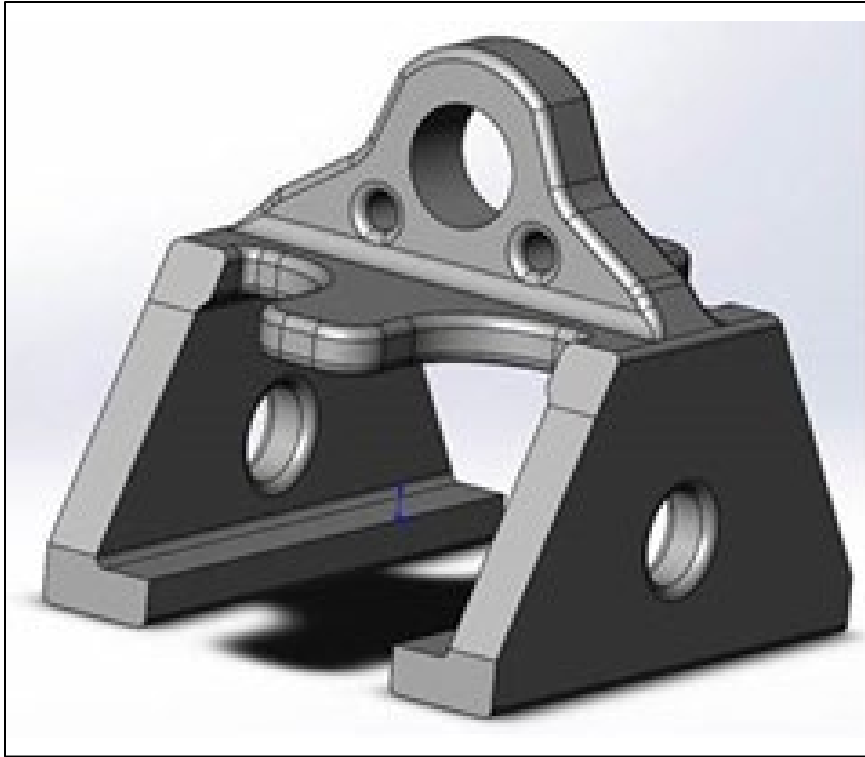


Figure 34.—Redesigned anchor block optimized for additive manufacturing.

3.2.2 Cost and Feasibility Estimates and Selections

SLM was selected for part fabrication after discussion between ORNL's MDF and Reclamation. Some of the aluminum alloys which can be printed on MDF's Concept Laser machine include AlSi10Mg, A205, AlCe Alloys, F357, and 7A77. AlSi10Mg was the alloy selected to additively manufacture the anchor blocks because data for most of the mechanical and thermal material properties of interest was obtainable and matched or exceeded those of the 6061 aluminum alloy that was used in the software during stress analysis. The first order from Reclamation was for six log boom anchors and two wall samples for mechanical testing). ORNL MDF ordered these from Volunteer Aerospace, Inc., because fabrication of these components on the Concept Laser machine at Volunteer Aerospace is cheaper than at ORNL MDF. Table 12 shows the cost and delivery time provided by Volunteer Aerospace, Inc. The cost decreases with quantity ordered.

Table 12.—Cost of Log Boom Anchor Blocks Produced from Additively Manufactured AlSi10Mg After Stress Relief and Without Overhead

Quantity	Price per Block (2020 USD)	Delivery Time
1	3,977.27	3–4 weeks
2	3,727.45	3–4 weeks
4	2,014.14	4–5 weeks
6	1,566.91	4–5 weeks

The estimated cost for six log boom anchors and two test walls was \$1,566.91 multiplied by 6 plus \$234.53 multiplied by 2 (test walls), for a total of \$9870.52 (2020 USD), plus appropriate overhead. The actual material cost for the first six log boom anchors and two test walls was \$13,319 (2021 USD) including overhead.

For testing and demonstrating purposes, Reclamation requested a second order for three additional log boom anchors. The actual material cost for four log boom anchors and two test walls was \$11,461 (2020 USD).

3.2.3 Additive Manufacturing Process

3.2.3.1 Printing and Stress Relief

The redesigned anchor blocks were produced from AlSi10Mg on EOS M290. AlSi10Mg is a spherical aluminum alloy powder. The particle size fraction of this material is 2.5 mils plus or minus (\pm) 0.8 mils ($63 \pm 20 \mu\text{m}$) and the chemical composition is aluminum with 10% silicon (Si) and 0.3% magnesium (Mg) by weight. Figure 35 shows the anchor blocks and walls, as printed. After the anchor blocks were printed, they were stress-relieved in air at $550^{\circ}\text{F} \pm 10^{\circ}\text{F}$ for 80–100 minutes and air cooled to ambient temperature. The ramp time for the parts to reach holding temperature was 47 minutes.



Figure 35.—Redesigned anchor parts and wall produced by additive manufacturing in as-printed state.

3.2.3.2 Finishing and Post Processing

Figure 36 shows the final anchor blocks and test wall after removal from the build plate. The anchor blocks were sent to Reclamation for finishing. Eight holes (four on each side) were drilled in the rail bars and plastic rails, made of Delrin (polyoxymethylene), were attached on top. Figure 37 shows the anchor blocks after finishing and after a stainless steel insert was press-fit into the top shackle.



Figure 36.—Redesigned anchor parts and wall produced by additive manufacturing after post-processing.



Figure 37.—Side and top view of the finished anchor blocks with the Delrin rails attached and the stainless steel insert pressed into the top shackle.

Figure 38 gives the results of a 3D scan taken of the printed log boom anchor overlaid with a color map indicating deviations in dimension between the designed part and the printed part. For the majority of the part, there was minimal deviation—between 0 and 8 mils (0 and 0.20 mm) difference—indicating good agreement between design and printed versions. At other portions, including bottom corners and around holes or other complex geometries, the deviation is up to 40 mils (1 mm) or more. A full set of views and 3D scan results can be found in Appendix I.

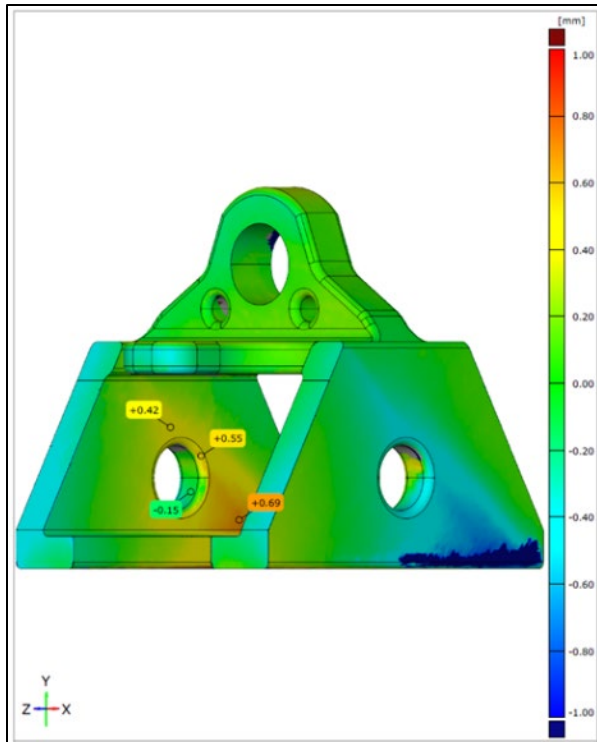


Figure 38.—Deviation between design and actual dimensions obtained through a 3D scan of the log boom anchor.

3.3 Laboratory Test Results

3.3.1 Mechanical Testing

Specimens for mechanical testing were machined from the printed walls. Figure 39 and Figure 40 show the orientation of the tensile bars and Charpy v-notch specimens which were cut from each wall piece in accordance with ASTM E23-18. Round tensile samples with a gauge length 4 times the diameter were machined in accordance with ASTM E8-16a, “FIG. 8, specimen 3.” Note that the test was printed vertically as shown in Figure 35. Table 13 and Table 14 give the resulting tensile and Charpy impact test results. See Appendix J for tensile test report.

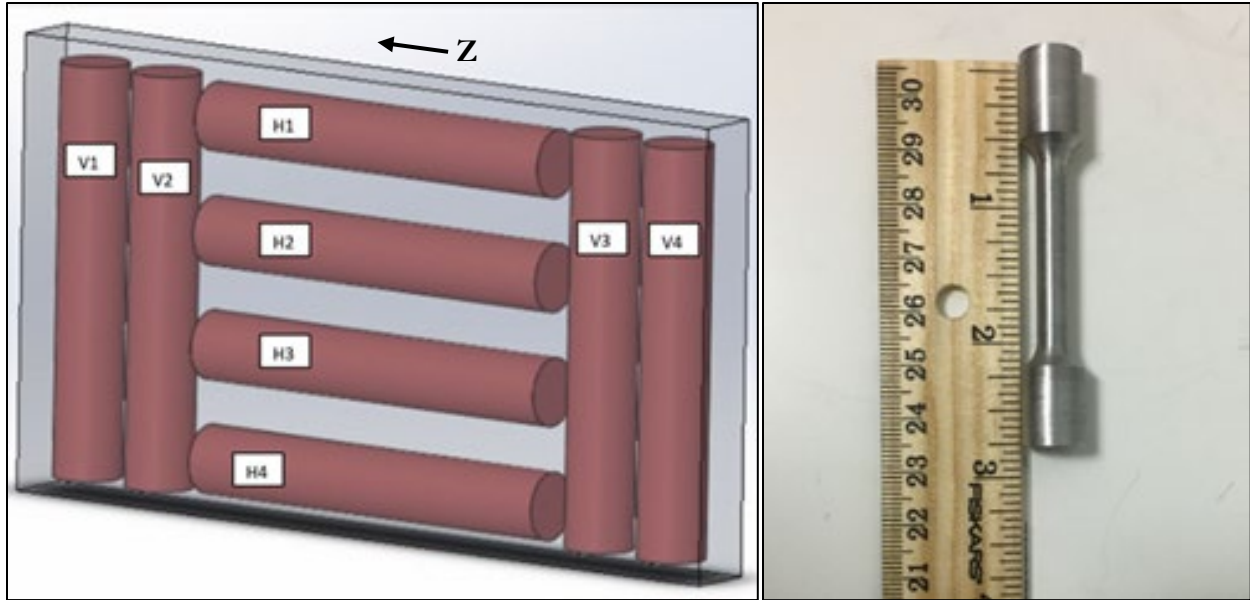


Figure 39.—Left: Schematic of tensile bar orientation machined from one wall piece. Right: Photograph of a representative machined tensile test bar.

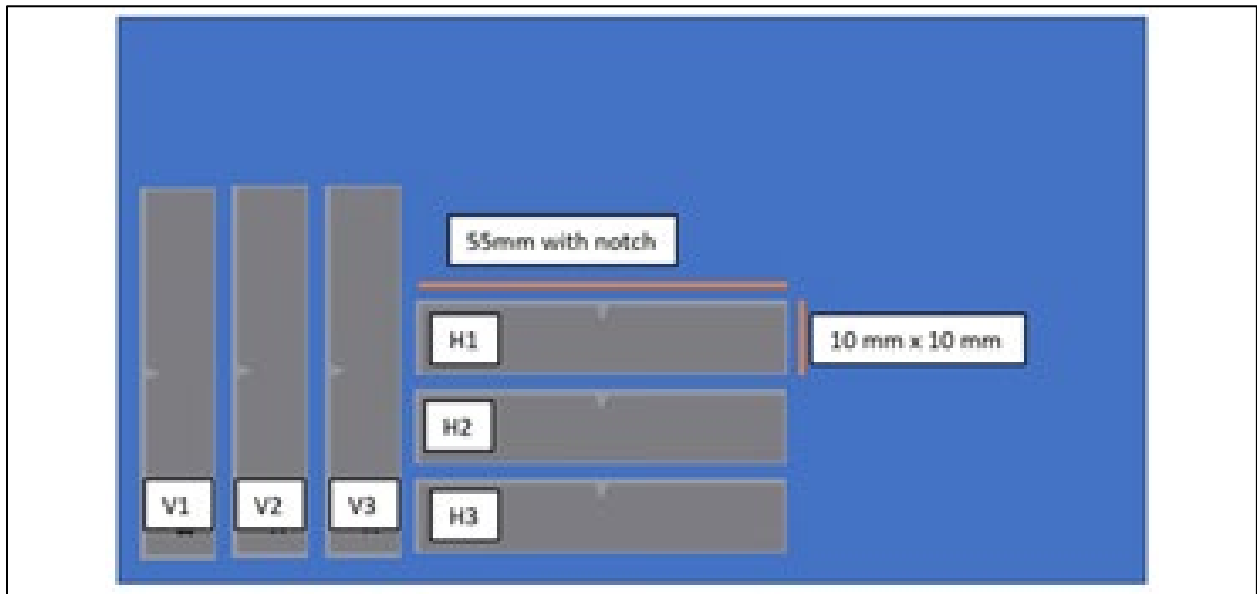


Figure 40.—Orientation of Charpy v-notch specimens machined from one wall piece.

Table 13.—Tensile Test Results from Test Bars and Published Literature Data for 3D Printed Material (As-Printed) and Cast Aluminum Alloy AlSi10Mg

Specimen	Yield Load (lb)	Yield Strength (lb/in ²)	Tensile Load (lb)	Tensile Strength (lb/in ²)	Elong. (in)	Elong. (%)	Diameter Reduction (in)	Area Reduction (%)
H1	1,358	31,900	1,968	46,200	1.08	8.5	0.2010	26
H2	1,516	35,300	1,993	46,300	1.10	9.5	0.1960	30
H3	1,357	32,700	1,930	46,500	1.11	11	0.1970	27
H4	1,374	32,500	1,966	46,500	1.13	13	0.1980	27
"H" Specimen Average	1,401	33,100	1,964	46,375	1.11	11	0.198	28
V1	1,349	31,900	1,900	44,900	1.14	14	0.1790	40
V2	1,378	31,900	1,945	45,000	1.16	16	0.1800	41
V3	1,370	32,200	1,920	45,100	1.13	13	0.1750	43
V4	1,386	31,600	1,990	45,300	1.16	16	0.1845	39
"V" Specimen Average	1,371	31,900	1,939	45,075	1.15	15	0.180	41
AlSi10Mg Literature Value (XY direction) [10]	-	39,160	-	66,717	-	9 ± 2	-	-
AlSi10Mg Literature Value (Z direction) [10]	-	34,809	-	66,717	-	6 ± 2	-	-
Cast AlSi10Mg Literature Value [11]	-	14,359	-	27,992	-	6.5	-	-

Note: Elong. = elongation and in² = square inches. "H" specimens are oriented in the Z direction whereas "V" specimens are oriented in the XY direction.

The average yield strength for the test bars was 31,900 lb/in² (220 MPa) and 33,100 lb/in² (228 MPa) for the XY orientation and Z orientation, respectively. Those values are slightly lower than the reported yield strengths for AlSi10Mg of 39,160 lb/in² (270 MPa) and 34,809 lb/in² (240 MPa) for XY and X directions, respectively. Both test bar orientations had similar average tensile strengths of 45,075 lb/in² (311 MPa) for the XY oriented bars and 46,375 lb/in² (320 MPa) for the Z oriented bars. The reported average tensile strength is 66,717 lb/in² (460 MPa) for both orientations. The XY test bars had an average elongation of 15%, compared to the 11% elongation of the Z bars. These measured elongation values were higher than reported values for XY and Z orientations of 9% and 6%, respectively. Elongation results coincide with reduction of area. Notably, there was an average of a 41% reduction of area for the XY bars, while the Z bars had an average 28% reduction.

Table 14.—Charpy Impact Testing Results

Specimen	Impact (ft-lb)
H1	12
H2	13
H3	12
V1	17
V2	18
V3	16

Note: ft-lb = foot-pound(s).

On average, the vertical bars had a higher impact strength, indicating more ductile behavior, than the horizontal bars. This is expected since the crack tip of the v-notch must propagate across layers as opposed to between layers. However, since aluminum and some of its alloys do not have a ductile-brittle transition temperature—meaning they stay ductile at all temperatures—Charpy testing on aluminum is not typically performed, and results cannot be compared to those of other materials.

Figure 41 shows the hardness testing results from the horizontal and vertical orientations of the anchor wall.

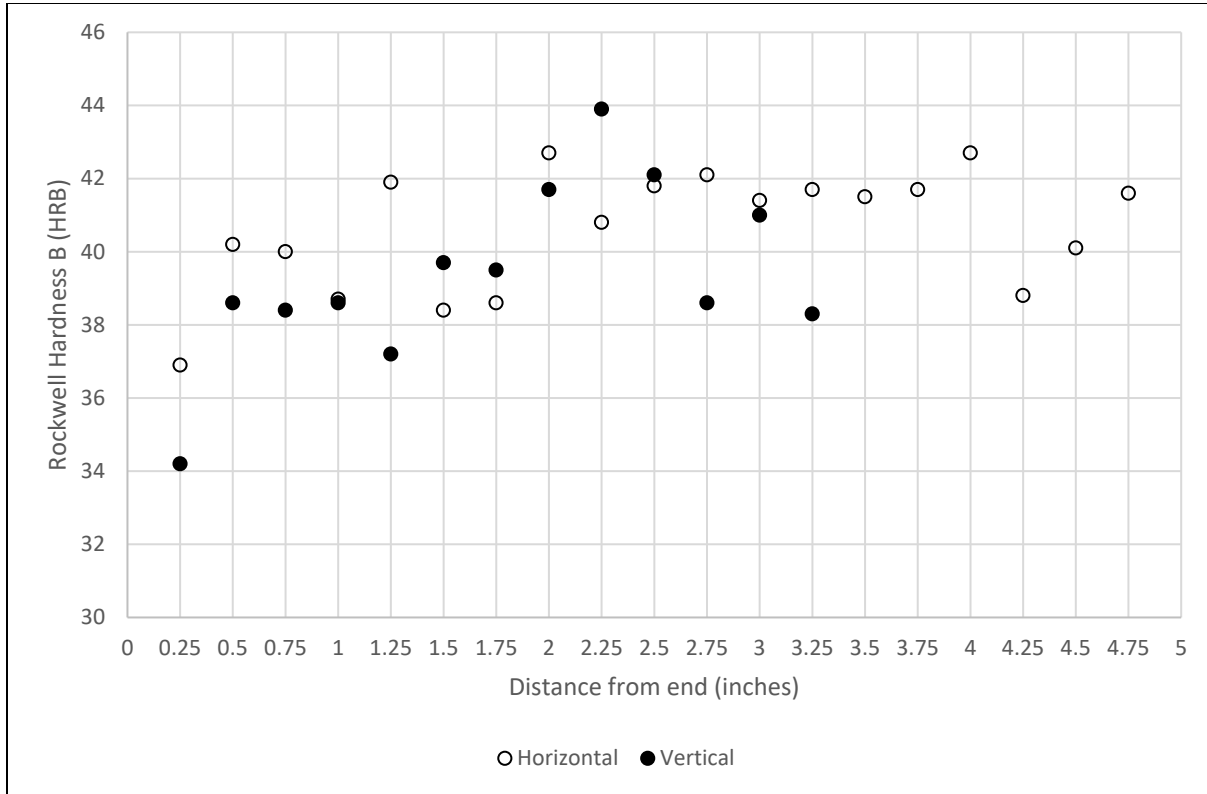


Figure 41.—Hardness test results for Horizontal and Vertical specimens showing that for both orientations, hardness increases from bar ends to the centers. Both orientations had similar average hardness values.

AlSi10Mg fabricated through SLM in both heat-treated (T6) and non-heat treated conditions is reported to have a hardness value of approximately 58–60 HRB [12], [10]. Cast and T6 heat-treated AlSi10Mg has a similar hardness of 60 HRB. Cast AlSi10Mg that has not been heat treated, however, has a significantly reduced hardness of 22 HRB. The average measured hardness for the anchor wall’s horizontal (XY) direction was 40.6 HRB, while the average for the vertical (Z) orientation was very similar at 39.4 HRB. The reason for the discrepancy between reported and measured hardness values is unknown but is likely due to differences in processing parameters between the anchor specimens and specimens used in the literature. For example, the anchor parts evaluated only underwent a stress relief heat treatment, not a full T6. For both orientations, the

hardness appears to increase slightly from the initial measurements at one end to the centers. For the vertical orientation, the hardness decreased as measurements reached the opposite end of the bar.

The printed log boom anchors themselves were tested in uniaxial tension using a custom designed test fixture, as shown in Figure 42. Free crosshead speed was set to 0.05 in per minute. A grid pattern was drawn on each piece and the tests were video recorded with a scale and load information in the frame for documentation.



Figure 42.—Test configuration for log boom anchors.

Anchor piece 1 was loaded to 6,500 lb (the estimated strength of the test fixture), at which point the test was terminated with no obvious deformation of the part. Anchor piece 2 was loaded to approximately 16,900 lb, at which point the test fixture failed. There was no noticeable deformation on anchor piece 2, as shown in Figure 43.

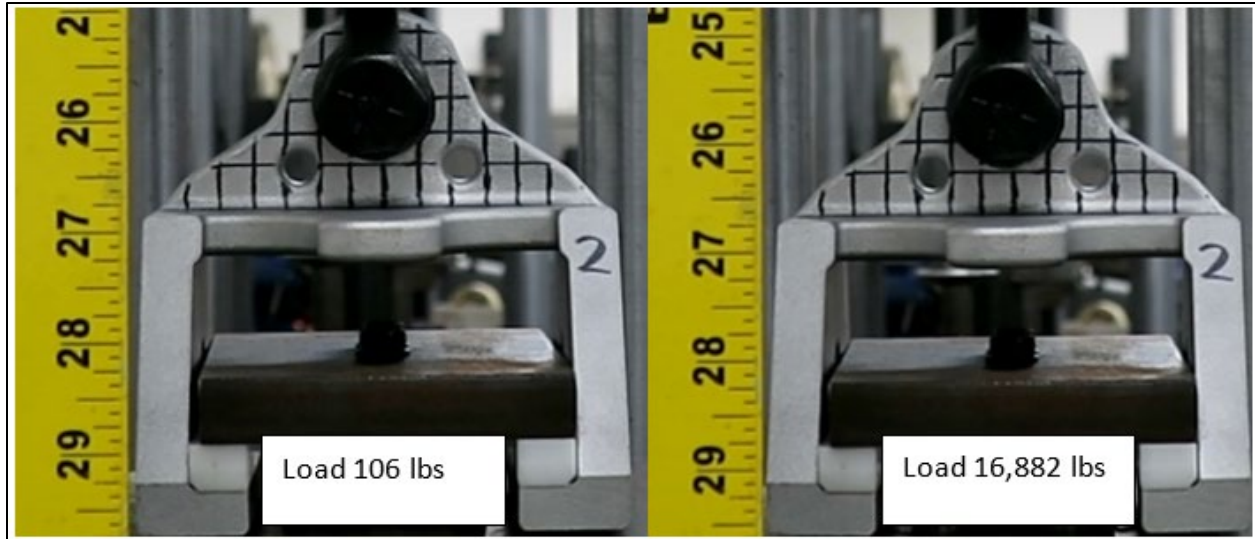


Figure 43.—Frame capture of anchor piece 2 during testing at 106 lb and 16,882 lb load with no visible deformation.

3.3.2 Metallography

Metallography was performed to analyze the microstructure of both the face and cross section of a horizontal and vertical tensile specimen. Metallography consists of sectioning, grinding, polishing, etching, and imaging. This process gives a representative image of the metal without any influence from cold working or other processing damage. The following procedure was used for each metallographic specimen:

1. Section metallographic specimens from the tested tensile specimens using an abrasive metallography saw. Specimens were taken from a horizontal (H) specimen and a vertical (V) specimen. The face (F) and cross section (X) of each specimen were analyzed for a total of four specimens—HF, HX, VF, and VX—as shown in Figure 18.
2. Cold mount specimens in epoxy and cure for a minimum of 24 hours.
3. Grind from coarser to finer grits:
 - a. 180 grit for 2 minutes
 - b. 400 for 2 minutes
 - c. 600 for 2 minutes
4. Polish to a mirror finish:
 - a. 9-micron diamond for 4 minutes
 - b. 6-micron diamond for 2 minutes
 - c. 3-micron diamond for 2 minutes
 - d. 1-micron diamond for 1 minute
5. Etch with sodium hydroxide (NaOH).

6. Image at the following magnifications using an optical microscope:
 - a. 20X, 50X, and 100X

Figure 44. shows representative 20X cross-section micrographs from the specimens evaluated. Since the face micrograph samples came from a cylinder, the orientation is undefined in the Z-direction and only the cross-section micrographs are shown.

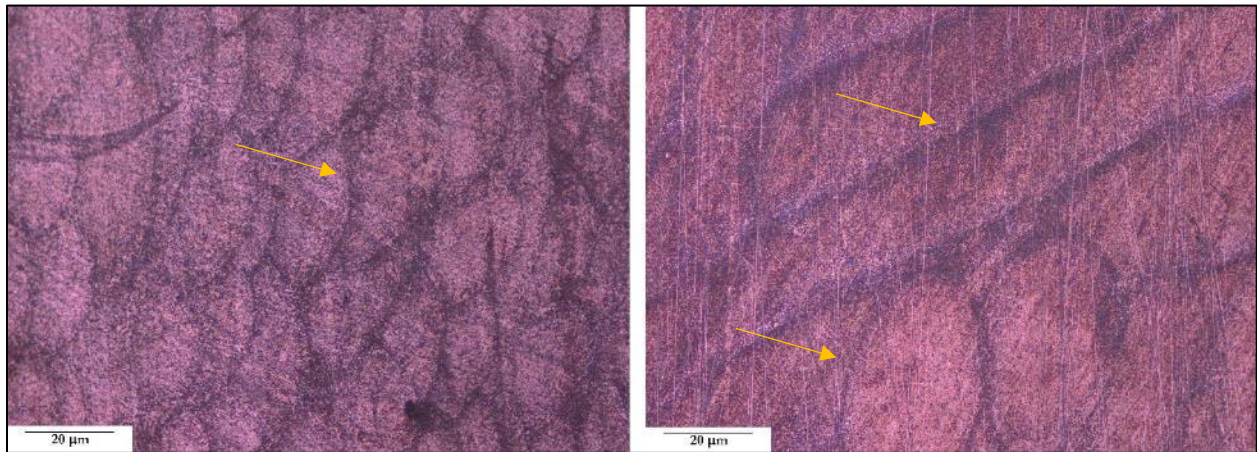


Figure 44.—250X micrographs of the HX (left) and VX (right) specimens. Melt pool boundaries are indicated with arrows. Specimens were stain etched with NaOH for 10 minutes (VX) and 5 minutes (HX).

The main microstructural feature visible are melt pool boundaries (indicated with arrows) which represent the print beads/laser path. The melt pool boundaries for VX are long and narrow, whereas the HX boundaries appear to show cross sections of multiple layers. The melt pool boundaries are not congruent to the grain boundaries which would only be visible through advanced imaging techniques (i.e., electron backscatter diffraction). Figure 45 shows a 100X micrograph of the HX specimen. Darker and lighter areas represent different elements within the microstructure. From literature for cast AlSi10Mg, the light portions are the aluminum matrix and the darker portions are the Si eutectic [13]. Similar features are seen in the printed AlSi10Mg and are assumed to be the same phases as the cast version, although the distribution of Si is more uniform and finer than in cast versions. This refined microstructure, due to the high solidification rate, results in a material with improved mechanical properties (higher yield and tensile strengths) from the cast version [11].

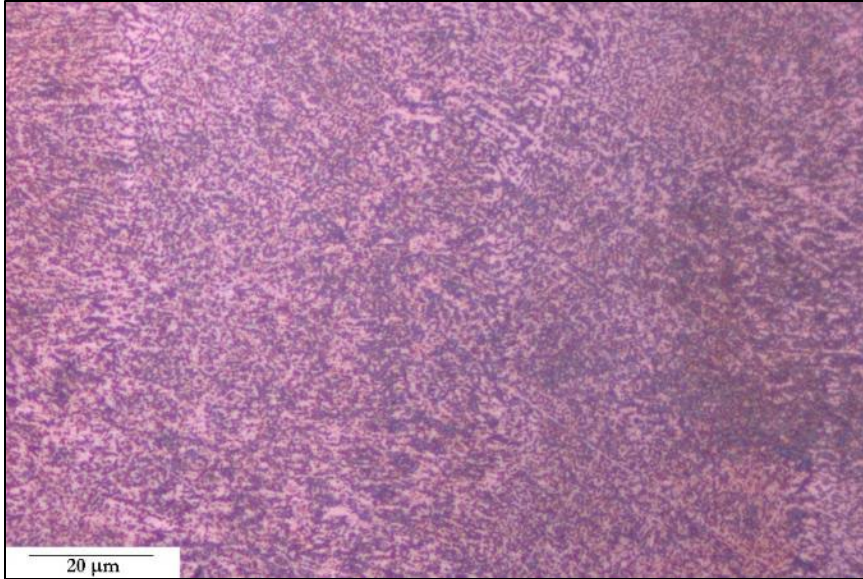


Figure 45.—100X micrograph of HX showing an aluminum matrix (light) with regions of Si eutectic (dark).

3.3.3 Fractography

Both specimen types exhibited very typical cup-and-cone fracture surfaces, as shown in Figure 46. As a moderately ductile fracture mode, this type of fracture typically occurs where there is a void or cavity in the material which expands to form a crack as more tension is applied [14]. The “H” specimens thus exhibited more complete cup-and-cone failure due to the test bar being pulled perpendicular to the print layers. The “V” specimens were pulled parallel to the print layers and the voids did not form cracks and separate as readily. Therefore, a partial cup-and-cone fracture mode is noted for the “V” specimens, with areas of brittle fracture (flat surfaces) in the very center of the fracture surface.

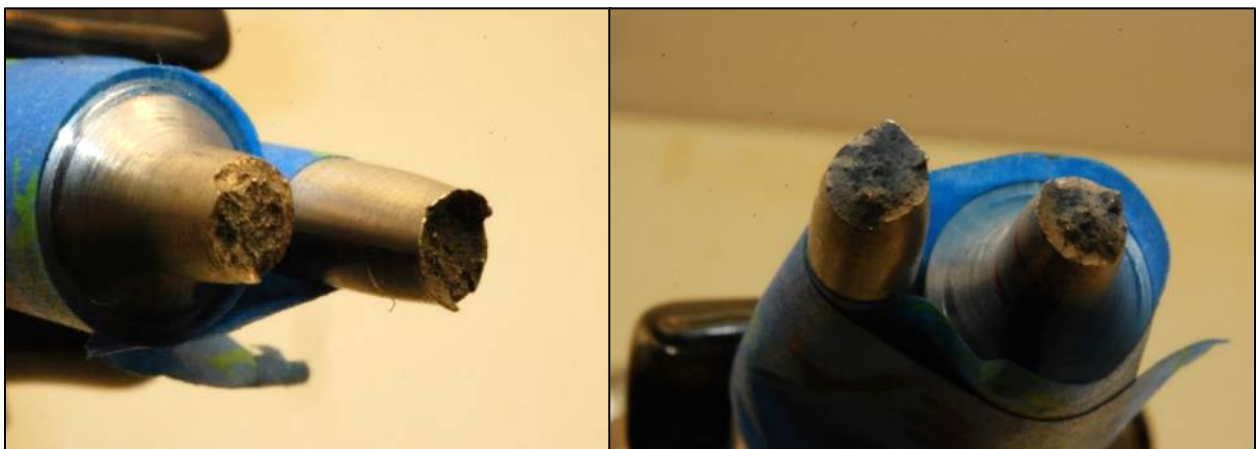


Figure 46.—The “H” specimens (left) and “V” specimens (right) both exhibited cup-and-cone fracture modes, with the H specimens showing more complete cup-and-cone fracture and the less ductile “V” specimens showing partial cup-and-cone with brittle fracture in the center of the fracture surface.

3.3.4 Density

Density testing was performed on one half of the broken test bars according to the procedure in Appendix K. Table 15 gives the density results of the evaluated parts. On average, the horizontally printed parts were slightly denser than the vertically printed parts, with average densities of 93.5% and 92.8%, respectively. The differences in standard deviation were also negligible, suggesting that print orientation did not greatly impact density. These results are congruent to the metallography findings which showed a similar amount and distribution of porosity among the two specimen types. The measured density was approximately 6–7% lower than the density reported in literature for PBF AlSi10Mg. As a conventional application, this alloy is also used in casting, but reported density values for cast AlSi10Mg were not found.

Table 15.—PBF AlSi10Mg Vertical and Horizontal Specimen Density Results

Specimen	Density (g/cm ³)	Percent Dense (%)
V1	2.52	93.2
V2	2.53	93.5
V3	2.49	92.3
V4	2.49	92.2
"V" Specimens Average	2.51	92.8
"V" Specimens Standard Deviation	0.016	0.006
H1	2.53	93.8
H2	2.54	94.0
H3	2.51	93.0
H4	2.51	93.1
"H" Specimens Average	2.52	93.5
"H" Specimens Standard Deviation	0.011	0.004
Literature Value (SLM) [15]	2.67	99.85

3.3.5 Field Results

While the intent is to install the new parts in the field at Nimbus Dam, as of this writing, limited staff availability has delayed installation plans and field trials are currently pending.

3.3.6 Cost-Benefit Analysis of Additive Manufacturing

As depicted in section 3.1.1 by Figure 33, traditional fabrication costs include machining multiple pieces of aluminum which are then attached together. The estimated cost of approximately \$1,800 (2020 USD) per anchor significantly increases if subtractive manufacturing is employed, which would involve directly machining the anchor from a single large block of aluminum. Alternatively, producing parts via additive manufacturing reduces the cost depending on quantity printed. For example, the cost for ORNL to print a single pier anchor was \$3,977 (2020 USD). However, that cost was reduced to \$1,566 (2020 USD) per anchor when six were printed at a time.

The decrease in cost is at the expense of approximately one-week additional delivery time. It is important to note that those costs include a stress relief heat treatment but do not include overhead. Table 12 in section 3.2.2 depicts how the price per pier anchor decreases with quantity.

Another consideration not captured in the cost analysis is the material wasted when fabricating these parts through traditional machining. While additive manufacturing methods utilize the exact amount of material needed, machining generates scrap pieces that would likely need to be disposed of. These and other similar costs are difficult to estimate, and for the purpose of this analysis, are not considered further.

4 Case Study C: Slinger Rings

4.1 Component Selection

For the third case study, researchers chose a pair of naval brass wear rings from a generator exciter bearing at Grand Coulee Dam, otherwise referred to as slinger rings. As with the previous parts, the slinger rings were identified during the team's initial consultations with research partners in area and project offices.

Grand Coulee operates several generator exciter units, each with varying quantities and sizes of bearing slinger rings. The unit selected for this project contains four rings of roughly 8.5-inch inner diameter (ID) (part no. G5365000530013RC) and two rings of roughly 10-inch ID (part no. G5365000530014RC). Each bearing has a pair of rings, as shown in Figure 47. For Case Study C, researchers chose the two larger ID slinger rings for reproduction by additive manufacturing.



Figure 47.—Pair of slinger rings on a bearing.

Conventionally, these slinger rings are manufactured in-house at the Grand Coulee machine shop from naval brass plate (CDA 464 or C46400, ASTM B171, O25 temper-hot rolled). The manufacturing process is time consuming and generates a significant amount of material waste.

While 3D printing would require final machining to ensure proper fit of the two slinger ring halves and appropriate surface finish, using additive manufacturing to produce a near net shape has the potential to greatly reduce machining time and the amount of material waste generated.

4.2 Component Functionality

The slinger ring acts as an oiler device to bring fresh lubricating and cooling oil to the center top of a horizontal bushing. The ring rests on the shaft by gravity and turns by friction contact with the shaft. The ring supplies oil to the shaft through oil shear; oil is pulled to areas between the babbitt and shaft journal. As oil is brought onto the shaft, the ring begins to ride on an oil film and the friction decreases.

The slinger ring must have the following characteristics:

- predictable, slow wear over time,
- a uniform cross section and circular ID to remain balanced on the shaft while rotating, and
- it must meet the critical dimensions and surface finish requirements to provide an appropriate and consistent oil delivery volume across the shaft.

As the ring wears, it must not contaminate the oil bath with suspended particulates that could foul the bearing. Metal particles will sink in the oil bath, whereas plastic particles may remain suspended longer and could possibly melt in a tight clearance choking oil flow.

Due to these requirements, it is best to use a metal that has a history of long performance, such as the naval brass material that is already installed. A typical slinger ring will be in service for up to 12–14 years, and they are inspected every six years during outages.

4.3 Conventional (Baseline) Components

4.3.1 Conventional Design and Fabrication

Historically, the slinger rings are subtractively manufactured from temper-hot rolled naval brass (C46400) plates. The rings are machined from the naval brass plates in halves. This process wastes most of the billet and requires large amounts of machine time. The high material waste and the desire to find a new manufacturing method made the slinger rings a good candidate for the additive manufacturing research study.

From a visual inspection of a spare ring provided by Grand Coulee, the conventional naval brass rings have a 62 micro-inch surface finish. The spare ring is pictured in Figure 48.



Figure 48.—Spare slinger ring received from Grand Coulee.

4.3.2 Conventional Costs

Traditional fabrication involves CNC machining to create two mating semi-circular parts from a solid plate of naval brass. ORNL obtained cost estimates for CNC machining the slinger rings from C360 Brass, the closest material to naval brass that was available in the Xometry estimating tool. The costs (listed in 2021 USD) were: \$667 for 16-day delivery, \$1,420 for 13-day delivery, and \$2,290 for 7-day delivery.

4.4 Additive Manufacturing Results

There is currently no developed procedure for printing naval brass. The process could be developed at ORNL but would be expensive, time-consuming, and outside of this project's scope, so printing the part from the original material is not feasible. This means that an alternate material is required for fabrication by additive manufacturing. The important properties in the alternate material are wear and hardness. In case of wear or corrosion, it is easier to replace the slinger rings rather than the generator shafts, so the rings should be made from a material that will wear or degrade more readily than the shaft.

For slinger ring additive manufacturing production, the team pursued two paths: 1) direct printing by a PBF process and 2) printing polymer patterns for use in an investment casting process.

4.4.1 Printed Aluminum Bronze Slinger Ring Parts

The first additive manufacturing process investigated for the slinger rings was direct printing through a PBF process. The material selected was the same aluminum bronze alloy (UNS C95300) used for the governor parts in Case Study A. This material fulfills the necessary material property requirements, i.e., has a hardness value close to naval brass. This is discussed in section 2.4.1.

ONRL does not have capacity to print this material, so printing was outsourced to a 3D printing materials research and development company, Elementum 3D.

To prepare for printing, the original slinger ring part model (Figure 49, top) was altered (Figure 49, bottom). The bottom chamfer was squared off so the full surface would contact the build plate with no supports required. Holes were filled so they could be accurately located and tapped at the machining stage. Material was added to the joint. Lastly, 0.125 inches of material was added to the ID and 0.040 inches added on all remaining surfaces as machining stock.

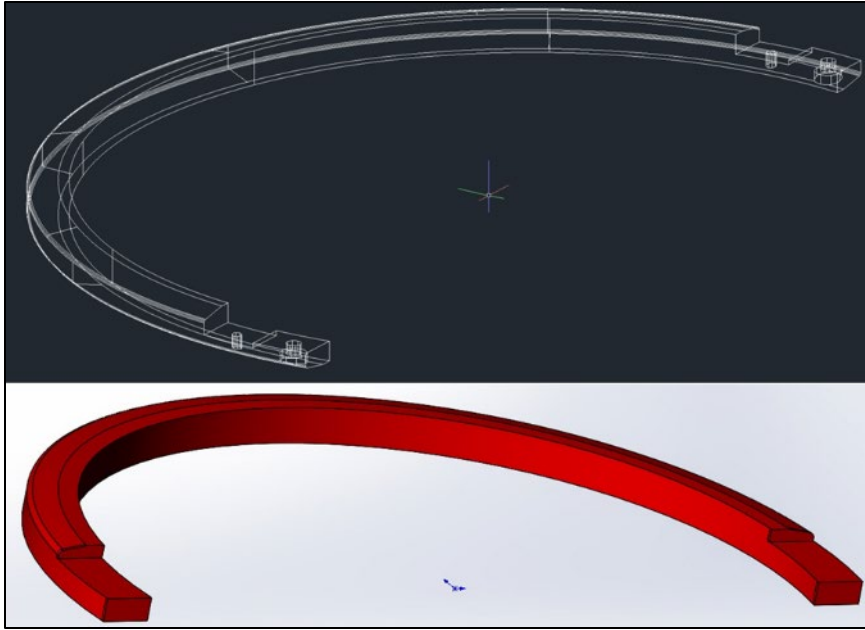


Figure 49.—Slinger ring part model. Top: Wireframe of original part model. Bottom: Final part model for printing with added material colored red.

Elementum 3D provided six ring halves printed by the PBF process. Developing the printing process with the new aluminum bronze material required a significant amount of time and effort to determine the correct printing parameters and heat treatments. Details on this process are included in section 2.4.2 and in Appendix D. The six ring halves are pictured in Figure 50.



Figure 50.—Six slinger ring halves as-received from Elementum3D. The ring ID numbers are based on IDs that were inscribed on the parts by Elementum 3D.

3D scans were performed in-house at Reclamation to quantify deviation between the CAD models and the as-printed ring halves (Figure 51). The summarized findings from the 3D scans are as follows:

- A2228- thickness over dimension (too large)
- A2229- ID and outer diameter (OD) under dimension (too small); thickness over dimension (too large)
- A2237- ID, OD, and thickness all within tolerance
- A2240- ID and OD under dimension (too small)
- A2247- ID and OD under dimension (too small)
- A2527- ID, OD, and thickness all within tolerance

See Appendix L for full 3D scan reports.

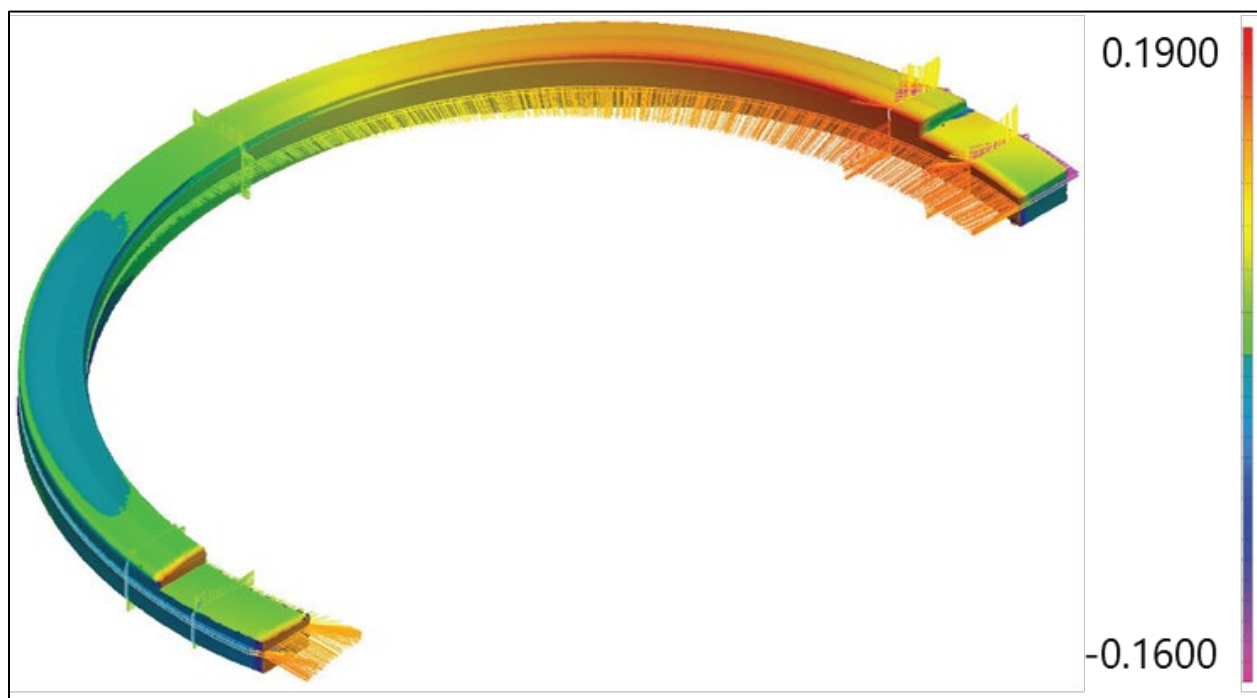


Figure 51.—Example of one control view from the 3D scan report of ring half A2229 showing the OD being under dimension. The greatest value on the color scale (red) is +0.1900 inches. The lowest value (pink) is -0.1600 inches.

Ring halves A2237 and A2527 were the only two of the six with all critical dimensions (ID, OD, and thickness) within tolerance. However, all rings had warpage in the Z-plane, which affects the circularity and prevents them from joining properly (Figure 52). Based on discussions with Elementum 3D, the warpage may have been due to incompatibility between the build plate and the part material, which caused the parts to peel up from the build plate during printing. This issue is also discussed in section 2.8 and section 2.9.2 for the Case Study A aluminum bronze governor part components.



Figure 52.—Representative photograph of the joint between two direct-printed slinger ring halves. Warpage and dimensions being out of tolerance cause the halves to not meet correctly. The left side of the photograph shows the top (based on print orientation) of ring half A2527 and the right side shows the bottom of ring half A2240.

With the observed warpage, the research team determined that it is not worth the time or effort to machine the printed slinger halves, as it would be more economical to start from a block of material and use traditional subtractive manufacturing. Since each of the printed halves are unique (warpage is not consistent), this prevents the same machining sequence from being programmed each time. Instead, a machinist would need to figure out exactly what is needed for each piece.

In an attempt to address the warpage of the ring halves, Elementum 3D printed one additional ring half, A2902, using an Inconel 718 (IN718) build plate (Figure 53). The IN718 build plate was reported to have improved adhesion when printing aluminum bronze than with 1045 mild steel or copper build plates.



Figure 53.—Photograph of ring half A2902, as-received condition.

The 3D scan report for A2902 shows no improvement from the first six ring halves, with all critical dimensions out of tolerance and warpage in the Z-plane (Figure 54). The full 3D scan report is included in Appendix L, with summarized findings as follows:

- A2902- ID, OD, and thickness over dimension (too large)

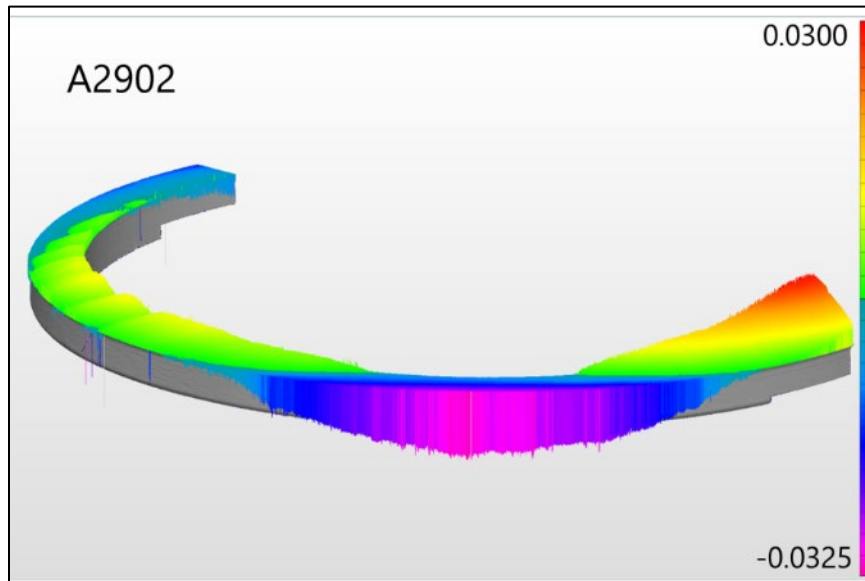


Figure 54.—Example of one control view from the 3D scan report of ring half A2902 showing warpage in the Z-plane. The greatest value on the color scale (red) is +0.0300 inches. The lowest value (pink) is -0.0325 inches.

4.4.2 Cast Slinger Ring Parts With Printed Polylactic Acid Pattern

The second additive manufacturing process investigated for the slinger rings was use of polymer 3D printing to fabricate a pattern, which was used to create an investment casting mold. For the investment casting process, C464 naval brass was able to be used.

Based on discussions with the foundry, several polymer materials which have been successfully used for investment-cast prototypes are stereolithography (SLA) resins, polylactic acid (PLA), and wax. SLA resin is intermediate cost and burns out well, leaving no ash content. PLA is less expensive but typically lower in resolution and does not burn out as well as SLA resin. Both SLA and PLA require the entire mold to be burned out, cooled, rinsed, and then fired for pouring, which adds risk and time to the process. Printed wax is a great option that can be run like a typical cast part because it melts out of the mold when autoclaved, and it has good resolution. However, it is a newer technology, and therefore still quite expensive.

ORNL has PLA-printing capabilities and printed a PLA test ring to evaluate the resolution, as shown in Figure 55. The printed parts were run through an acetone mist finisher to smooth the surface. Upon visual inspection, the surface finish of the PLA test rings after finishing is equivalent to or better than the traditionally manufactured naval brass rings, and therefore it was determined that PLA would provide sufficient resolution for the slinger ring patterns.



Figure 55.—Printed PLA ring halves to test the resolution for use as investment casting patterns.

With PLA selected as the material for the patterns, the slinger ring part model was altered for the PLA-printing process by ORNL MDF staff. Extra material (machining stock) was added to the ID and interfacing surfaces, including the alignment step, so that adequate dimensions and surface finish could be attained post-machining. The hardware holes were filled in to be tapped later at the machining stage. Then, the altered model was sent to the foundry to be updated with a gating system, which provides channels for molten metal flow during the casting process. The part model was also scaled up by the foundry to account for dimensional shrinkage after casting. Using the final altered part model, ORNL printed five test patterns at the ORNL machine shop (Figure 56, left).

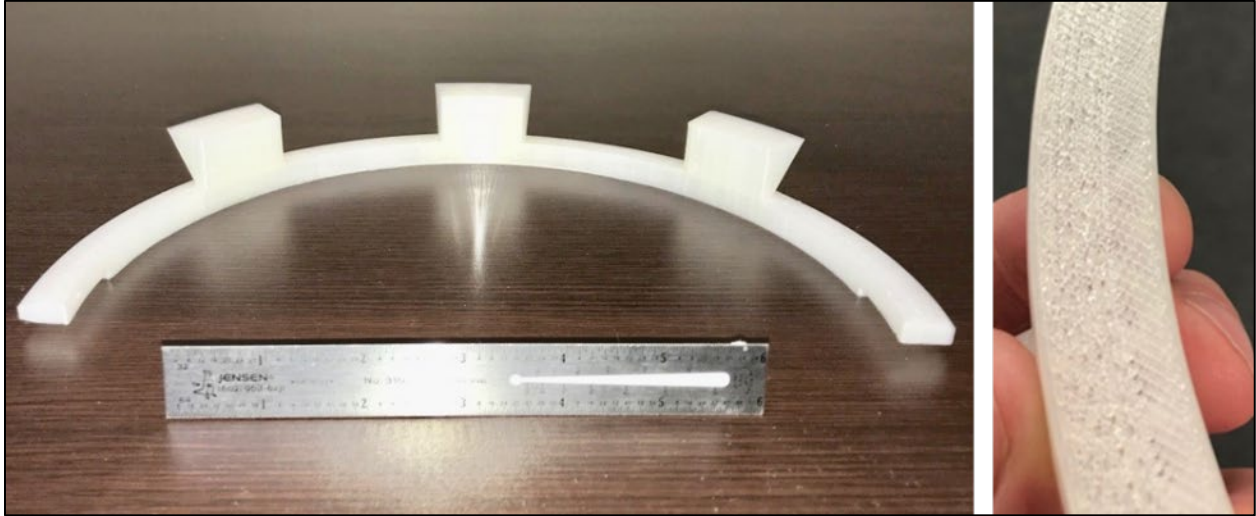


Figure 56.—Left: Printed PLA ring half pattern with gating system. Right: Small voids in the printed PLA ring surface due to incorrect print settings.

The test patterns were shipped to the foundry to be used to create test castings to check quality and shrinkage. The foundry found that, due to an error with the infill print settings, the test patterns had small gaps and holes on the surface opposite to the gating system (Figure 56, right). These voids exposed the interior of the pattern and would cause issues during casting. To try and avoid this, the foundry filled in the voids with patching material and smoothed out the patches. However, during casting, patch material from one pattern floated to two other patterns on the same tree, causing all three pieces to be unsuccessful and resulting in only two successful test castings. Aside from the patch issues, the foundry reported that melting and pouring of the metal went well. The two successful test castings are shown in Figure 57.



Figure 57.—Naval brass test castings prior to sand blasting to achieve final surface finish. Left: Two successful test castings. Right: Closeup view of surface texture on test casting.

The test castings were sandblasted at the foundry to achieve the final surface finish, and then underwent dimensional analysis. The foundry arbitrarily labeled the test castings as Half 1 and Half 2 and measured the critical dimensions for each half (Figure 58 and Table 16).

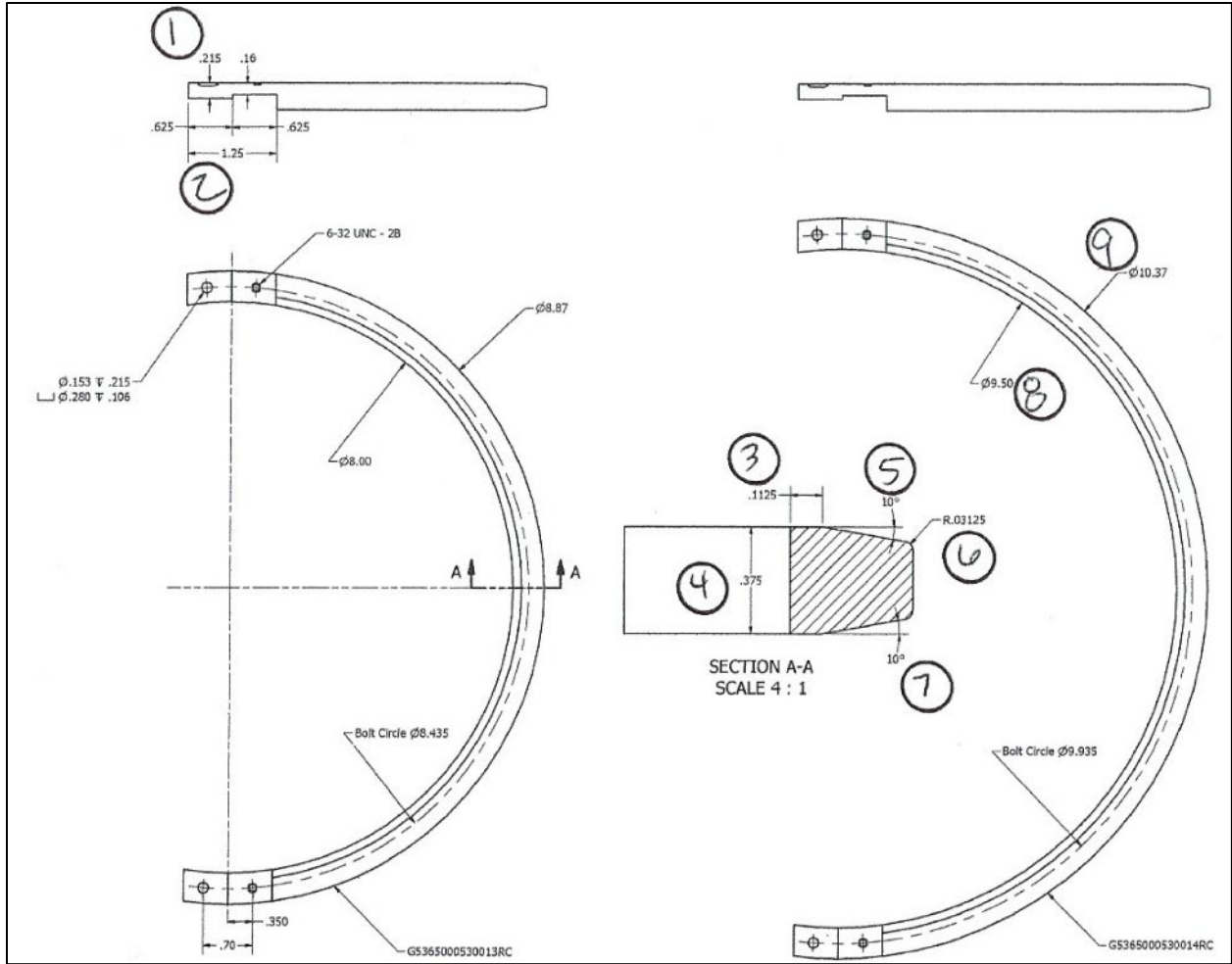


Figure 58.—Labeling of critical slinger ring dimensions with bubbles numbered 1–9 for cast slinger ring dimensional analysis.

Table 16.—Dimensional Analysis of Slinger Ring Test Castings

Bubble No.	Dimension	Requirement	Units	Gage Used	Half 1 Results	Half 1 Delta	Half 2 Results	Half 2 Delta
1	Joint notch thickness	0.215	inches	Calipers	0.245	-0.030	0.240	0.005
1	Joint notch thickness	0.215	inches	Calipers	0.247	-0.032	0.233	0.014
2	Joint notch length	1.25	inches	Calipers	1.193	0.0570	1.173	0.020
2	Joint notch length	1.25	inches	Calipers	1.186	0.064	1.182	0.004
3	Outer non-tapered width	0.1125	inches	Calipers	0.264	-0.152	0.248	0.016
4	Ring thickness	0.375	inches	Calipers	0.354	0.021	0.357	-0.003
5	Outer taper top angle	10	degrees	CMM	8.56	1.44	10.74	-2.18
6	Outer edge radius	R 0.03125	inches	Radius gage	R 0.031	0.000	R 0.031	0.000
7	Outer taper bottom angle	10	degrees	CMM	8.81	1.19	9.61	-0.80
8	Ring inner diameter	9.50	inches	CMM	10.0286	-0.5286	9.7778	0.2508
9	Ring outer diameter	10.37	inches	CMM	11.1008	-0.7308	10.8208	0.2800

Note: CMM = coordinate measuring machine.

The dimensional analysis from the foundry found that the rings did not meet requirements due to the ID and OD being out of dimension. These findings were confirmed once the test castings were shipped to Reclamation for inspection. The inspection by Reclamation also found warpage of the test castings, which caused them to lose circularity (Figure 59).

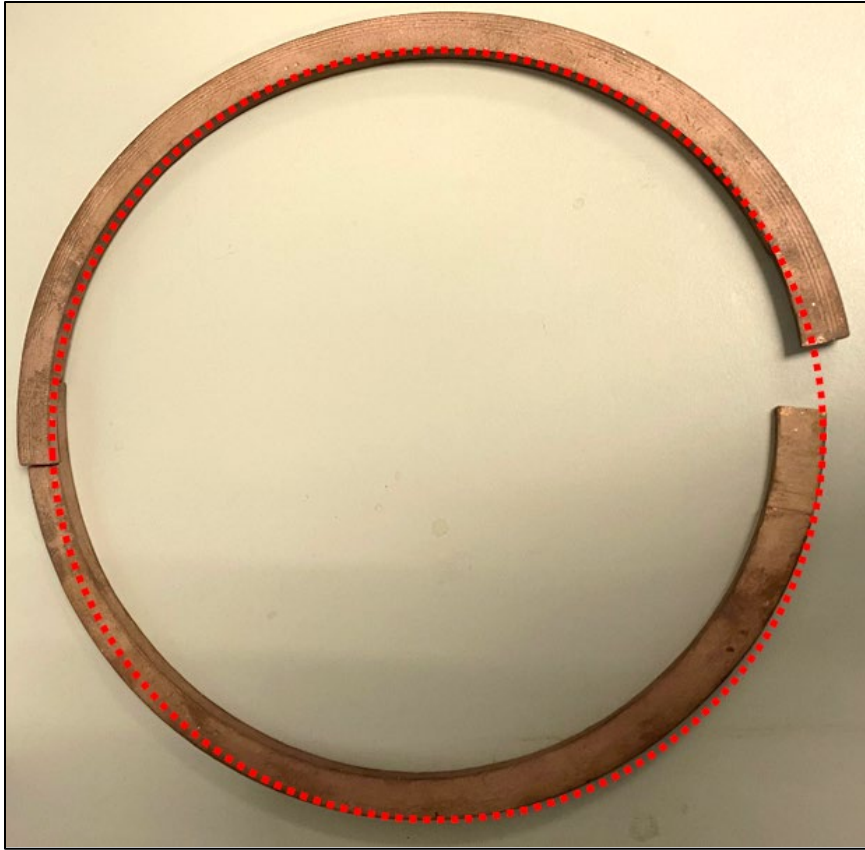


Figure 59.—Test castings in as-received condition. Warping causes the two halves to not line up properly and affects circularity, as represented by the overlaid red dashed circle.

While it is possible that the test castings could be bent into shape to fit the halves together as intended, this could impact material properties. And because the circularity of the slinger ring is a critical factor in its operation, researchers decided to abandon this production option until the cause of the warping could be identified and resolved.

Although the casting process was abandoned, ORNL printed two additional PLA patterns with the correct 100% infill to determine if this would address the void issue (Figure 60). The adjustment to an infill setting of 100% successfully solved the void issue, but also greatly increased print time since the patterns were now solid and not hollow. These additional PLA test patterns were not sent to the foundry (due to the concerns with warping), and therefore it is not known how the changes made to the patterns would affect the casting process.

A summary of the print settings for the two additional PLA test patterns is listed below. Unlisted settings were left at default. Screenshots of the full print machine settings pages are also included in Appendix M.

- Machine: MakerGear Ultra One
- Slicing Software: Simplify 3D
- Layer: Increased to 0.006 inches, which is when the print would stick to the build platform
- Additions: Brim with 0 offset from part
- Infill: 100%
- Temperature: Bed heater turned off at layer 3, nozzle is 205 °C
- Cooling: Turned on at layer 3
- Speed: Reduced to 43.3 mm/s, which is when the print would stick to the build platform

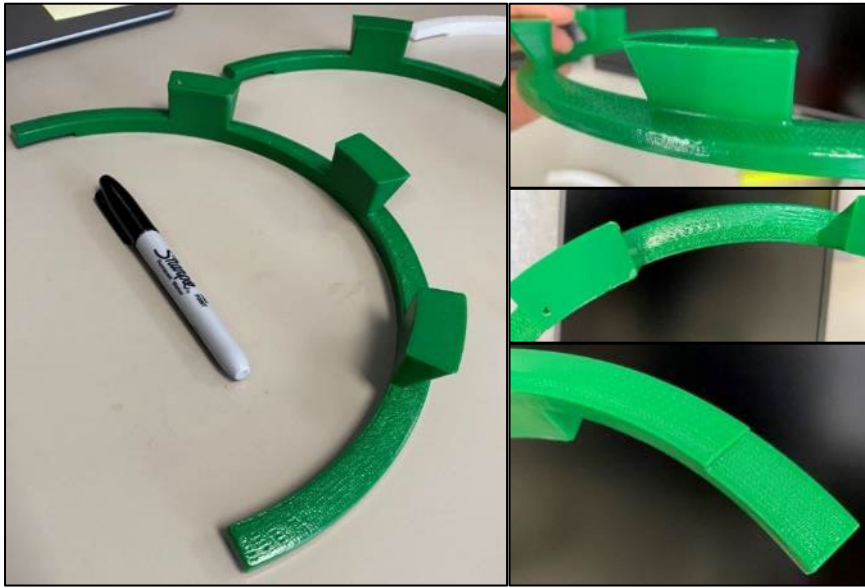


Figure 60.—Additional PLA test patterns printed by ORNL with 100% infill to address the void issue in the original PLA test patterns.

4.4.3 Laboratory and Field Test Results

4.4.3.1 Printed Aluminum Bronze Laboratory Results

Refer to section 2.8 for aluminum bronze laboratory results.

4.4.3.2 Cast Brass Laboratory Results

The component warpage of the cast slinger rings resulted in abandonment of this casting process as an option for slinger ring production. As such, no laboratory testing was performed on the cast brass material.

4.5 Additive Manufacturing Cost Estimates

4.5.1 Printed Aluminum Bronze Slinger Ring Parts

The cost to produce the printed aluminum bronze (UNS C95300) slinger rings is combined with the cost for the governor parts, and includes development of feed material, print parameters, and heat treatment. The unit price of a final printed slinger ring part without development cost is unknown. The total cost for printing a slinger ring using a PBF process was significant in this project due to the need to develop process parameters; however, future costs could be reduced substantially if aluminum bronze process parameters are already fully developed by that time.

4.5.2 Printed Polylactic Acid Slinger Ring Patterns

The cost information for the 100% infill PLA rings (green-colored rings) is included below:

- Nominal print time for two rings: 29 hours, 35 minutes.
- Material: 11 ounces (311.95 grams), prorated cost: \$13.10 (2021 USD).
- Labor: Because of issues with the machine, 3–4 hours. Without issues, less than 1 hour.

4.5.3 Cast Slinger Ring Parts

The PLA ring halves printed by ORNL were provided to the foundry for use as patterns to create the investment casting molds. The slinger ring halves were cast in C464 naval brass, with each half having an estimated weight of 0.65 lb. The investment casting tolerance was listed as ± 0.005 in/in surface finish was 125 roughness average (Ra) microinches minimum, and the final castings were annealed. The foundry provided pricing on a lot-charge basis, as shown in the Table 17.

Table 17.—Lot Pricing for Slinger Ring Castings

Number of Pieces	Prices per Half Ring Casting (2021 USD)
2	1,540.00 lot charge
5	1,565.00 lot charge
10	1,575.00 lot charge

The following certifications were included as part of the lot charge:

- Physical properties of a 0.252 in test bar
- Heat treating certification
- Chemical analysis

The foundry also offered an optional first article inspection, with cost being \$900.00 (2021 USD) per part. For the purposes of this project, the foundry provided two test castings to verify that casting quality and dimensions met the project needs. The test castings and dimension analysis were provided at no charge, and no additional castings were ordered since the test pieces did not meet project needs.

4.6 Cost-Benefit Analysis of Additive Manufacturing

For traditional fabrication, the slinger rings are machined from a plate of naval brass and involves CNC machining to create two mating semi-circular parts. ORNL obtained cost estimates for CNC machining the slinger rings from C360 Brass, the closest material to naval brass that was available in the Xometry estimating tool used by ORNL. The costs (listed in 2021 USD) were: \$667 for 16-day delivery, \$1,420 for 13-day delivery, and \$2,290 for 7-day delivery. While the cost is not prohibitive, the traditional process creates significant material waste, which is where additive manufacturing may provide the most benefit. For additive manufacturing fabrication, this research investigated two methods: 1) direct printing aluminum bronze by a PBF process and 2) the use of printed PLA patterns in investment casting of naval brass.

The PBF process allowed for significant reduction in material waste. However, it is not a cost-effective alternative at this time, and will likely not become cost-effective until techniques for PBF production of bronze and brass materials become well-established. The current state of the technology still requires significant further investment into development of printing parameters and heat treatment to prevent the material issues seen in this research, such as warpage that prevents the parts from being useable. Once the process is better established, the cost-benefit analysis of direct printing slinger rings by a powder bed fusion process could be revisited.

For the second method, the team was able to print PLA patterns within dimension and surface finish requirements, and the patterns were successfully used in investment casting of test pieces. The casting process, unlike the PBF process, allowed the ring halves to be produced in the original material (naval brass). However, the casting process had similar issues to the PBF process with warpage of the parts that prevented them from being usable. Due to these issues, the team did not progress beyond the test castings, and therefore did not obtain final cost and time information for this multi-step fabrication process. Further investigation would be needed to determine total cost through the end of the process, including post-processing and final machining.

5 Summary of Hydropower Component Additive Manufacturing Case Studies

5.1 Lessons Learned and Recommendations for Process Improvement

Governor Parts.—The governor parts were considered unsuccessful due to the following:

- The components were selected for geometric complexity, however the post-processing requirements of the parts offset any cost saving.
- The lack of additional material to grip the components made post-print machining difficult.
- Reverse engineering of intricate parts increased the risk of producing design errors and non-conforming components.
- Selection of parts made from less-common additive manufacturing materials created additional challenges (development of print parameters and heat treatment, selection of feedstock, etc.) to overcome.
- Selecting a part made of multiple components and multiple materials compounded the issues above.

Log Boom Anchor.—The log boom anchor was considered successful, which can be attributed to several factors:

- The part was able to be redesigned for additive manufacturing, the original part was changed and optimized for strength and weight. Also, the part was comprised of multiple components that could be combined into a single piece allowing for strengthening and cost savings.
- Familiar material, aluminum is a common material used in additive manufacturing with well-established print parameters for PBF. Additionally, the powder feedstock is widely available.
- The part size fit within commonly used PBF equipment.
- The part did not require extensive post-processing such as machining to obtain a required surface finish.
- The original design presented an opportunity for significant machine time reduction and material savings.

Slinger Rings.—The slinger rings were considered to be unsuccessful due to the following:

- The PBF ring halves had similar challenges as faced with the aluminum bronze components of the governor parts (print parameters, precise dimensions, and final machining needed to achieve the specified surface finish, heat treatment, feedstock selection, etc.).
- The overall size of the printed parts and aspect ratio caused issues with adhesion to the baseplate and thermal distortion, which made the ring halves unusable.
- Investment casting allowed for use of the original naval brass material, and the PLA test patterns were successful; however, the test castings had warpage issues affecting the ring circularity, which is critical to its function.
- The benefit of material savings was outweighed by the above issues.

5.2 Priorities for Future Efforts

Throughout the project, the research team identified several key areas for additional research which were outside the scope of the current project. A discussion of these applications is presented in the following sections.

5.2.1 Hybrid Additive Manufacturing Technology and In Situ Repairs

Hybrid processes include both additive and subtractive capabilities integrated into a single unit. Most additive processes require some type of post processing to achieve the specified surface finish, and manual post processing can be a labor-intensive process that impacts the fabrication costs. Incorporating a milling bit into a direct (or directed) energy deposition (DED) robot can save time, reduce labor and lower the overall costs. This approach could also be incorporated into a field-ready machine to facilitate in-situ repairs. The SCOMPI robot developed by Quebec Hydro is a good example of a robot designed to automated in situ cavitation repairs to hydro turbines. Reclamation could benefit from this technology if and/or when it becomes commercially available.

5.2.2 Printing More Advanced Parts Including a Turbine Runner or Pump Impellor

The expertise and intellectual property placed these parts outside the scope of the current project. In the future, a potential partnership with a turbine manufacturer could be explored with a targeted research proposal.

5.2.3 Embedded Sensors and Smart Design

Additive manufacturing may allow unique designs which incorporate embedded sensors, such as strain gauges for loading condition or structure health monitoring applications. This example of value-added capability is an area of interest to ORNL and could be incorporated into a future research project.

5.2.4 Corrosion Susceptibility of Additively Manufactured Parts

It is important to note that corrosion properties can vary between additively manufactured parts and traditional parts depending on the alloy and additive manufacturing process used. There are ongoing efforts in the additive manufacturing community to characterize corrosion performance of additively manufactured parts. Reclamation does not need to duplicate these efforts but should stay informed as new developments unfold.

5.2.5 Using Additive Manufacturing to Create Parts With Enhanced Properties

Friction stir welding using additive manufacturing is one possibility. Pacific Northwest National Laboratory has performed some research in this area. The U.S. Army Corps of Engineers (USACE) also has active research using friction stir welding for repairing fatigue-damaged parts such as rails. USACE is also evaluating the use of mixed metal oxide materials using cold spray and DED methods for enhanced impact resistance.

5.3 Implications for the Entire Reclamation Hydropower Fleet

There may be opportunities for additive manufacturing to be deployed selectively within Reclamation's aging infrastructure, but careful consideration must be made for the amount of post-processing required for parts. Additive manufacturing is a viable alternative for components that can be updated, changed, or optimized for strength, weight (or material reduction), or for printing. Another prerequisite for use of additive manufacturing is that the design must allow for materials with established print parameters to be used.

6 References

- [1] ASM International. 1990. ASM Handbook Volume 1 Properties and Selection: Irons, Steels, and High-Performance Alloys, Metals Park: ASM International.
- [2] Kurzynowski, T., K. Gruber, W. Stopyra, B. Kuźnicka, and E. Chlebus. 2018. "Correlation between process parameters, microstructure and properties of 316 L stainless steel processed by selective laser melting." *Materials Science and Engineering: A*, vol. 718, pp. 64–73.
- [3] Qiu, C., M. Al Kindi, A. Aladawi, and I. Al Hatmi. 2018. "A comprehensive study on microstructure and tensile behaviour of a selectively laser melted stainless steel." *Scientific Reports*, vol. 8:7785.
- [4] Charmi, A., R. Falkenberg, L. Avila, G. Mohr, K. Sommer, A. Ulbricht, M. Sprengel, R. Saliwan Neumann, B. Skrotzki, and A. Evans. 2021. "Mechanical Anisotropy of Additively Manufactured Stainless Steel 316L: An experimental and numerical Study." *Materials Science and Engineering: A*, vol. 799, 140154.
- [5] Im, Y.D., K.H. Kim, K.H. Jung, Y.K. Lee, and K.H. Song. 2019. "Anisotropic Mechanical Behavior of Additive Manufactured AISI 316L Steel." *Metallurgical and Materials Transactions A*, vol. 50, no. 4, pp. 2014–2021.
- [6] Niendorf, T., S. Leuders, A. Riemer, et. al. 2013. "Highly Anisotropic Steel Processed by Selective Laser Melting." *Metallurgical and Materials Transactions B*, vol. 44, no. 8, pp. 794–796.
- [7] ASM International. 2008. Elements of Metallurgy and Engineering Alloys, Ohio: ASM International.
- [8] Huang, H., M. Nie, Y. Luan, X. Liu, and J. Xie. 2012. "Fatigue Property of Single-Crystal and Columnar-Grained Polycrystalline Cu-12wt.%Al Alloys." *Procedia Engineering*, vol. 27, pp. 1686–1693.
- [9] Copper Development Association, Inc. 1994. Copper Casting Alloys, New York: Copper Development Association, Inc.
- [10] Cerri, E.G.E. 2020. "AlSi10Mg alloy produced by Selective Laser Melting: Relationships between vickers microhardness, Rockwell hardness and mechanical properties." *International Journal of the Italian Association for Metallurgy*, pp. 7–17.
- [11] Kempen, K., L. Thijs, J.V. Humbeeck, and J. Kruth. 2012. "Mechanical Properties of AlSi10Mg Produced by Selective Laser Melting." *Physics Procedia*, vol. 39, pp. 439–446.
- [12] Zygula, K., B. Nosek, H. Pasiowicz, and N. Szysiak. 2018. "Mechanical properties and microstructure of AlSi10Mg alloy obtained by casting and SLM technique." *World Scientific News*, vol. 104, pp. 462–472.

- [13] Hatch, J. 1984. "Microstructure of Alloys," *in* Aluminum Properties and Physical Metallurgy, Microstructure of Alloys, pp. 58–104.
- [14] Callister, J.W.D. and D.G. Rethwisch. 2013. "Failure," *in* Materials Science and Engineering: An Introduction, Hoboken, John Wiley & Sons.
- [15] EOS GmbH - Electro Optical Systems. 2014. "EOS Aluminum AlSi10Mg." May 2014. Available at: https://fathommg.com/wp-content/uploads/2020/11/EOS_Aluminium_AlSi10Mg_en.pdf.

6.1 Additional References—ASTM Standards

ASTM International (ASTM):

1. ASTM B171 Standard Specification for Copper-Alloy Plate and Sheet for Pressure Vessels
2. ASTM B822 Standard Test Method for Particle Size Distribution of Metal Powders and Related Compounds by Light Scattering
3. ASTM E8/E8M-16a Standard Test Methods for Tension Testing of Metallic Materials
4. ASTM E23-18 Standard Test Methods for Notched Bar Impact Testing of Metallic Materials
5. ASTM E290-14 Standard Test Methods for Bend Testing of Material for Ductility
6. ASTM E466-15 Standard Practice for Conducting Force Controlled Constant Amplitude Axial Fatigue Tests of Metallic Materials
7. ASTM F3184-16 Standard Specification for Additive Manufacturing Stainless Steel Alloy (UNS S31603) with Powder Bed Fusion

7 Supporting Datasets

Additional files associated with this project can be accessed via:

- **File Path.**—T:\Jobs\DO_NonFeature\Science and Technology\2018-PRG-Additive Manufacturing Investigation and Demonstration for Hydropower Applications
- **Point of Contact.**—Dave Tordonato, dtordonato@usbr.gov, 303-445-2394
- **Short Description of Data.**—Files primarily include mechanical property test data, part models, photographs of case study parts, project management files, email correspondences, relevant literature, and test standards.
- **Keywords.**—Additive manufacturing, 3D printing, aging infrastructure, governor valve, log boom anchor, slinger ring, fabrication, powder bed fusion, stainless steel, aluminum bronze, polylactic acid.
- **Approximate Total File Size.**—3,623 Files, 264 Folders, 28.0 GB

Appendix A

Colorado Metallurgical Services Mechanical Property Data of
Service Parts



Colorado Metallurgical Services

10605 East 25th Avenue Aurora, CO 80010 T/303 780 9800 F/303 780 9402 testmetals.com



Date: January 21, 2020

Company: Bureau of Reclamation

P.O. #

ATTN: Matthew Jermyn

Ref. #

Address: Denver Federal Center (86-68540)

Material: Stainless Steel & Brass

Address: Denver, CO 80225

Specification: ASTM E18-19 | ASTM 1086-14 | CMS SOP-10-01-1

Lab#: 2001-115

HARDNESS

Indent	Stainless Sample (HRB)	Brass Sample (HRB)
1	86	77
2	88	77
3	87	78
Average	87	77

[X] Information Only

CHEMICAL ANALYSIS	Stainless Sample	UNS S30300
Carbon	0.05	0.15 max
Sulfur	0.345	0.15 min
Phosphorus	0.032	0.20 max
Silicon	0.73	1.00 max
Chromium	17.31	17.0-19.0
Nickel	8.97	8.0-10.0
Manganese	1.60	2.00 max
Copper	0.57	
Molybdenum	0.43	
Columbium	<0.01	
Titanium	0.01	
Aluminum	<0.01	
Vanadium	0.08	
Cobalt	0.14	
Tungsten	<0.01	
Tin	0.02	
Iron	Base	Base

Chemistry Run By: OES

Percent By Weight

[X] Meets Specification Requirements for UNS S30300



Colorado Metallurgical Services

10605 East 25th Avenue Aurora, CO 80010 T/303 780 9800 F/303 780 9402 testmetals.com



<u>CHEMICAL ANALYSIS</u>	<u>Brass Sample</u>	<u>UNS C46400</u>
Silicon	<0.01	
Iron	0.01	0.10 max
Manganese	<0.01	
Nickel	<0.01	
Zinc	39.7	Remainder
Lead	0.04	0.20 max
Tin	0.70	0.50-1.0
Beryllium	0.01	
Cobalt	<0.01	
Aluminum	<0.01	
Phosphorous	<0.01	
Sulfur	<0.01	
Carbon	<0.01	
Copper	59.5	59.0-62.0
Cu + Named Elements	99.96	99.6 min

Chemistry Run By: OES
 Percent By Weight
 Meets Specification Requirements for UNS C46400

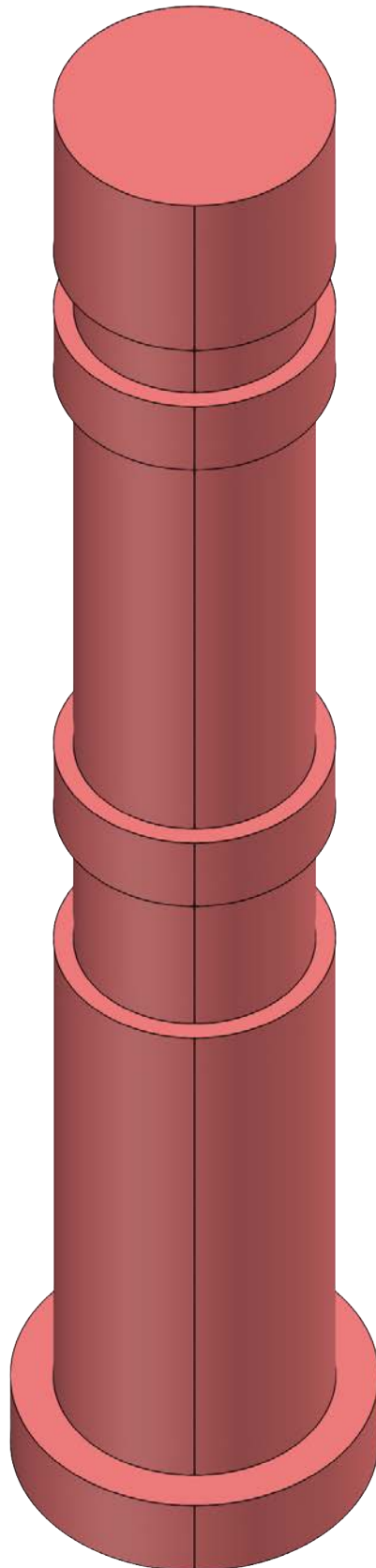
Respectfully Submitted,

Josh Belt
Materials Engineer

Appendix B

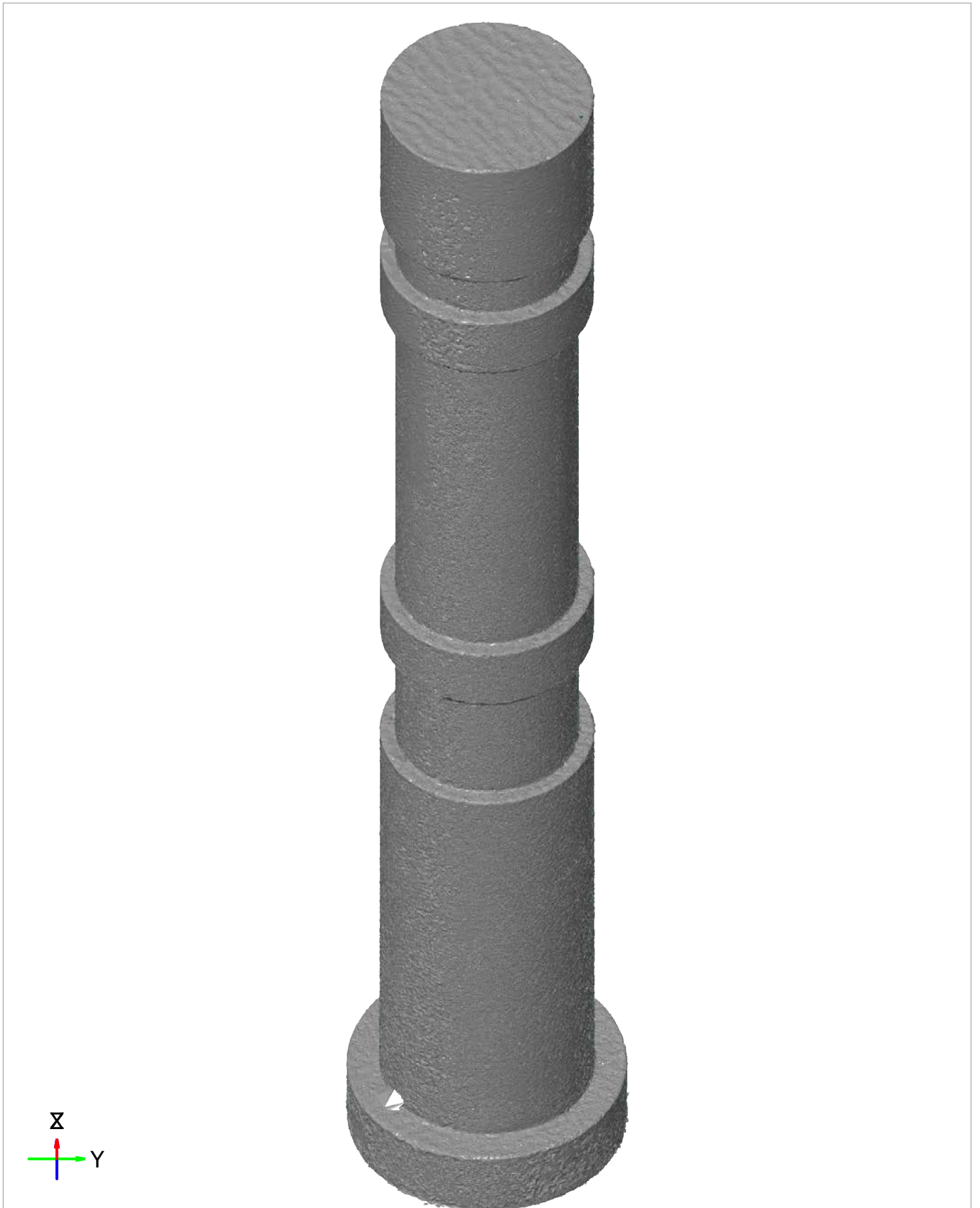
3D Scan Results of Stainless Steel Governor Parts As-Printed

CAD



Length unit: mm

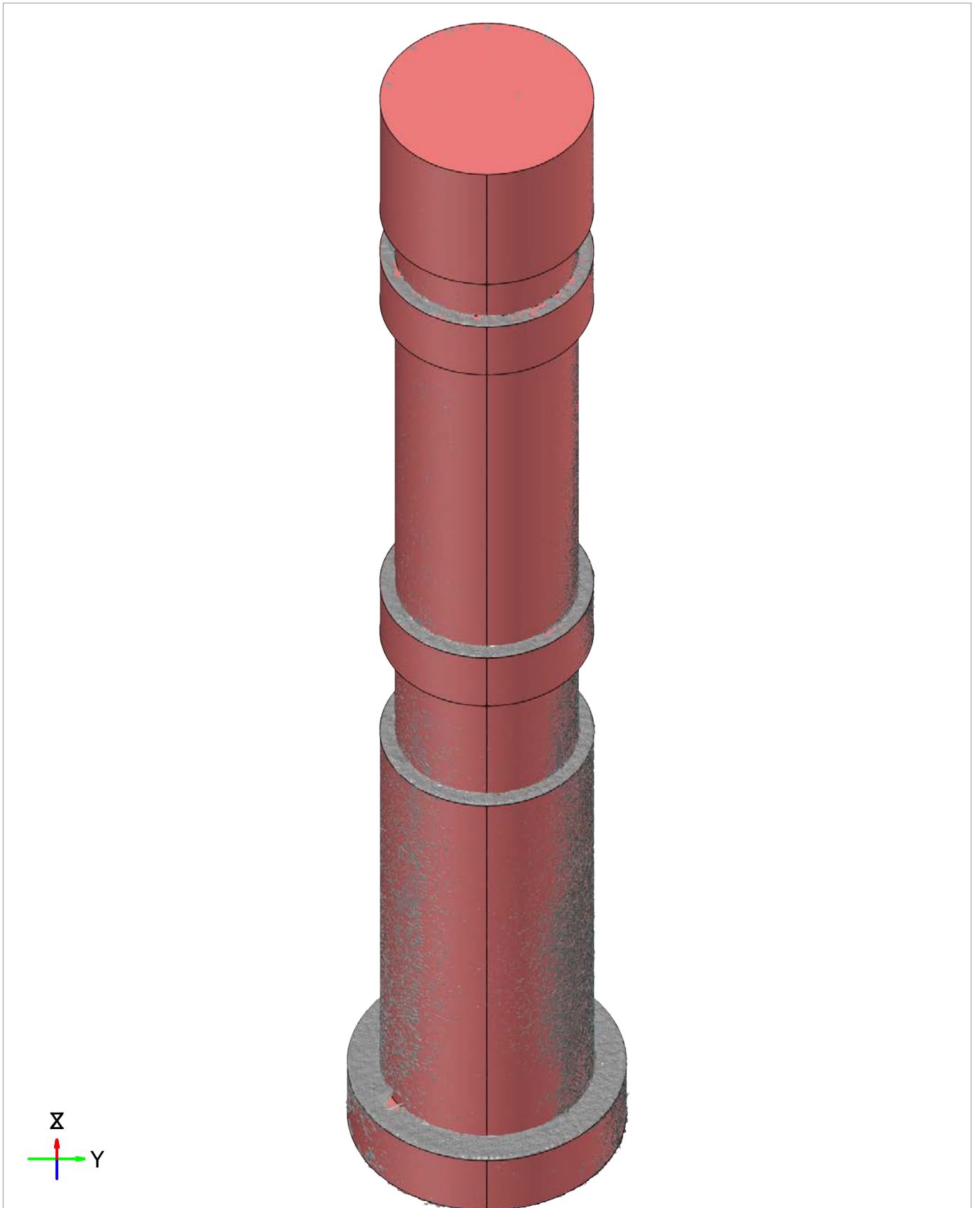
Mesh



Prealignment

Length unit: mm

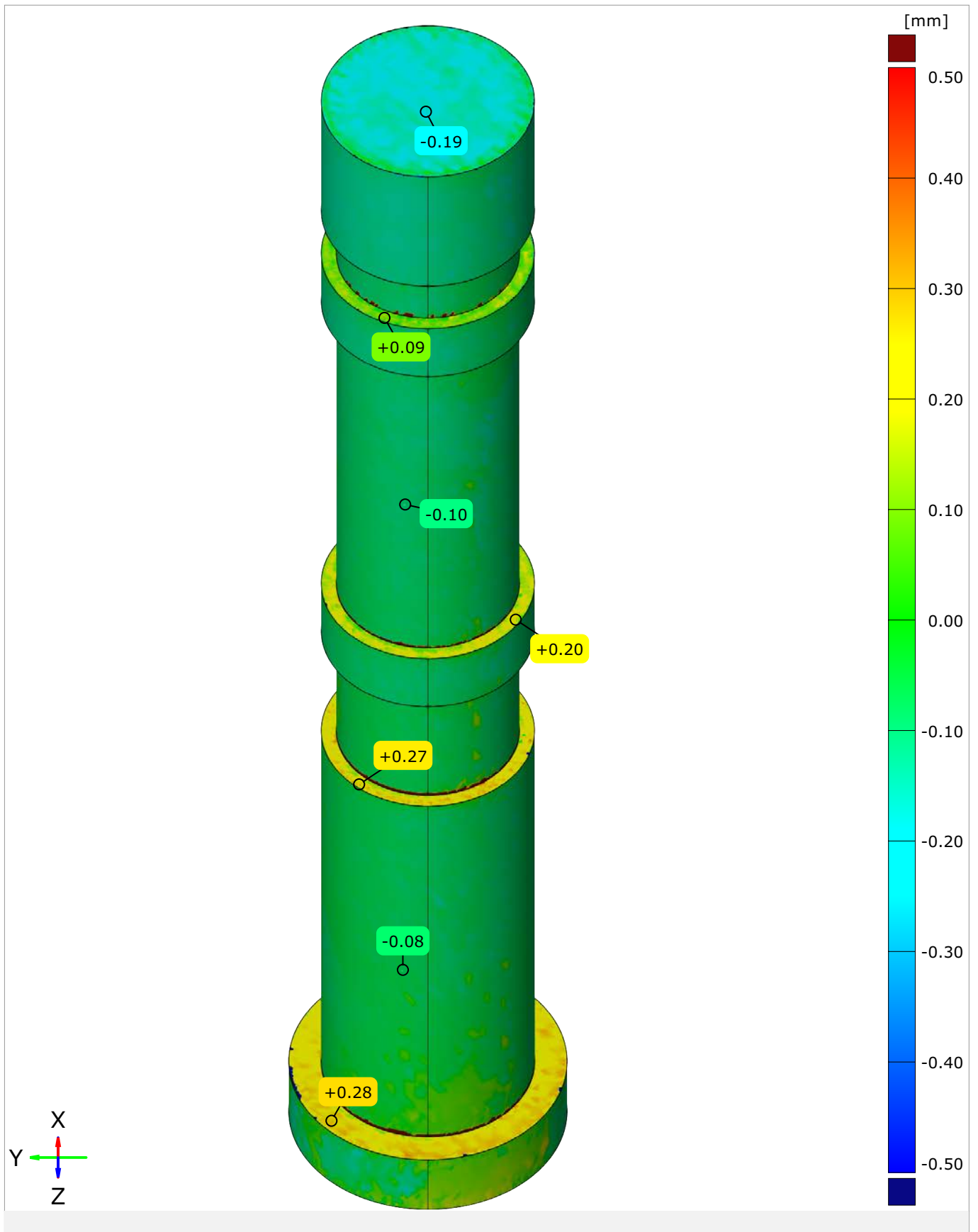
Alignment



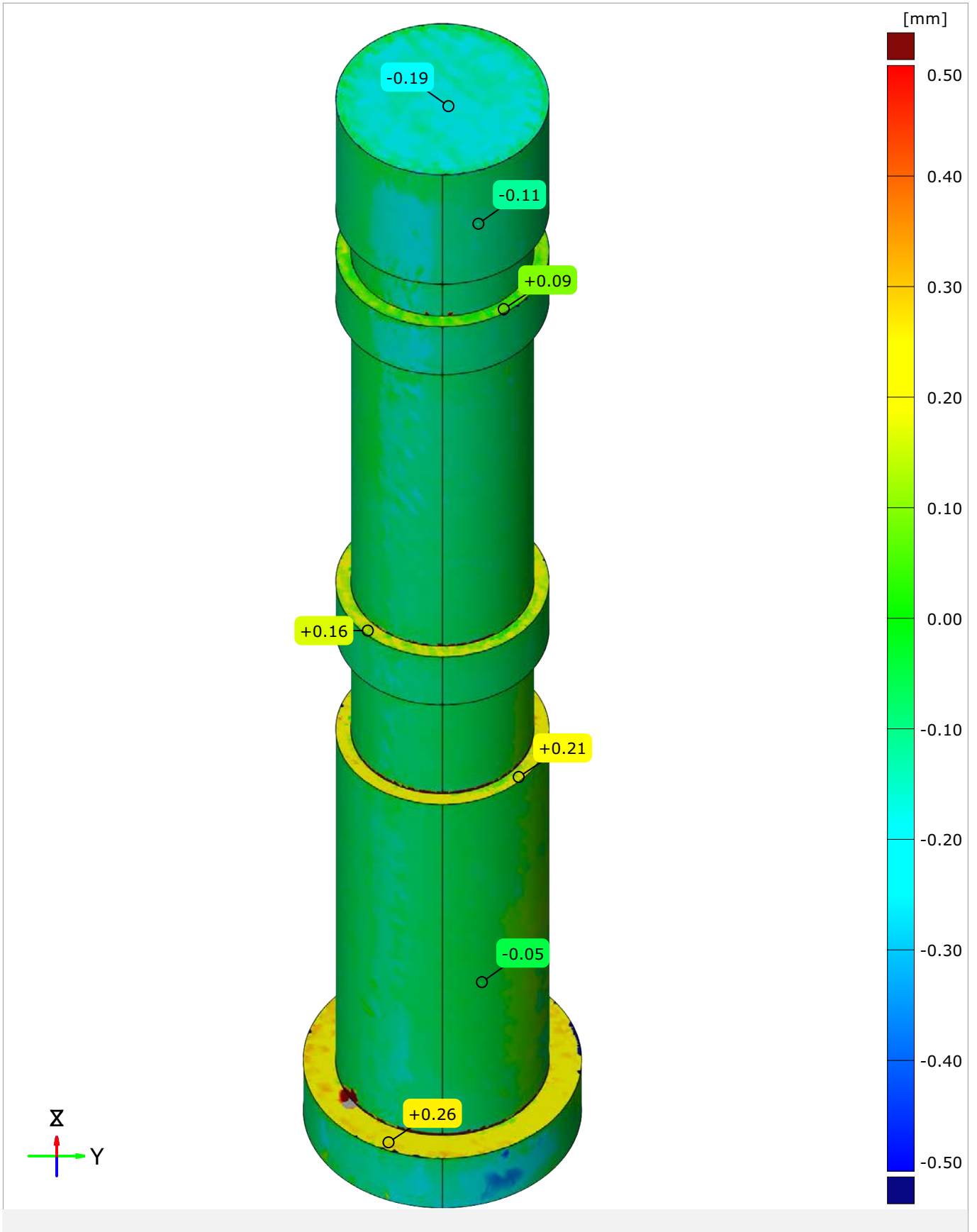
Prealignment

Length unit: mm

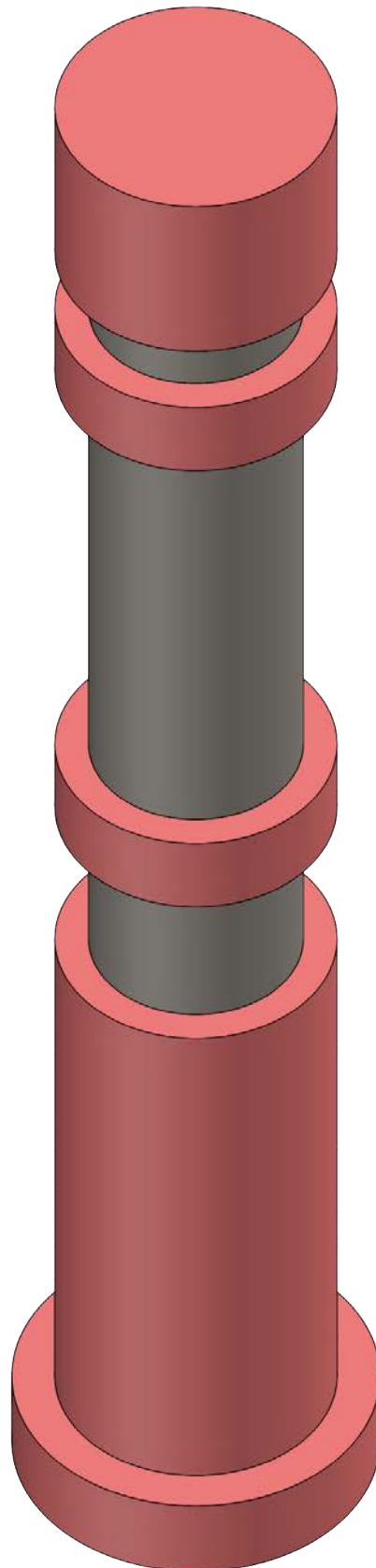
Surface Comparison



Surface Comparison Opposite Side

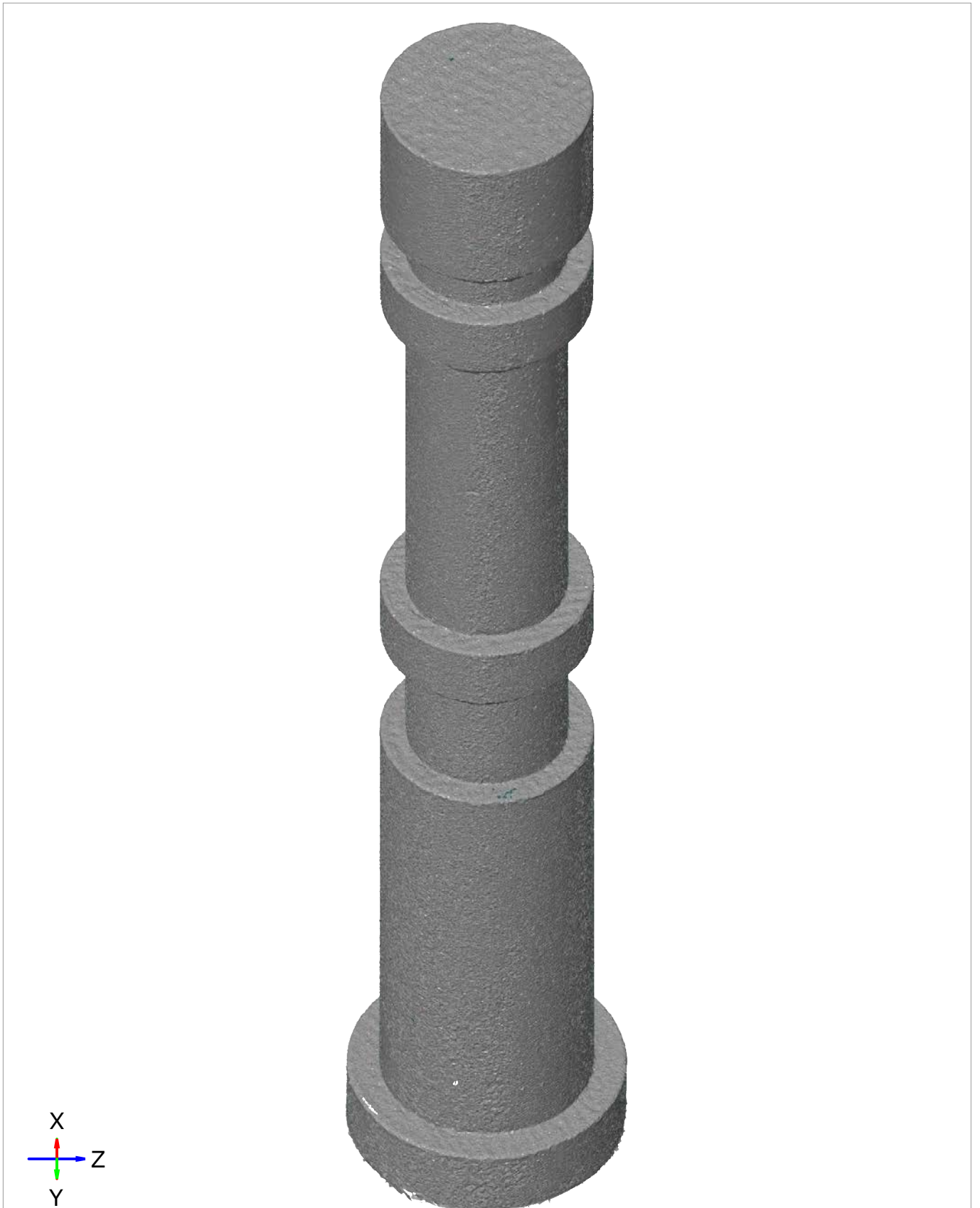


CAD

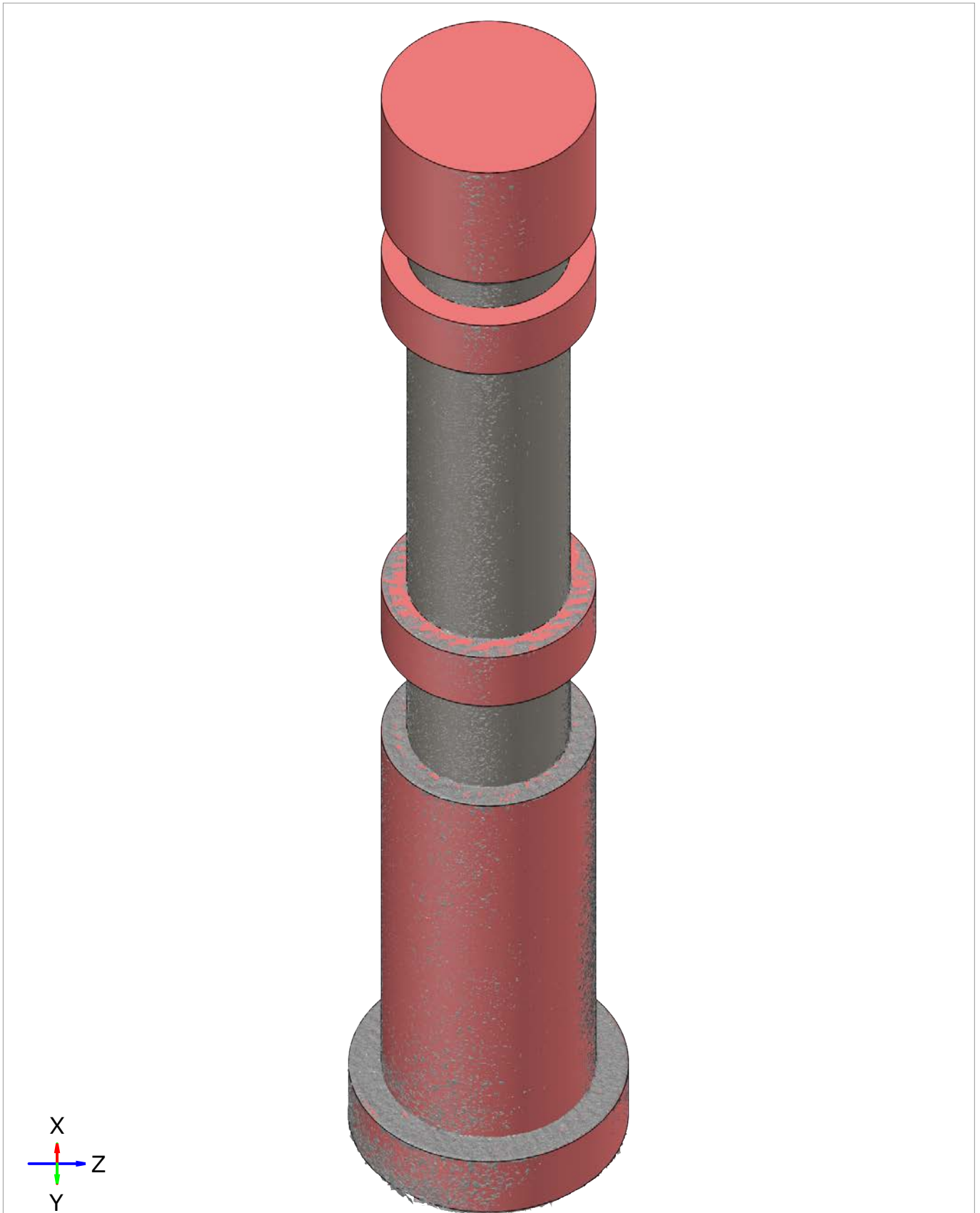


Length unit: mm

Mesh



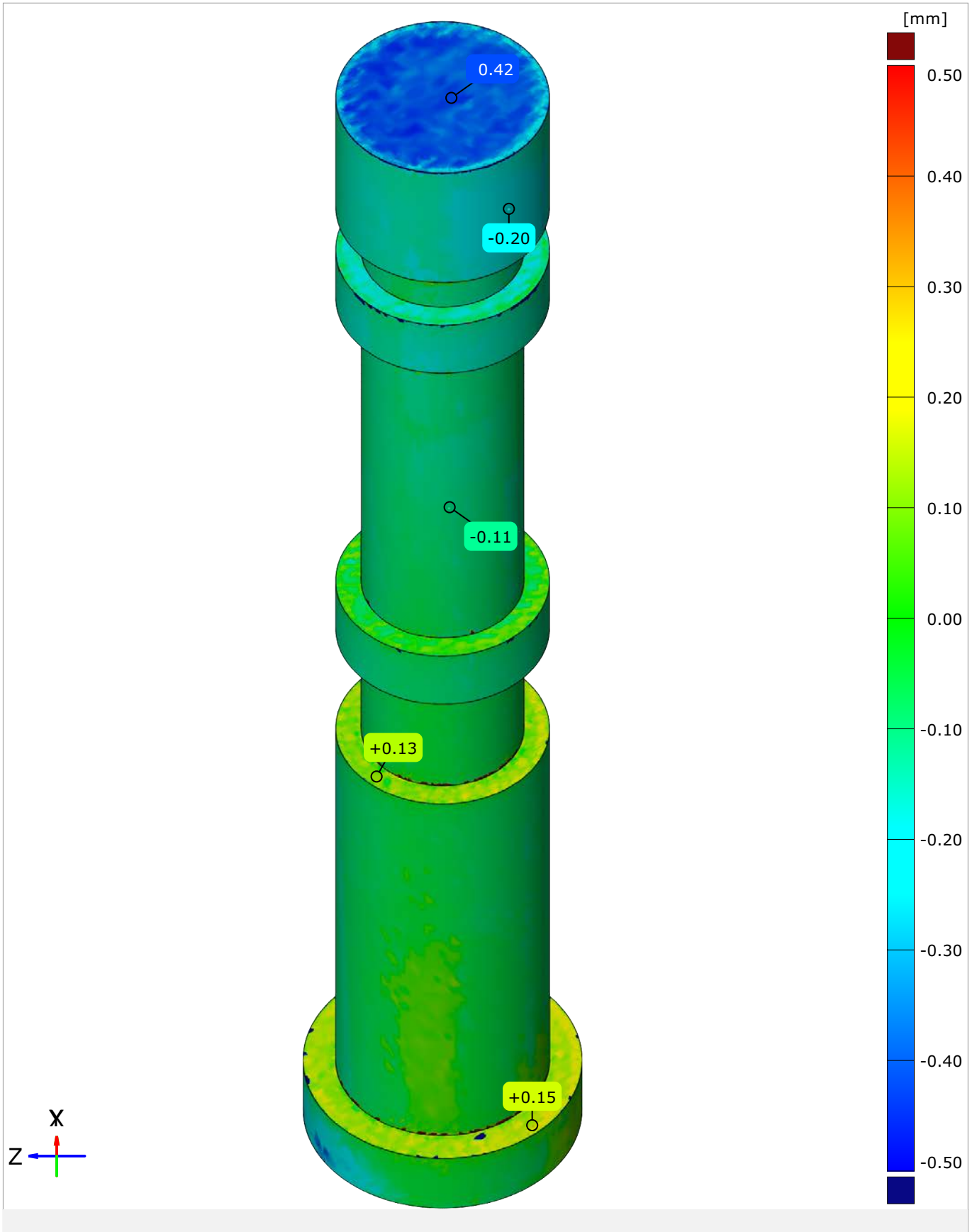
Alignment



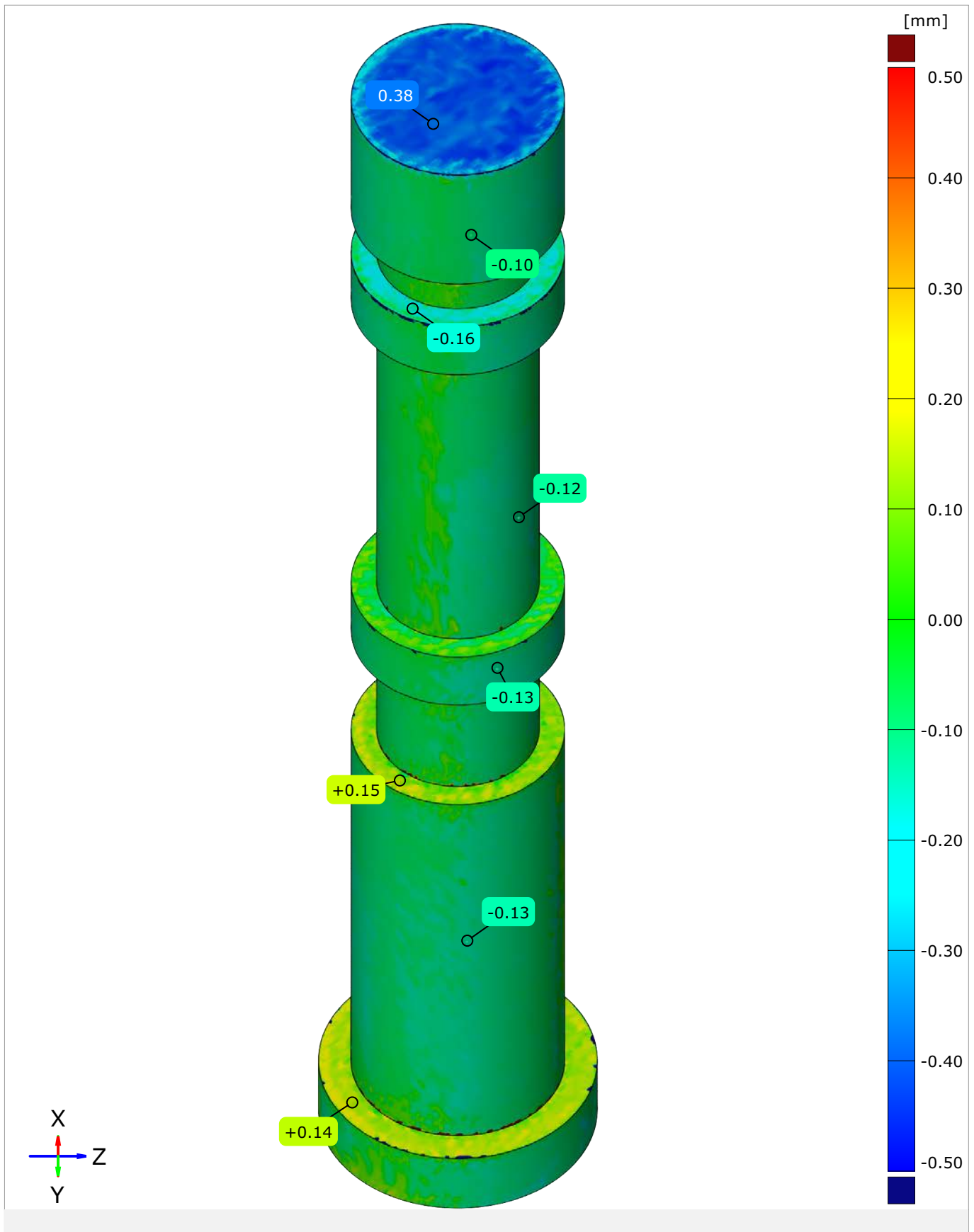
Prealignment

Length unit: mm

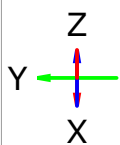
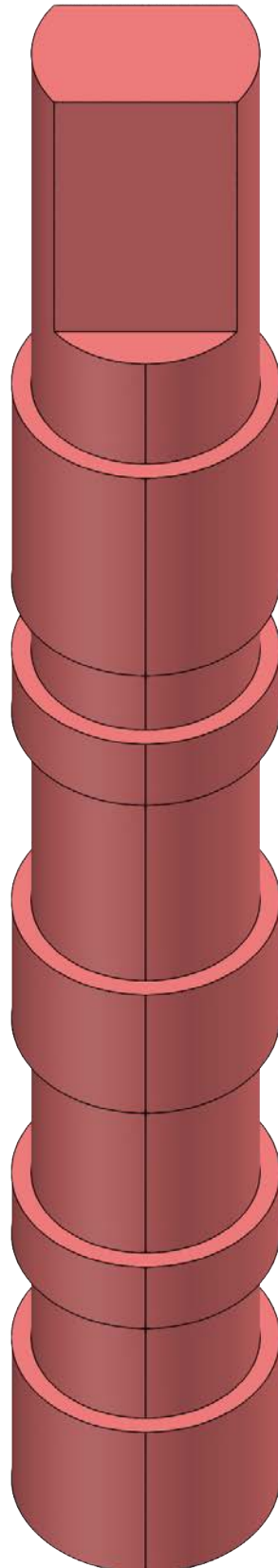
Surface Comparison



Surface Comparison Opposite Side

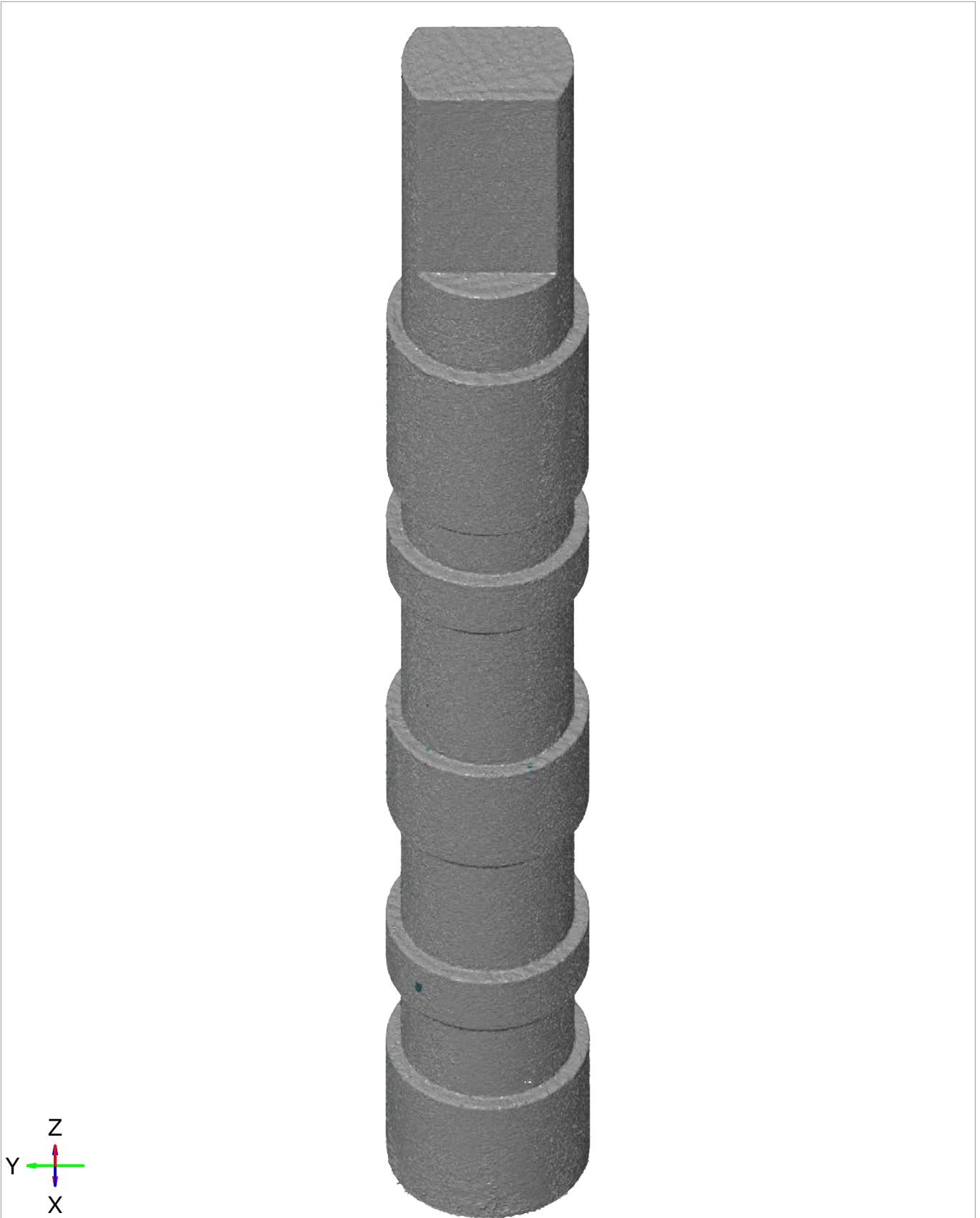


CAD



Length unit: mm

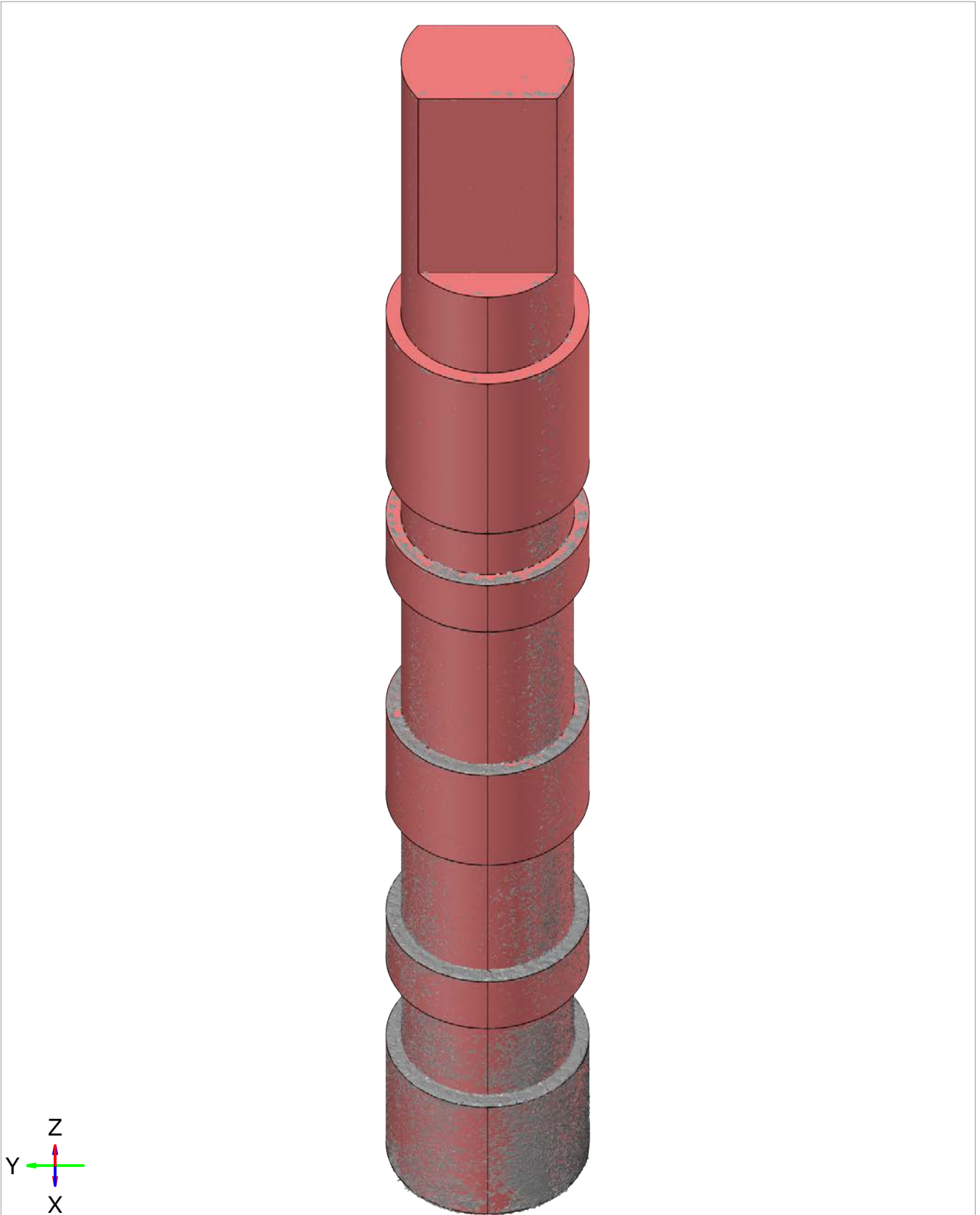
Mesh



Prealignment

Length unit: mm

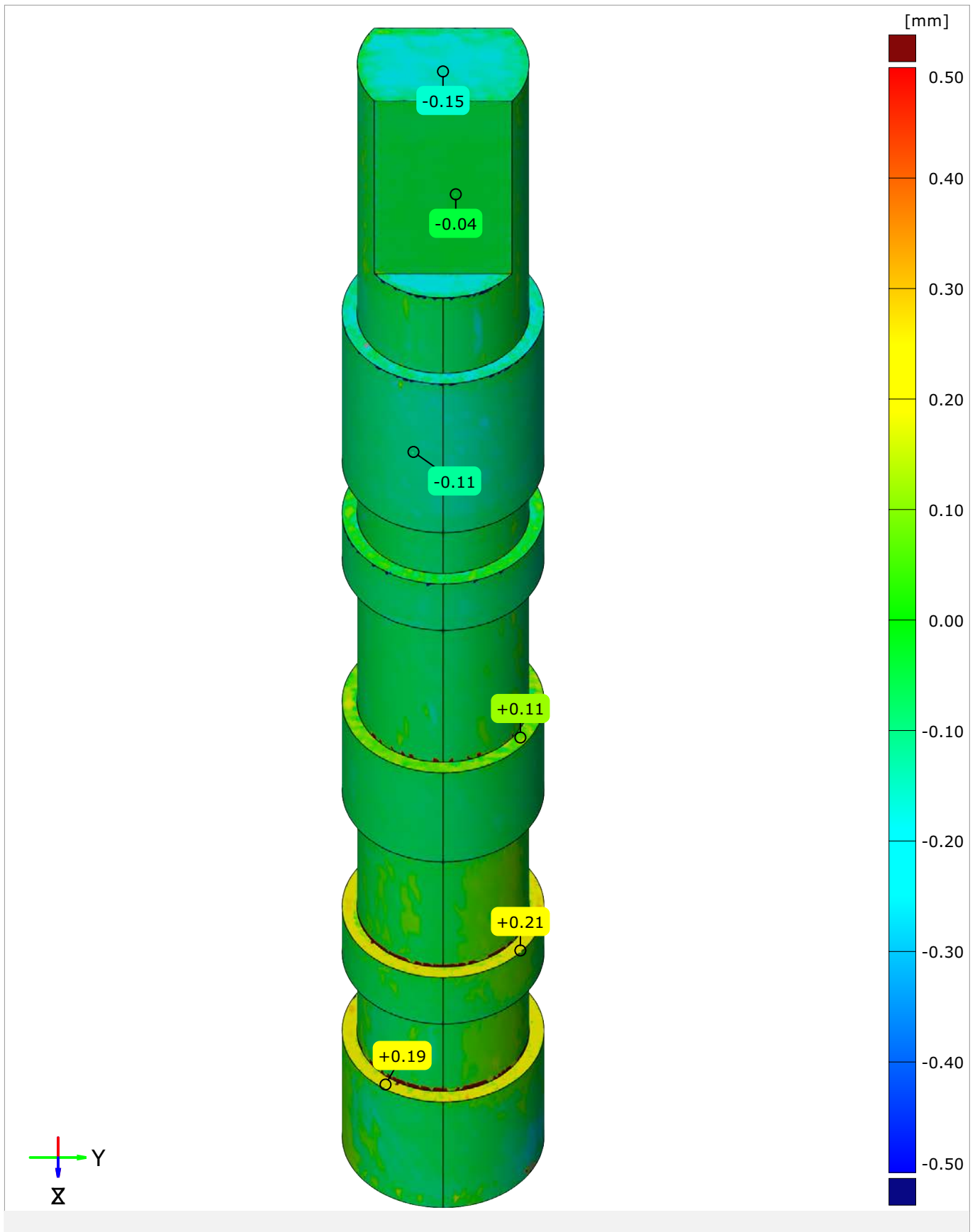
Alignment



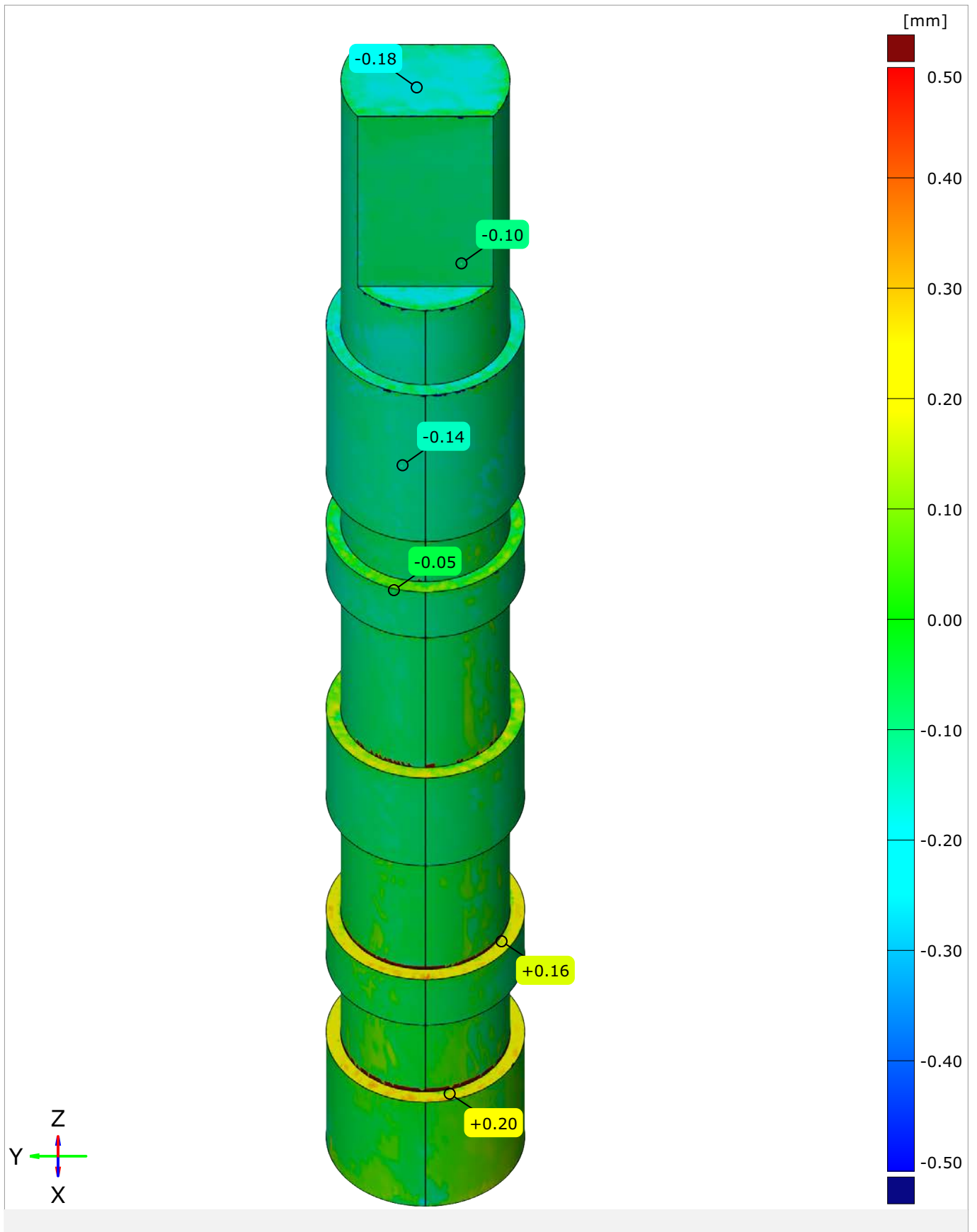
Prealignment

Length unit: mm

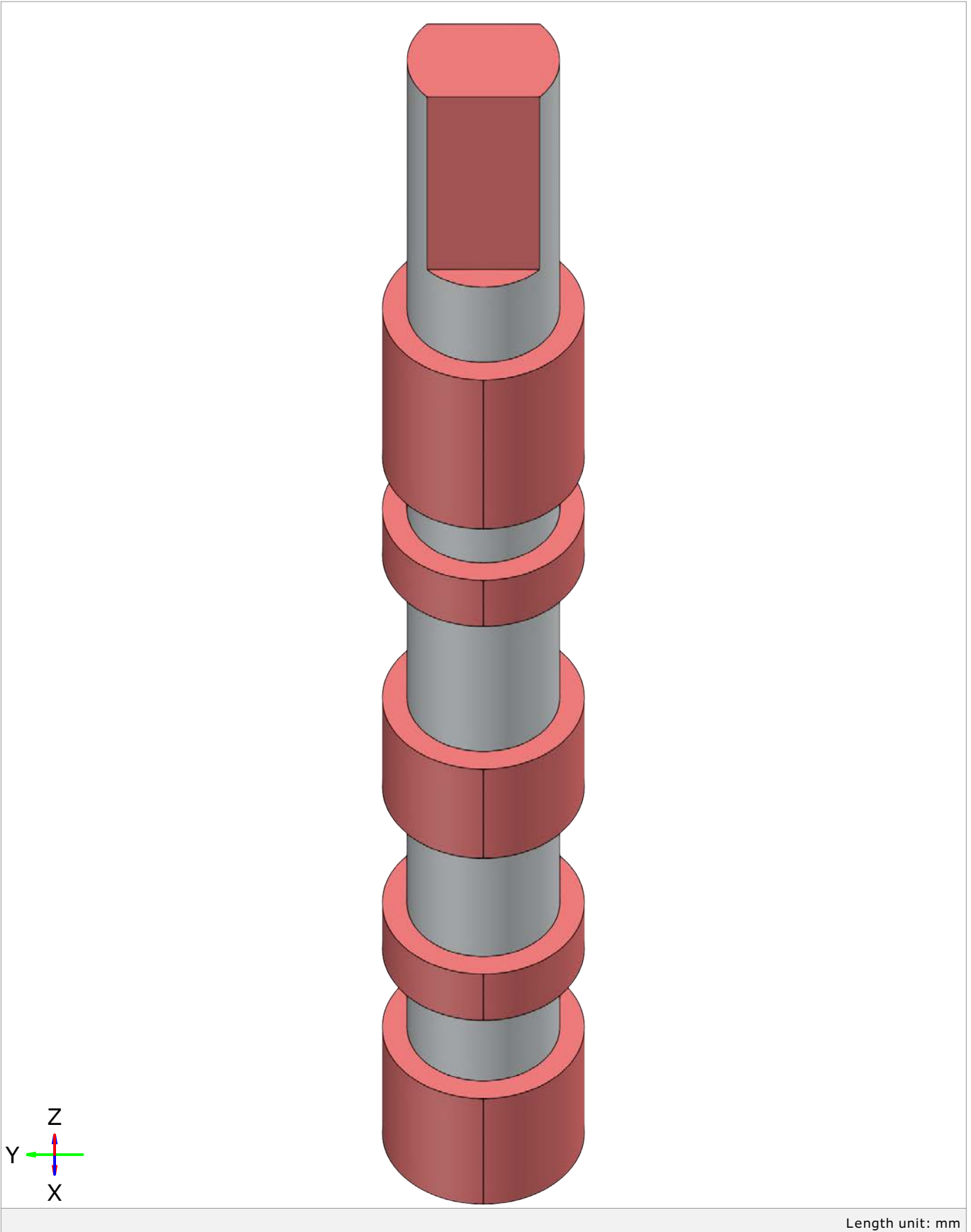
Surface Comparison



Surface Comparison Opposite Side

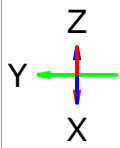
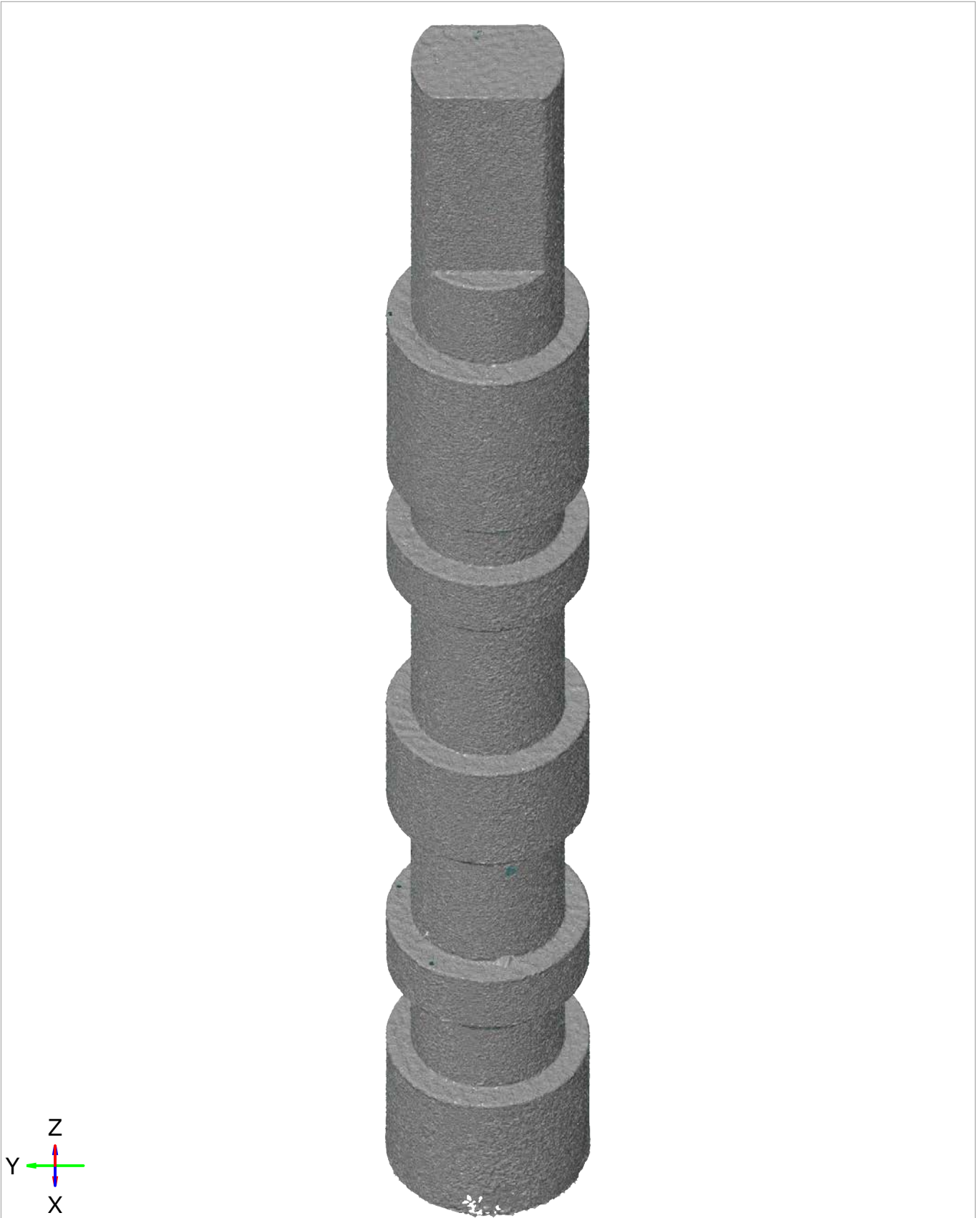


CAD



Length unit: mm

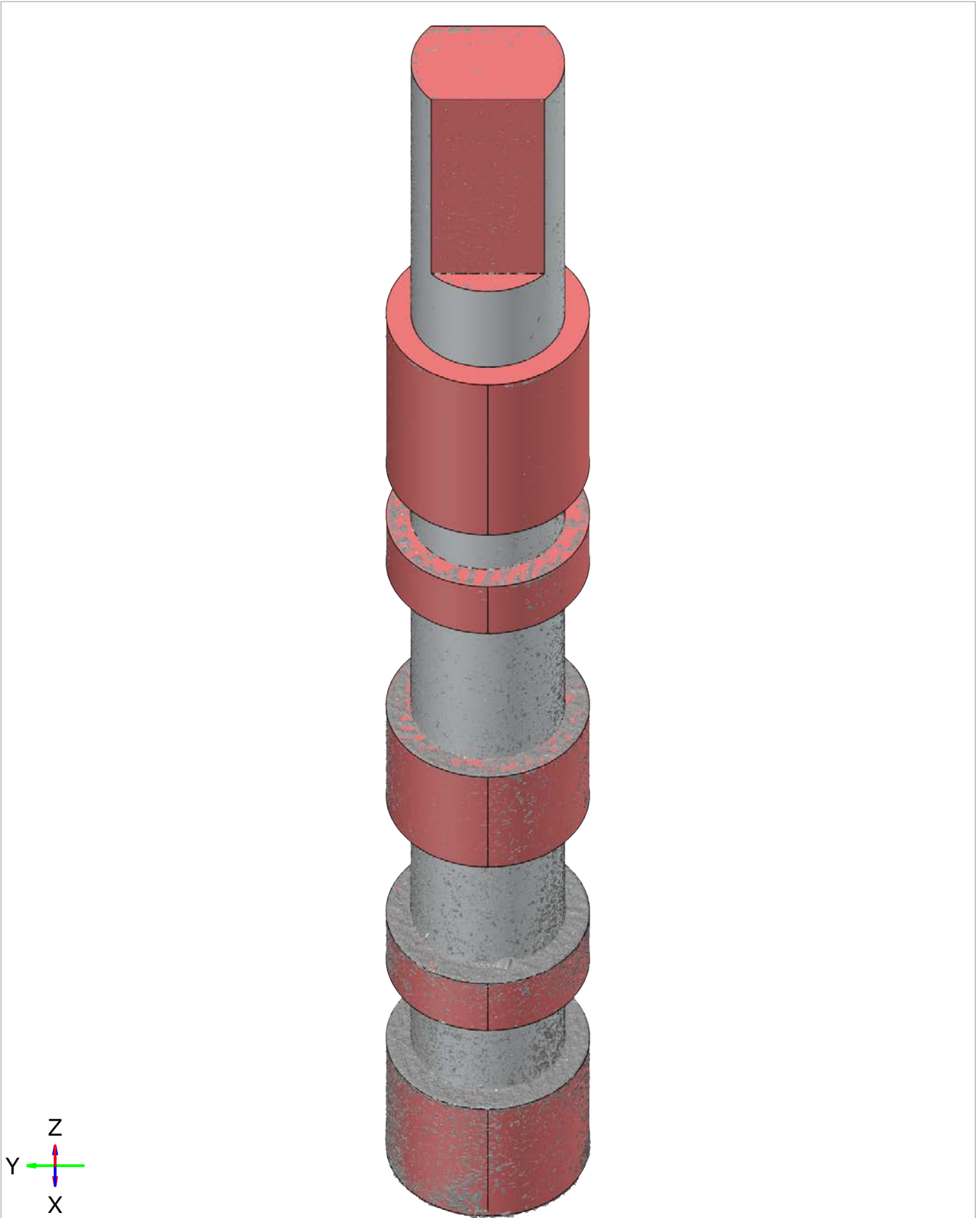
Mesh



Prealignment

Length unit: mm

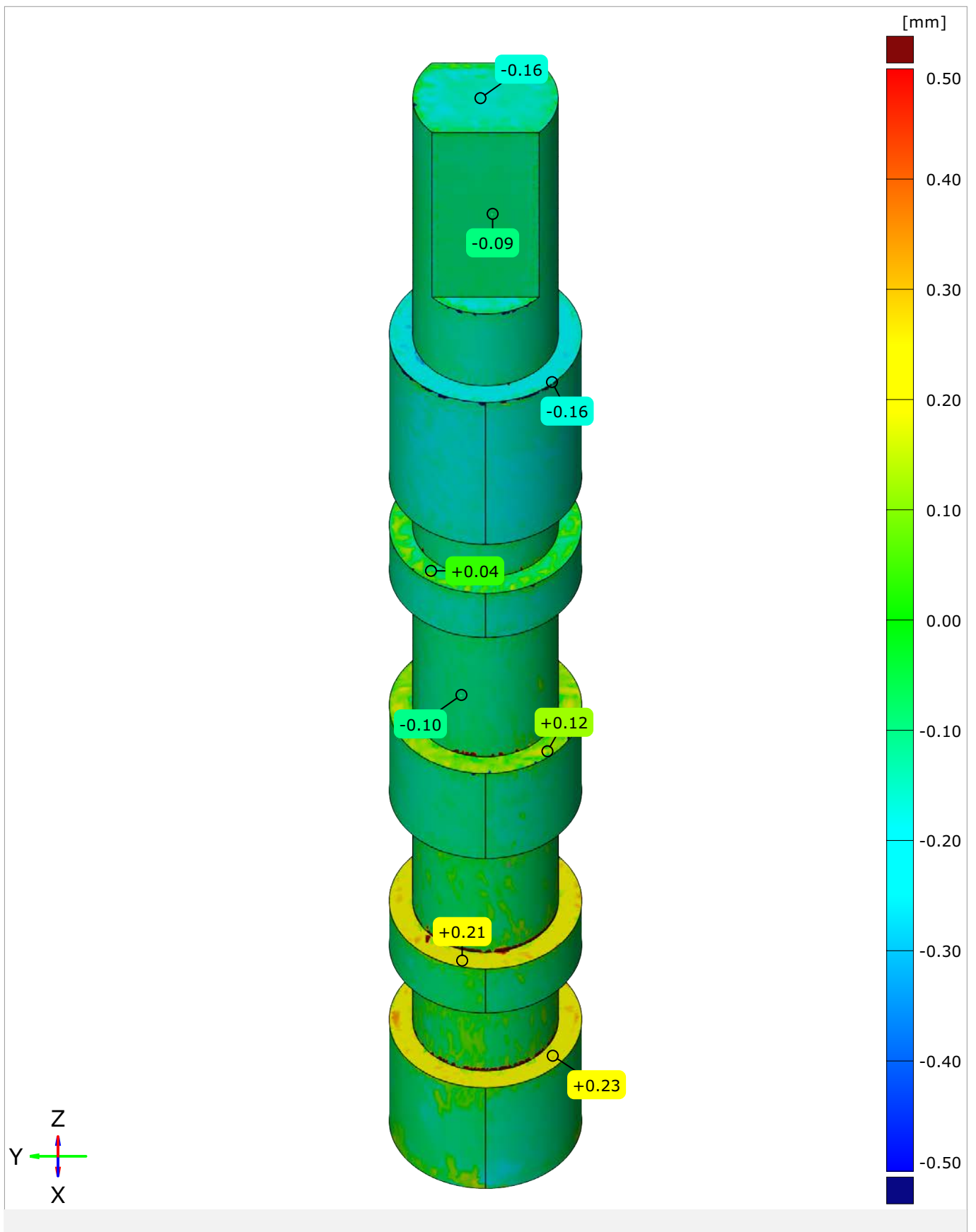
Alignment



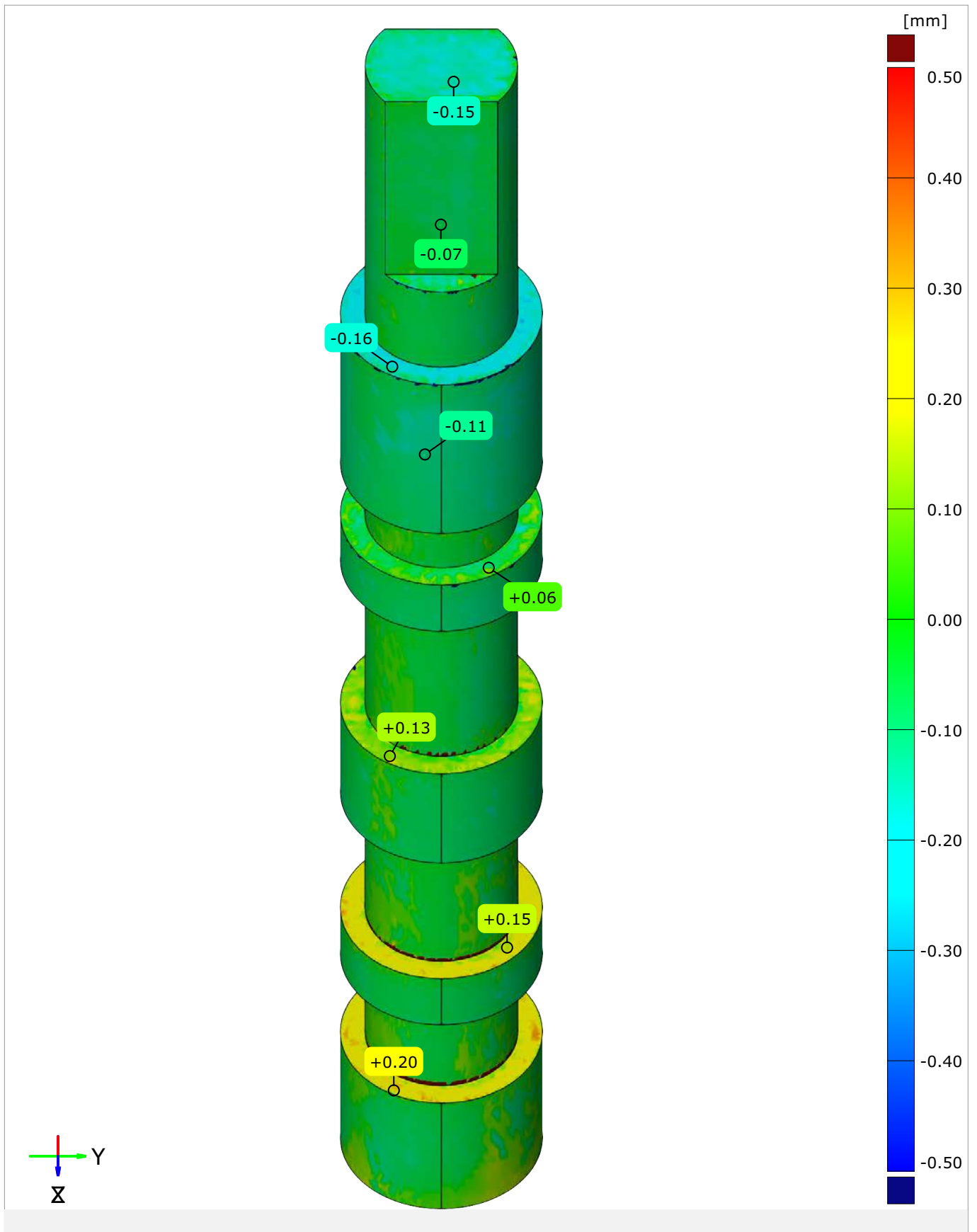
Prealignment

Length unit: mm

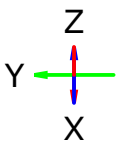
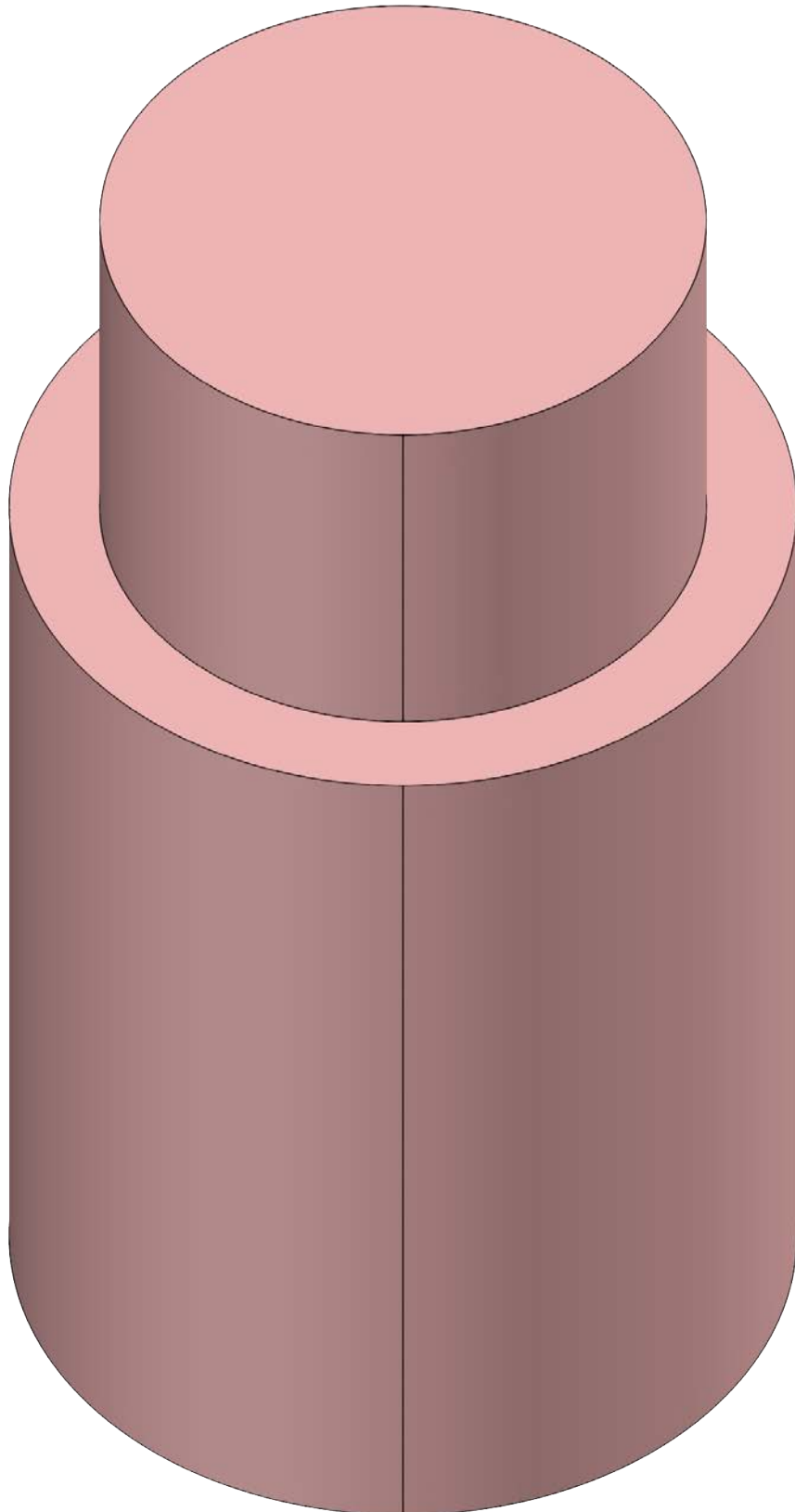
Surface Comparison



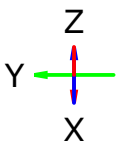
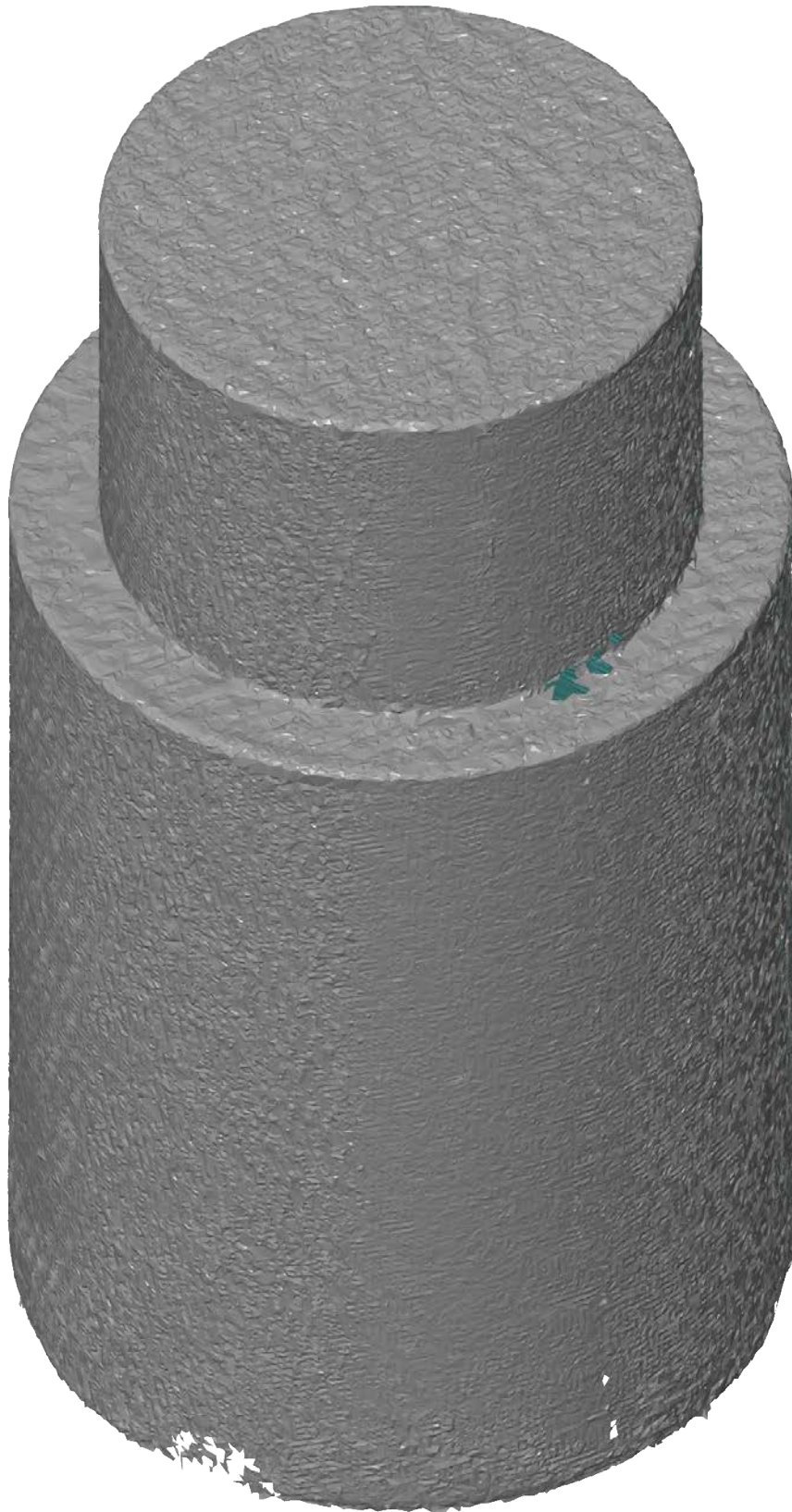
Surface Comparison Opposite Side



CAD



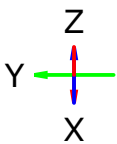
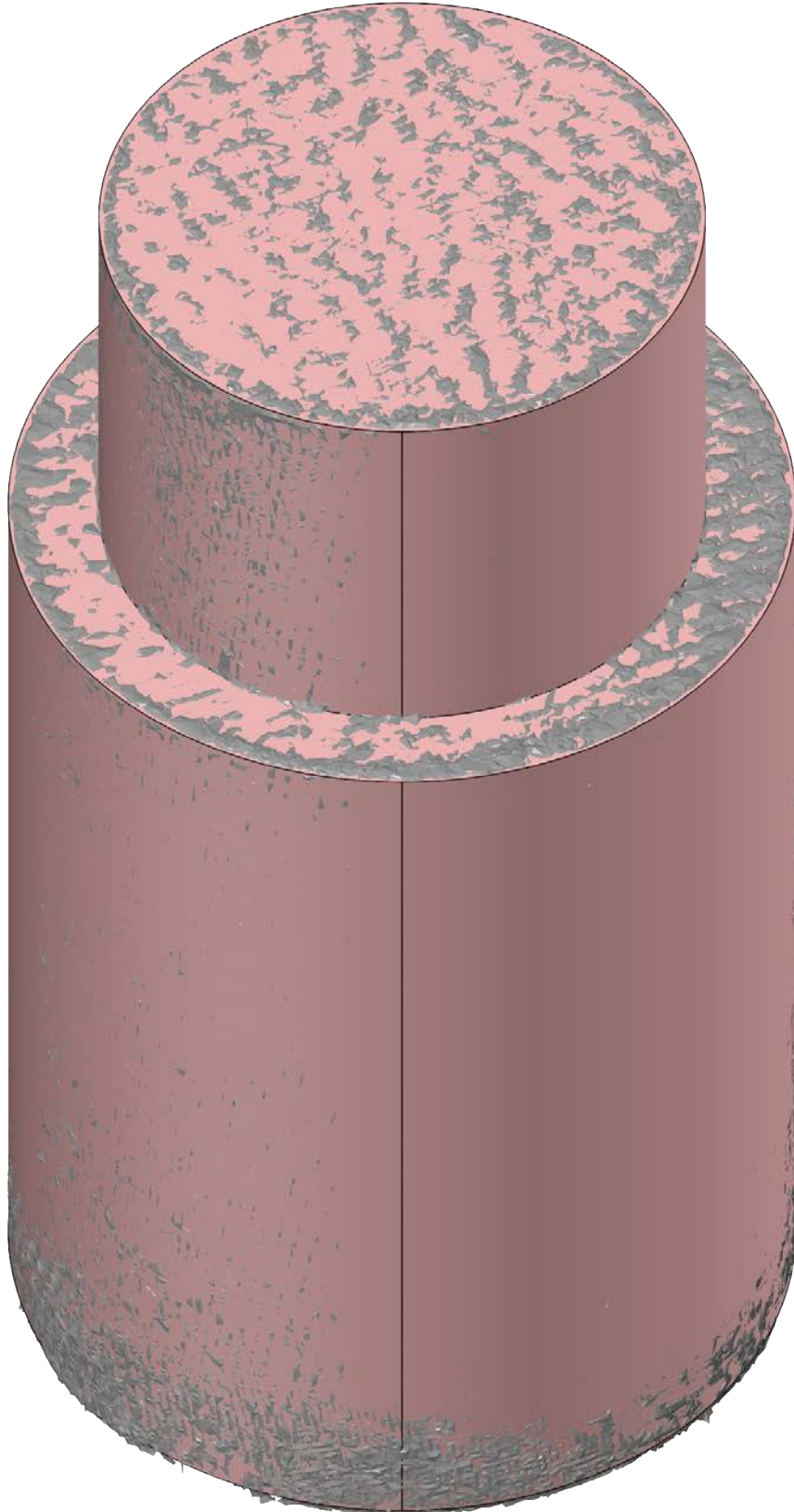
Mesh



Prealignment

Length unit: mm

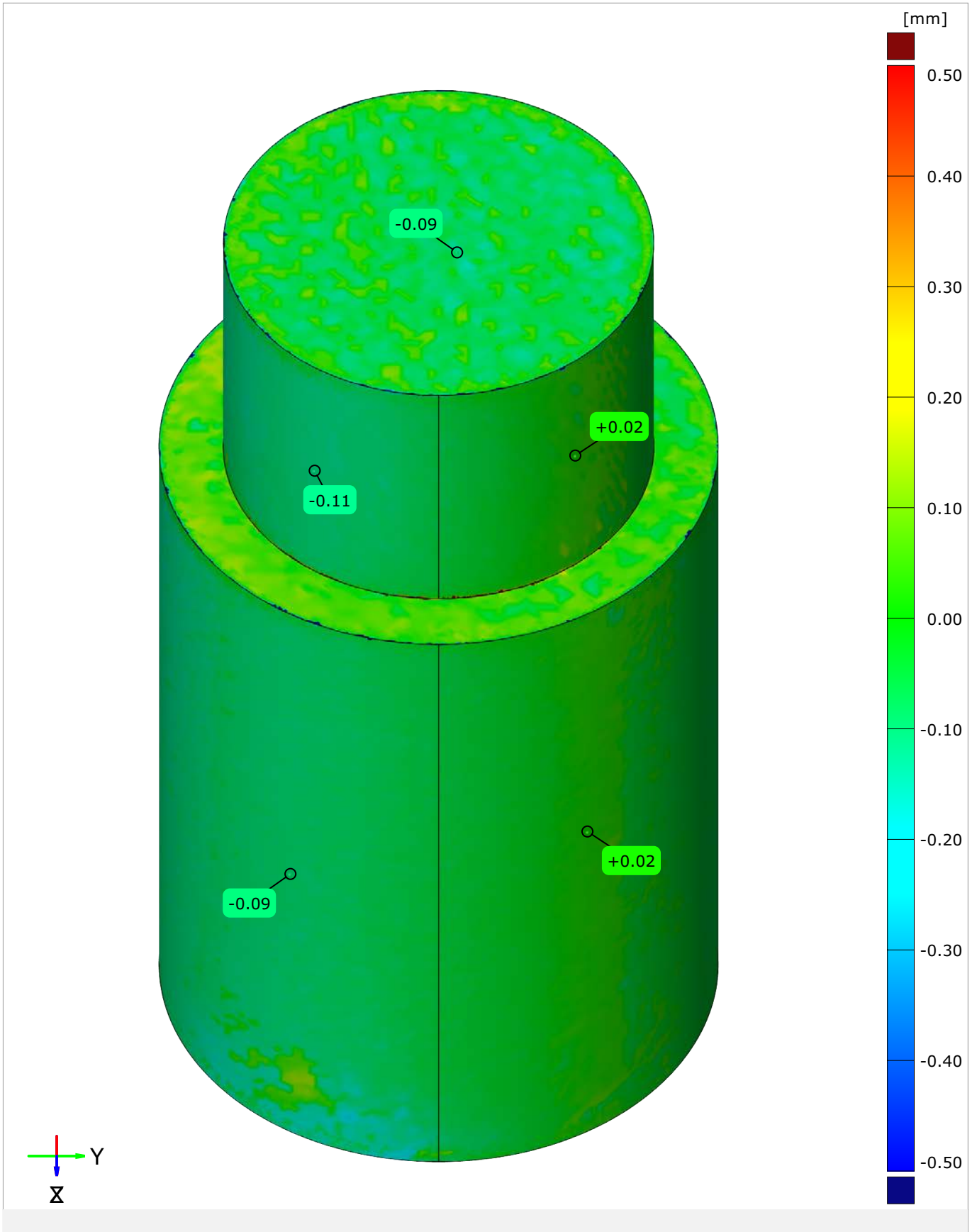
Alignment



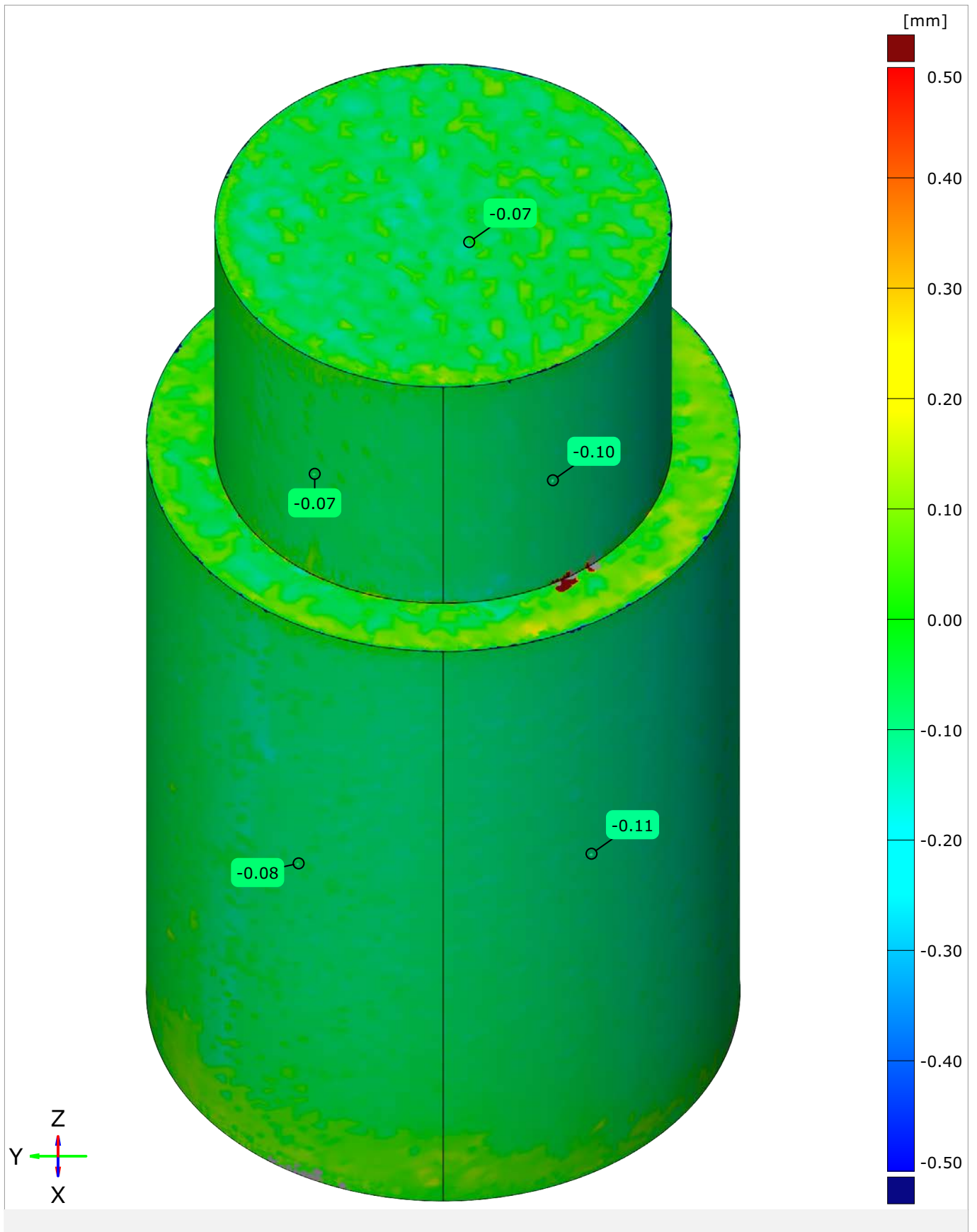
Prealignment

Length unit: mm

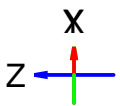
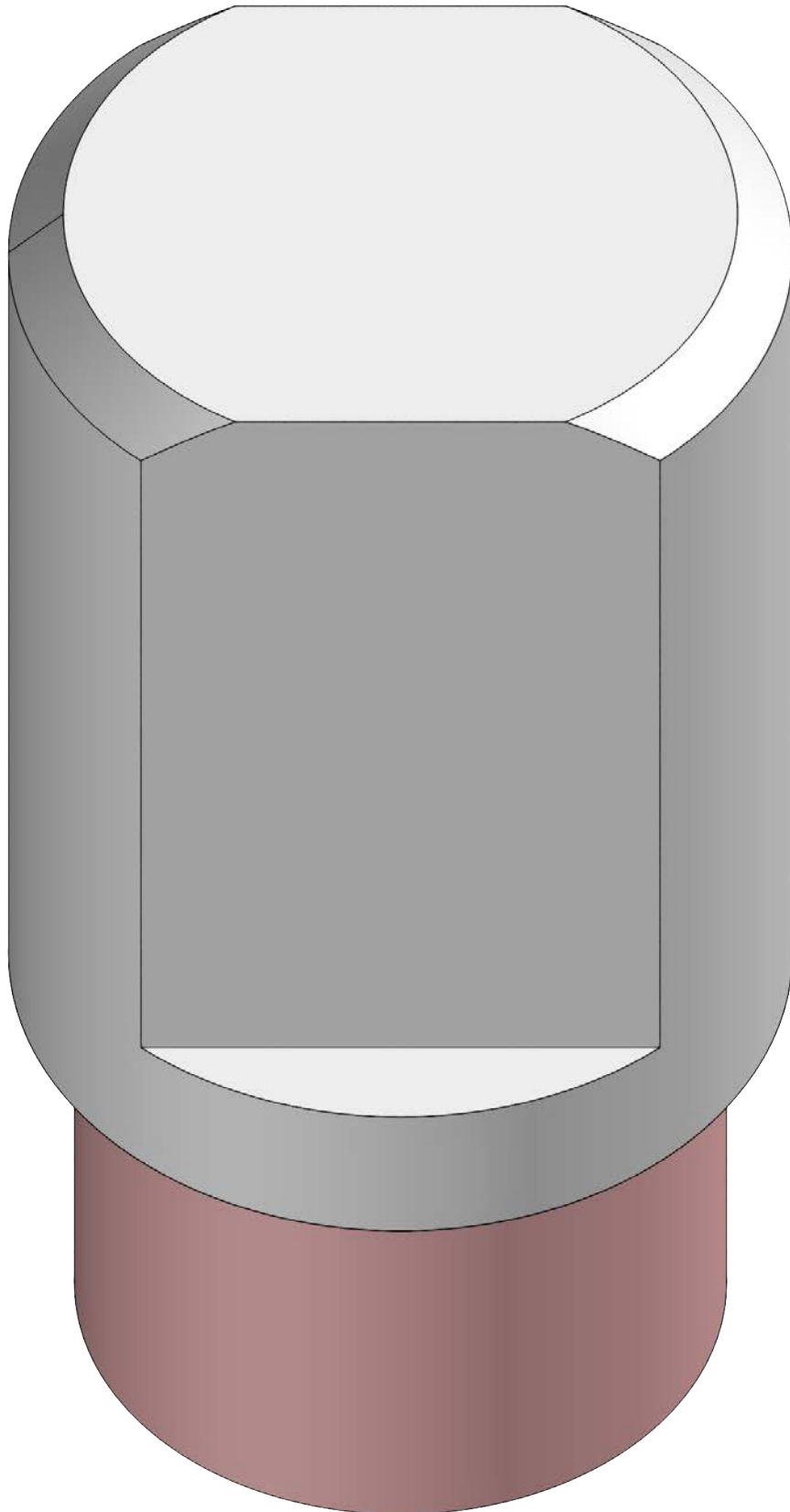
Surface Comparison



Surface Comparison Opposite Side



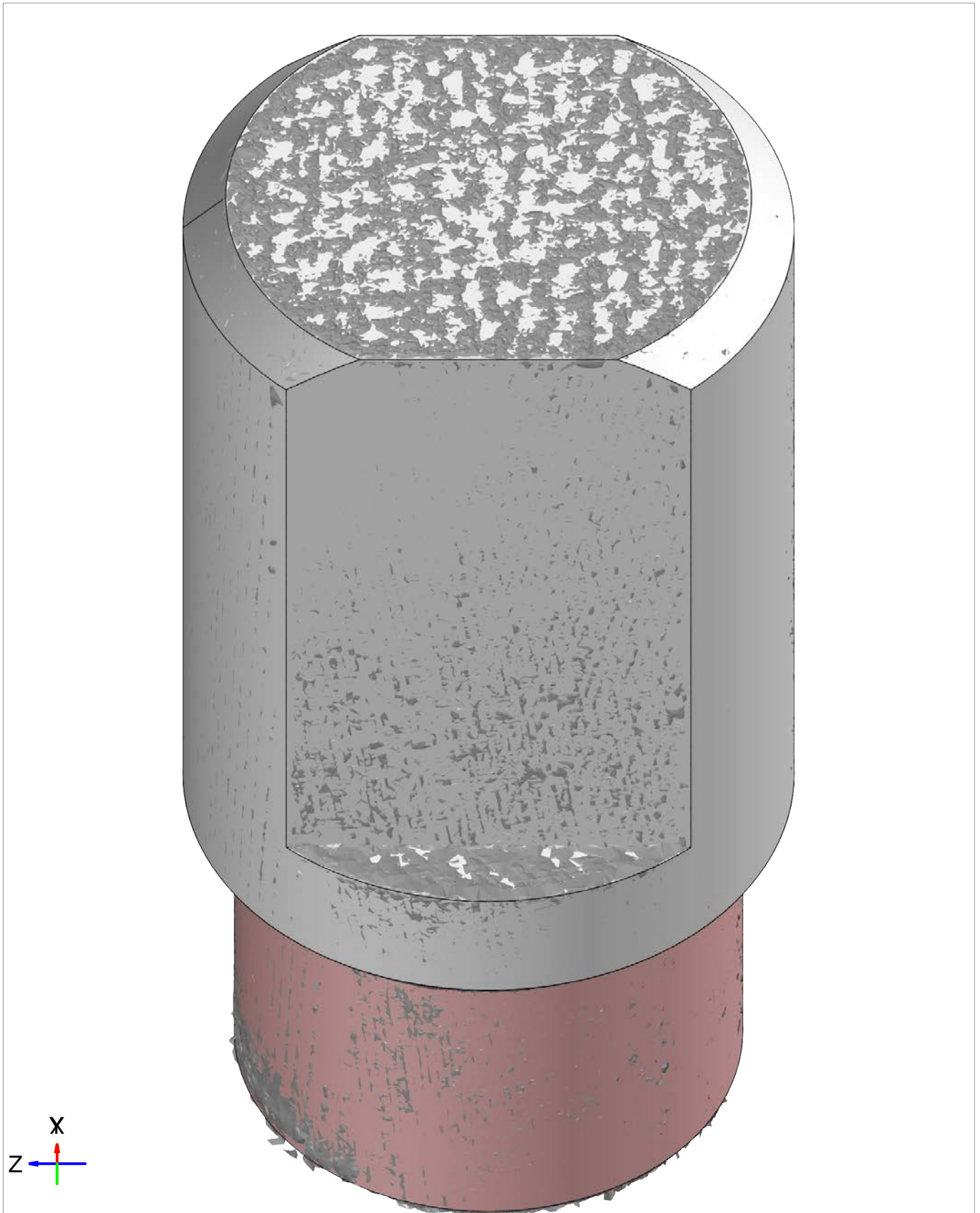
CAD



Mesh



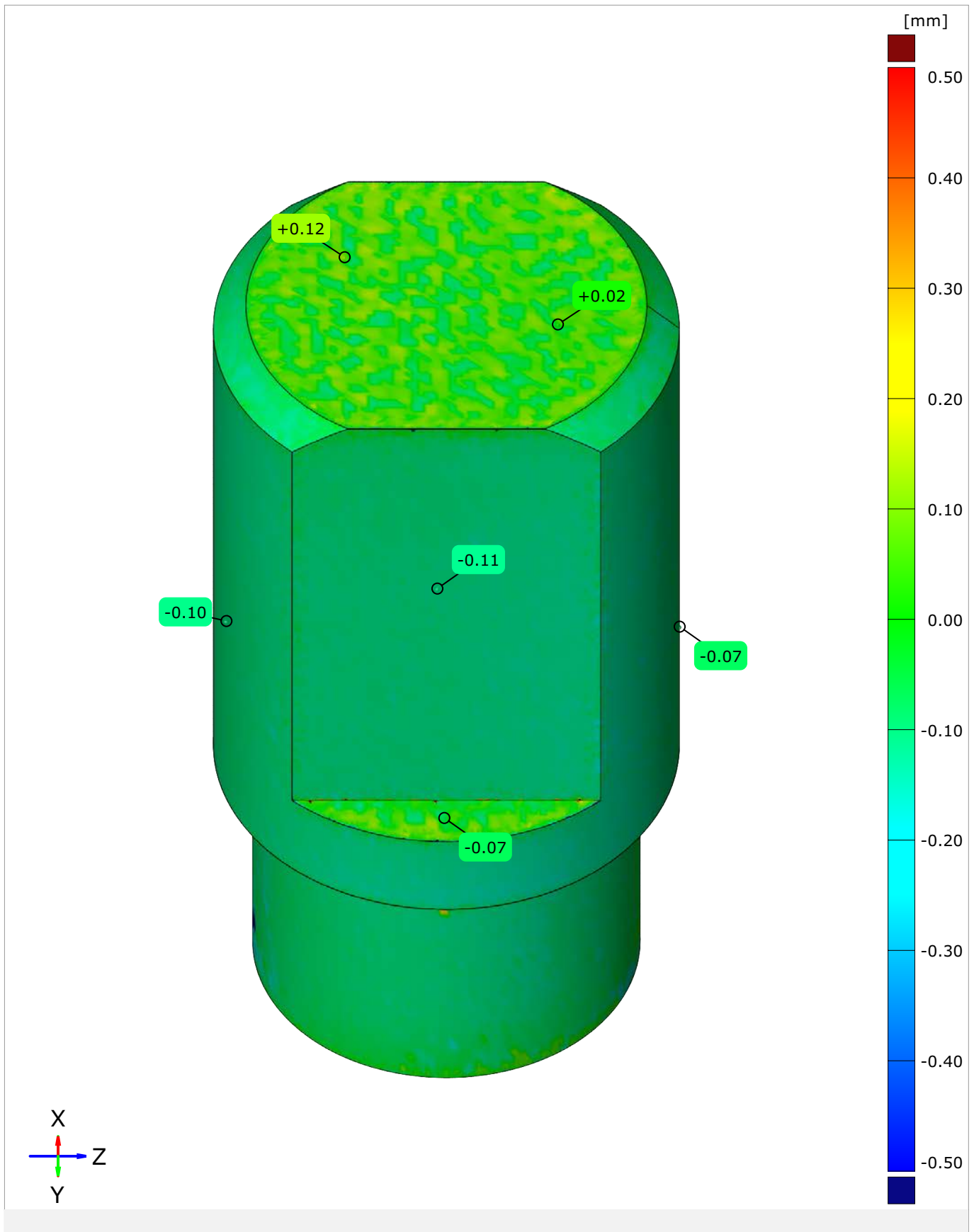
Alignment



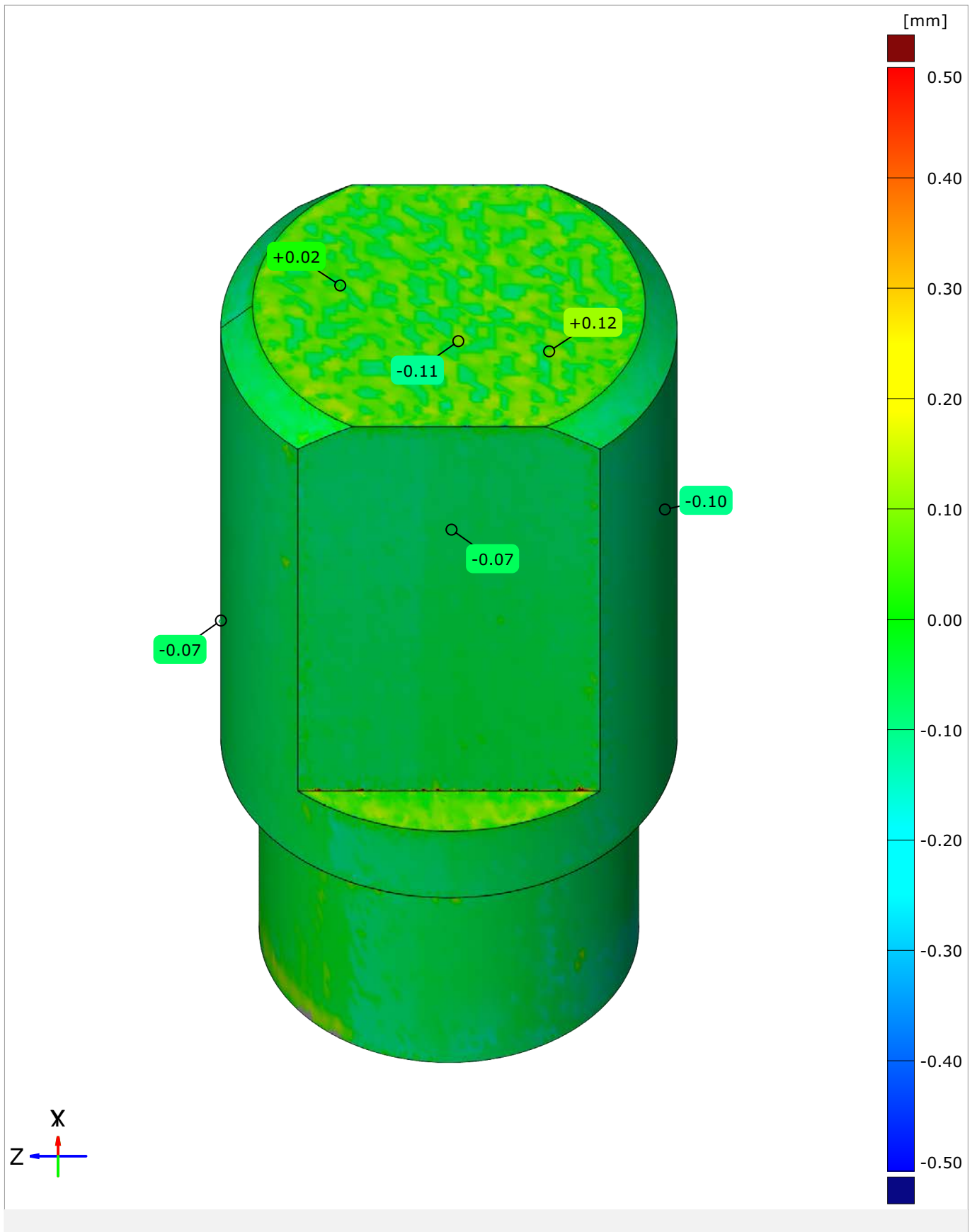
Prealignment

Length unit: mm

Surface Comparison



Surface Comparison Opposite Side



Appendix C

3D Scan Results of Stainless Steel Governor Parts As-Machined



Metal 3D Printed Part

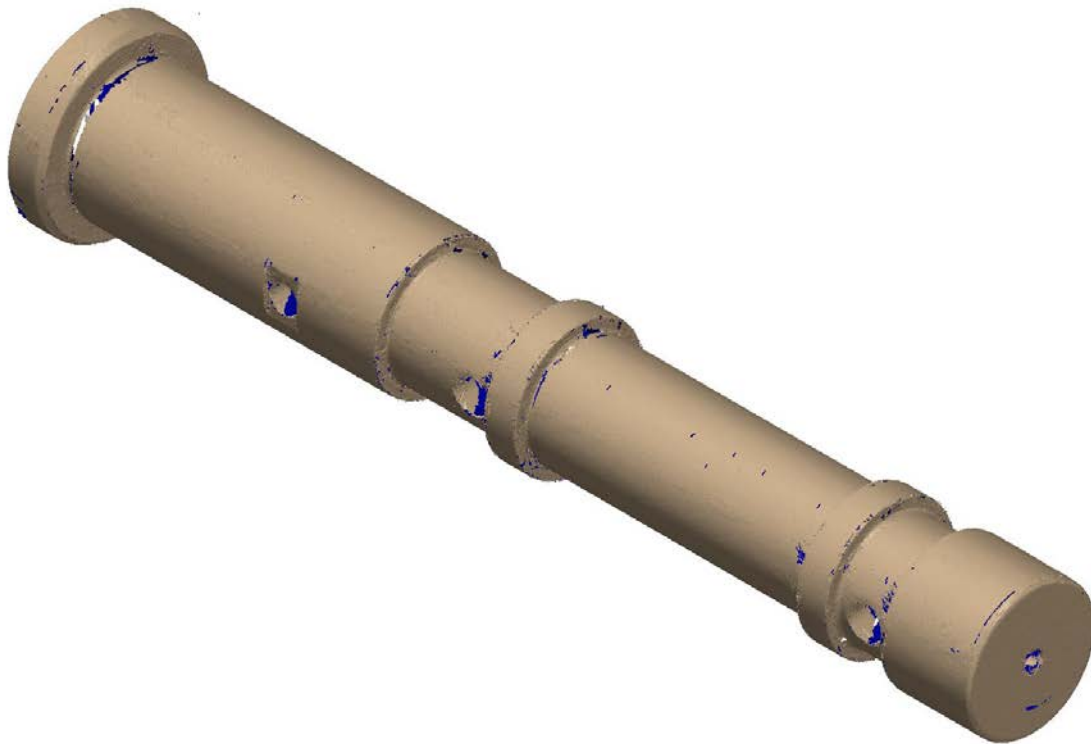
Part number: Cylinder H41365-C

Workspace: Jermyn 3D Printed Material

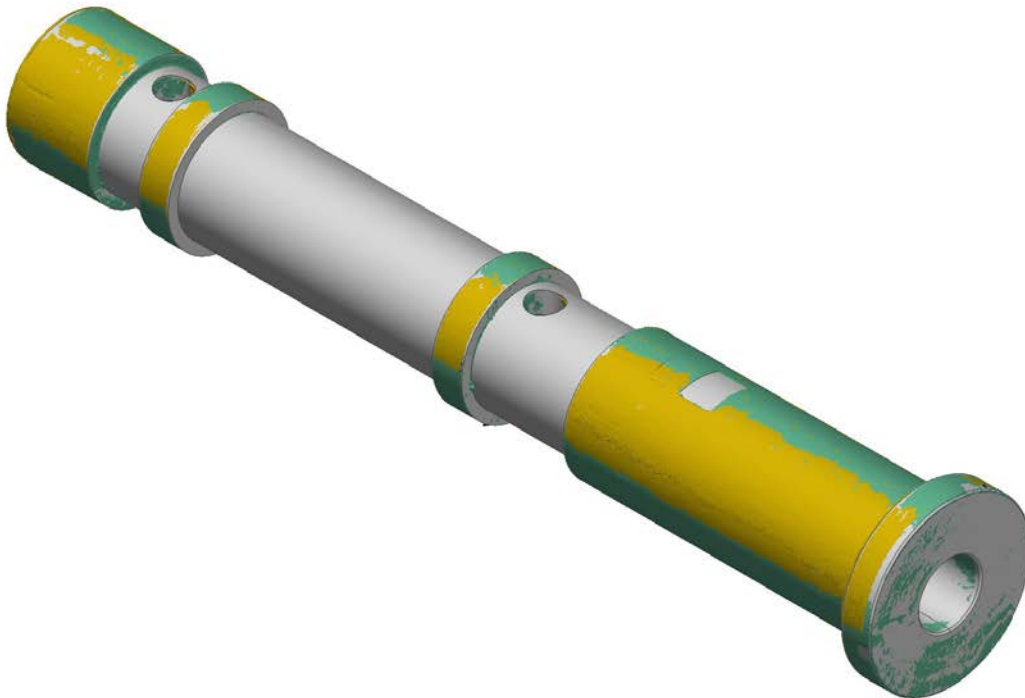
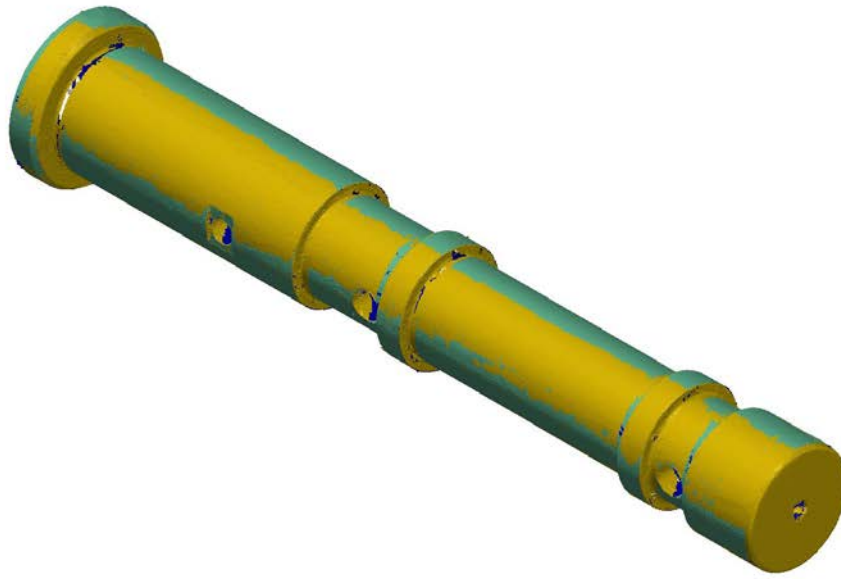
Project: SS Machined 2 - piece 1

Report Author: Chad Paulson

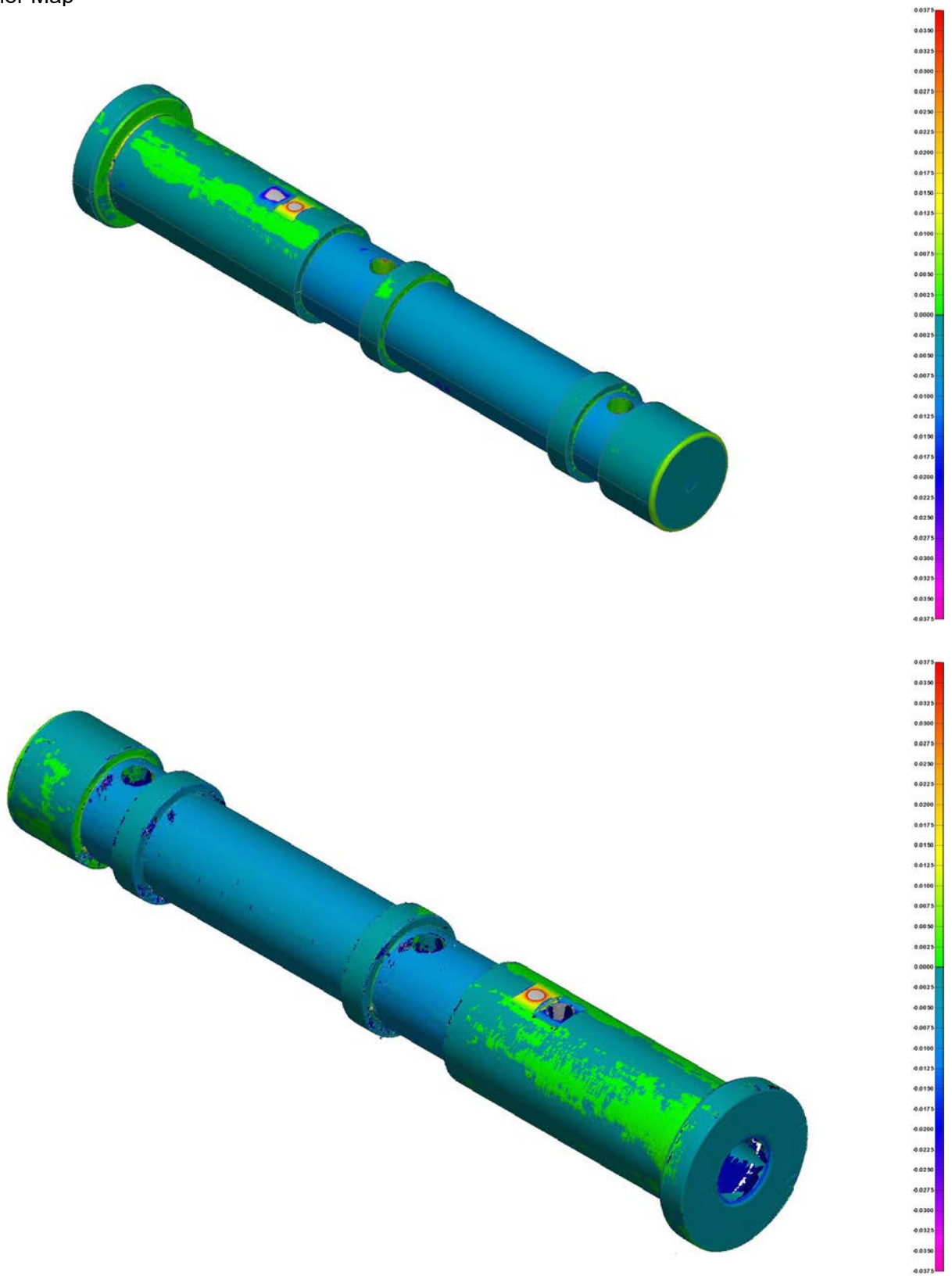
Date: 12/6/2022



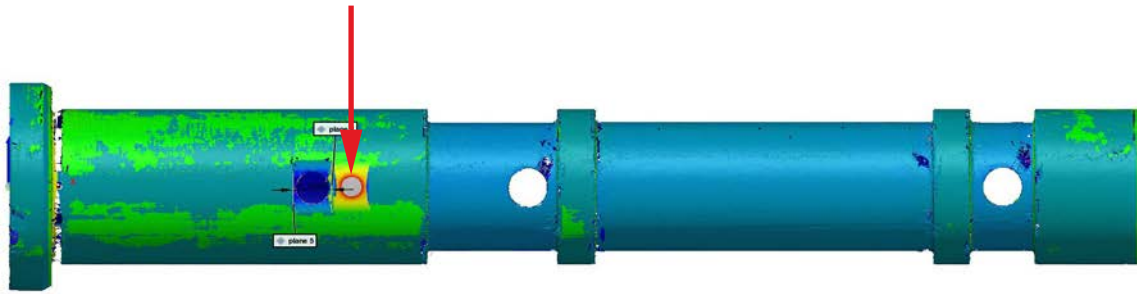
Scan Alignment



Deviation Color Map



Flat Surface on Cylinder in wrong location by 0.1862"



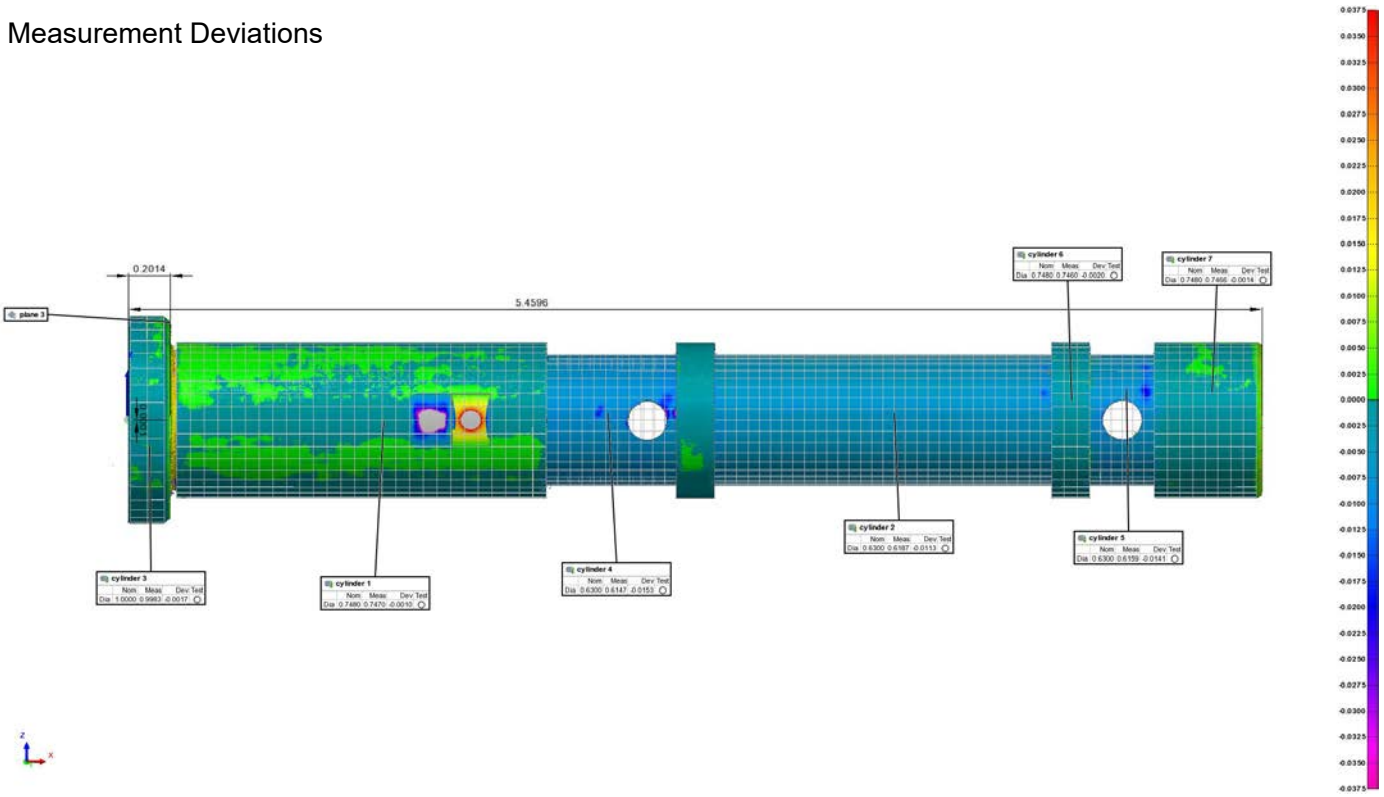
Control View

Control View Name control view 2
 Units Inches
 Coordinate Systems world
 Data Alignments best-fit to ref 1 (alignment group 1), best-fit to ref 2 (alignment group 2), original (alignment group 3)
 All Statistics Total: 1, Measured: 0 (0.0000%), Pass: 0 (0.0000%), Fail: 0 (0.0000%), Warning: 0 (0.0000%)



Object Name	Control	Nom	Meas	Dev
Defect Distance	3D Distance	0.1862		

Measurement Deviations



Control View

Control View Name control view 1
 Units Inches
 Coordinate Systems world
 Data Alignments best-fit to ref 1 (alignment group 1), best-fit to ref 2 (alignment group 2), original (alignment group 3)
 All Statistics Total: 10, Measured: 10 (100.0000%), Pass: 10 (100.0000%), Fail: 0 (0.0000%), Warning: 0 (0.0000%)

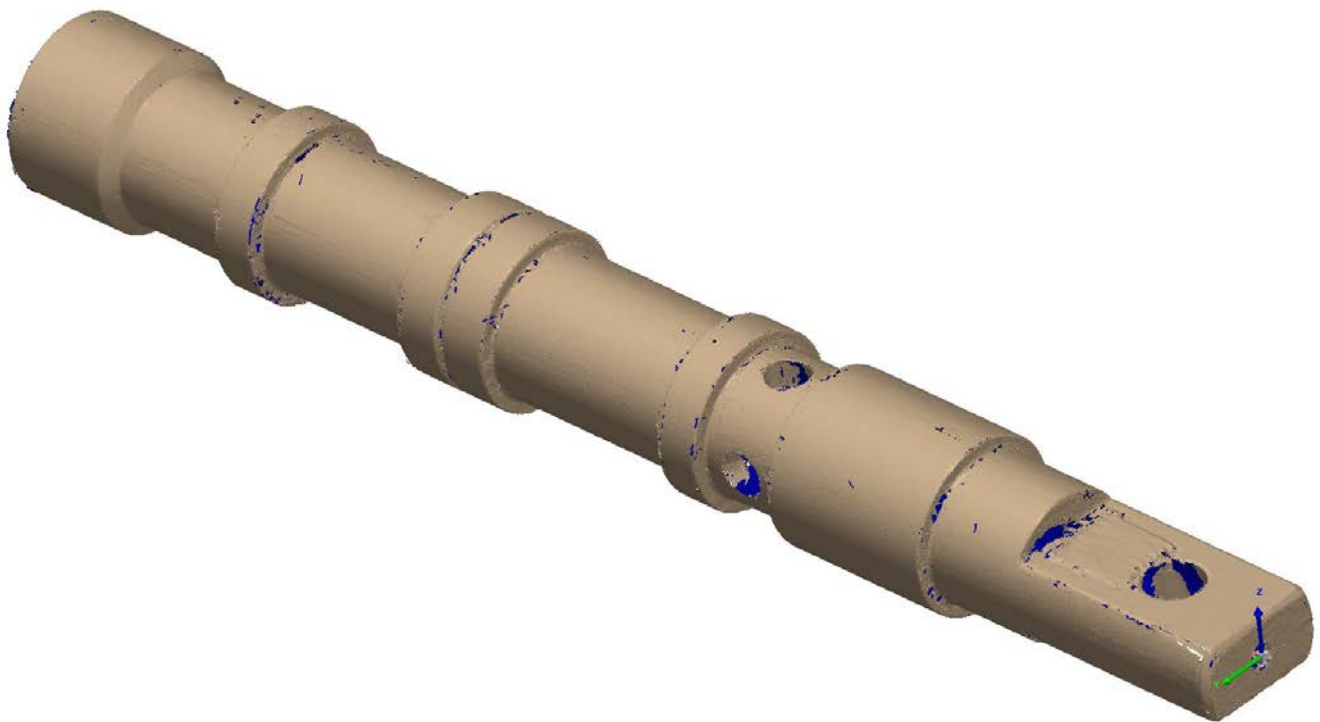
Object Name	Control	Nom	Meas	Dev
cylinder 1	Diameter	0.7480	0.7470	-0.0010
cylinder 2	Diameter	0.6300	0.6187	-0.0113
distance 1	X Distance	5.4630	5.4596	-0.0034
cylinder 3	Diameter	1.0000	0.9983	-0.0017
cylinder 4	Diameter	0.6300	0.6147	-0.0153
cylinder 5	Diameter	0.6300	0.6159	-0.0141
cylinder 6	Diameter	0.7480	0.7460	-0.0020
cylinder 7	Diameter	0.7480	0.7466	-0.0014
distance 2	X Distance	0.2030	0.2014	-0.0016
distance 2	Z Distance	0.0000	0.0001	0.0001



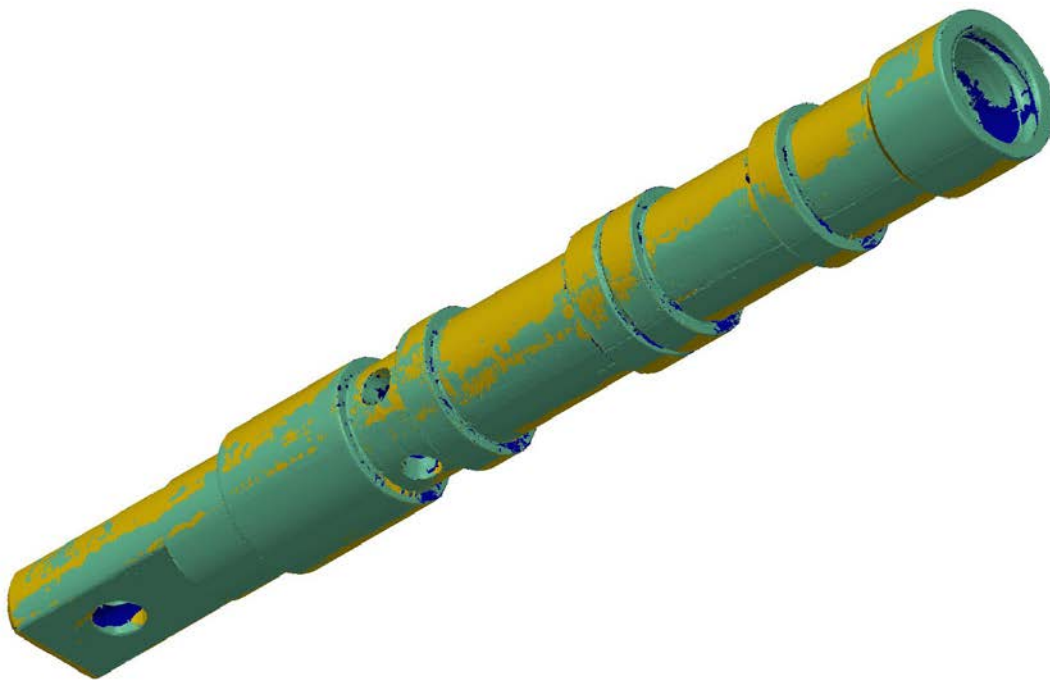
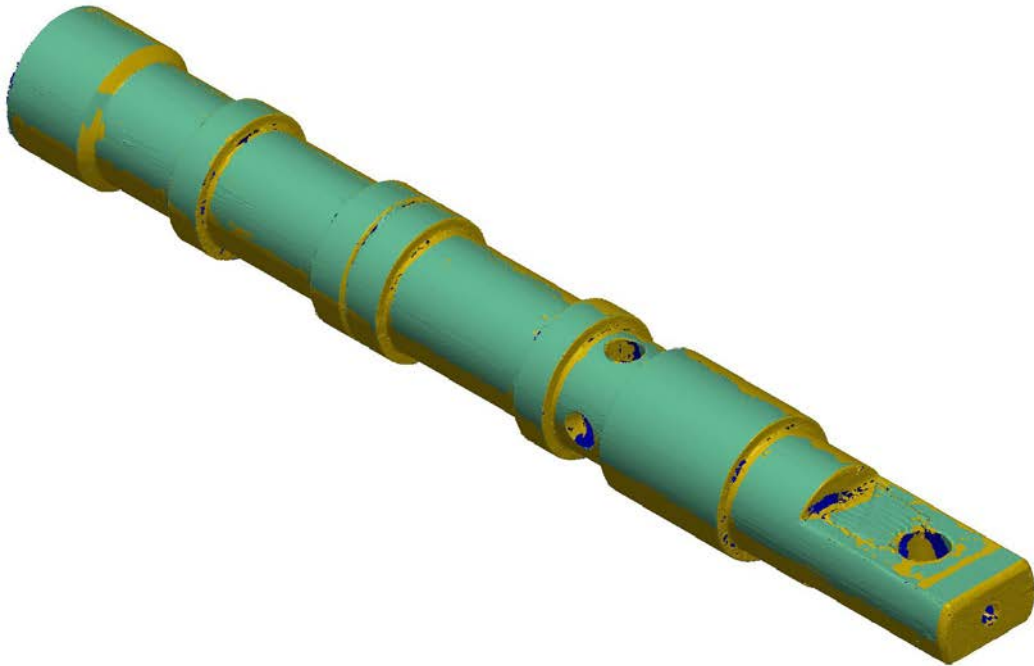
Metal 3D Printed Part

Part number: H41365-D

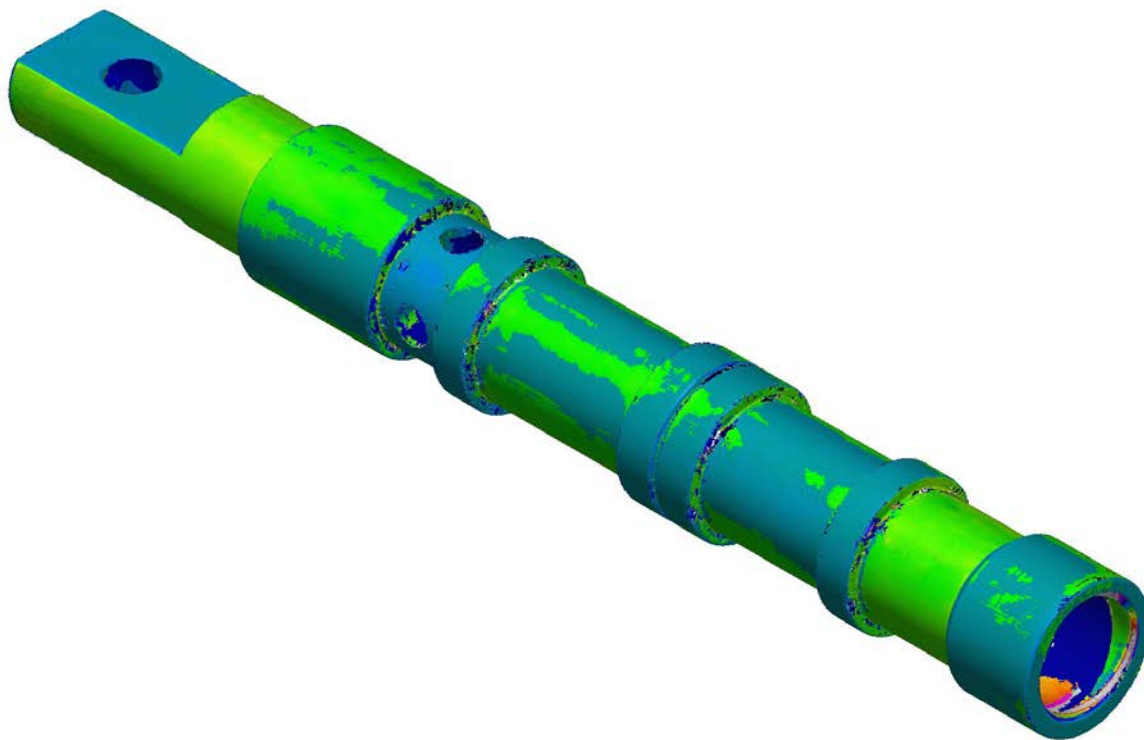
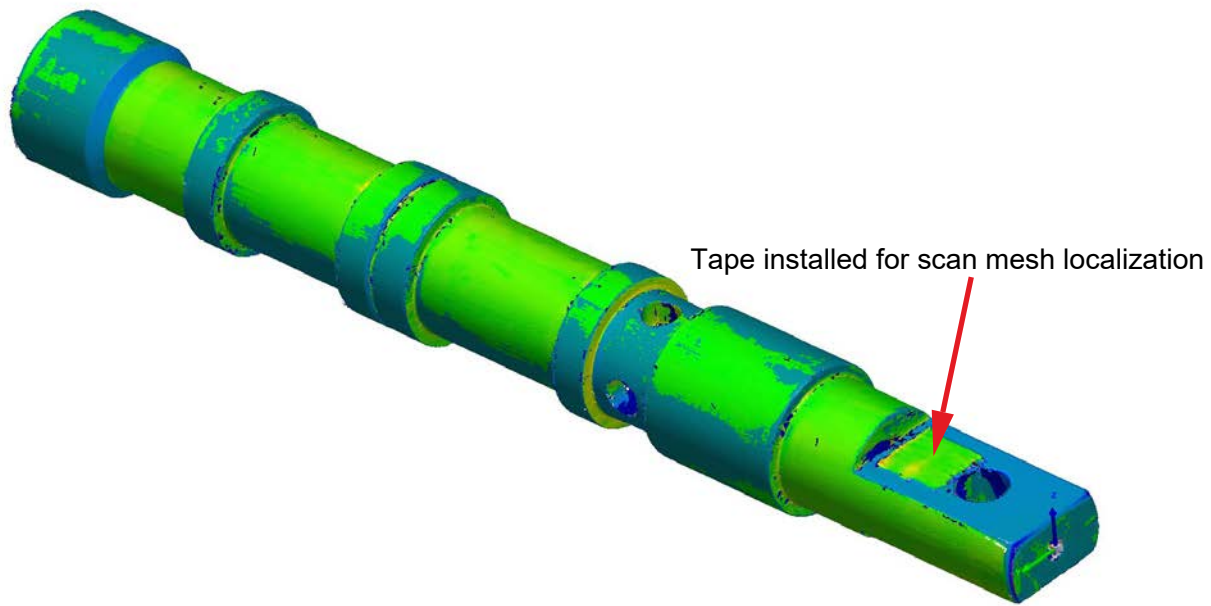
Workspace: Jermyn 3D Printed Material
Project: SS Machined 1 - piece 1
Report Author: Chad Paulson
Date: 12/7/2022



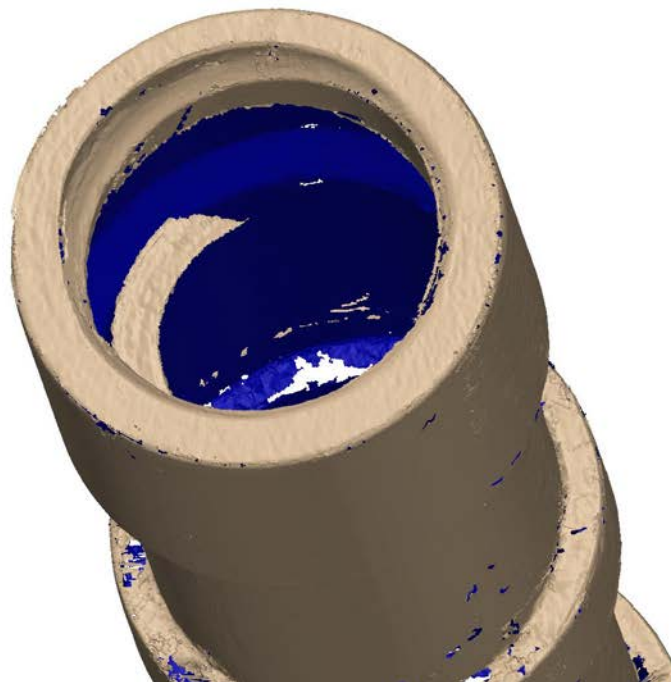
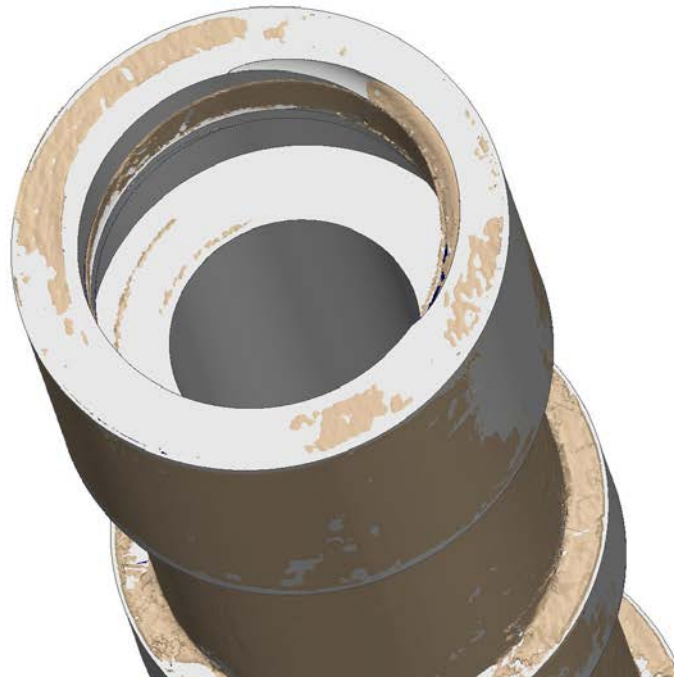
Scan Alignment



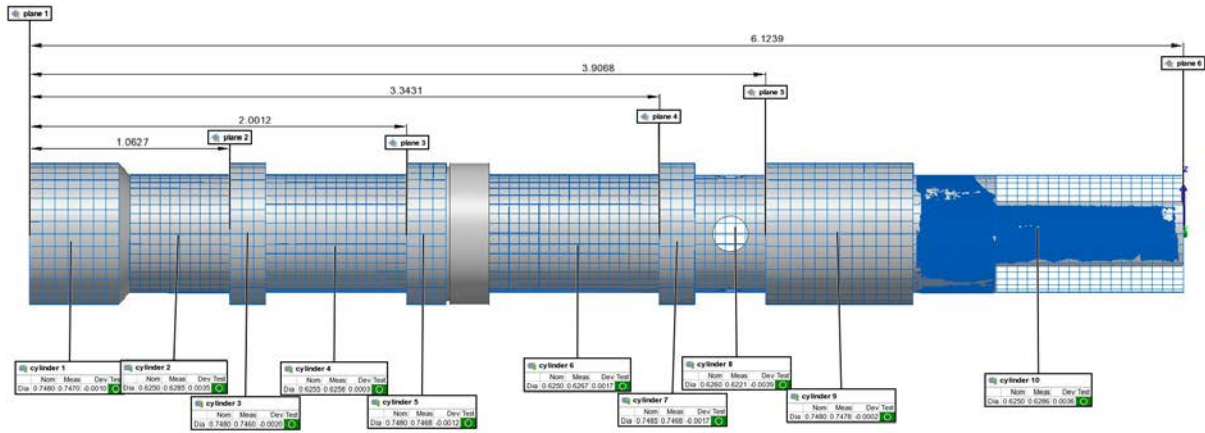
Deviation Color Maps



Threading on the end appears to be rotating the opposite direction.



Measurement Deviations



Control View

Control View Name control view 2
 Units Inches
 Coordinate Systems world
 Data Alignments best-fit to ref 1 (alignment group 2), best-fit to ref 2 (alignment group 3), original (alignment group 5)
 All Statistics Total: 15, Measured: 15 (100.0000%), Pass: 15 (100.0000%), Fail: 0 (0.0000%), Warning: 0 (0.0000%)

Object Name	Control	Nom	Meas	Dev
cylinder 1	Diameter	0.7480	0.7470	-0.0010
cylinder 2	Diameter	0.6250	0.6285	0.0035
cylinder 3	Diameter	0.7480	0.7460	-0.0020
cylinder 4	Diameter	0.6255	0.6258	0.0003
cylinder 5	Diameter	0.7480	0.7468	-0.0012
cylinder 6	Diameter	0.6250	0.6267	0.0017
cylinder 7	Diameter	0.7485	0.7468	-0.0017
cylinder 8	Diameter	0.6260	0.6221	-0.0039
cylinder 9	Diameter	0.7480	0.7478	-0.0002
cylinder 10	Diameter	0.6250	0.6286	0.0036
distance 6	X Distance	1.0655	1.0627	-0.0028
distance 7	X Distance	2.0030	2.0012	-0.0018
distance 8	X Distance	3.3435	3.3431	-0.0004
distance 9	X Distance	3.9090	3.9068	-0.0022
distance 10	X Distance	6.1250	6.1239	-0.0011

Appendix D

Aluminum Bronze L-PBF Development Report



Requisition/Purchase Number: 4000186100

Aluminum Bronze L-PBF Development

Elementum 3D
400 Young Ct., Unit 1
Erie, CO 80516

2022.08.26



TABLE OF CONTENTS

LIST OF FIGURES	3
LIST OF TABLES	3
INTRODUCTION	4
WORK PERFORMED DURING PERIOD	4
PROBLEMS AND CORRECTIVE ACTION	8
CONCLUSION	10

LIST OF FIGURES

Figure 1. E3D aluminum bronze initial density development build4

Figure 2. Third aluminum bronze dev build layout5

Figure 3. SEM microscopy images (A) before heat treatment and (B) after heat treatment.....6

Figure 4. Final build printing individual test specimens7

Figure 5. (A) Governors build and (B) mechanical test specimens build8

Figure 6. Part delamination due to lack of adhesion to build plate9

Figure 7. Horizontal specimens printing on IN718 build plate9

LIST OF TABLES

Table 1. Volumetric energy density and respective relative density measurements5

Table 2. Aluminum bronze L-PBF measured properties.....7

Introduction

The United States Bureau of Reclamation (USBR) is interested in aluminum bronze alloy material development for additive manufacturing (AM, also known as 3D printing). USBR is particularly interested in the hardness of these materials for hydraulic applications. Elementum proposed selecting an aluminum bronze alloy for concept testing under a Phase I development project. Phase I of this project included: raw material selection and sourcing, 3-4 iterations of development builds on an EOS M290 DMLS machine, and evaluation of density, hardness, modulus, and microstructure. Additionally, Elementum 3D was to manufacture deliverable test components for USBR using the selected material and developed processing parameters.

Work Performed During Period

Elementum 3D began with sourcing an aluminum bronze alloy with appropriate particle size distribution for use in Laser Powder Bed Fusion (L-PBF) applications. E3D procured 330 pounds of a pre-alloyed aluminum bronze material (UNS C95300) for use in the development project. E3D started the development with an initial build of 30 density cubes with a design of experiments (DOE) that altered the laser power, laser speed, and hatch spacing process parameters. The initial DOE tested a volumetric energy density range from 78.1 [J/mm³] to 133.9 [J/mm³]. These initial cubes are shown below in Figure 1.

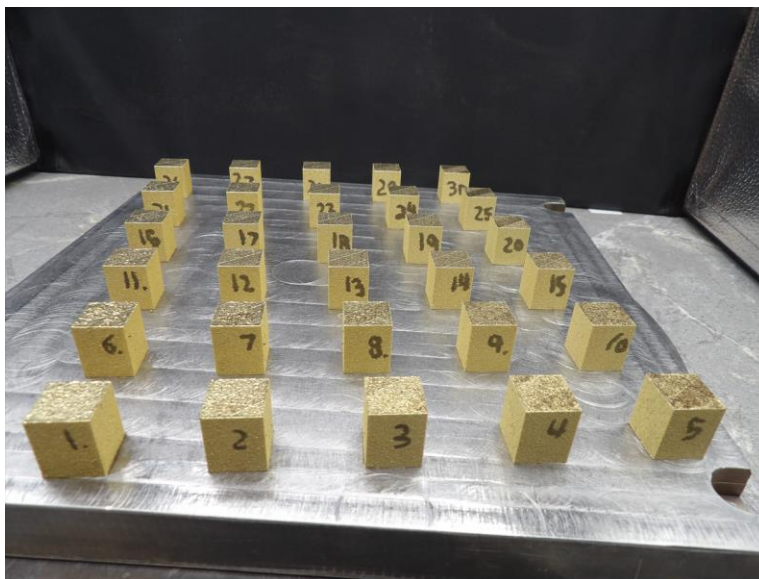


Figure 1. E3D aluminum bronze initial density development build

Elementum 3D performed the density measurements of the 30 cubes in-house using an analytical balance and calculations derived from Archimedes' principle of water displacement per

ASTM B311-17. The density results indicated a large processing window with relatively consistent measured densities ranging from 98.41% to 99.87%. The second iterative density build included a set of 21 cubes which were also processed by Elementum 3D using their in-house measurement equipment. The data from the first two builds allowed Elementum 3D to down select three process parameters to compare. Figure 2 below illustrates the third build which was set up to test the three selected parameters sets and had additional specimens aimed to develop contour parameter settings for improved surface finish.

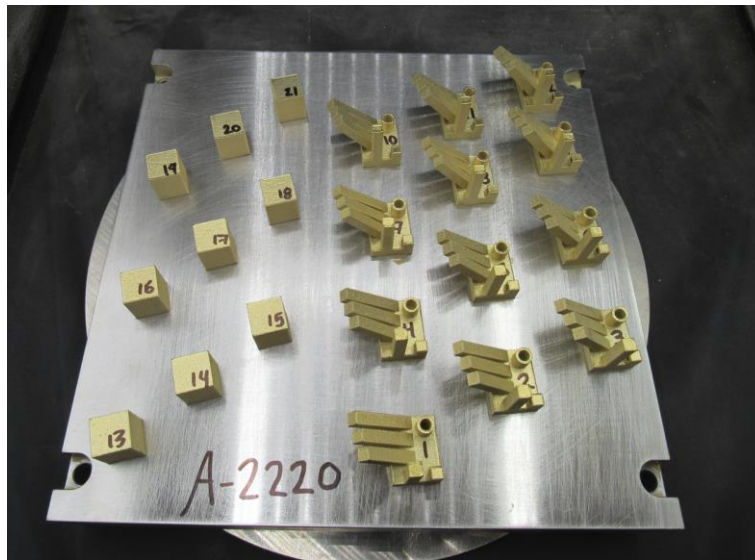


Figure 2. Third aluminum bronze dev build layout

Table 1. Volumetric energy density and respective relative density measurements

Volumetric Energy Density [J/mm ³]	Relative Density [%]
72.1	99.92
78.1	99.93
91.1	99.91

Table 1 above shows the averaged relative density results for each of the selected parameter sets tested in the third development build. Optical density measurements were also completed by Elementum 3D via their Keyence optical microscope and measured 99.9% density. These measurements, however, are for reference only as the Keyence microscope was not calibrated at the time of the analysis. Elementum 3D selected the parameter set with the lowest volumetric energy density to avoid potential issues with overheating due to the material's low thermal conductivity. Additionally, E3D evaluated the surface finish of the different specimens from the third build and selected the contour parameters which provided the best improvement in surface

finish. The surface finish measurements were completed by E3D using a calibrated profilometer. Further optimization of the contour process parameters could be performed to improve the surface finish, but the initial results allowed E3D to move forward with a parameter set that would be used to produce the deliverables for USBR.

After completion of the preliminary process parameter development Elementum 3D proceeded with developing the heat treatment required to achieve the desired material hardness. The heat treatment studies were performed in-house using Elementum 3D's high temperature argon furnace. Elementum 3D initially worked through numerous single stage heat treatments which were aimed at reducing the complexity of the thermal processing steps. Development included varying the furnace temperature, varying the hold times, and performing either a water quench, air cool, or furnace cool. These single stage heat treatments resulted in measured hardness values that were either higher or lower than the desired hardness. Therefore, Elementum 3D proceeded with development of a multi-step heat treatment strategy which resulted in achieving the desired material hardness values. The first step of the developed heat treatment includes holding the parts at 860°C for 2 hours per inch of section thickness followed by a water quench. The second step of the heat treatment includes holding the parts for 3 hours at 675°C followed with a furnace cool. Figure 3 below compares the microstructure of the printed parts (A) before and (B) after heat treatment. In the as-printed state (A) there are visible columnar grains which are oriented in the LPBF print direction. After completion of the thermal processing (B) the grains are more equiaxed. Along with achieving the desired average 78 HRB hardness the thermal processing will also lead to more isotropic physical and mechanical properties due to the modified grain structure.

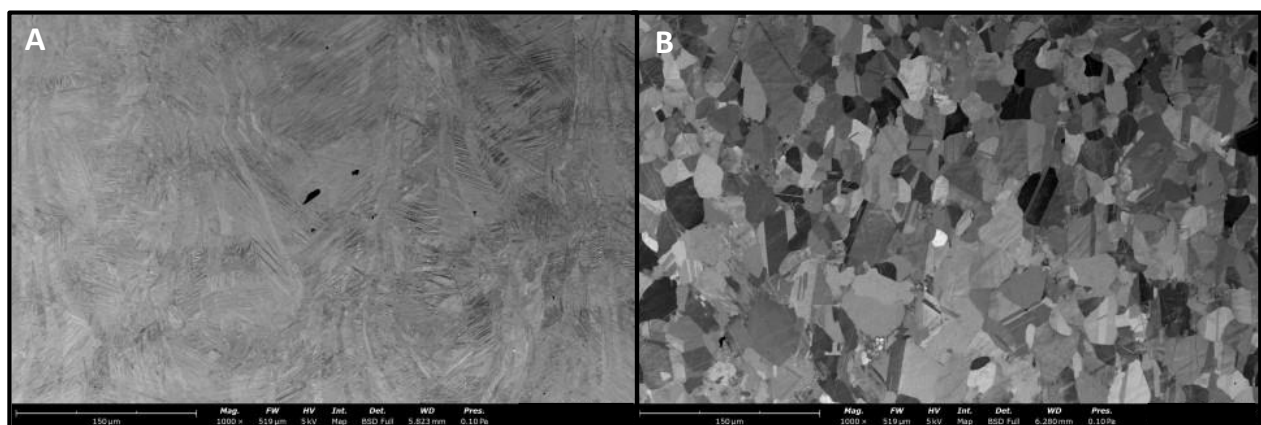


Figure 3. SEM microscopy images (A) before heat treatment and (B) after heat treatment at 1000x magnification

Additional testing performed in-house by Elementum 3D includes modulus testing by using the calibrated Olympus Modulus Device. This equipment measures the compression velocity

and shear velocity of a printed sample at various thicknesses to calculate Poisson’s ratio, Young’s (E) Modulus, Shear (G) Modulus, and Bulk (K) Modulus. Table 2 below outlines the average values recorded using this equipment.

Table 2. Aluminum bronze L-PBF measured properties

Poisson’s Ratio	Young’s (E) Modulus [GPa]	Shear (G) Modulus [GPa]	Bulk (K) Modulus [GPa]
0.328	117.5	45.8	121.6

With the initial process parameters and thermal processing development completed Elementum 3D was able to proceed with manufacturing the remaining deliverables. The deliverables included 6 slinger rings, 4 governors, and 19 mechanical test specimens which were completed in 8 individual builds. Six of those individual builds were used to complete the slinger ring geometry which, as shown below in Figure 4, requires a full EOS M290 build plate due to its large diameter.

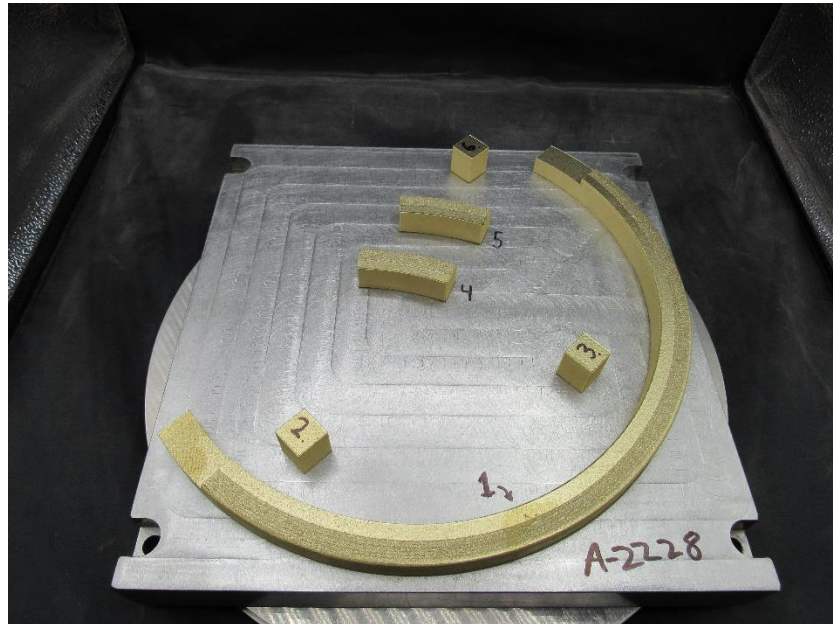


Figure 4. Slinger ring build layout

The remaining two builds with successful deliverable components can be seen below in Figure 5. The governors build (A) was completed on a copper build plate and the test specimens build (B) successfully completed on an IN718 build plate. The manufactured deliverable components were then heat treated using the developed thermal processing steps.

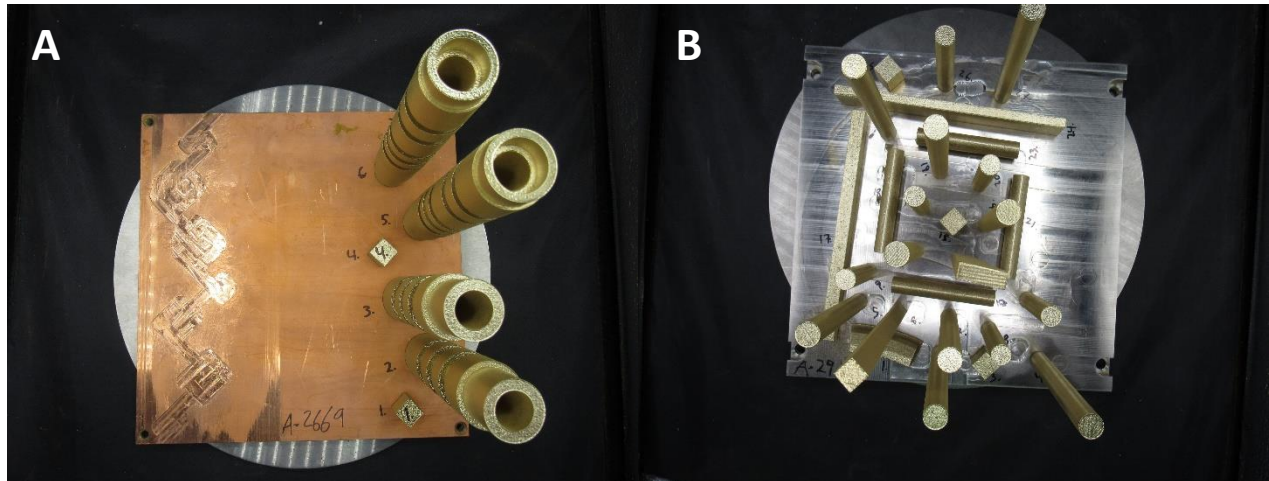


Figure 5. (A) Governors build and (B) mechanical test specimens build

Problems and corrective action

Elementum 3D has experienced 5 build failures during this period of work. The part failures were caused by part delamination which is a result of poor adhesion to the build plate. E3D performed various tests using different build plate materials and strategies for increasing part adhesion to the build plate. The build plate materials tested include mild steel, stainless steel, aluminum, and copper which all experienced some level of part delamination. An example of part delamination is shown below in Figure 6. This delamination is a result of poor adhesion and large internal stresses. The corrective action for successfully manufacturing aluminum bronze components was to increase the part's adhesion to the build plate and to manufacture geometries which would result in less internal stresses.

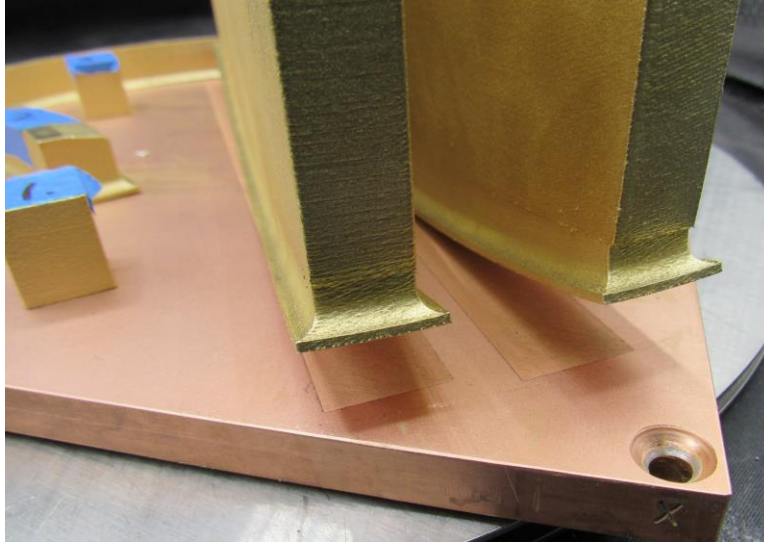


Figure 6. Part delamination due to lack of adhesion to build plate

To improve the part adhesion E3D machined a IN718 build plate to be used for manufacturing aluminum bronze components. Printing on the IN718 plate was successful as Elementum 3D was able to complete the printing of a slinger ring, vertical bars, and horizontal mechanical tests specimens with no part delamination from the build plate. Figure 7 below shows the long horizontal test specimens which have printed without any delamination from the IN718 build plate. Future builds manufacturing aluminum bronze components will utilize IN718 build plates.

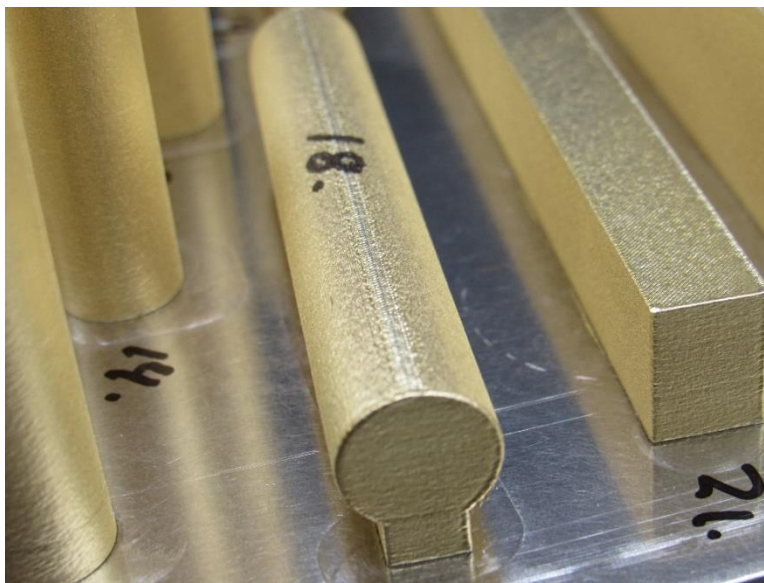


Figure 7. Horizontal specimens printing on IN718 build plate

Conclusion

Elementum 3D has been able to successfully develop process parameters for printing Aluminum Bronze in the EOS M290 L-PBF machine which provided 99.9% apparent relative densities, develop a multi-step heat treatment to achieve the desired HRB hardness values, and manufacture the specific deliverable components for the customer under the preliminary Phase I project. Further optimization of the process should be performed to improve the as-printed surface finish if desired by the customer. Any future manufacturing of aluminum bronze components will be complete using an IN718 build plate. Next steps are to collect the mechanical property data to complete the evaluation of the material for use in LPBF.

Appendix E

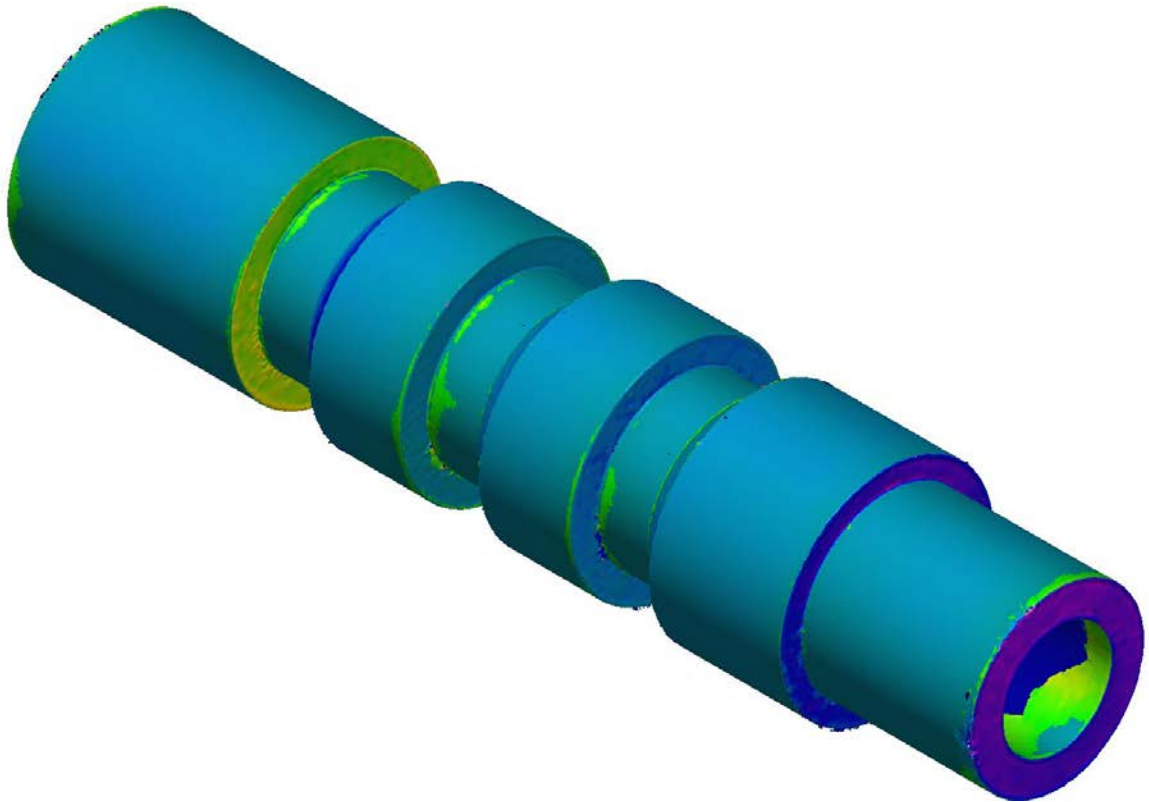
3D Scan Results of Aluminum Bronze Governor Parts As-Printed

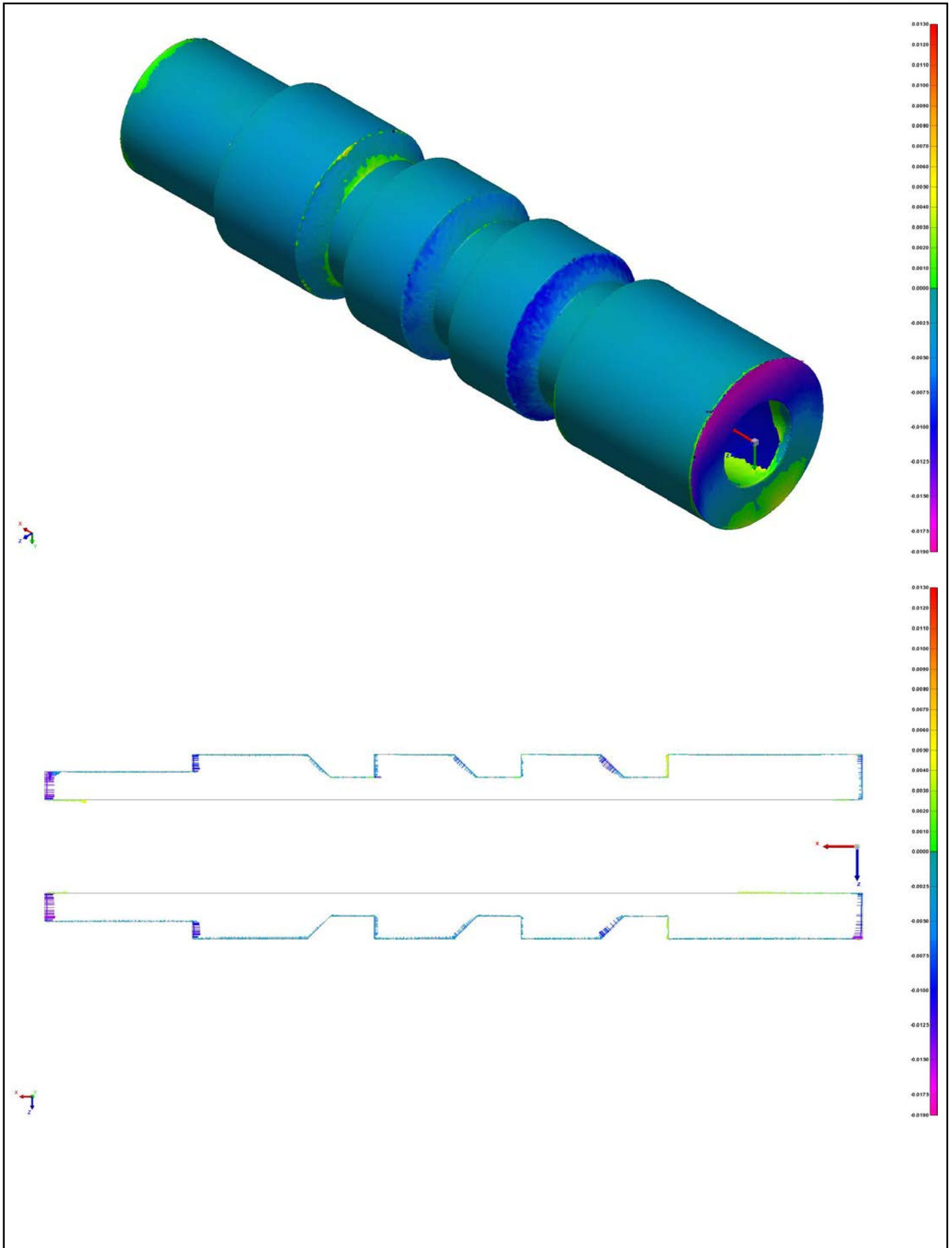


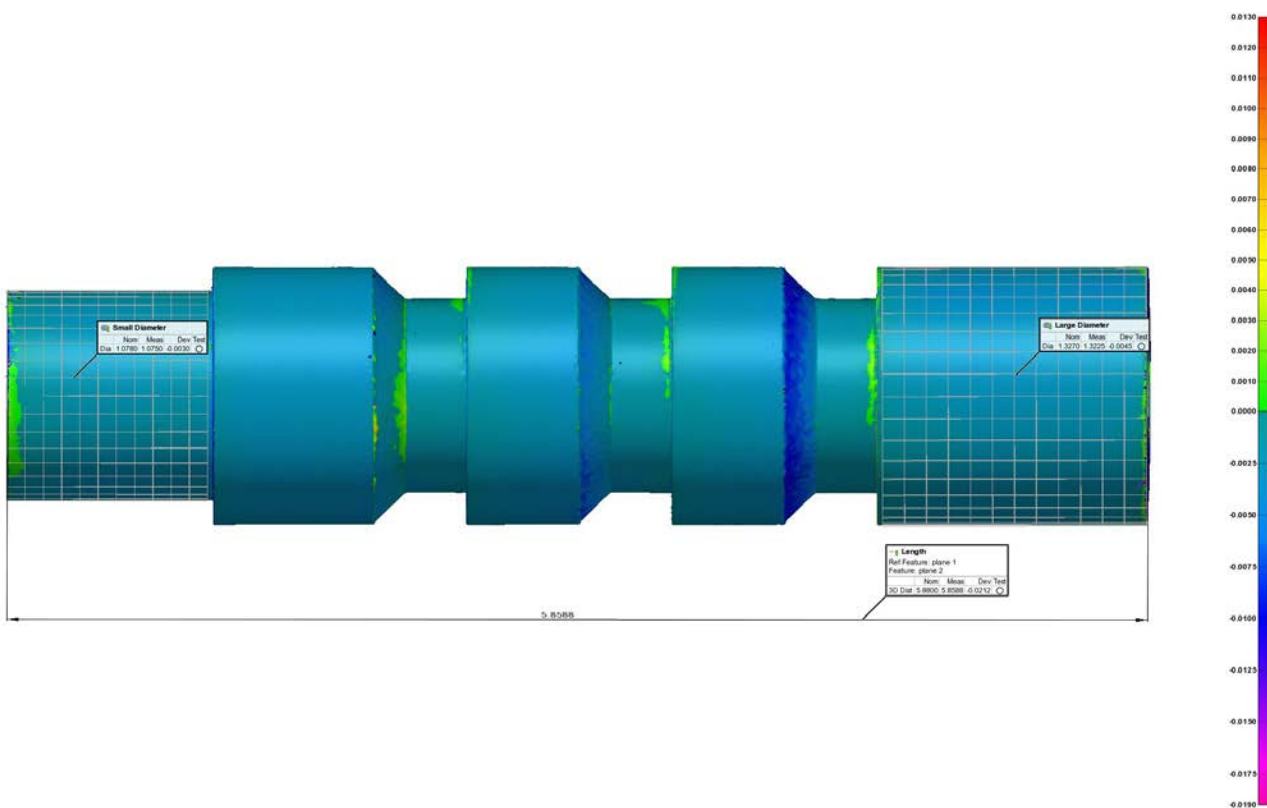
Metal 3D Printed Part

Part number: Cylinder A2669-2

Workspace: Jermyn 3D Printed Material
Project: Cylinder A2669-2 - piece 1
Report Author: Chad Paulson
Date: 4/7/2022







Control View

Control View Name Side Colormap (2)
 Units Inches
 Coordinate Systems world
 Data Alignments best-fit to ref 1 (alignment group 1), best-fit to ref 1 (alignment group 2), best-fit to ref 1 (alignment group 3)
 All Statistics Total: 3, Measured: 3 (100.0000%), Pass: 3 (100.0000%), Fail: 0 (0.0000%), Warning: 0 (0.0000%)

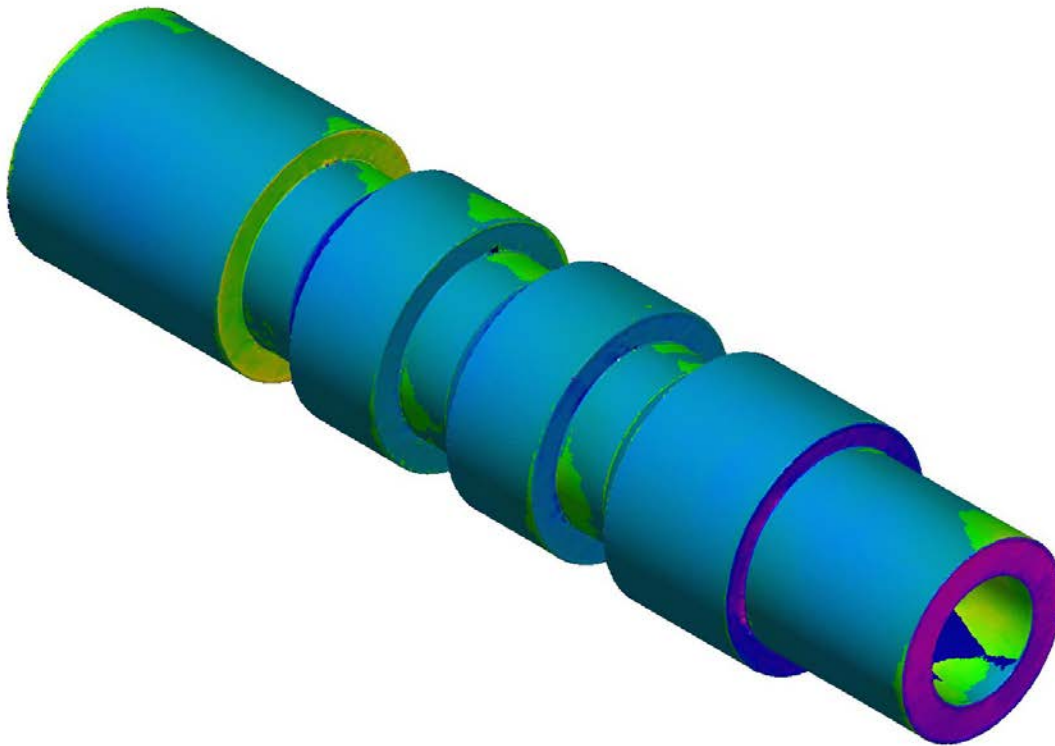
Char No.	Object Name	Control	Nom	Meas	Tol	Dev	Test	Out Tol
	Large Diameter	Diameter	1.3270	1.3225	±0.0394	-0.0045	Pass	
	Small Diameter	Diameter	1.0780	1.0750	±0.0394	-0.0030	Pass	
	Length	3D Distance	5.8800	5.8588	±0.0394	-0.0212	Pass	

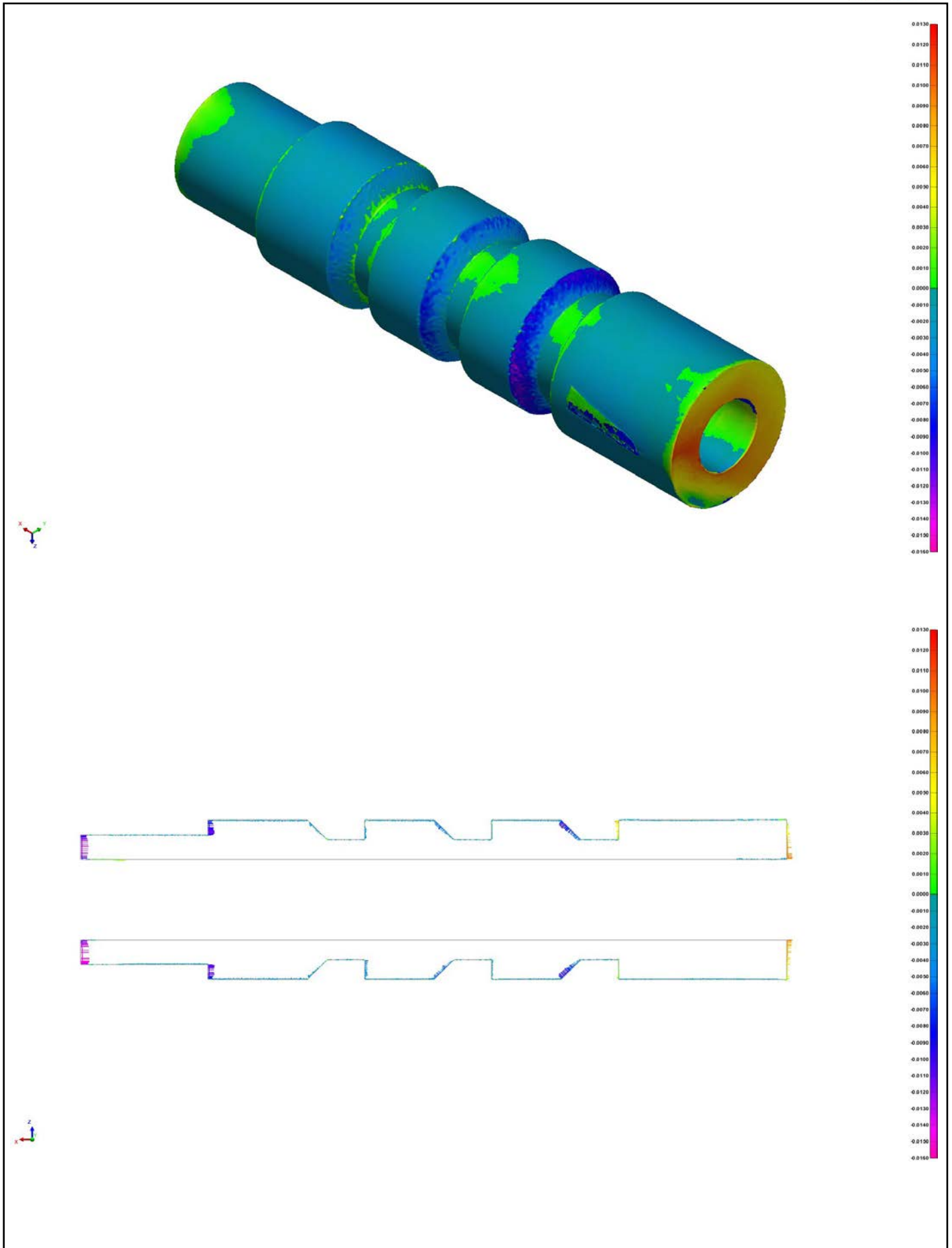


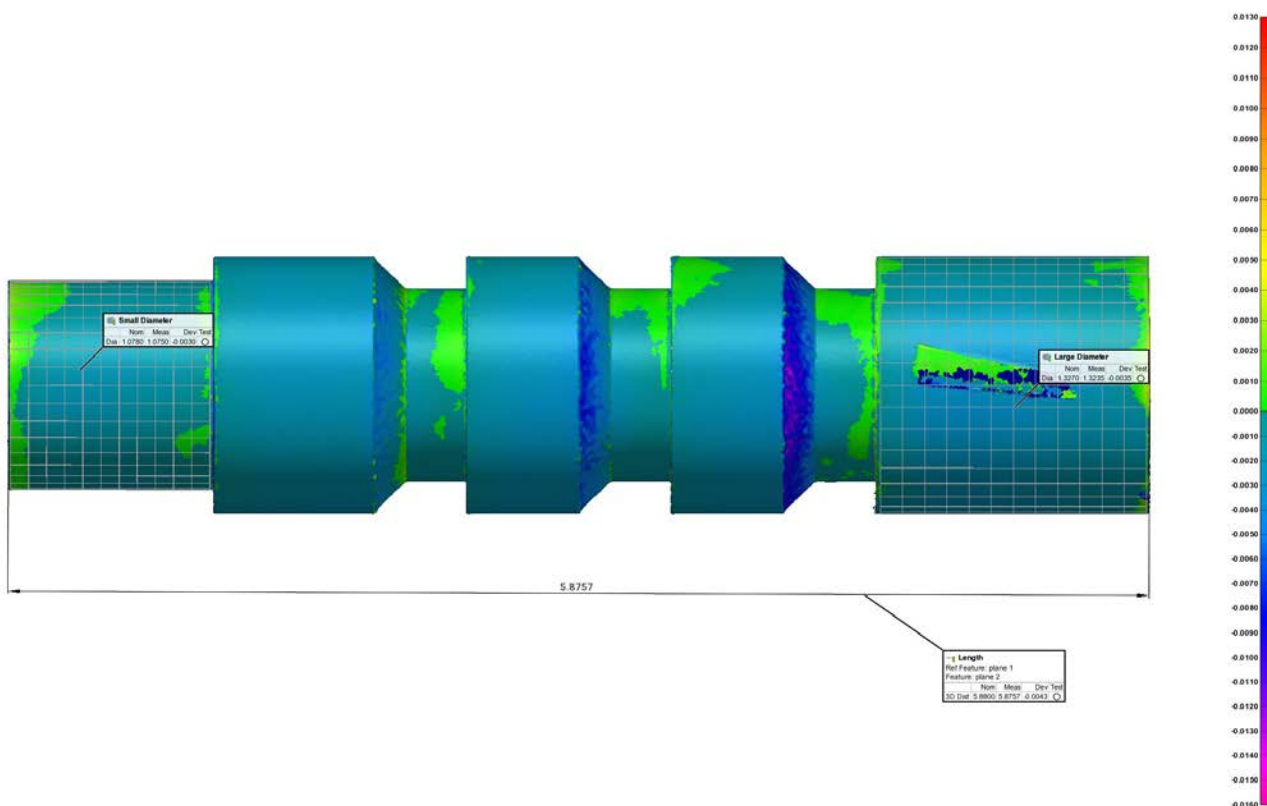
Metal 3D Printed Part

Part number: Cylinder A2669-3

Workspace: Jermyn 3D Printed Material
Project: Cylinder A2669-3 - piece 1
Report Author: Chad Paulson
Date: 4/7/2022







Control View

Control View Name Side Colormap
 Units Inches
 Coordinate Systems world
 Data Alignments best-fit to ref 1 (alignment group 1), best-fit to ref 1 (alignment group 2), best-fit to ref 1 (alignment group 3)
 All Statistics Total: 3, Measured: 3 (100.0000%), Pass: 3 (100.0000%), Fail: 0 (0.0000%), Warning: 0 (0.0000%)

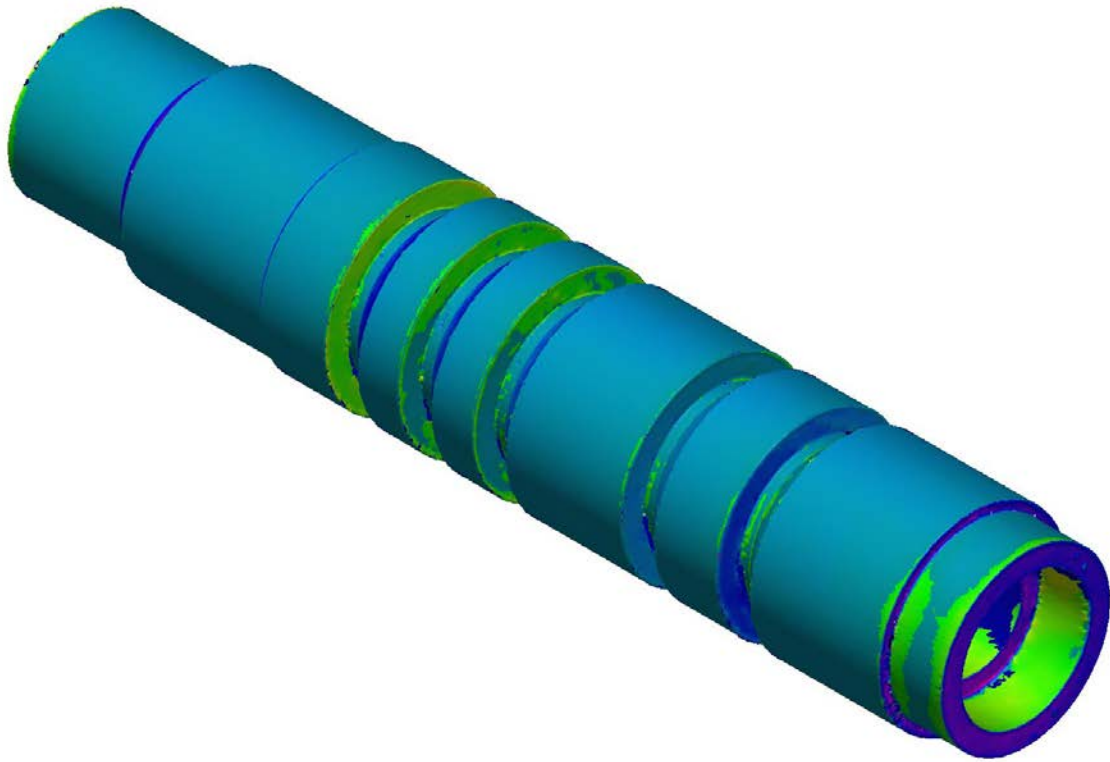
Char No.	Object Name	Control	Nom	Meas	Tol	Dev	Test	Out Tol
	Large Diameter	Diameter	1.3270	1.3235	±0.0300	-0.0035	Pass	
	Small Diameter	Diameter	1.0780	1.0750	±0.0300	-0.0030	Pass	
	Length	3D Distance	5.8800	5.8757	±0.0300	-0.0043	Pass	

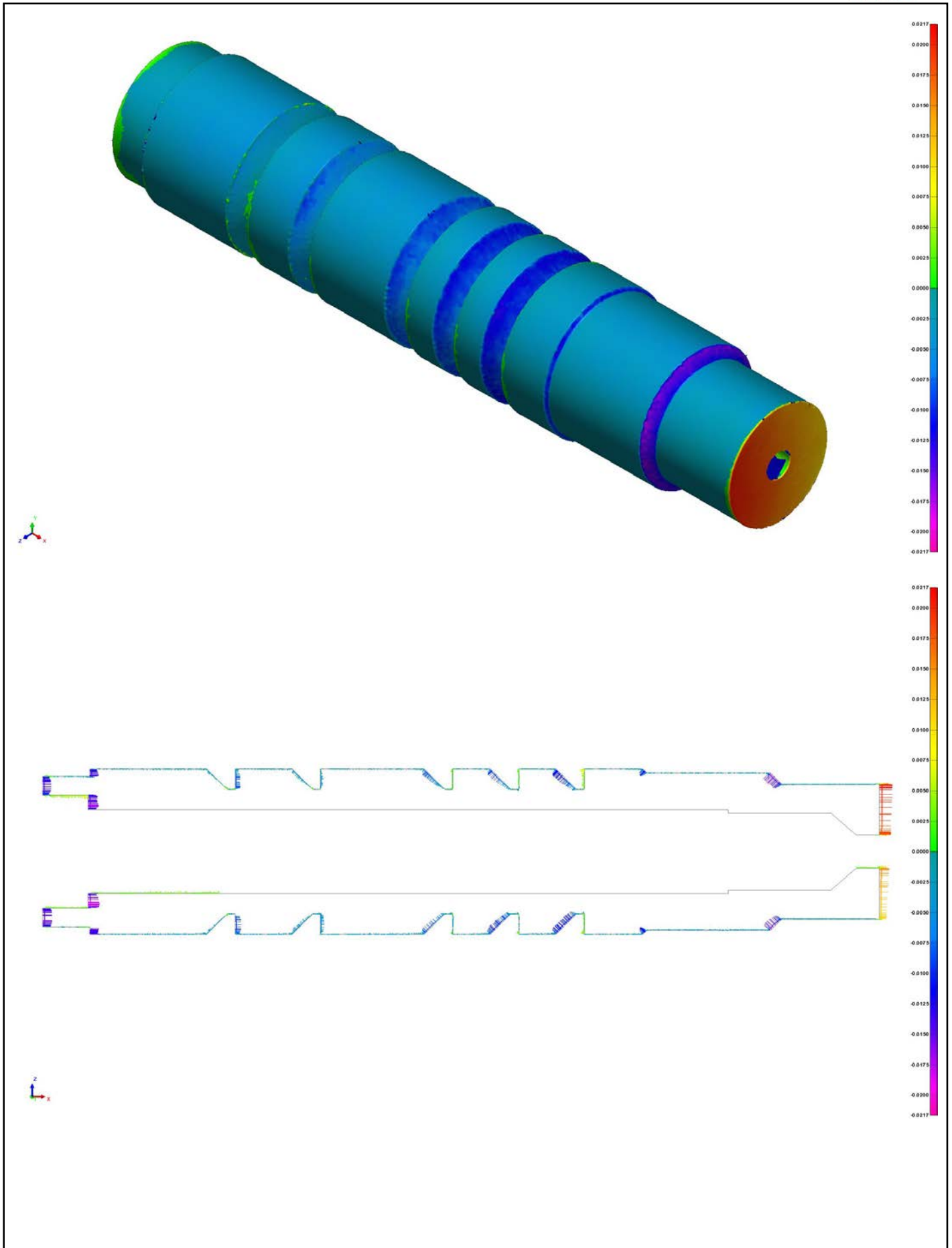


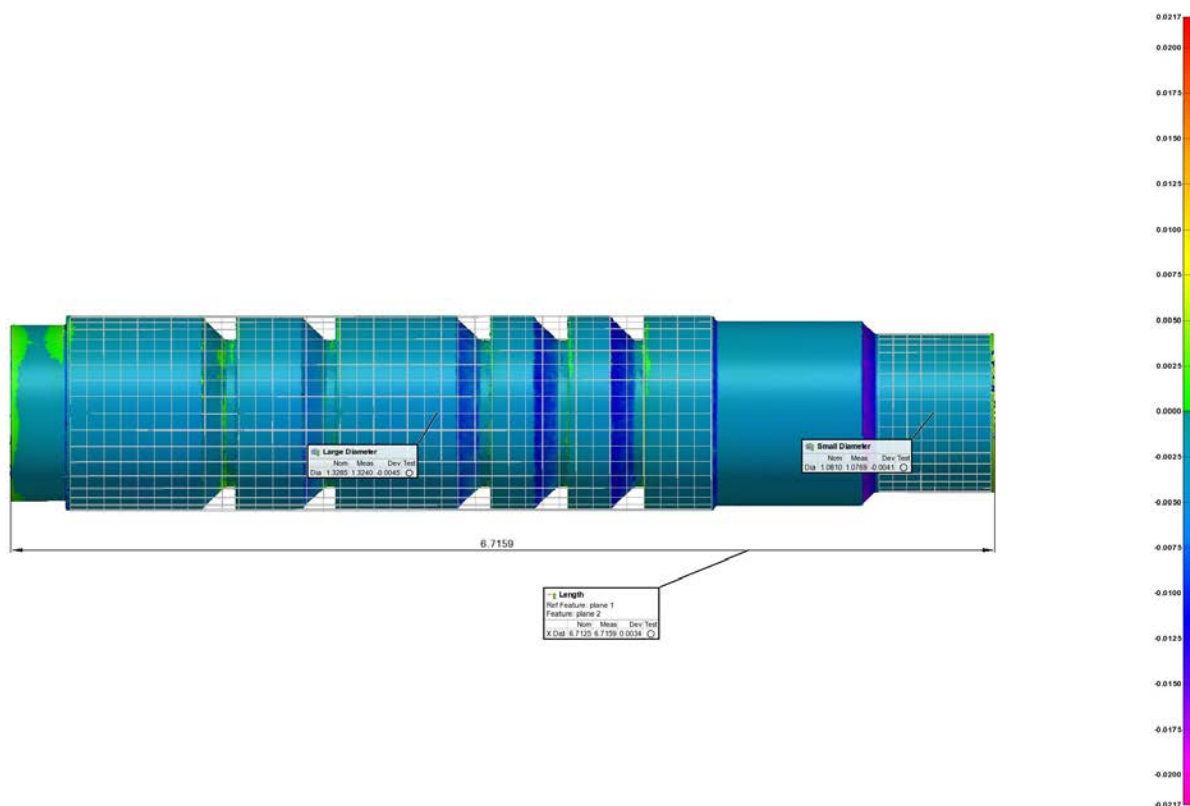
Metal 3D Printer Part

Part number: Cylinder A2669-5

Workspace: Jermyn 3D Printed Material
Project: Cylinder A2669-5 - piece 1
Report Author: Chad Paulson
Date: 4/7/2022







Control View

Control View Name Side Colormap (2)
 Units Inches
 Coordinate Systems world
 Data Alignments best-fit to ref 1 (alignment group 1), best-fit to ref 1 (alignment group 2), best-fit to ref 1 (alignment group 3)
 All Statistics Total: 3, Measured: 3 (100.0000%), Pass: 3 (100.0000%), Fail: 0 (0.0000%), Warning: 0 (0.0000%)

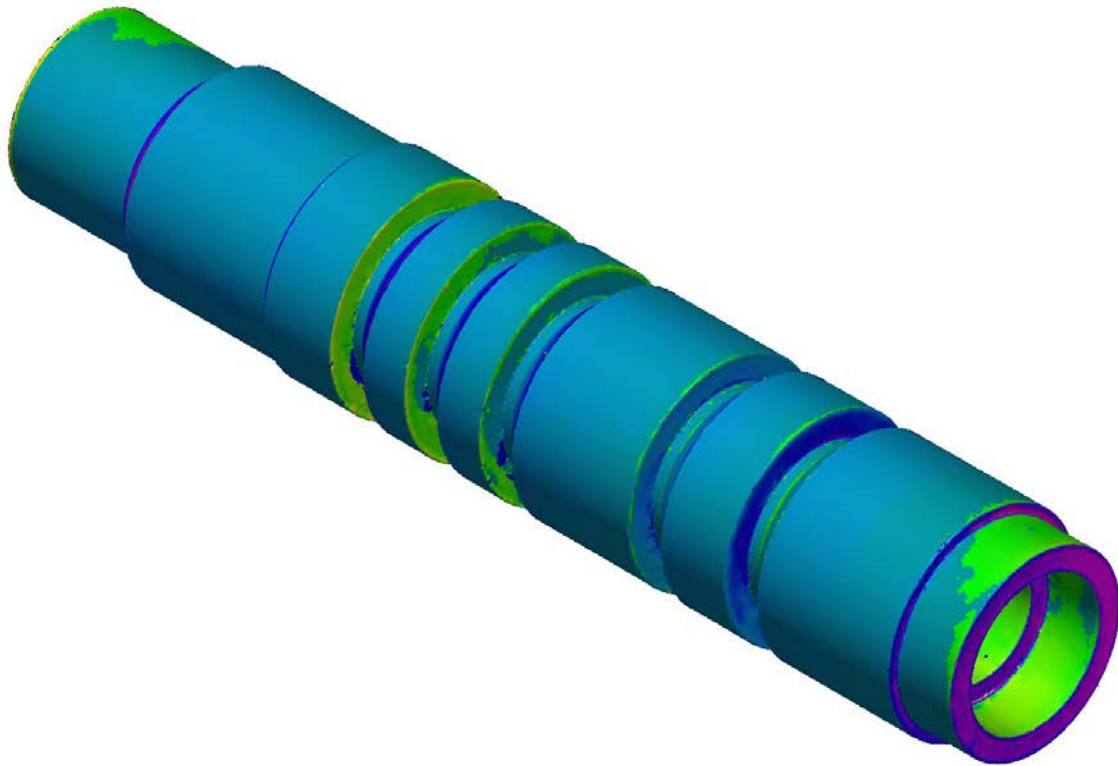
Char No.	Object Name	Control	Nom	Meas	Tol	Dev	Test	Out Tol
	Large Diameter	Diameter	1.3285	1.3240	±0.0300	-0.0045	Pass	
	Small Diameter	Diameter	1.0810	1.0769	±0.0300	-0.0041	Pass	
	Length	X Distance	6.7125	6.7159	±0.0300	0.0034	Pass	

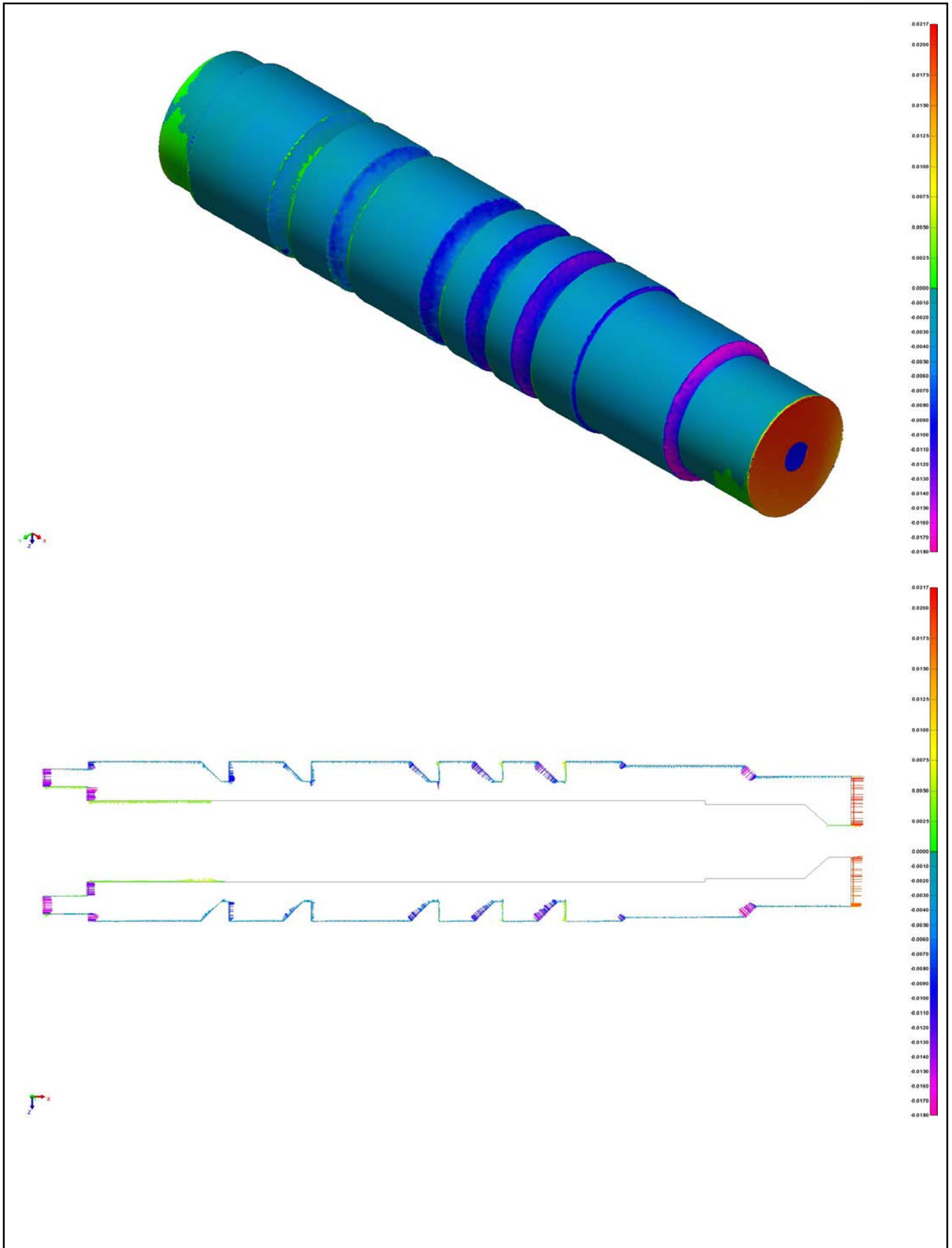


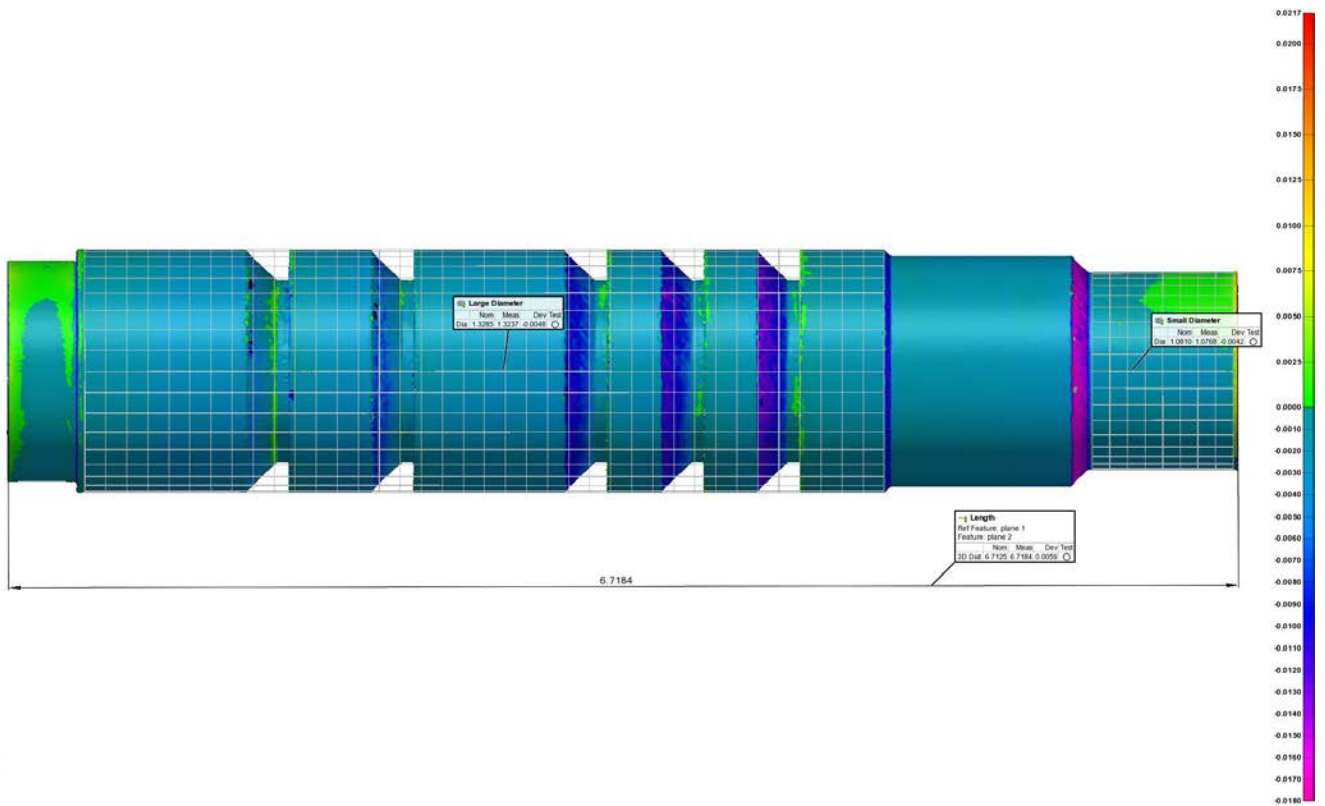
Metal 3D Printed Part

Part number: Cylinder A2669-6

Workspace: Jermyn 3D Printed Material
Project: Cylinder A2669-6 - piece 1
Report Author: Chad Paulson
Date: 4/7/2022







Control View

Control View Name: Side Colormap (4)
 Units: Inches
 Coordinate Systems: world
 Data Alignments: best-fit to ref 1 (alignment group 1), best-fit to ref 1 (alignment group 2), best-fit to ref 1 (alignment group 3)
 All Statistics: Total: 3, Measured: 3 (100.0000%), Pass: 3 (100.0000%), Fail: 0 (0.0000%), Warning: 0 (0.0000%)

Char No.	Object Name	Control	Nom	Meas	Tol	Dev	Test	Out Tol
	Large Diameter	Diameter	1.3285	1.3237	±0.0300	-0.0048	Pass	
	Small Diameter	Diameter	1.0810	1.0768	±0.0300	-0.0042	Pass	
	Length	3D Distance	6.7125	6.7184	±0.0300	0.0059	Pass	

Appendix F

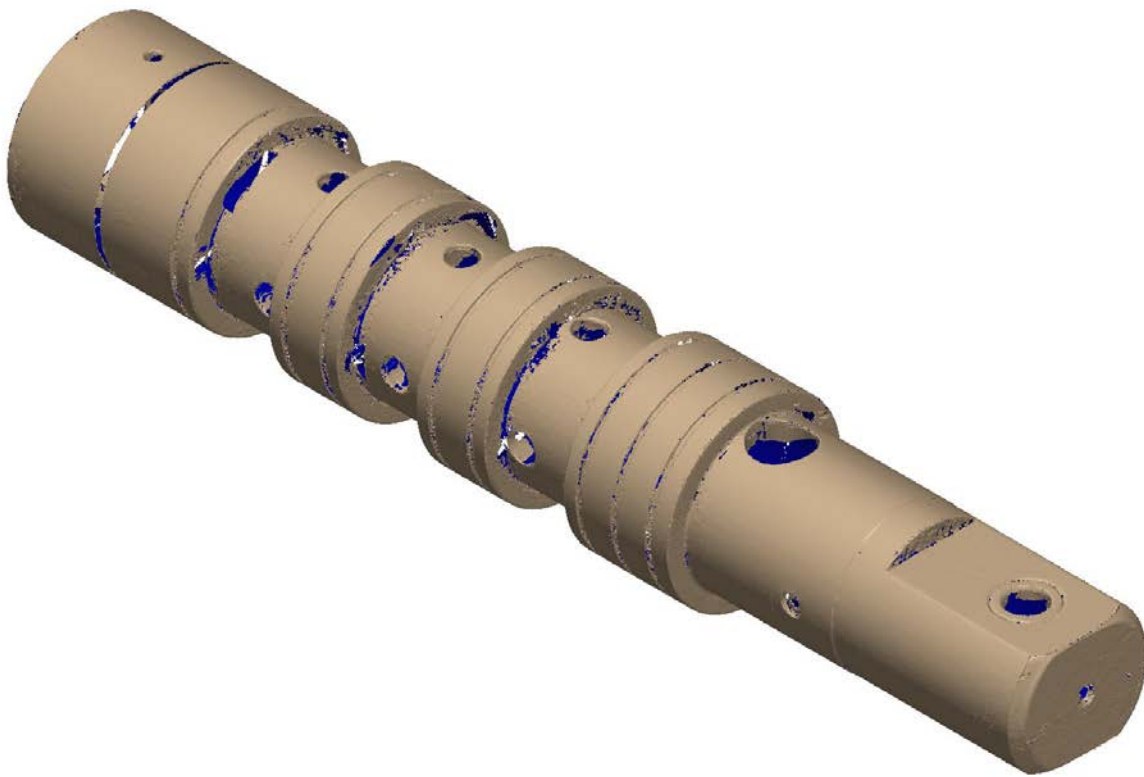
3D Scan Results of Aluminum Bronze Governor Parts As-Machined



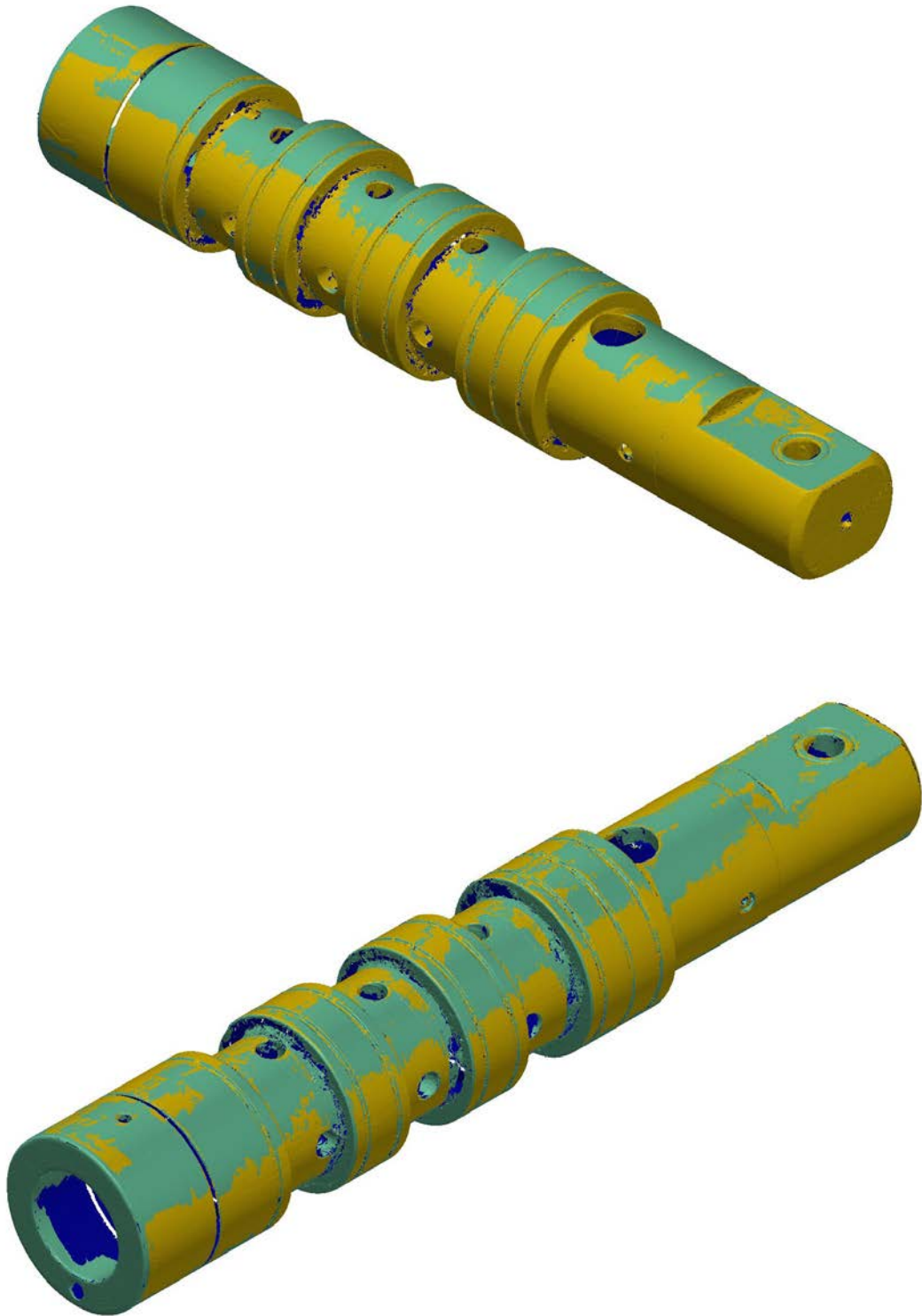
Metal 3D Printed Part

Part number: H41365-A

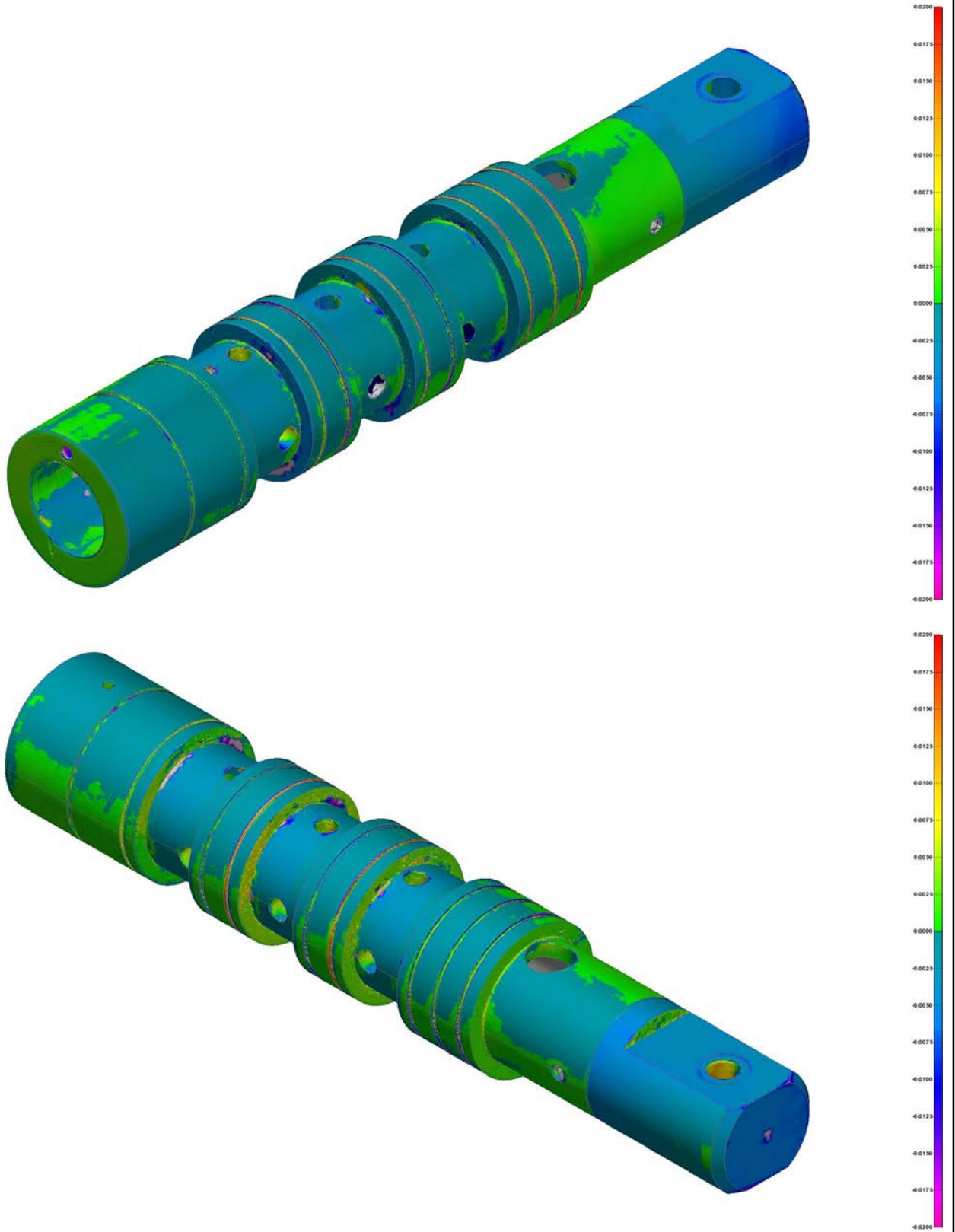
Workspace: Jermyn 3D Printed Material
Project: Brass Machined 1 - piece 1
Report Author: Chad Paulson
Date: 12/7/2022



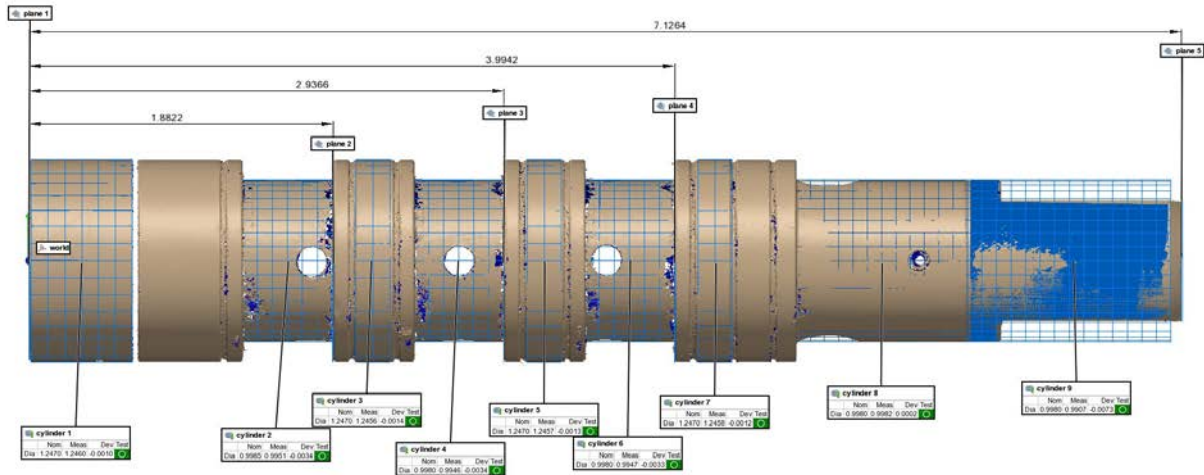
Scan Alignment



Deviation Color Map



Measurement Deviations



Control View

Control View Name control view 2
 Units Inches
 Coordinate Systems world
 Data Alignments best-fit to ref 1 (alignment group 1), best-fit to ref 2 (alignment group 2), original (alignment group 3)
 All Statistics Total: 13, Measured: 13 (100.0000%), Pass: 13 (100.0000%), Fail: 0 (0.0000%), Warning: 0 (0.0000%)

Object Name	Control	Nom	Meas	Dev
cylinder 1	Diameter	1.2470	1.2460	-0.0010
cylinder 2	Diameter	0.9985	0.9951	-0.0034
cylinder 3	Diameter	1.2470	1.2456	-0.0014
cylinder 4	Diameter	0.9980	0.9946	-0.0034
cylinder 5	Diameter	1.2470	1.2457	-0.0013
cylinder 6	Diameter	0.9980	0.9947	-0.0033
cylinder 7	Diameter	1.2470	1.2458	-0.0012
cylinder 8	Diameter	0.9980	0.9982	0.0002
cylinder 9	Diameter	0.9980	0.9907	-0.0073
distance 1	X Distance	1.8760	1.8822	0.0062
distance 2	X Distance	2.9330	2.9366	0.0036
distance 3	X Distance	3.9900	3.9942	0.0042
distance 4	X Distance	7.1300	7.1264	-0.0036



Metal 3D Printed Part

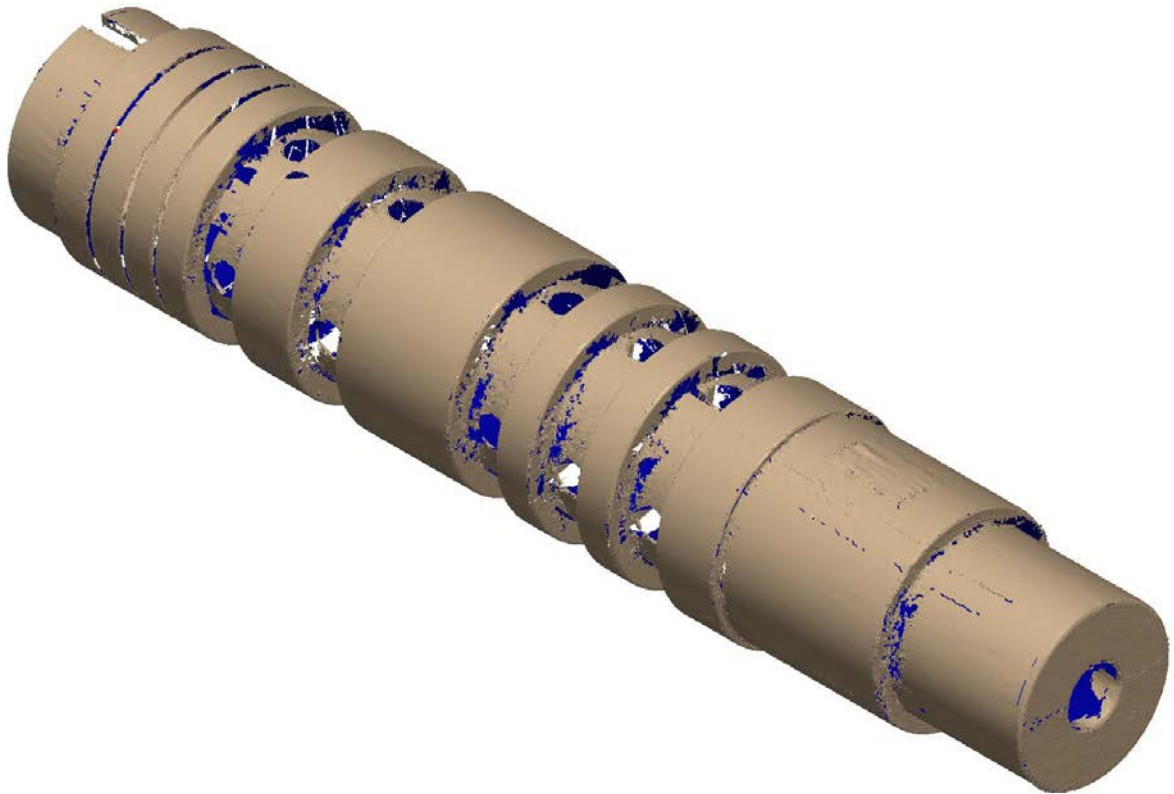
Part number: Cylinder H41365-B

Workspace: Jermyn 3D Printed Material

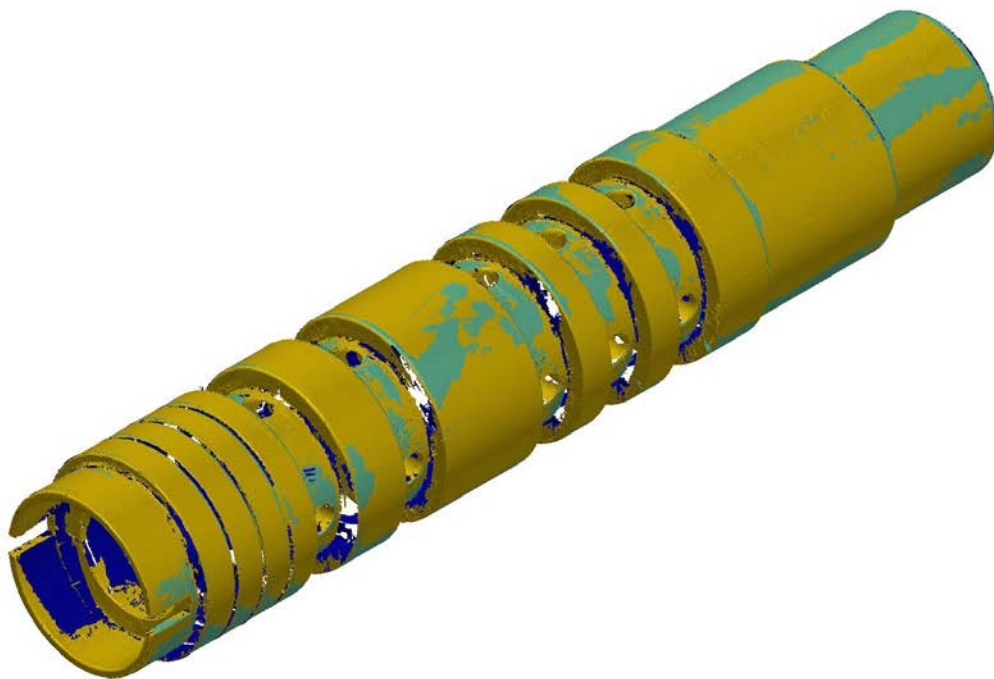
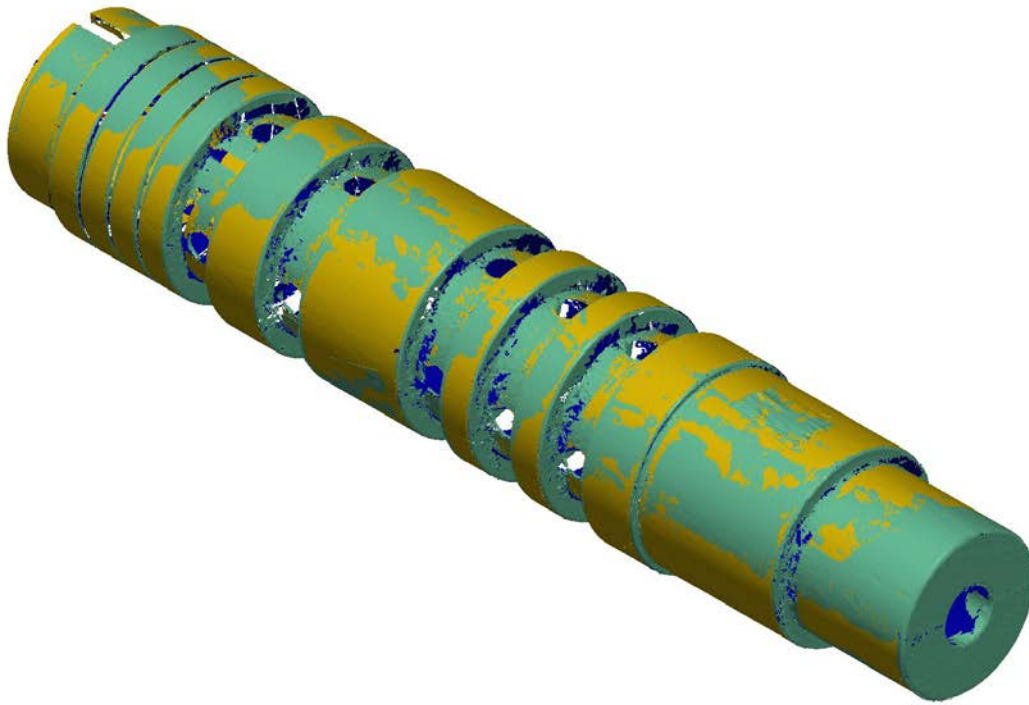
Project: Brass Machined 2 - piece 1

Report Author: Chad Paulson

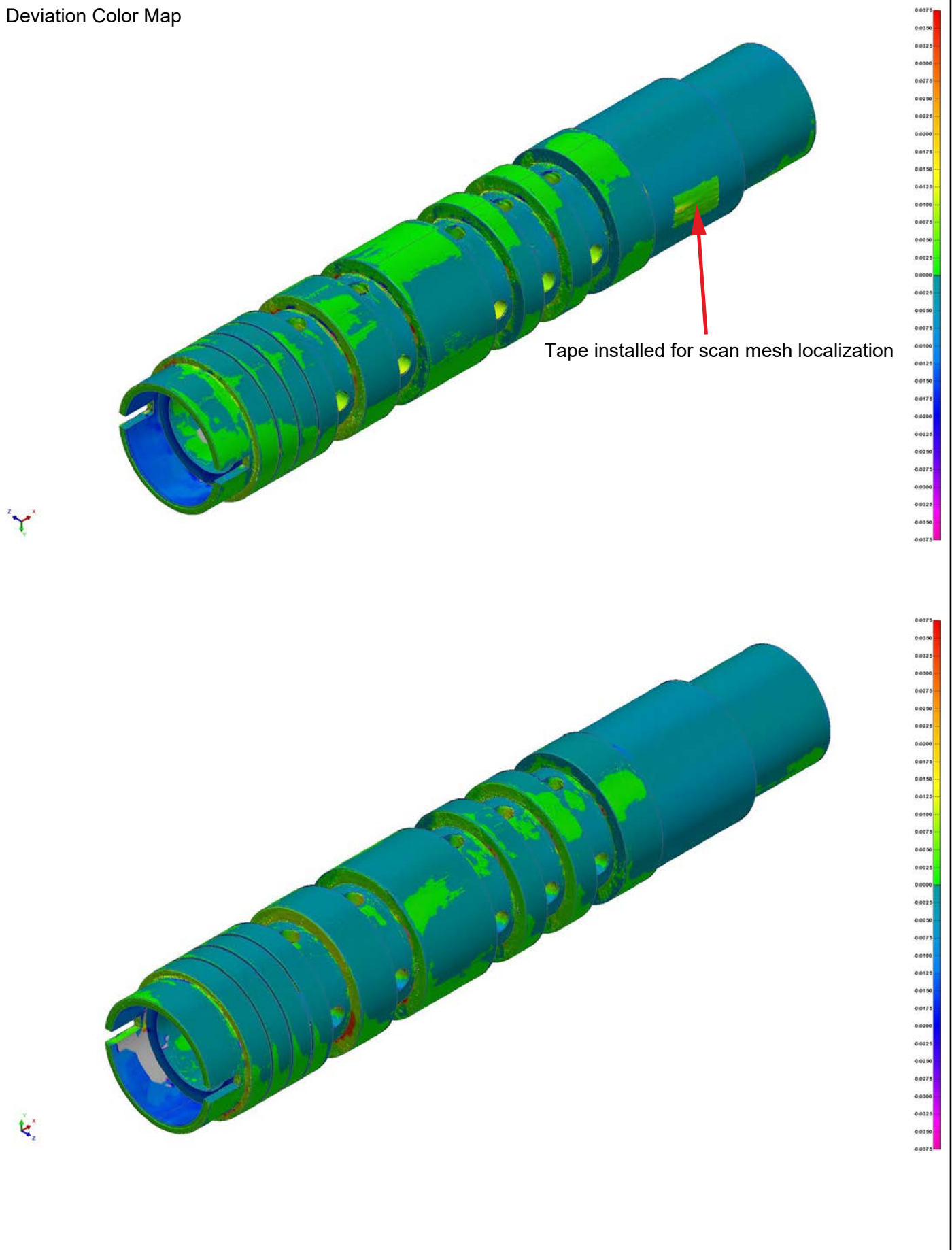
Date: 12/6/2022



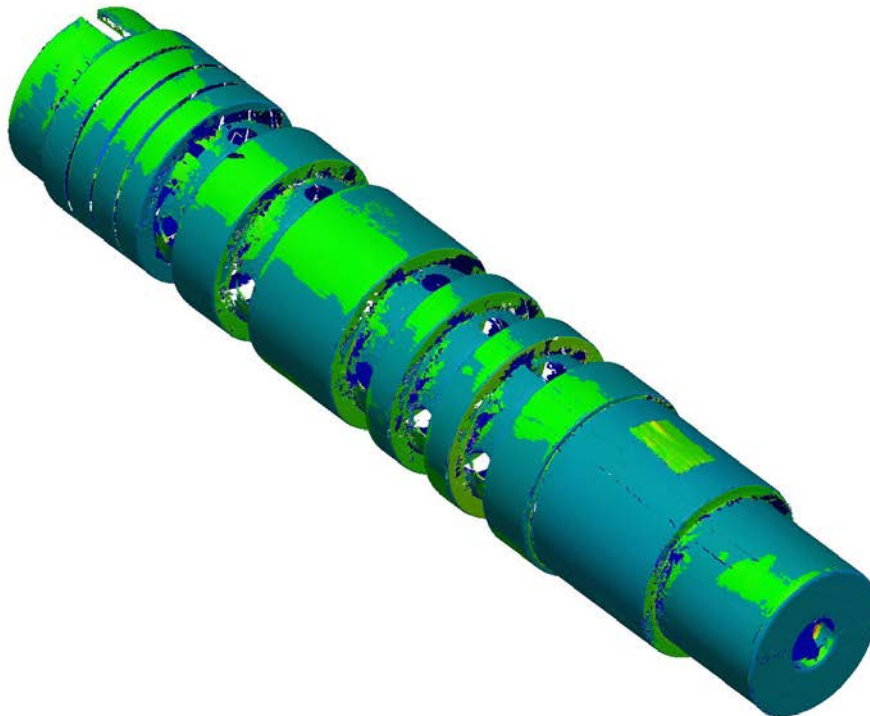
Scan Alignment



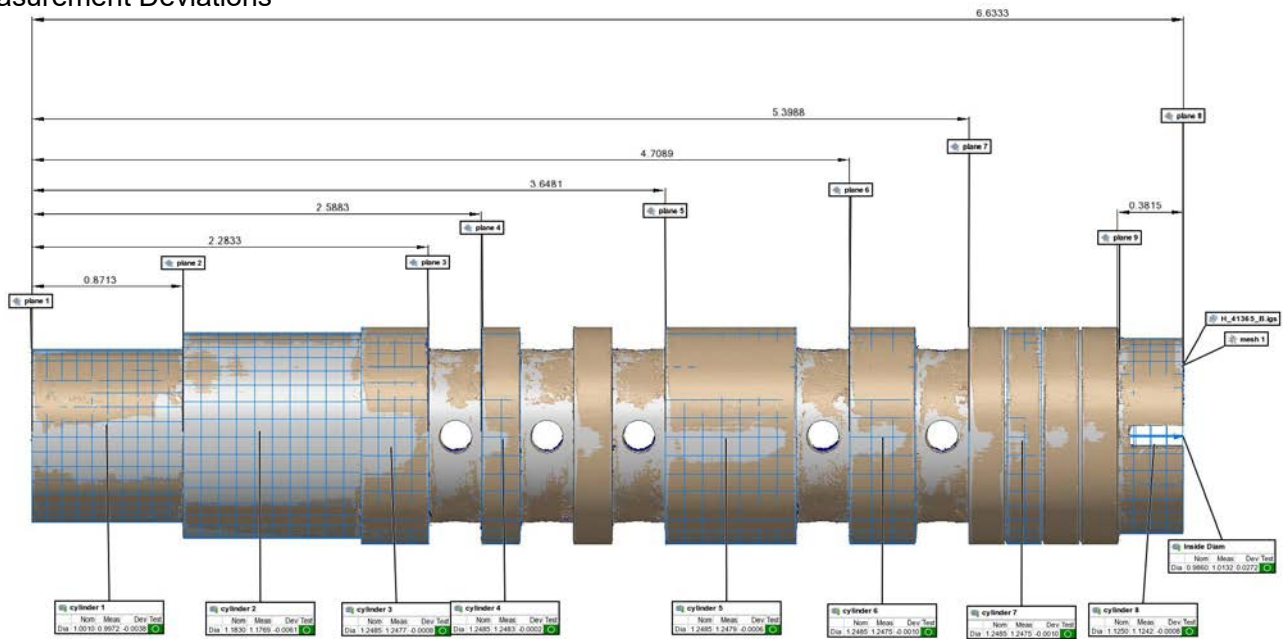
Deviation Color Map



Deviation Color Map



Measurement Deviations



Control View

Control View Name: control view 1
 Units: Inches
 Coordinate Systems: world
 Data Alignments: best-fit to ref 2 (alignment group 1), best-fit to ref 3 (alignment group 2), original (alignment group 3)
 All Statistics: Total: 17, Measured: 17 (100.0000%), Pass: 17 (100.0000%), Fail: 0 (0.0000%), Warning: 0 (0.0000%)

Object Name	Control	Nom	Meas	Dev
cylinder 1	Diameter	1.0010	0.9972	-0.0038
cylinder 2	Diameter	1.1830	1.1769	-0.0061
cylinder 3	Diameter	1.2485	1.2477	-0.0008
cylinder 4	Diameter	1.2485	1.2483	-0.0002
cylinder 5	Diameter	1.2485	1.2479	-0.0006
cylinder 6	Diameter	1.2485	1.2475	-0.0010
cylinder 7	Diameter	1.2485	1.2475	-0.0010
cylinder 8	Diameter	1.1250	1.1242	-0.0008
Inside Diam	Diameter	0.9860	1.0132	0.0272
distance 1	X Distance	0.8750	0.8713	-0.0037
distance 2	X Distance	2.2875	2.2833	-0.0042
distance 3	X Distance	2.5975	2.5883	-0.0092
distance 4	X Distance	3.6535	3.6481	-0.0054
distance 5	X Distance	4.7135	4.7089	-0.0046
distance 6	X Distance	5.3985	5.3988	0.0003
distance 7	X Distance	6.6325	6.6333	0.0008
distance 8	X Distance	0.3650	0.3815	0.0165

Appendix G

Colorado Metallurgical Services Mechanical Property Data of
Printed Stainless Steel



Date: March 11, 2021

Company: Bureau of Reclamation

P.O. #:

ATTN: Stephanie Prochaska

Ref. #: Samples H1-4, V1-4

Address: PO Box 25007, Mail Code 86-68530

Material: Additively manufactured 316L stainless steel

Address: Denver, CO 80225-0007

Specification: ASTM E8/E8M-16ae1 | ASTM E290-14

Lab #: 2103-124

TENSILE TEST

CMS 130			Yield Strength		Tensile Strength		Elongation		Reduction of Area		Fracture	
	Identity	Diameter in	Area in ²	Load (lb)	lb / in ²	Load (lb)	lb / in ²	(in)	%	Diameter in	%	Location
	H1	0.2490	0.0487	2,681	55,000	4,069	83,500	1.52	52%	0.1455	66%	g
	H2	0.2490	0.0487	2,630	54,000	4,061	83,500	1.55	55%	0.1420	68%	g
	H3	0.2490	0.0487	2,573	53,000	4,134	85,000	1.60	60%	0.1490	64%	g
	H4	0.2480	0.0483	2,657	55,000	4,027	83,500	1.53	53%	0.1440	66%	g
	V1	0.2490	0.0487	2,735	56,000	4,209	86,500	1.50	50%	0.1320	72%	g
	V2	0.2490	0.0487	2,767	57,000	4,236	87,000	1.49	49%	0.1400	68%	g
	V3	0.2490	0.0487	2,876	59,000	4,281	88,000	1.47	47%	0.1380	69%	g
	V4	0.2490	0.0487	2,889	59,500	4,249	87,000	1.46	46%	0.1430	67%	g

Yield Strength Determined By: 0.2% Offset

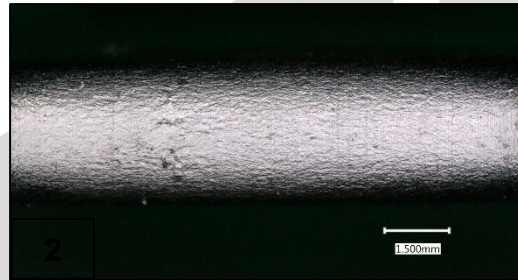
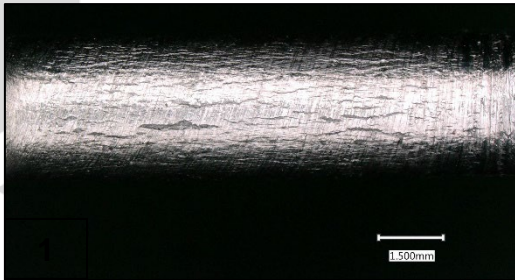
[g] Fractured thru gage marks or within specimen width of gage marks.

[X] Information Only

BEND TEST (ASTM E290)

Sample	Bend 1 (1t)	Bend 2 (flattening)
1	No Defects	Many Visible Cracks
2	No Defects	One Small Crack

[X] Information Only



Respectfully Submitted,

Josh Belt
Josh Belt
Materials Engineer

Appendix H

Mechanical Property Data of Printed Aluminum Bronze Samples



Date: September 20, 2022
P.O. #:
Ref. #: Group 1 H1, H, H3, V1, V2, V3
Material: Aluminum Bronze
Specification: ASTM E8/E8M-21
Lab #: 2208-006-Rev1

Company: Bureau of Reclamation
ATTN: Stephanie Prochaska
Address: Denver Federal Center Bldg 56, Rm 1400
Address: PO Box 25007 (86-68540)

TENSILE TEST

Table with 12 columns: CMS 130, Identity, Diameter in, Area in², Yield Strength (Load (lb), lb / in²), Tensile Strength (Load (lb), lb / in²), Elongation (in, %), Reduction of Area (Diameter in, %), Fracture (Location). Rows include samples 006-H1 through 006-V3.

Yield Strength Determined By: 0.2% Offset
[G] Fractured outside gage marks.
[g] Fractured thru gage marks or within specimen width of gage marks.
[X] Information Only

BEND TEST (ASTM E290)

Table with 3 columns: Sample, Bend 1 (4t), Bend 2 (flattening). Rows show results for samples 1 and 2.

[X] Information Only

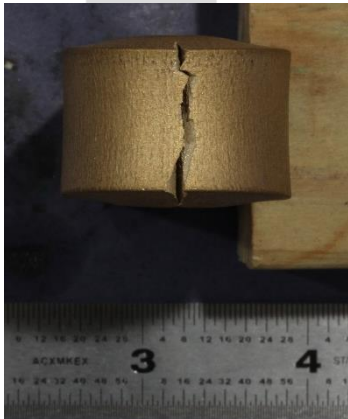


Figure 1: Sample 1

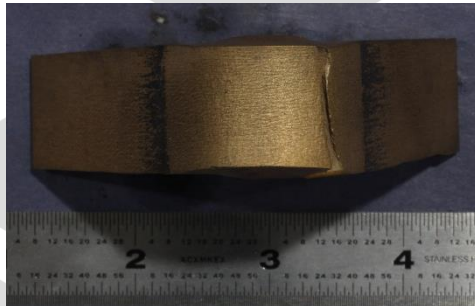


Figure 2: Sample 2 Top-Down View

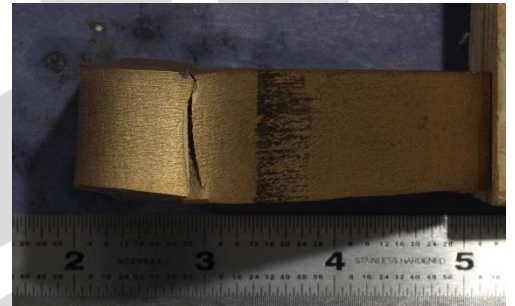


Figure 3: Sample 2 Focused on crack

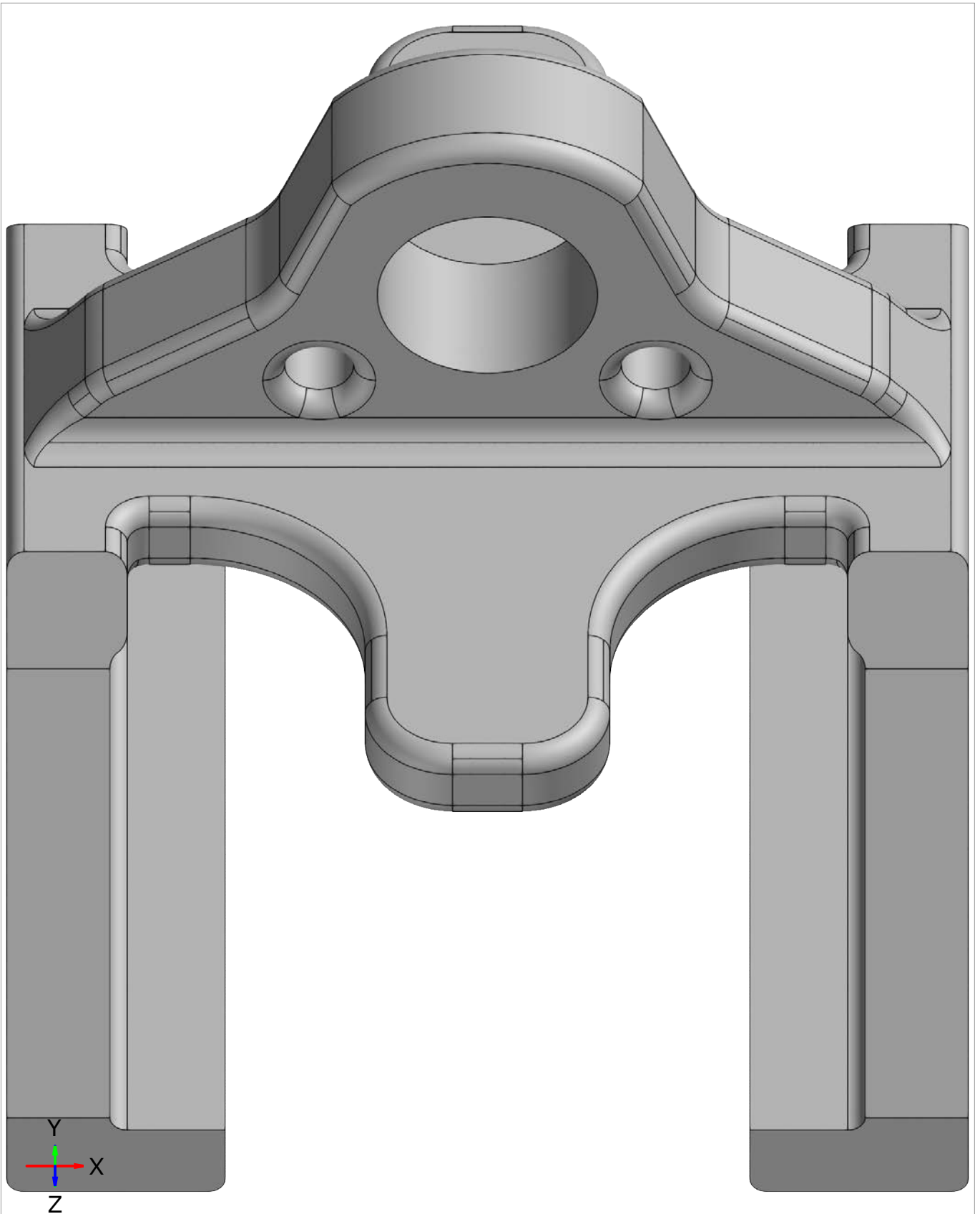
Respectfully Submitted,

Nick Rollman
Nick Rollman
Materials Engineer

Appendix I

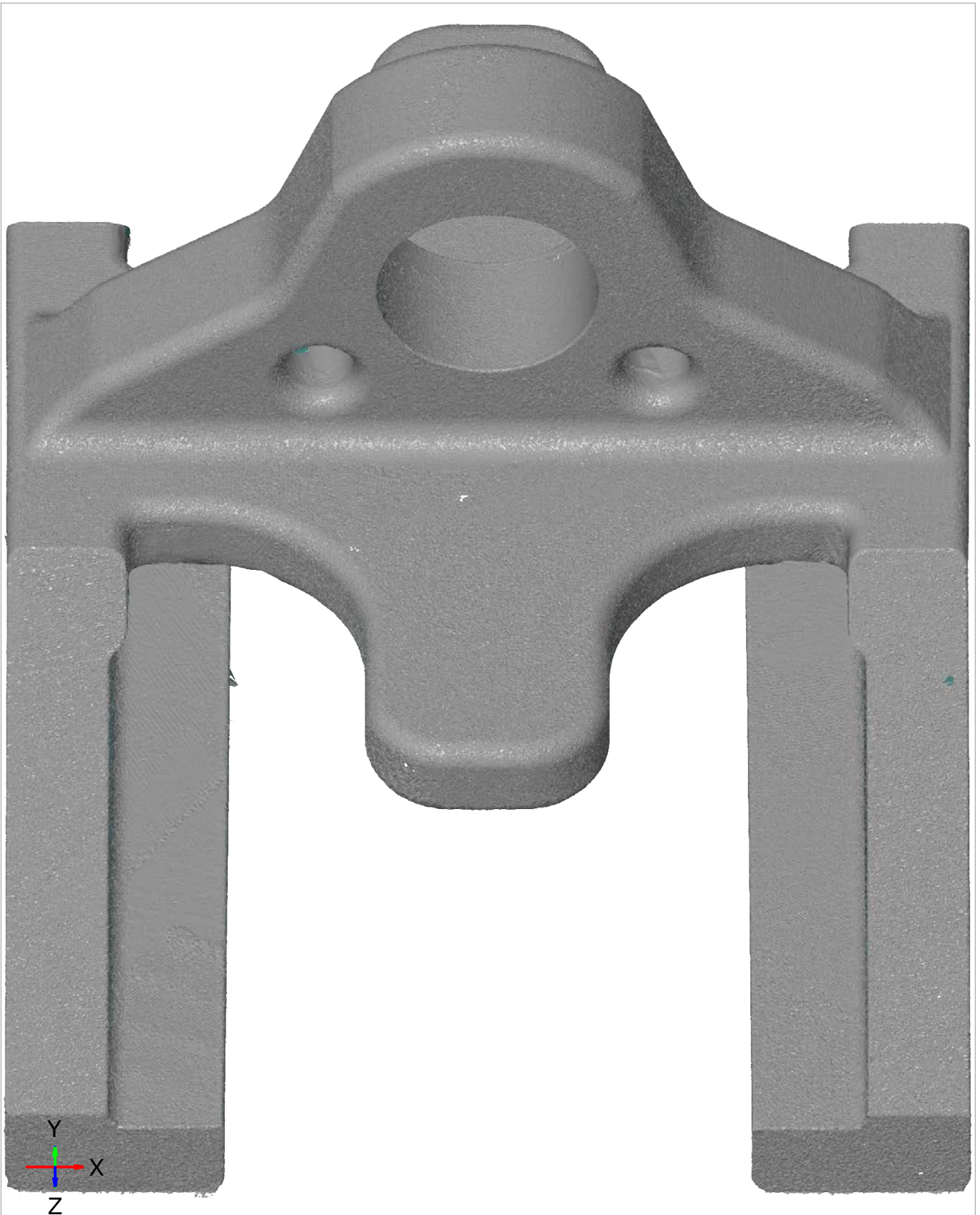
3D Scan Results of Aluminum Log Boom Anchor As-Printed

CAD



Length unit: mm

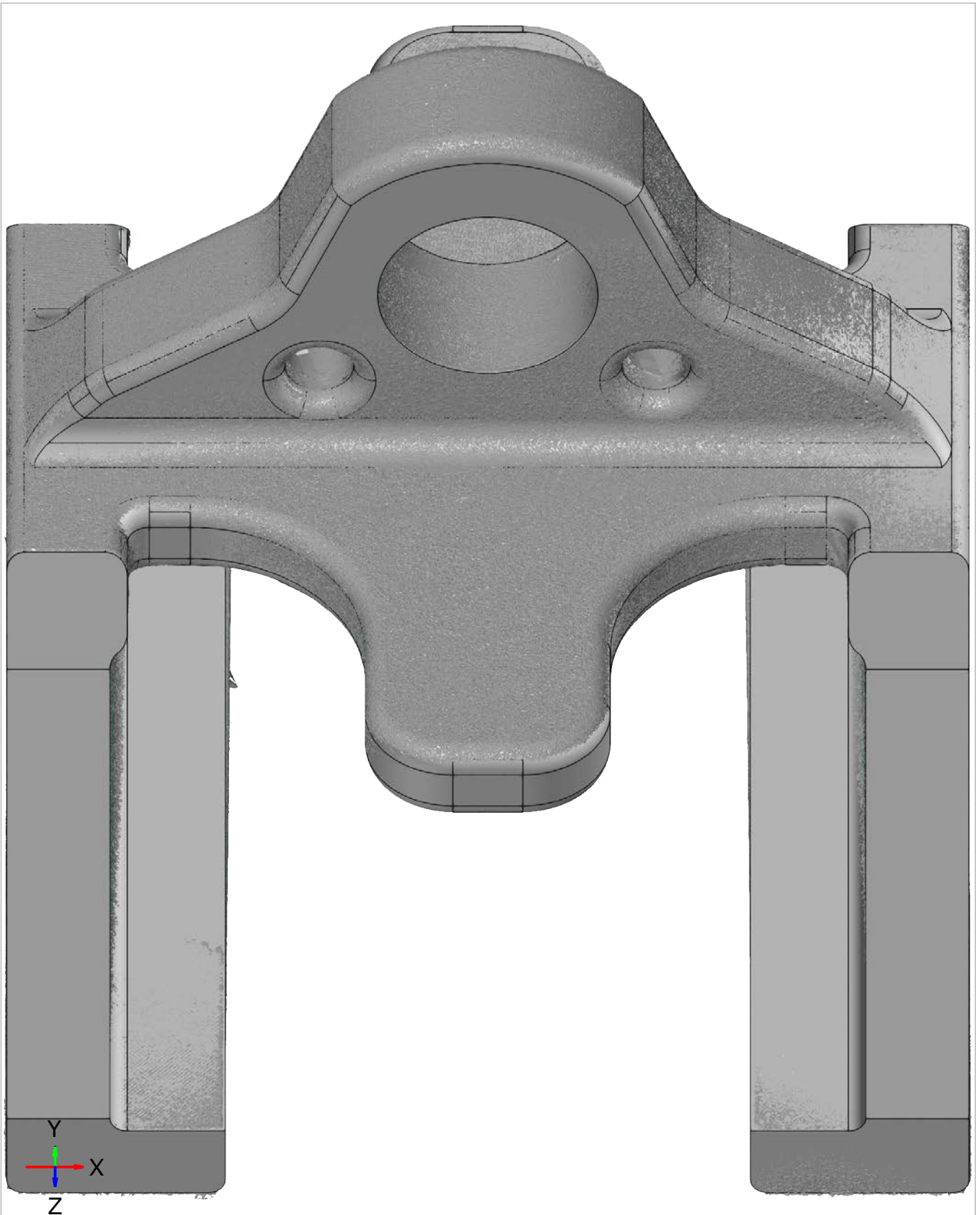
Mesh



Local best-fit

Length unit: mm

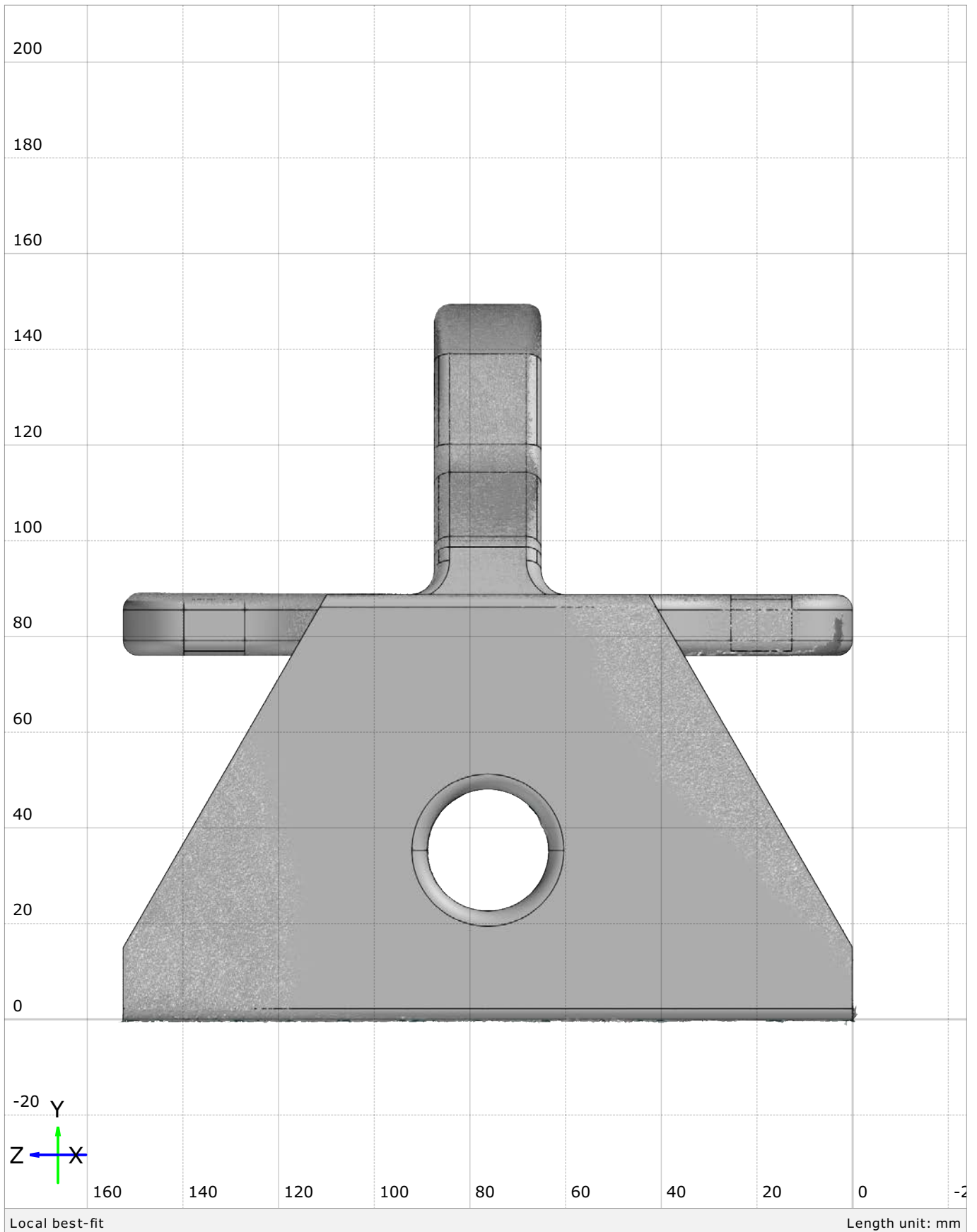
Alignment



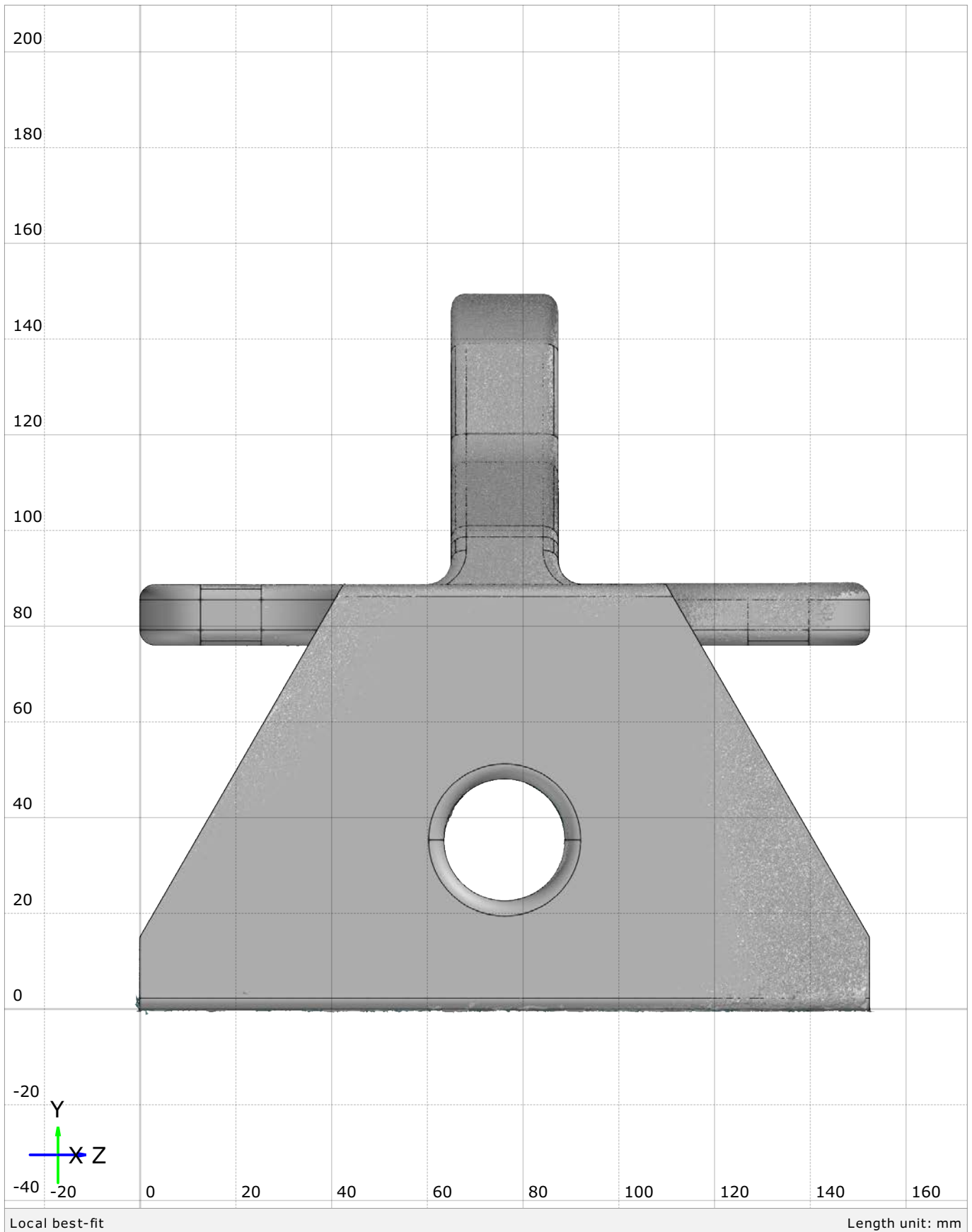
Local best-fit

Length unit: mm

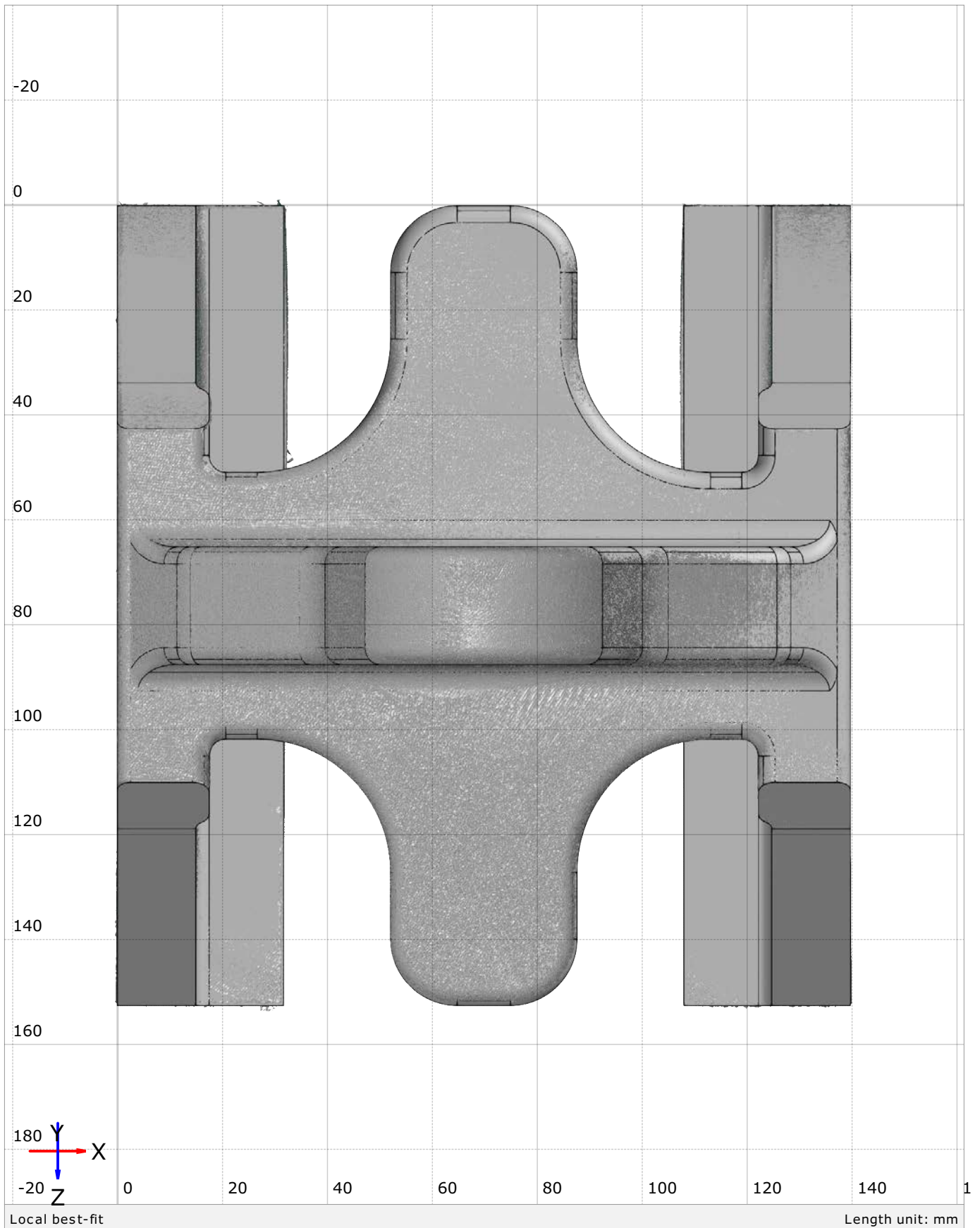
Alignment Cont. Left



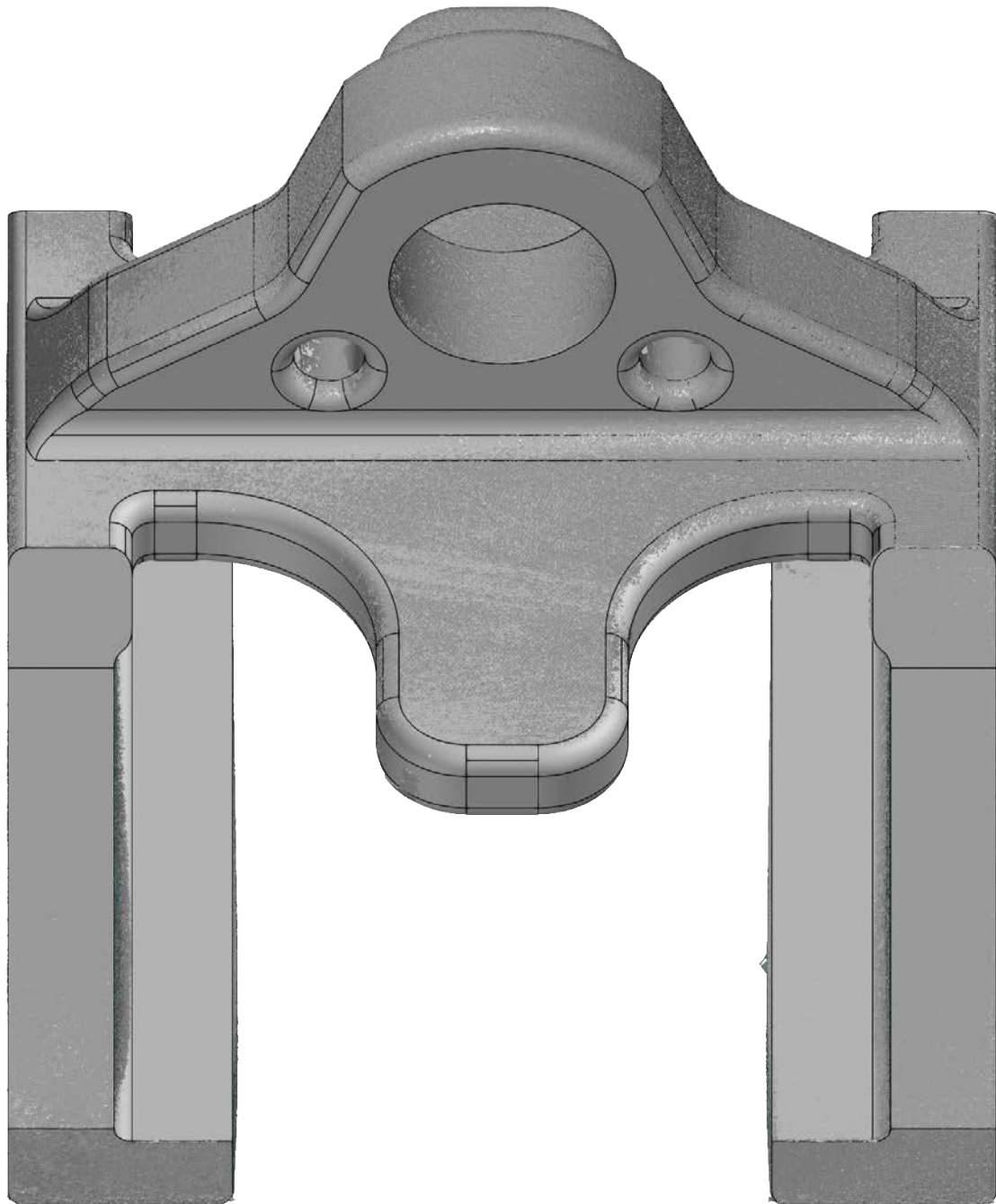
Alignment Cont. Right



Alignment Cont.



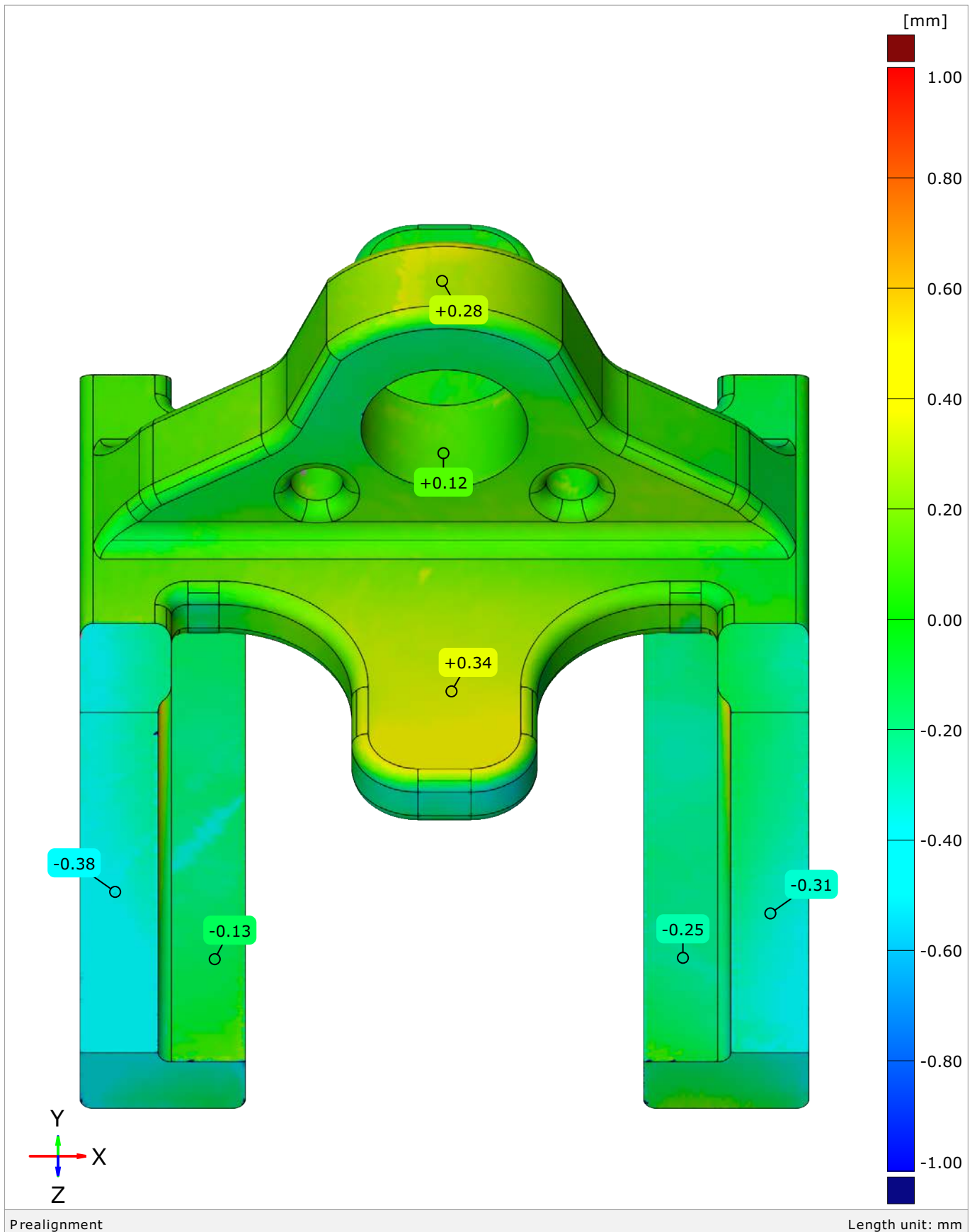
Alignment Cont.



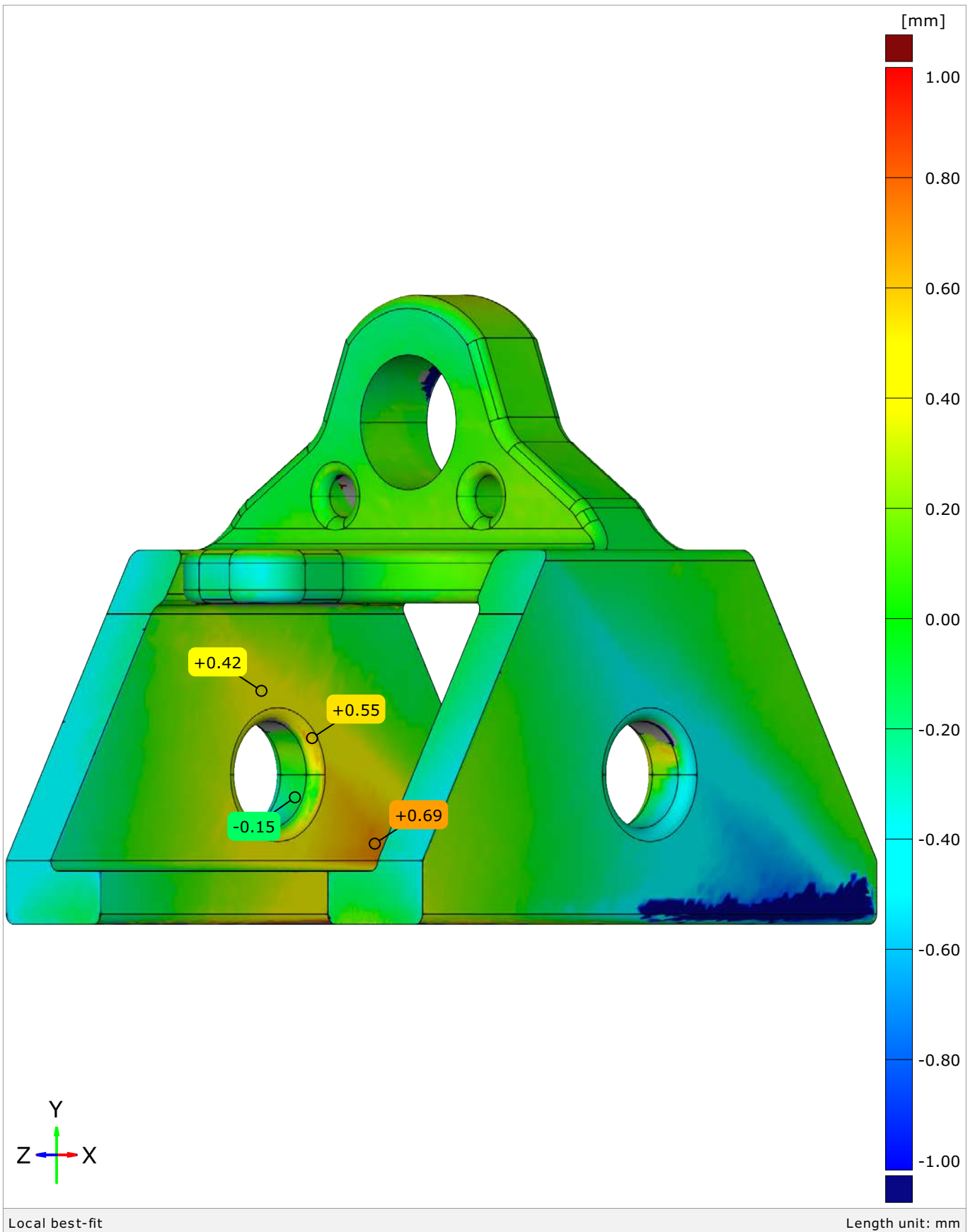
Local best-fit

Length unit: mm

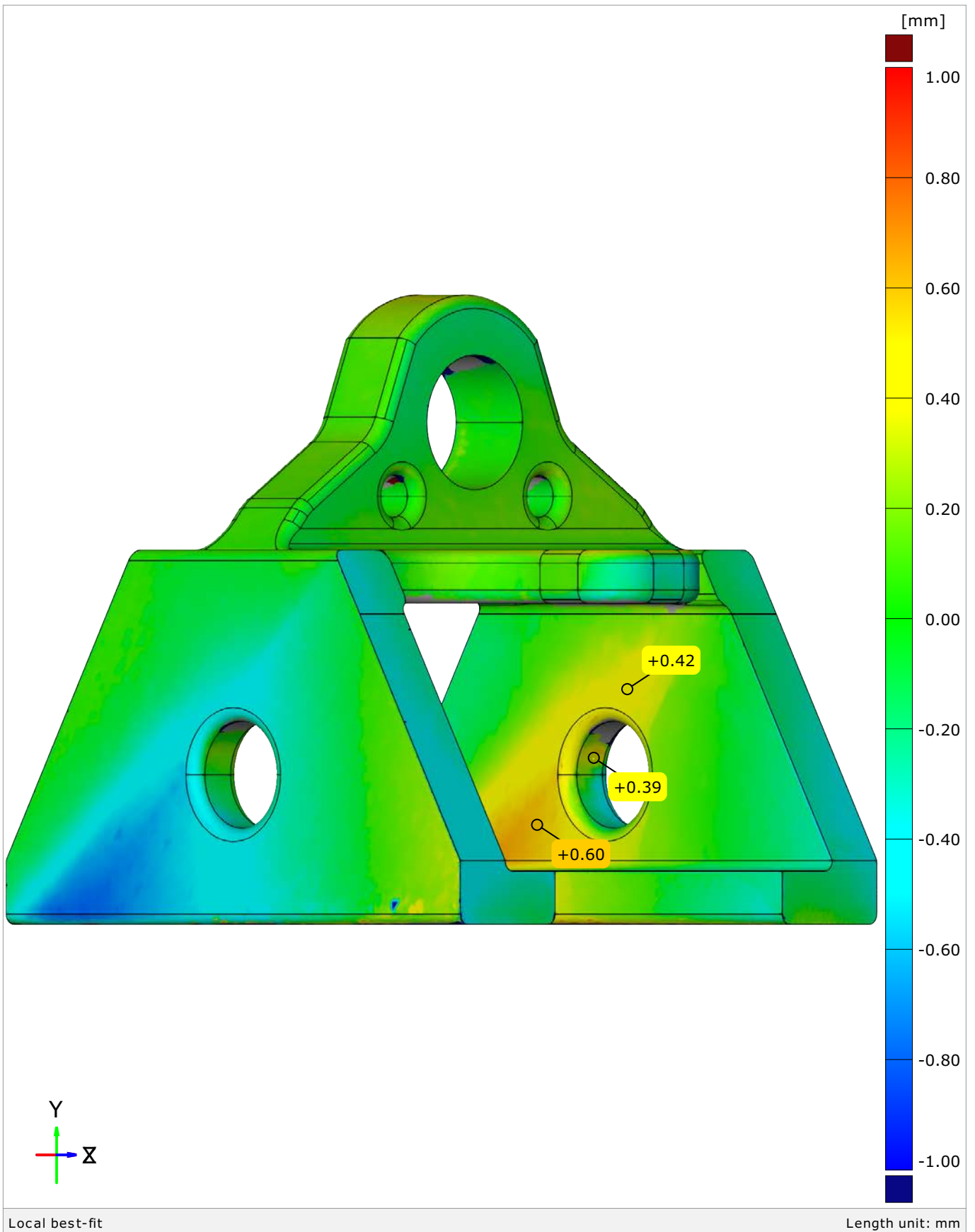
Surface Comparison



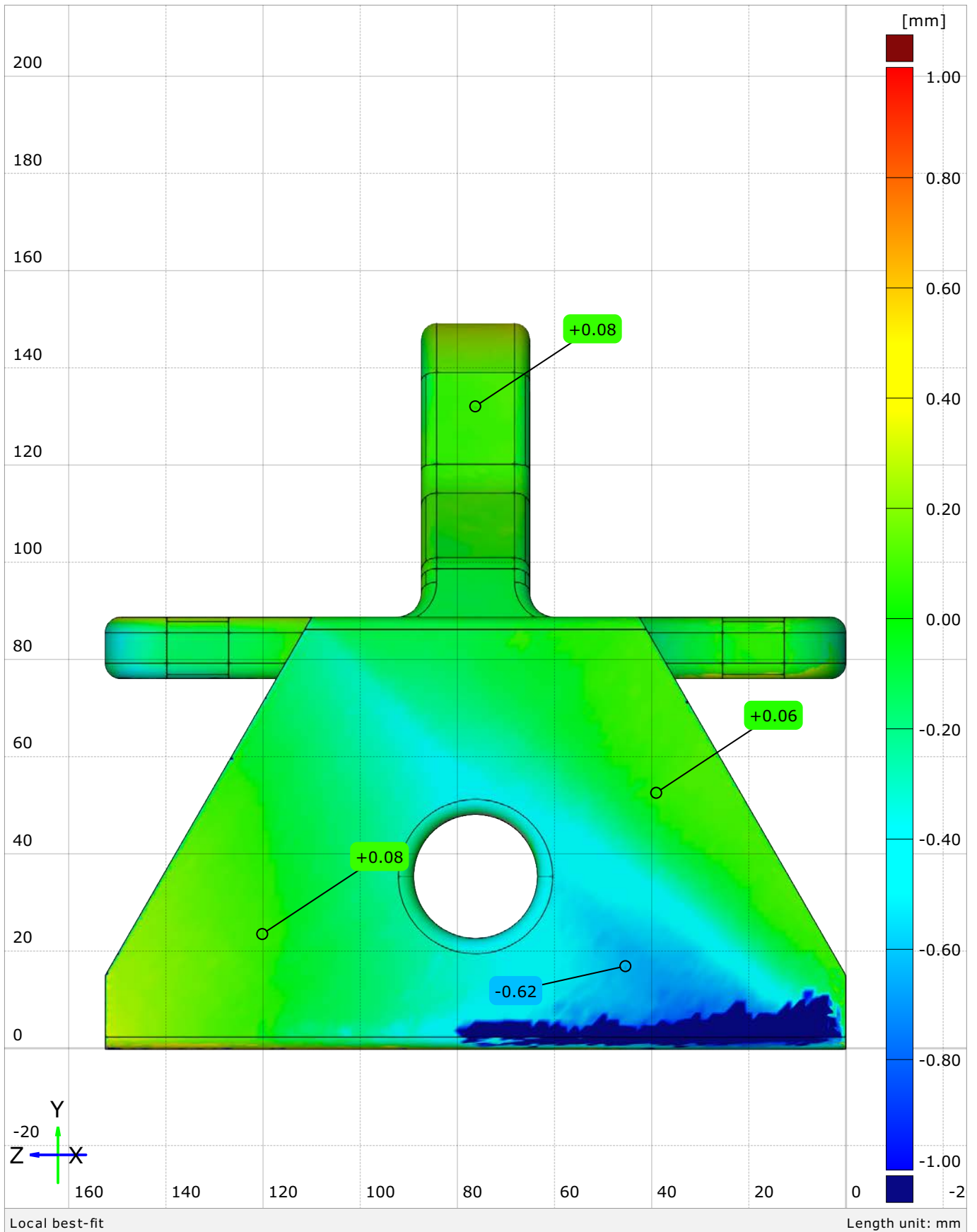
Surface Comparison Inside Left



Surface Comparison Inside Right



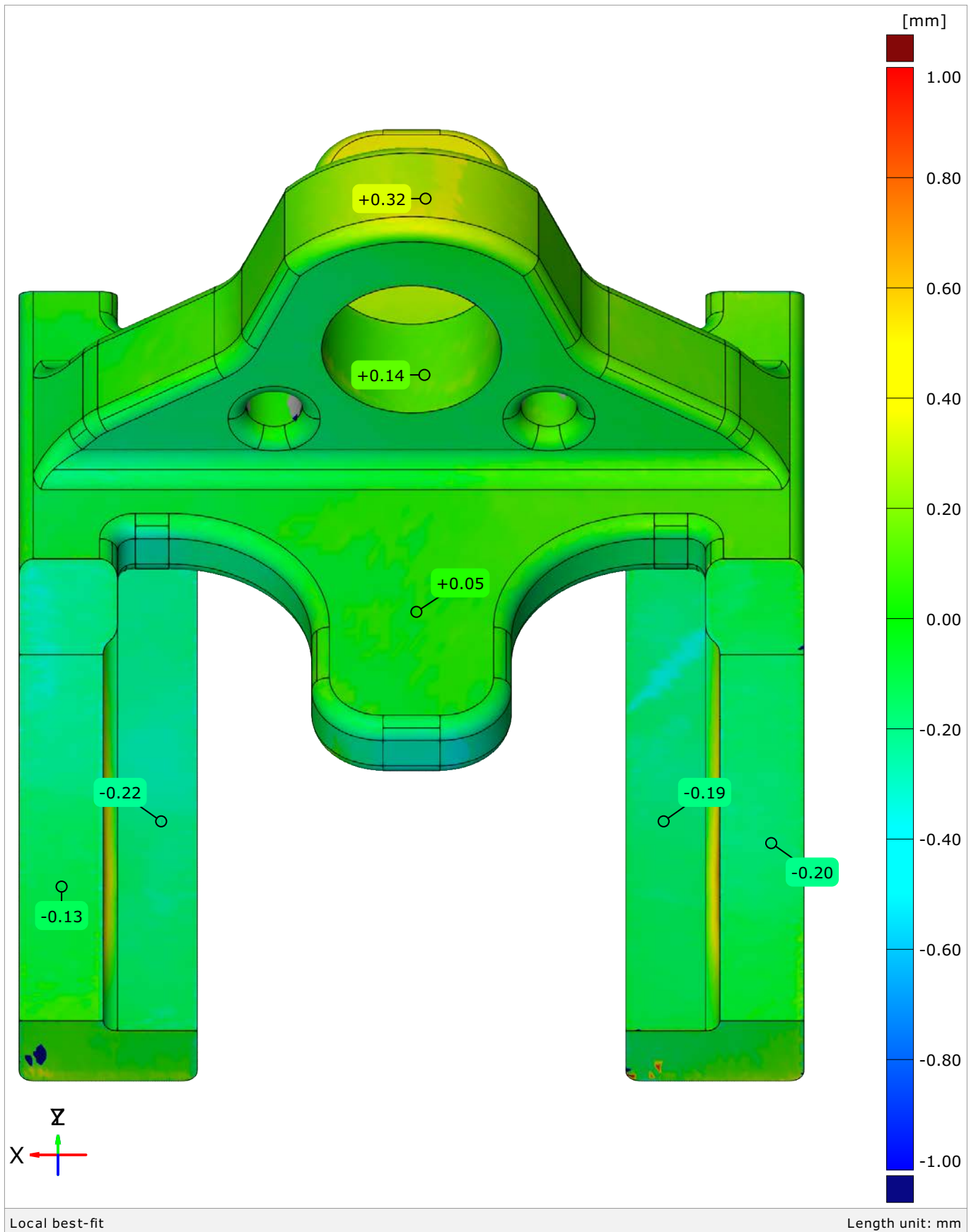
Surface Comparison 90° right



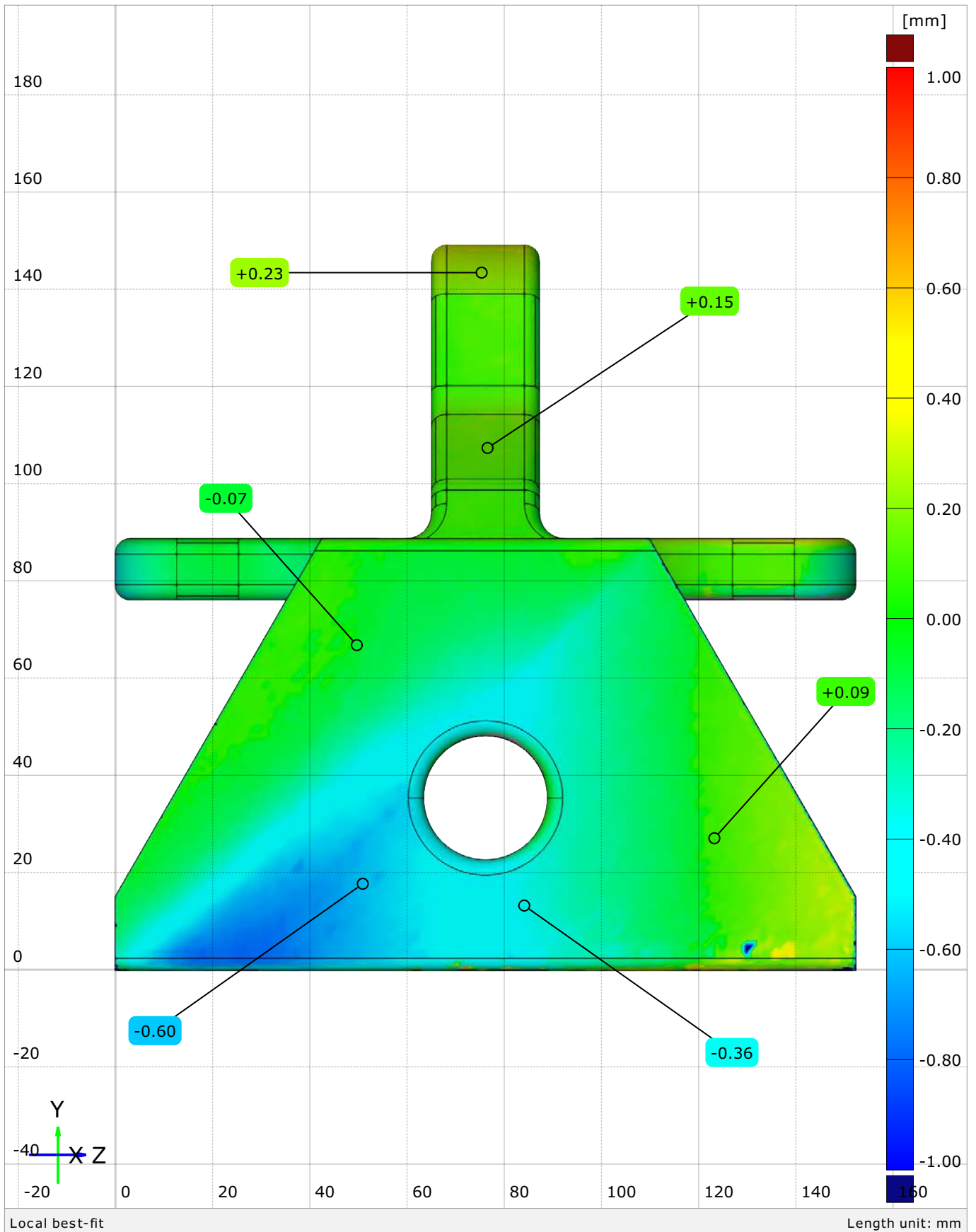
Local best-fit

Length unit: mm

Surface Comparison Back



Surface Comparison 90° right from Back



Appendix J

Mechanical Property Data of Printed Aluminum



Date: January 14, 2021

Company: Bureau of Reclamation

P.O. #:

ATTN: Stephanie Prochaska

Ref. #: Samples H1-4, V1-4

Address: PO Box 25007, Mail Code 86-68530

Material: AlSi10Mg Aluminum Alloy

Address: Denver, CO 80225-0007

Specification: ASTM E8/E8M-16ae1

Lab #: 2101-078

TENSILE TEST

CMS 209 Identity	Diameter in	Area in ²	Yield Strength		Tensile Strength		Elongation		Reduction of Area		Fracture
			Load (lb)	lb / in ²	Load (lb)	lb / in ²	(in)	%	Diameter in	%	Location
H1	0.2330	0.0426	1,358	31,900	1,968	46,200	1.08	8.5%	0.2010	26%	g
H2	0.2340	0.0430	1,516	35,300	1,993	46,300	1.10	9.5%	0.1960	30%	g
H3	0.2300	0.0415	1,357	32,700	1,930	46,500	1.11	11%	0.1970	27%	g
H4	0.2320	0.0423	1,374	32,500	1,966	46,500	1.13	13%	0.1980	27%	g
V1	0.2320	0.0423	1,349	31,900	1,900	44,900	1.14	14%	0.1790	40%	g
V2	0.2345	0.0432	1,378	31,900	1,945	45,000	1.16	16%	0.1800	41%	g
V3	0.2330	0.0426	1,370	32,200	1,920	45,100	1.13	13%	0.1750	43%	g
V4	0.2365	0.0439	1,386	31,600	1,990	45,300	1.16	16%	0.1845	39%	g

Yield Strength Determined By: 0.2% Offset

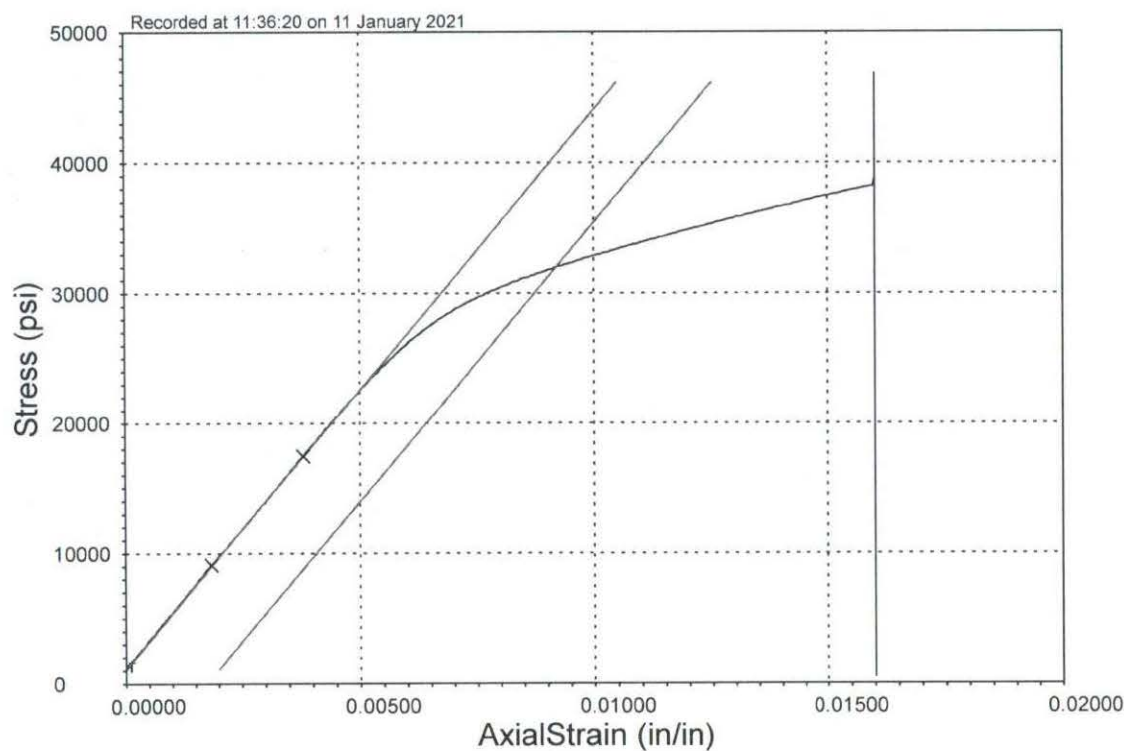
[g] Fractured thru gage marks or within specimen width of gage marks.

[X] Information Only

Respectfully Submitted,

Josh Belt
Materials Engineer

2101-078-H1



Specimen Identifier: 2101-078-H1
Instruments Used for Dimensions: #221 #232 #123 #124 #12
CMS Tensile Machine: #130
ADMET: #194
Technician: NLM
Temperature of Room: 69 F

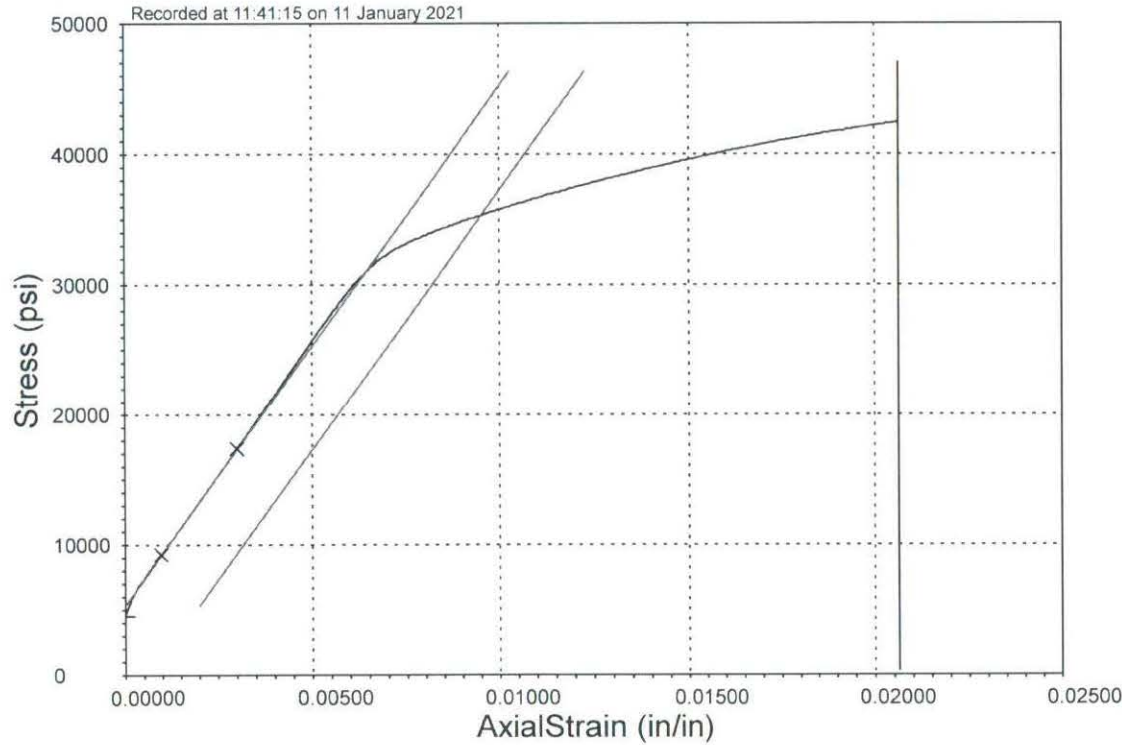
Test Date: 11 January 2021
Start Time: 11:36:20
End Time: 11:37:33

Geometry: Round
Diameter: 0.2330 in
Axial Strain Gauge Length: 2.0000 in
Area: 0.0426 sq in

Analysis Results

<u>Manual Elongation at Break</u>	
Elongation	8.35 %
Initial Gauge Length	1.0000 in
Final Gauge Length	1.0835 in
<u>Maximum Load</u>	
Load	1968 lb
<u>Maximum Stress</u>	
Maximum Stress	46158 psi
<u>Modulus of Elasticity</u>	
Modulus	4292518 psi
<u>Reduction of Area</u>	
Reduction	25.58160 %
Final Diameter	0.2010 in
<u>Yield by Offset (Load)</u>	
Yield	1358 lb
Offset	0.200 %
<u>Yield by Offset (Stress)</u>	
Yield	31839 psi
Offset	0.200 %

2101-078-H2



Specimen Identifier: 2101-078-H2
Instruments Used for Dimensions: #221 #232 #123 #124 #12
CMS Tensile Machine: #130
ADMET: #194
Technician: NLM
Temperature of Room: 69 F

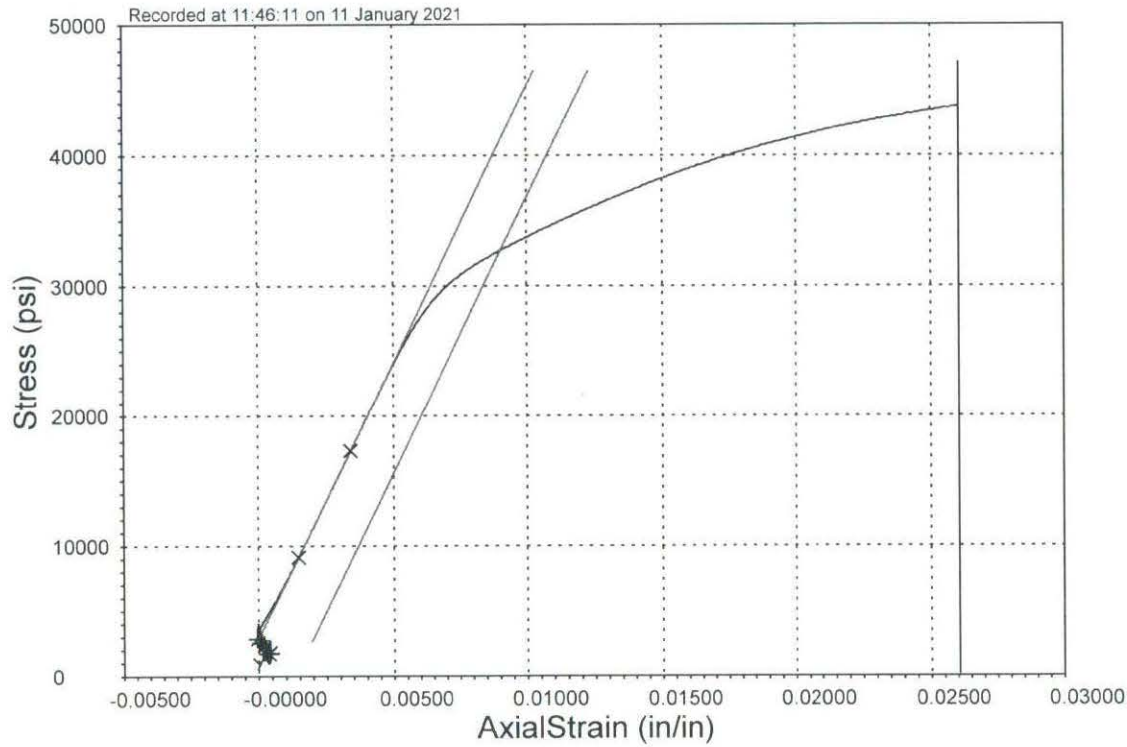
Test Date: 11 January 2021
Start Time: 11:41:15
End Time: 11:42:22

Geometry: Round
Diameter: 0.2340 in
Axial Strain Gauge Length: 2.0000 in
Area: 0.0430 sq in

Analysis Results

<u>Manual Elongation at Break</u>	
Elongation	9.55 %
Initial Gauge Length	1.0000 in
Final Gauge Length	1.0955 in
<u>Maximum Load</u>	
Load	1993 lb
<u>Maximum Stress</u>	
Maximum Stress	46339 psi
<u>Modulus of Elasticity</u>	
Modulus	3990353 psi
<u>Reduction of Area</u>	
Reduction	29.84149 %
Final Diameter	0.1960 in
<u>Yield by Offset (Load)</u>	
Yield	1516 lb
Offset	0.200 %
<u>Yield by Offset (Stress)</u>	
Yield	35249 psi
Offset	0.200 %

2101-078-H3



Specimen Identifier: 2101-078-H3
Instruments Used for Dimensions: #221 #232 #123 #124 #12
CMS Tensile Machine: #130
ADMET: #194
Technician: NLM
Temperature of Room: 69 F

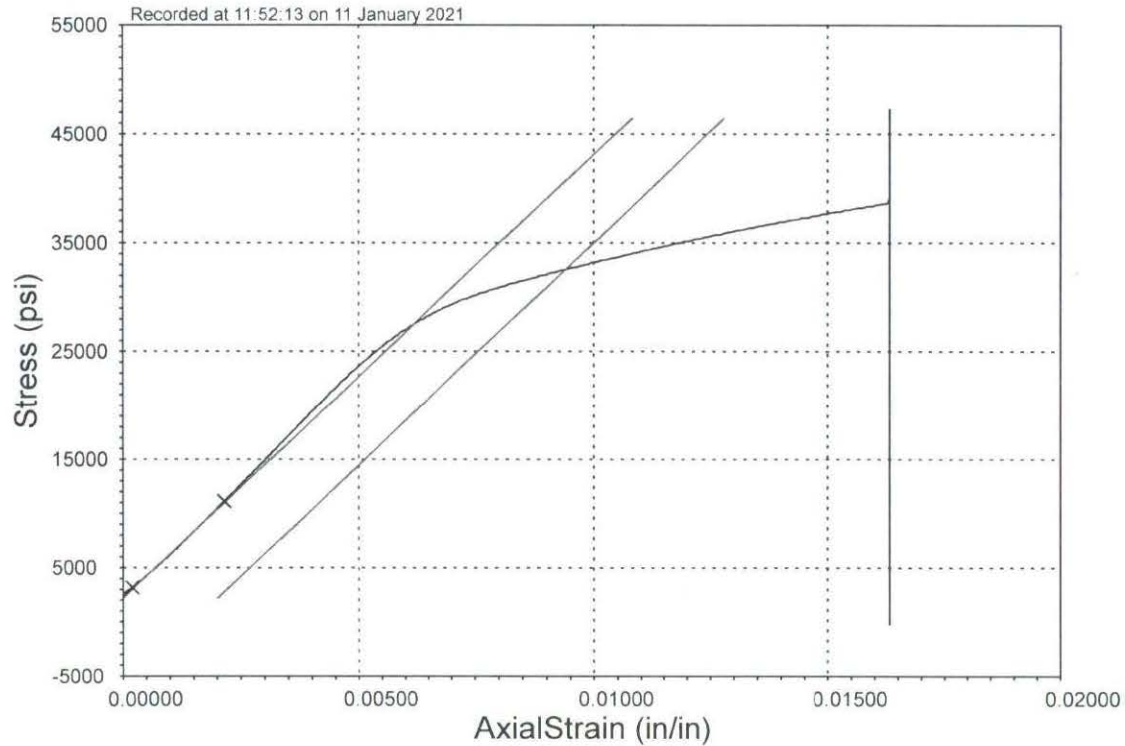
Test Date: 11 January 2021
Start Time: 11:46:11
End Time: 11:48:26

Geometry: Round
Diameter: 0.2300 in
Axial Strain Gauge Length: 2.0000 in
Area: 0.0415 sq in

Analysis Results

<u>Manual Elongation at Break</u>	
Elongation	11.20 %
Initial Gauge Length	1.0000 in
Final Gauge Length	1.1120 in
<u>Maximum Load</u>	
Load	1930 lb
<u>Maximum Stress</u>	
Maximum Stress	46465 psi
<u>Modulus of Elasticity</u>	
Modulus	4234516 psi
<u>Reduction of Area</u>	
Reduction	26.63706 %
Final Diameter	0.1970 in
<u>Yield by Offset (Load)</u>	
Yield	1357 lb
Offset	0.200 %
<u>Yield by Offset (Stress)</u>	
Yield	32651 psi
Offset	0.200 %

2101-078-H4



Specimen Identifier: 2101-078-H4
Instruments Used for Dimensions: #221 #232 #123 #124 #12
CMS Tensile Machine: #130
ADMET: #194
Technician: NLM
Temperature of Room: 69 F

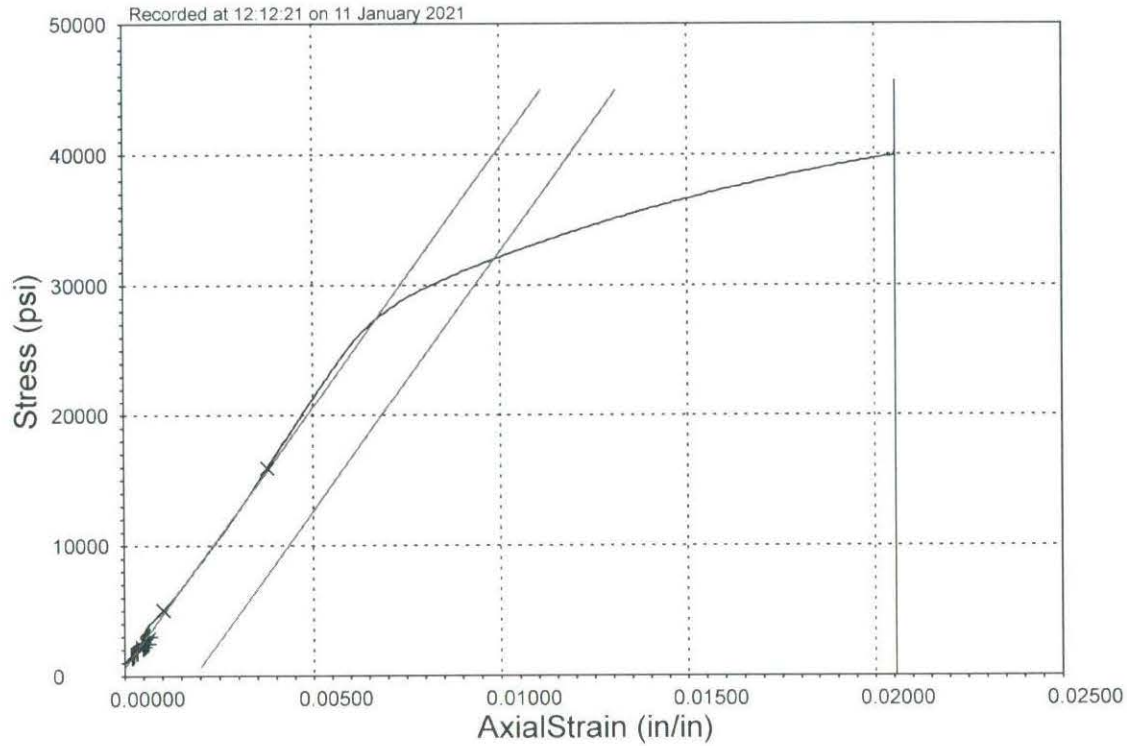
Test Date: 11 January 2021
Start Time: 11:52:13
End Time: 11:53:13

Geometry: Round
Diameter: 0.2320 in
Axial Strain Gauge Length: 2.0000 in
Area: 0.0423 sq in

Analysis Results

<u>Manual Elongation at Break</u>	
Elongation	13.20 %
Initial Gauge Length	1.0000 in
Final Gauge Length	1.1320 in
<u>Maximum Load</u>	
Load	1966 lb
<u>Maximum Stress</u>	
Maximum Stress	46510 psi
<u>Modulus of Elasticity</u>	
Modulus	4097469 psi
<u>Reduction of Area</u>	
Reduction	27.16259 %
Final Diameter	0.1980 in
<u>Yield by Offset (Load)</u>	
Yield	1374 lb
Offset	0.200 %
<u>Yield by Offset (Stress)</u>	
Yield	32512 psi
Offset	0.200 %

2101-078-V1



Specimen Identifier: 2101-078-V1
Instruments Used for Dimensions: #221 #232 #123 #124 #12
CMS Tensile Machine: #130
ADMET: #194
Technician: NLM
Temperature of Room: 69 F

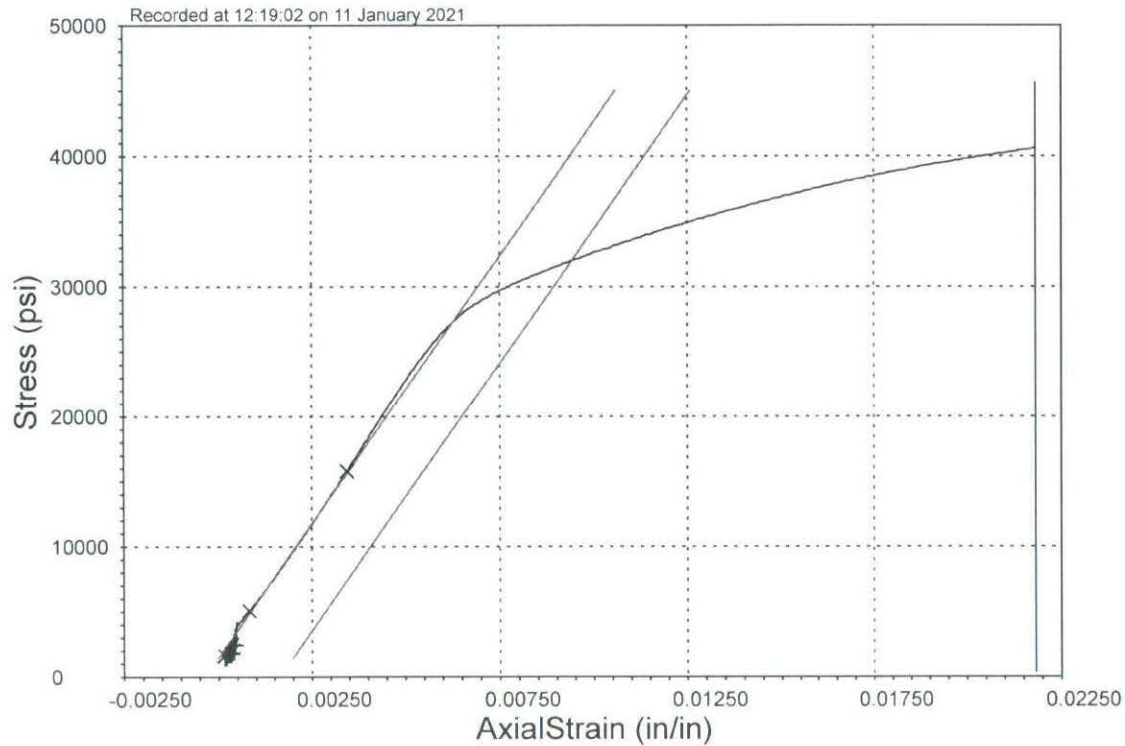
Test Date: 11 January 2021
Start Time: 12:12:21
End Time: 12:14:24

Geometry: Round
Diameter: 0.2320 in
Axial Strain Gauge Length: 2.0000 in
Area: 0.0423 sq in

Analysis Results

<u>Manual Elongation at Break</u>	
Elongation	13.60 %
Initial Gauge Length	1.0000 in
Final Gauge Length	1.1360 in
<u>Maximum Load</u>	
Load	1900 lb
<u>Maximum Stress</u>	
Maximum Stress	44941 psi
<u>Modulus of Elasticity</u>	
Modulus	3989259 psi
<u>Reduction of Area</u>	
Reduction	40.47079 %
Final Diameter	0.1790 in
<u>Yield by Offset (Load)</u>	
Yield	1349 lb
Offset	0.200 %
<u>Yield by Offset (Stress)</u>	
Yield	31904 psi
Offset	0.200 %

2101-078-V2



Specimen Identifier: 2101-078-V2
Instruments Used for Dimensions: #221 #232 #123 #124 #12
CMS Tensile Machine: #130
ADMET: #194
Technician: NLM
Temperature of Room: 69 F

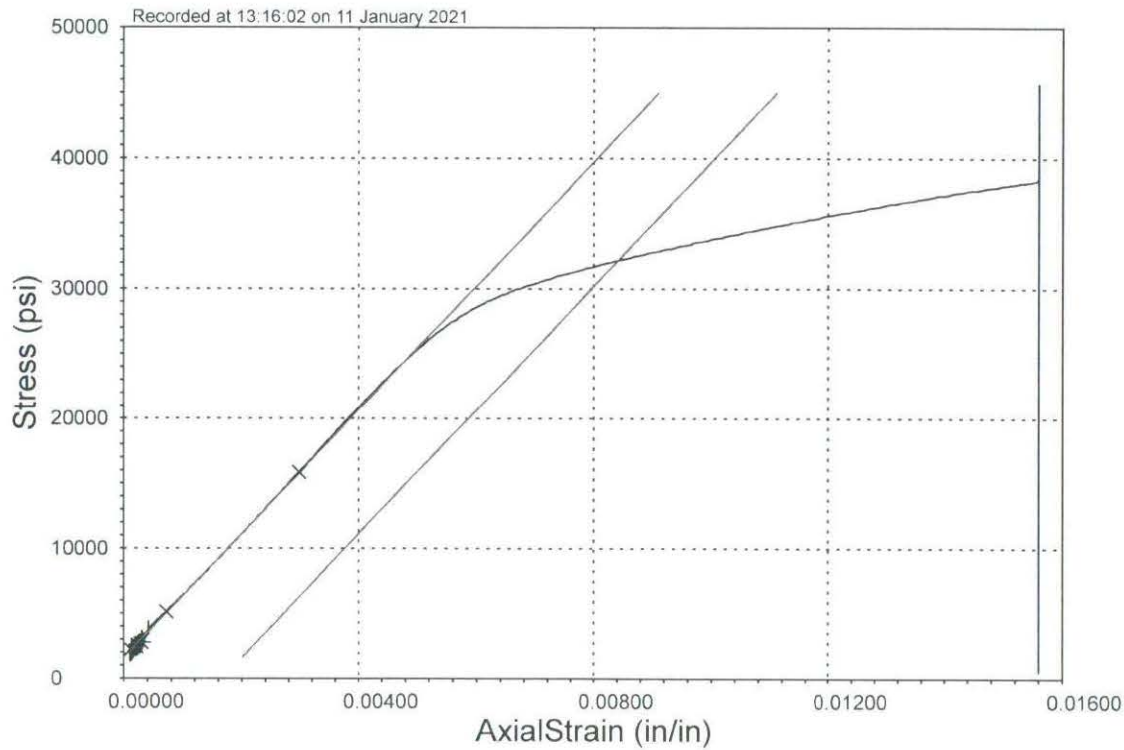
Test Date: 11 January 2021
Start Time: 12:19:02
End Time: 12:21:10

Geometry: Round
Diameter: 0.2345 in
Axial Strain Gauge Length: 2.0000 in
Area: 0.0432 sq in

Analysis Results

<u>Manual Elongation at Break</u>	
Elongation	15.50 %
Initial Gauge Length	1.0000 in
Final Gauge Length	1.1550 in
<u>Maximum Load</u>	
Load	1945 lb
<u>Maximum Stress</u>	
Maximum Stress	45042 psi
<u>Modulus of Elasticity</u>	
Modulus	41152999 psi
<u>Reduction of Area</u>	
Reduction	41.08046 %
Final Diameter	0.1800 in
<u>Yield by Offset (Load)</u>	
Yield	1378 lb
Offset	0.200 %
<u>Yield by Offset (Stress)</u>	
Yield	31914 psi
Offset	0.200 %

2101-078-V3



Specimen Identifier: 2101-078-V3
Instruments Used for Dimensions: #221 #232 #123 #124 #12
CMS Tensile Machine: #130
ADMET: #194
Technician: NLM
Temperature of Room: 69 F

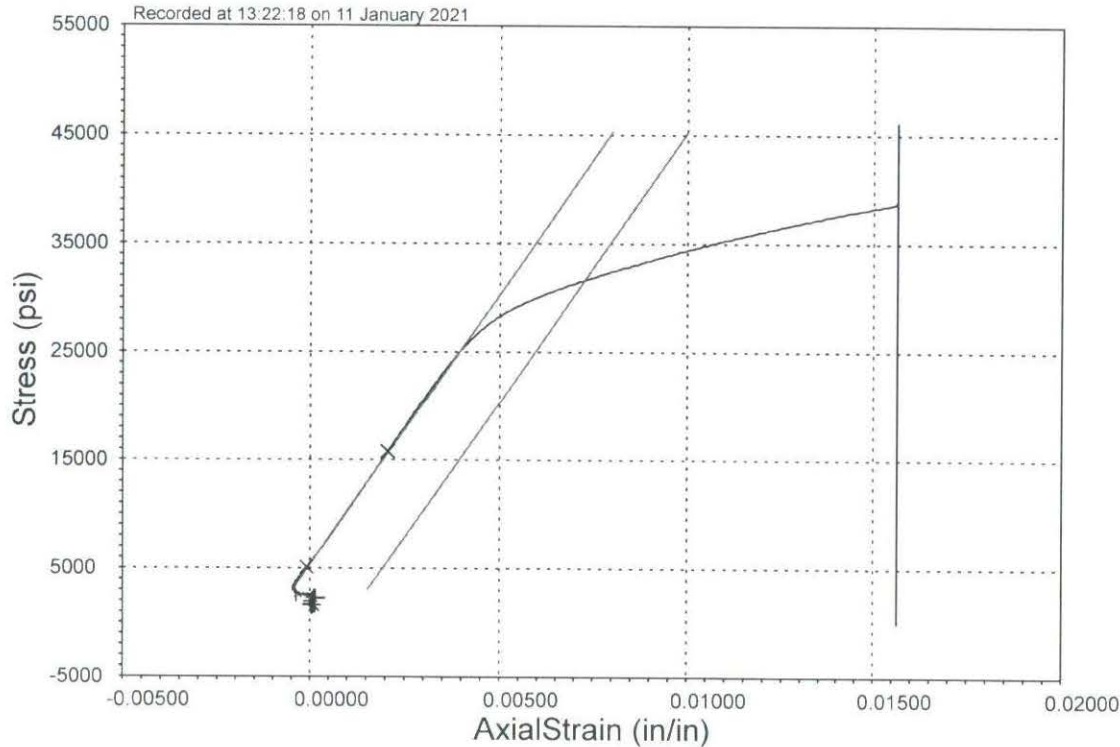
Test Date: 11 January 2021
Start Time: 13:16:02
End Time: 13:18:46

Geometry: Round
Diameter: 0.2330 in
Axial Strain Gauge Length: 2.0000 in
Area: 0.0426 sq in

Analysis Results

<u>Manual Elongation at Break</u>	
Elongation	13.20 %
Initial Gauge Length	1.0000 in
Final Gauge Length	1.1320 in
<u>Maximum Load</u>	
Load	1920 lb
<u>Maximum Stress</u>	
Maximum Stress	45021 psi
<u>Modulus of Elasticity</u>	
Modulus	4767538 psi
<u>Reduction of Area</u>	
Reduction	43.58894 %
Final Diameter	0.1750 in
<u>Yield by Offset (Load)</u>	
Yield	1370 lb
Offset	0.200 %
<u>Yield by Offset (Stress)</u>	
Yield	32141 psi
Offset	0.200 %

2101-078-V4



Specimen Identifier: 2101-078-V4
Instruments Used for Dimensions: #221 #232 #123 #124 #12
CMS Tensile Machine: #130
ADMET: #194
Technician: NLM
Temperature of Room: 69 F

Test Date: 11 January 2021
Start Time: 13:22:18
End Time: 13:24:13

Geometry: Round
Diameter: 0.2365 in
Axial Strain Gauge Length: 2.0000 in
Area: 0.0439 sq in

Analysis Results

Manual Elongation at Break

Elongation	15.75 %
Initial Gauge Length	1.0000 in
Final Gauge Length	1.1575 in
<u>Maximum Load</u>	
Load	1990 lb
<u>Maximum Stress</u>	
Maximum Stress	45297 psi
<u>Modulus of Elasticity</u>	
Modulus	4991573 psi
<u>Reduction of Area</u>	
Reduction	39.14022 %
Final Diameter	0.1845 in
<u>Yield by Offset (Load)</u>	
Yield	1386 lb
Offset	0.200 %
<u>Yield by Offset (Stress)</u>	
Yield	31557 psi
Offset	0.200 %

Appendix K

Density Measurement Procedure

Density Measurement Procedure

The density of the additive manufacturing materials evaluated in this study were tested in accordance with ASTM B962-17, *Standard Test Methods for Density of Compacted or Sintered Powder Metallurgy (PM) Products Using Archimedes' Principle*. This standard provides multiple procedures for infiltrating specimens with oil and recommends the use of vacuum infiltration. Due to material and time constraints, researchers implemented an adjusted procedure, taking advantage of surface pressure reduction by boiling. Since boiling causes the surface pressure on a submerged specimen to drop below one atmosphere, boiling specimens in mineral oil with viscosity between 20–65 centistokes (cSt) at 38 °C will allow the oil to infiltrate any surface-connected porosity. For these tests, specimens were boiled in mineral oil with a viscosity of 32 cSt for 1 hour.

The adjusted procedure requires three mass measurements:

1. Mass of sintered part in air
2. Mass of oil-impregnated part in air
3. Mass of oil-impregnated part in water

Each mass reading was taken three times per specimen and averaged to obtain the final reading. Using these masses and the density of the water, the density was calculated using the following equation:

$$\text{Sintered Density} = D_s = \frac{A\rho_w}{B - C}$$

Appendix L

3D Scan Results of Aluminum Bronze Slinger Rings As-Printed



3D Printed Part A2228

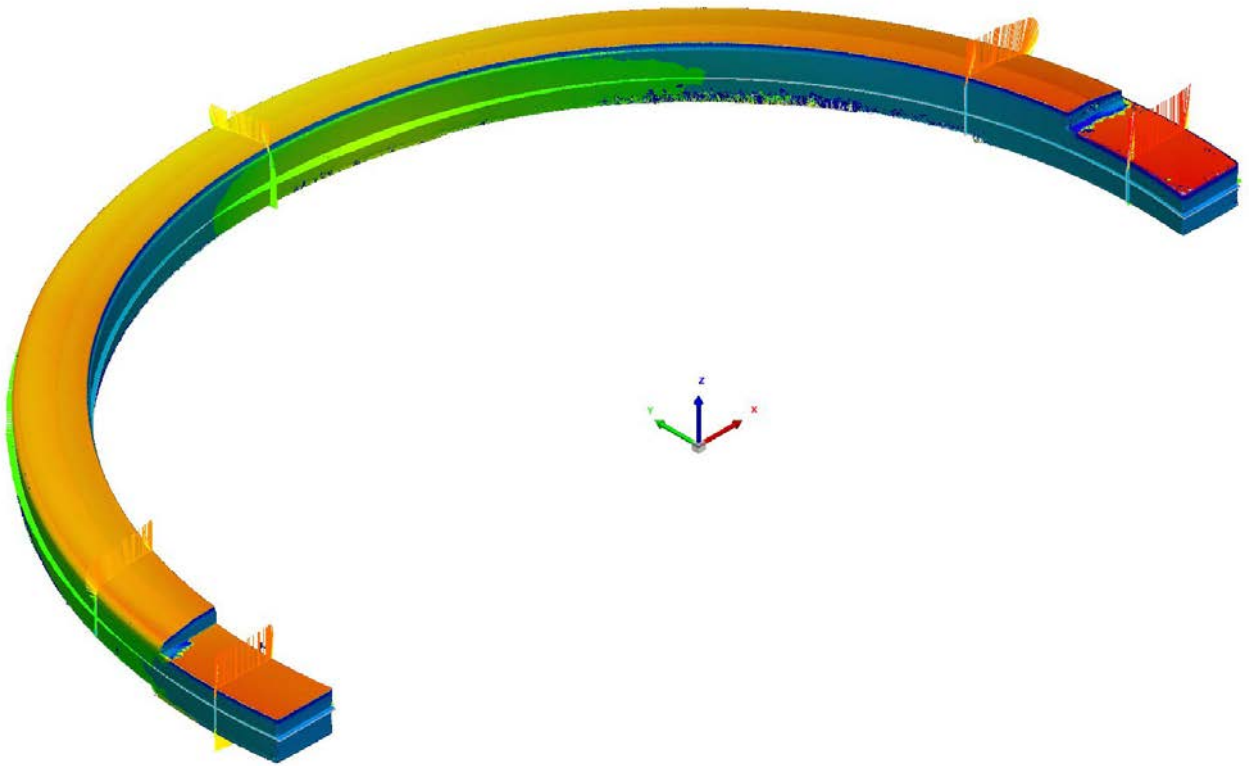
Part number: Slinger Ring A2228

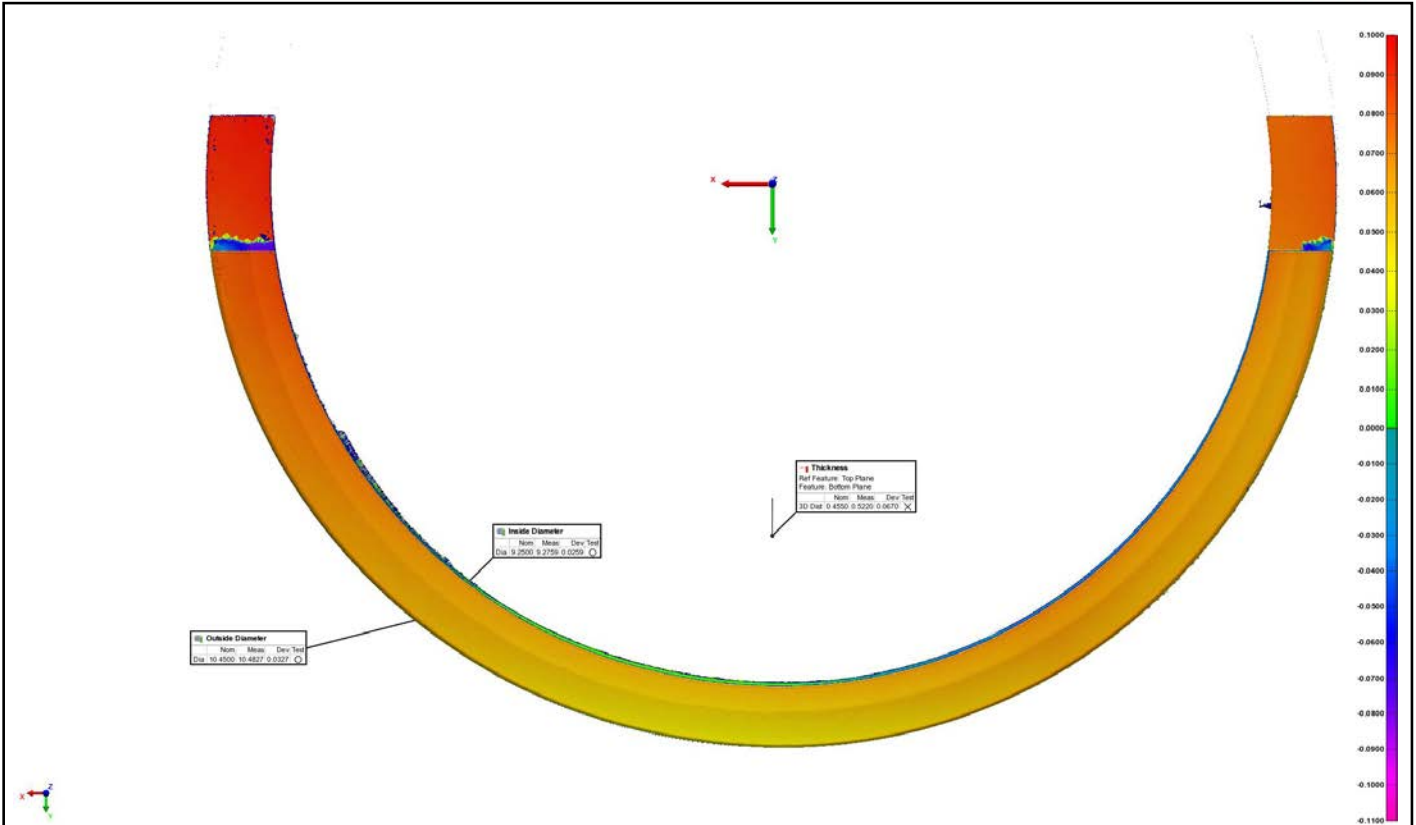
Workspace: Jermyn 3D Printed Material

Project: Part A2228 - piece 1

Report Author: Chad Paulson

Date: 4/22/2022

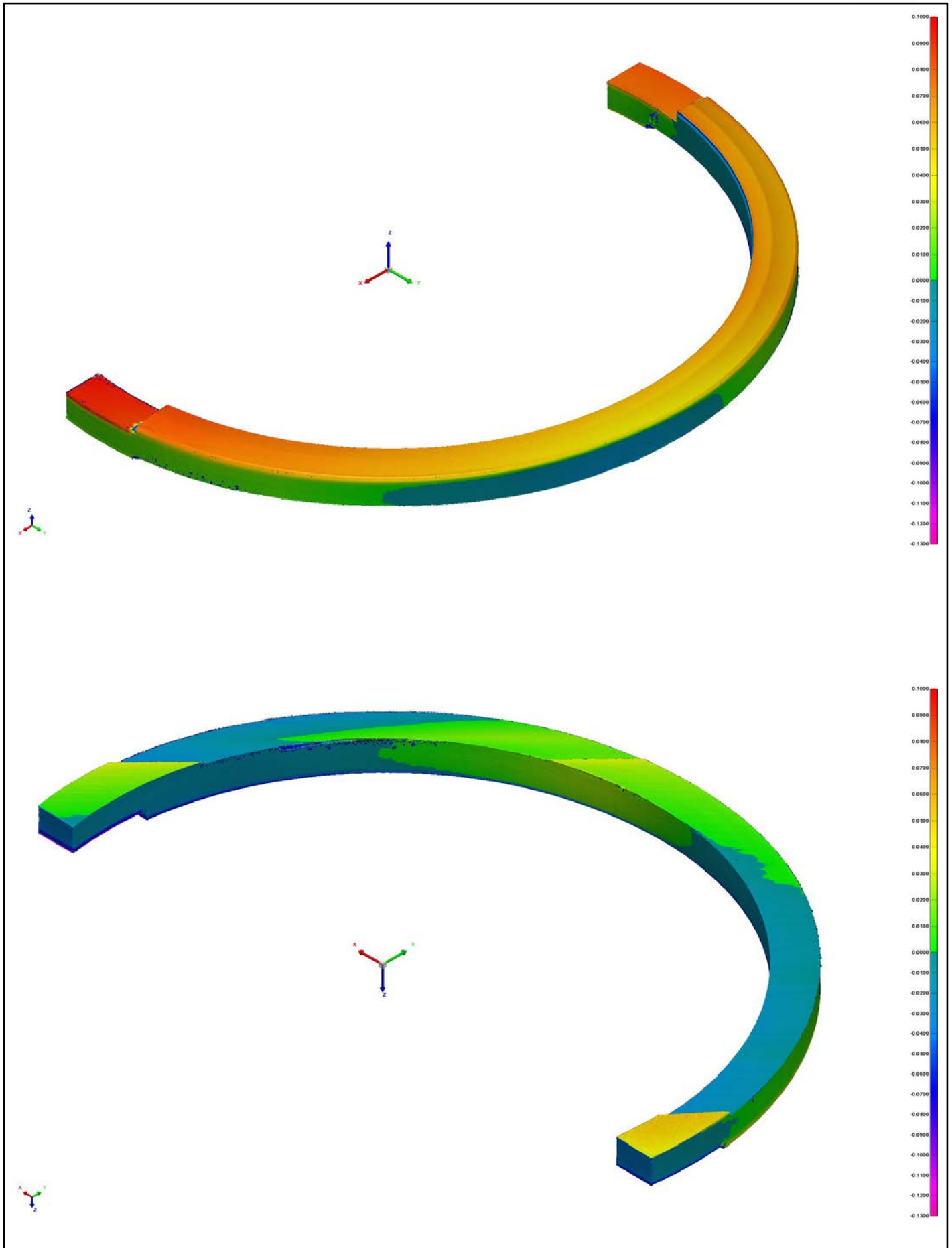


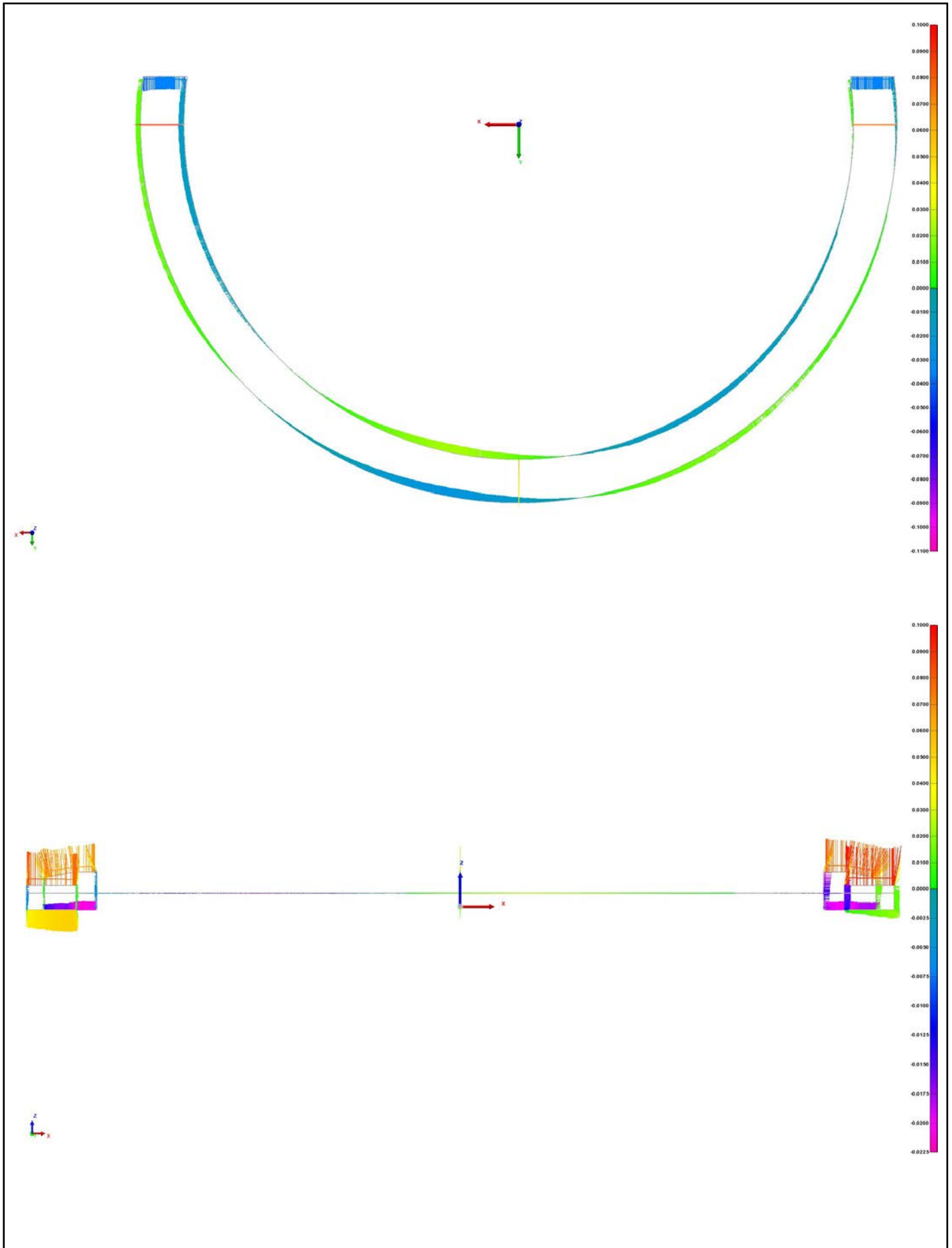


Control View

Control View Name Diameter Comparison
 Units Inches
 Coordinate Systems world
 Data Alignments best-fit to ref 1 (alignment group 2), best-fit to ref 1 (alignment group 6), best-fit to ref 1 (alignment group 5)
 All Statistics Total: 3, Measured: 3 (100.0000%), Pass: 2 (66.6667%), Fail: 1 (33.3333%), Warning: 0 (0.0000%)

Char No.	Object Name	Control	Nom	Meas	Tol	Dev	Test	Out Tol
	Inside Diameter	Diameter	9.2500	9.2759	±0.0394	0.0259	Pass	
	Outside Diameter	Diameter	10.4500	10.4827	±0.0394	0.0327	Pass	
	Thickness	3D Distance	0.4500	0.5220	±0.0394	0.0670	Fail	0.0276







3D Printed Part A2229

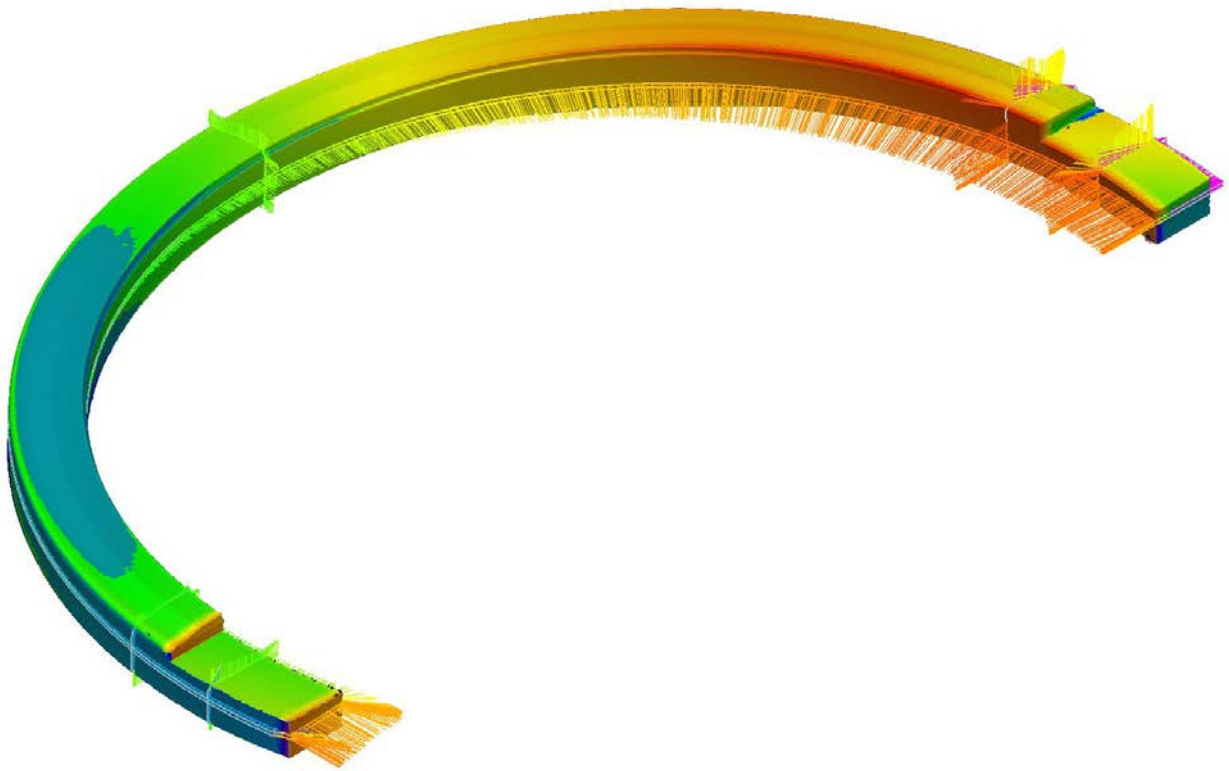
Part number: A2229

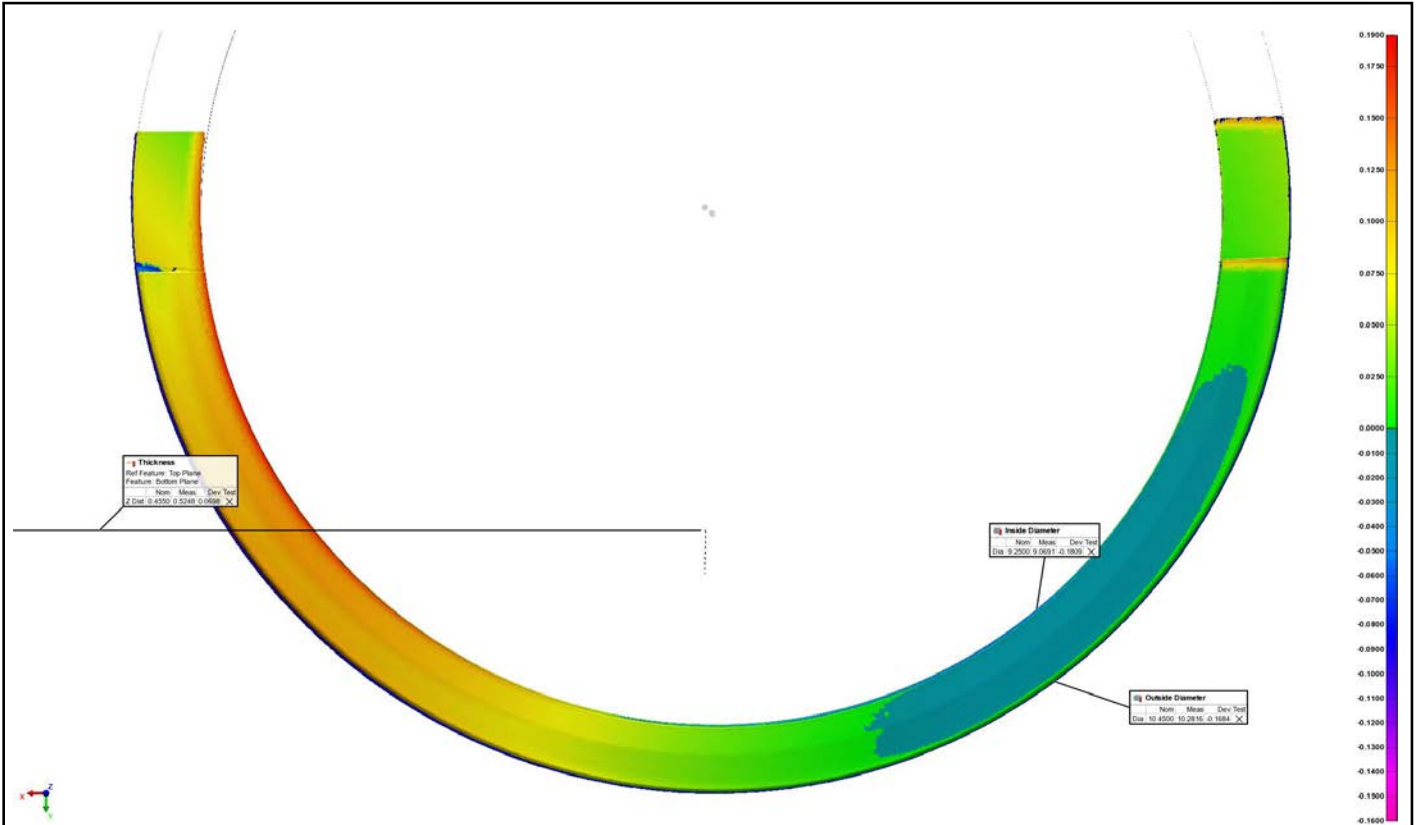
Workspace: Jermyn 3D Printed Material

Project: Part A2229 - piece 1

Report Author: Chad Paulson

Date: 4/22/2022

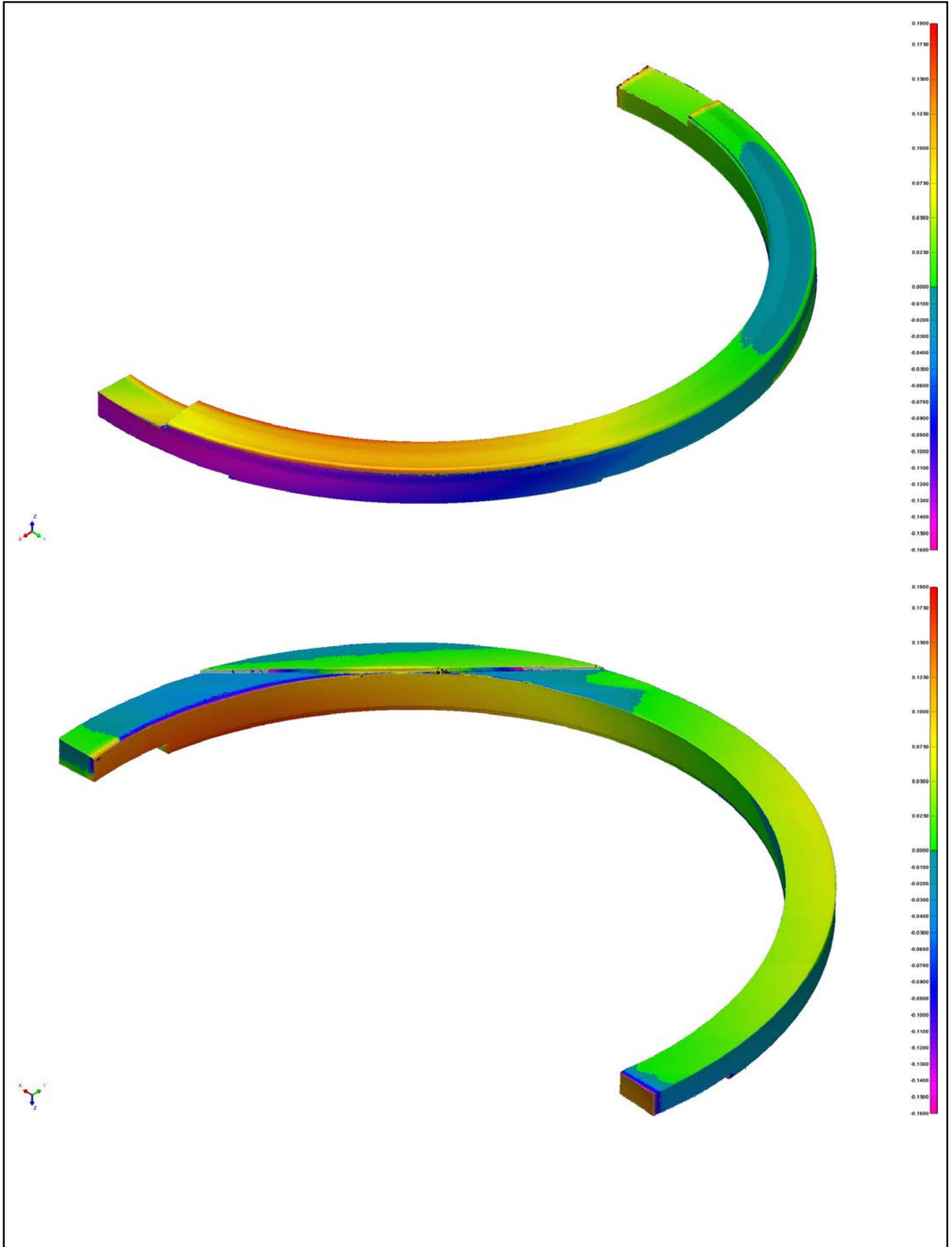


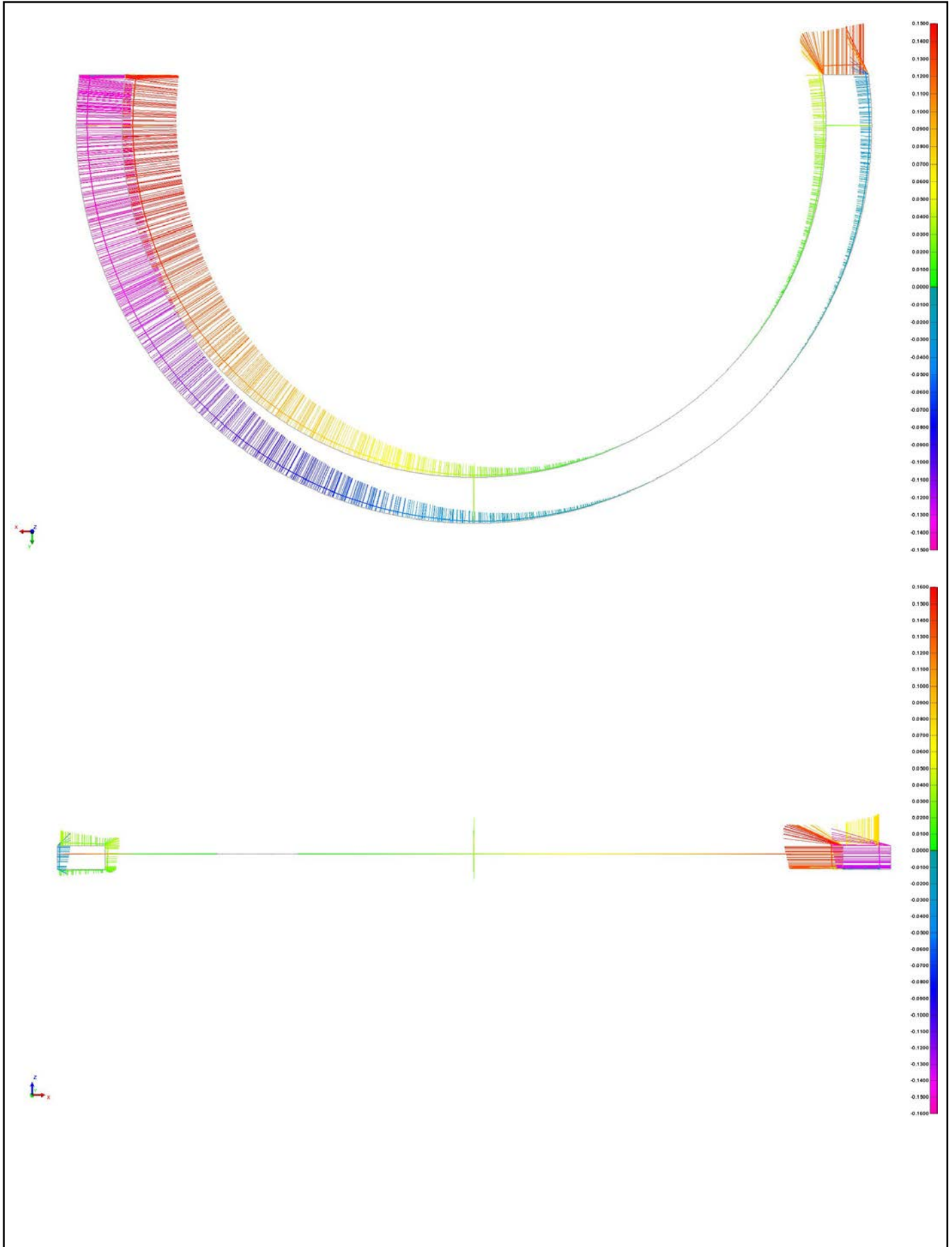


Control View

Control View Name Diameter Comparison (2)
 Units Inches
 Coordinate Systems world
 Data Alignments best-fit to ref 1 (alignment group 1), best-fit to ref 1 (alignment group 2), best-fit to ref 1 (alignment group 3)
 All Statistics Total: 3, Measured: 3 (100.0000%), Pass: 0 (0.0000%), Fail: 3 (100.0000%), Warning: 0 (0.0000%)

Char No.	Object Name	Control	Nom	Meas	Tol	Dev	Test	Out Tol
	Inside Diameter	Diameter	9.2500	9.0691	±0.0394	-0.1809	Fail	-0.1415
	Outside Diameter	Diameter	10.4500	10.2816	±0.0394	-0.1684	Fail	-0.1290
	Thickness	Z Distance	0.4550	0.5248	±0.0394	0.0698	Fail	0.0304







3D Printed Part A2237

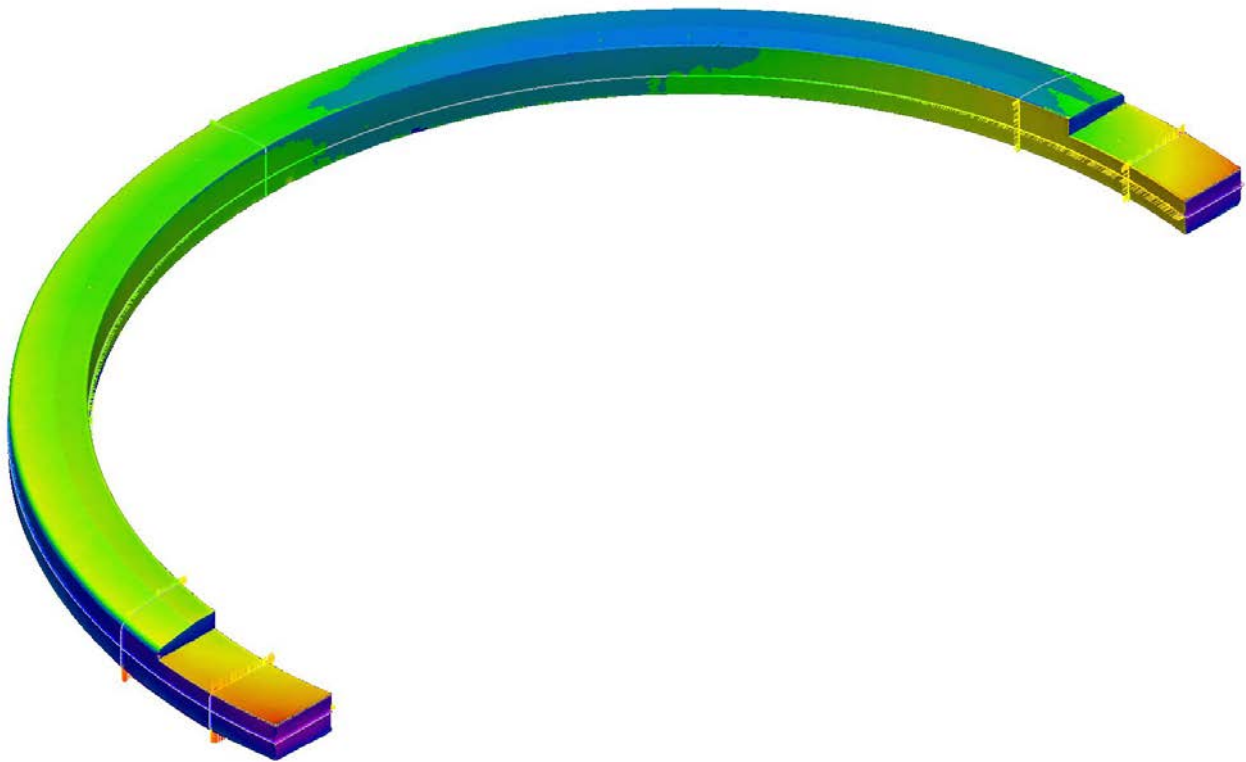
Part number: Slinger Ring A2237

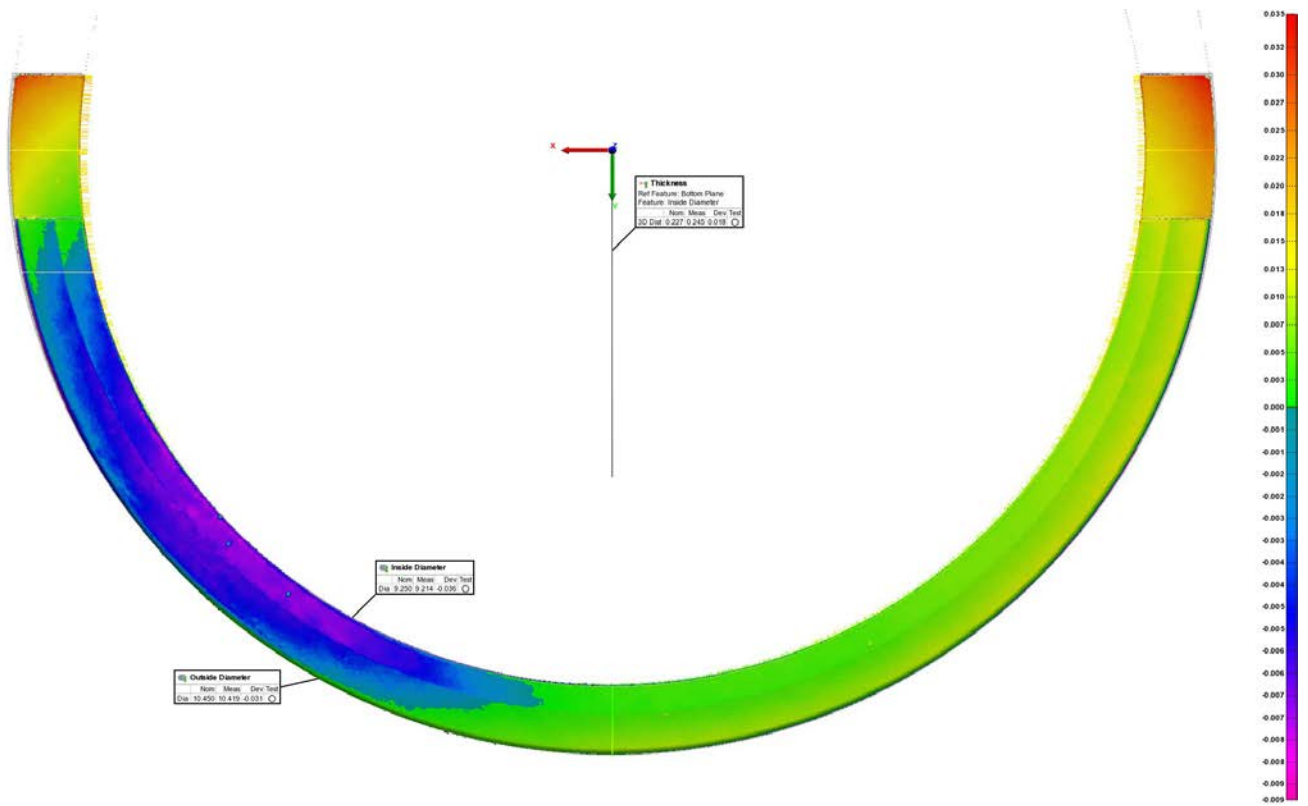
Workspace: Jermyn 3D Printed Material

Project: Part A2237 - piece 1

Report Author: Chad Paulson

Date: 4/22/2022

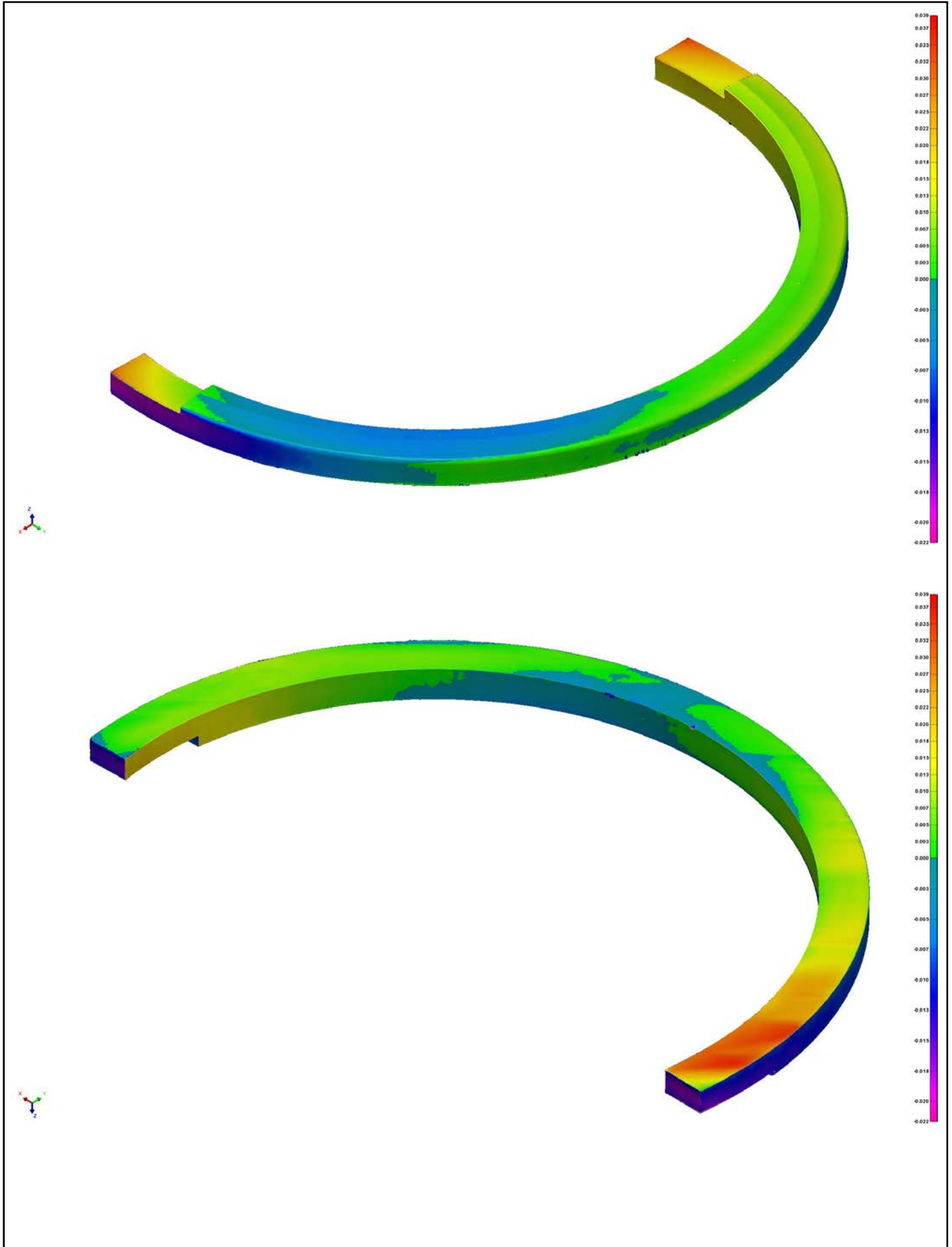


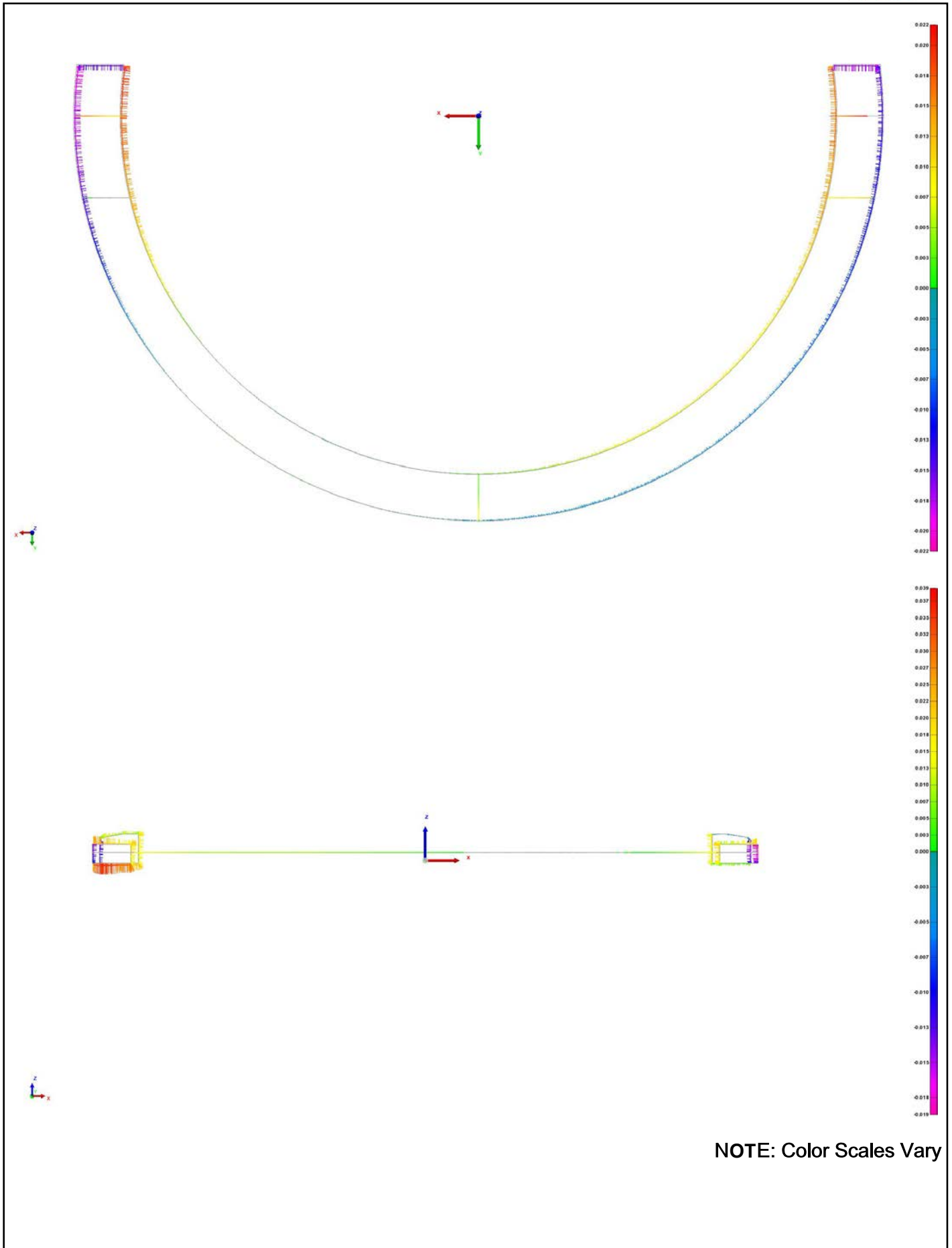


Control View

Control View Name Diameter Comparison
 Units Inches
 Coordinate Systems world
 Data Alignments best-fit to ref 1 (alignment group 1), best-fit to ref 1 (alignment group 2), best-fit to ref 1 (alignment group 3)
 All Statistics Total: 3, Measured: 3 (100.0000%), Pass: 3 (100.0000%), Fail: 0 (0.0000%), Warning: 0 (0.0000%)

Char No.	Object Name	Control	Nom	Meas	Tol	Dev	Test	Out Tol
	Inside Diameter	Diameter	9.2500	9.2141	±0.0394	-0.0359	Pass	
	Outside Diameter	Diameter	10.4500	10.4188	±0.0394	-0.0312	Pass	
	Thickness	3D Distance	0.2275	0.2454	±0.0394	0.0179	Pass	





NOTE: Color Scales Vary



3D Printed Part A 2240

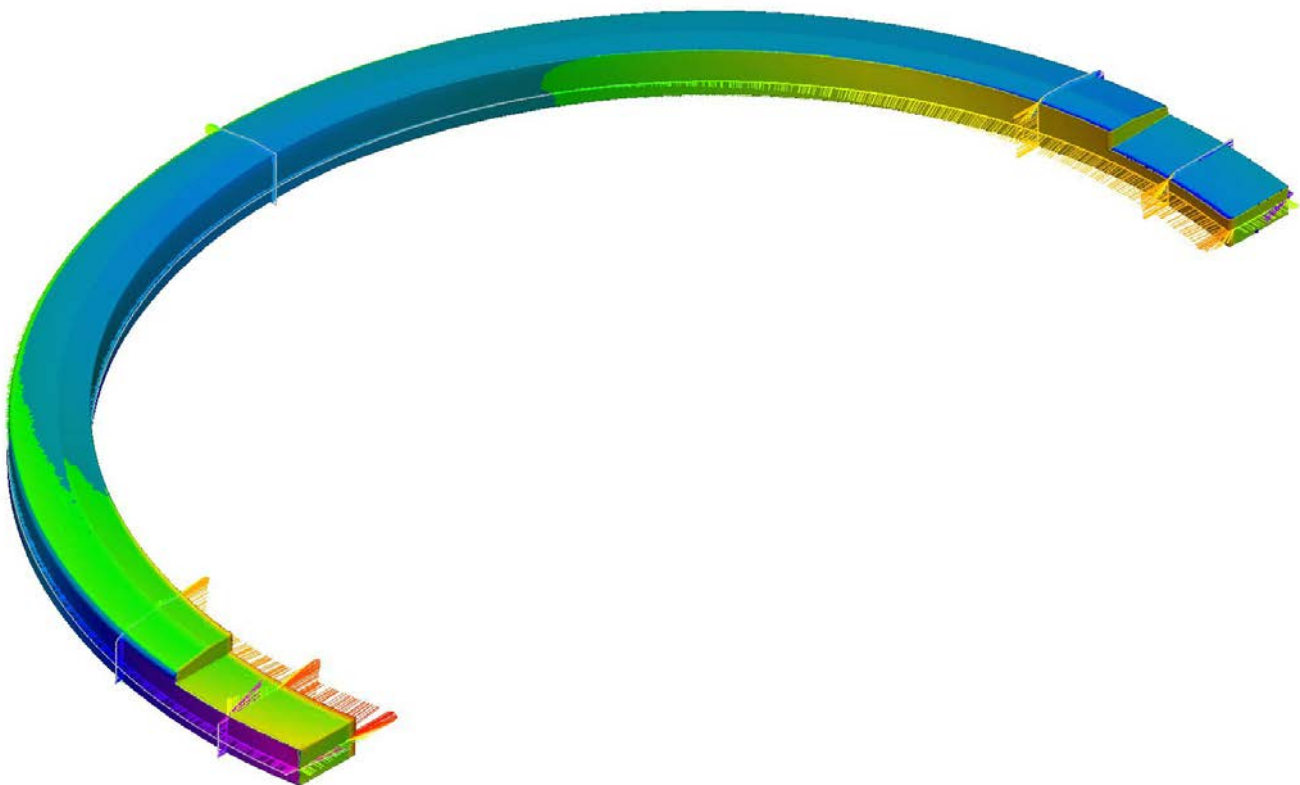
Part number: Slinger Ring A2240

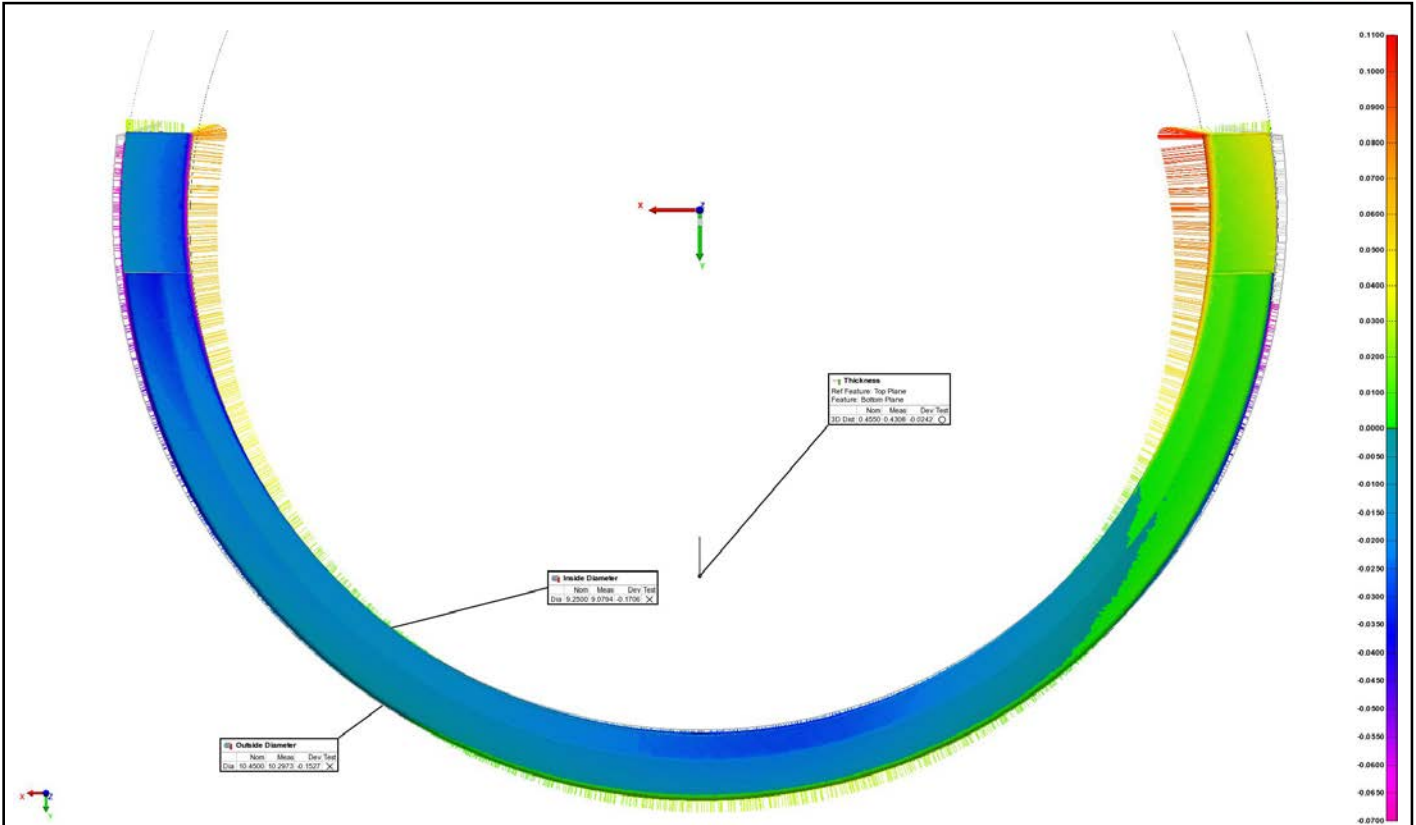
Workspace: Jermyn 3D Printed Material

Project: Part A2240 - piece 1

Report Author: Chad Paulson

Date: 4/22/2022

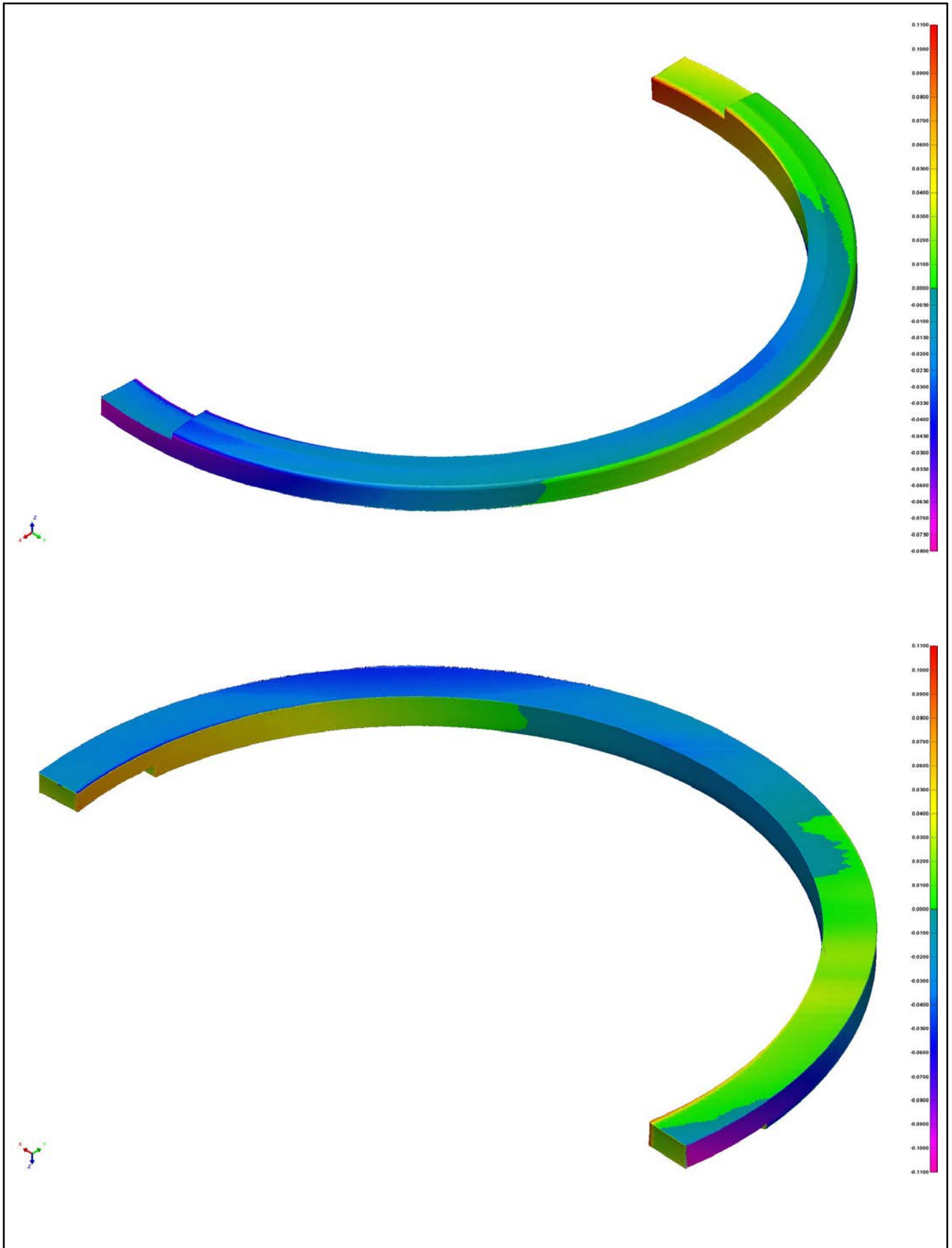


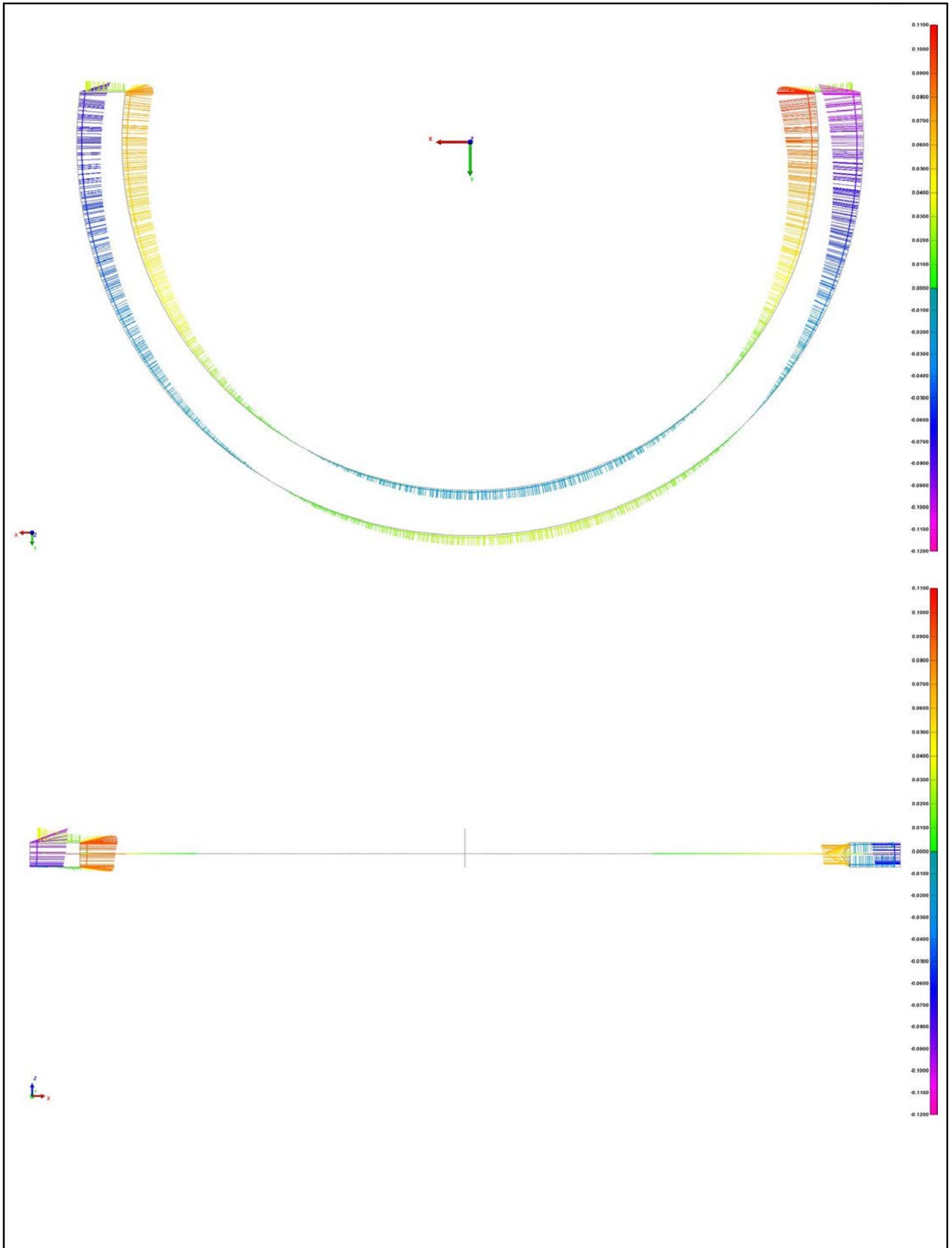


Control View

Control View Name Diameter Comparison (2)
 Units Inches
 Coordinate Systems world
 Data Alignments best-fit to ref 1 (alignment group 1), best-fit to ref 1 (alignment group 2), best-fit to ref 1 (alignment group 3)
 All Statistics Total: 3, Measured: 3 (100.0000%), Pass: 1 (33.3333%), Fail: 2 (66.6667%), Warning: 0 (0.0000%)

Char No.	Object Name	Control	Nom	Meas	Tol	Dev	Test	Out Tol
	Inside Diameter	Diameter	9.2500	9.0794	±0.0394	-0.1706	Fail	-0.1312
	Outside Diameter	Diameter	10.4500	10.2973	±0.0394	-0.1527	Fail	-0.1133
	Thickness	3D Distance	0.4550	0.4308	±0.0394	-0.0242	Pass	







3D Printed Part A2247

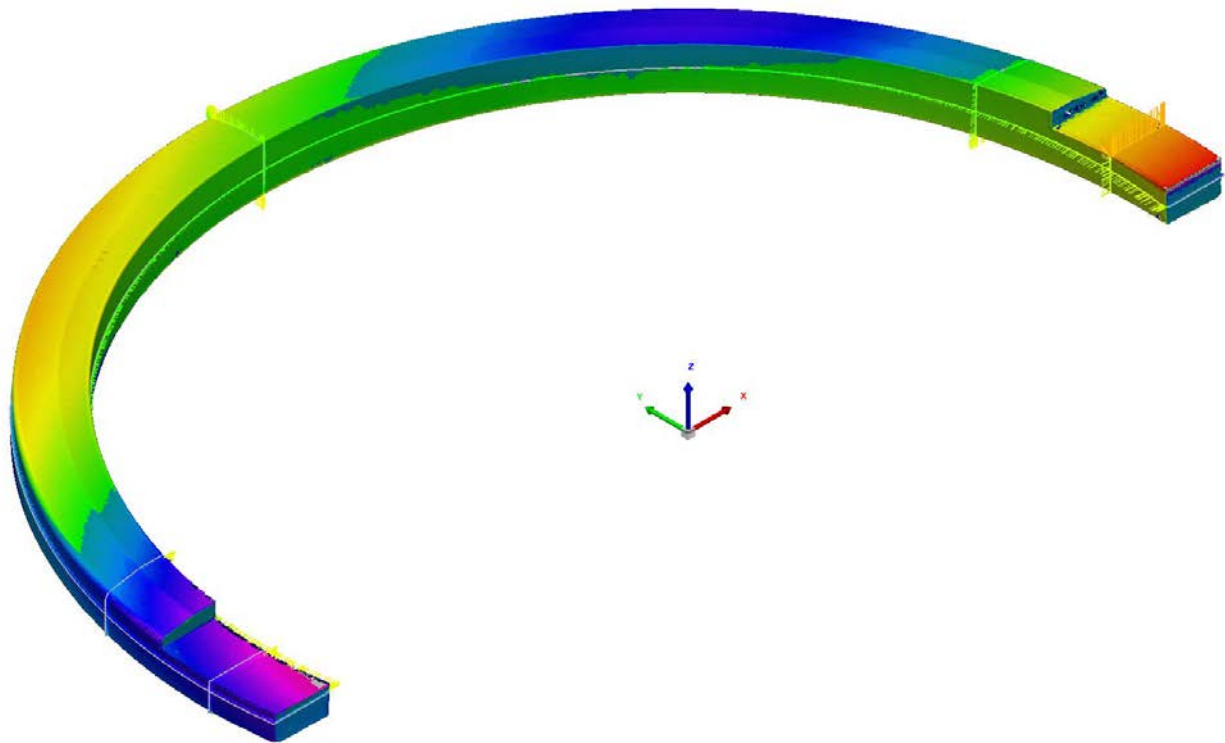
Part number: A2247

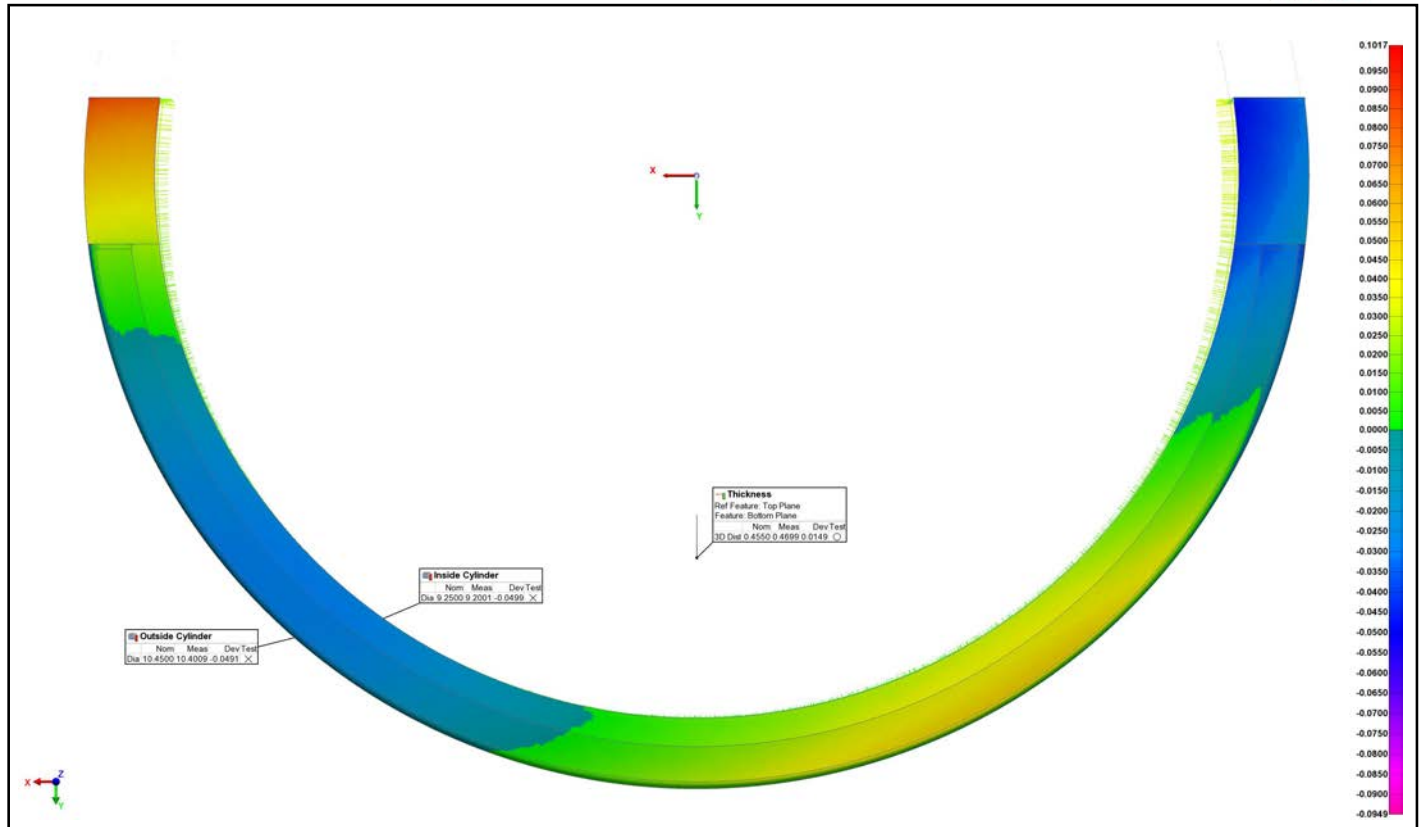
Workspace: Jermyn 3D Printed Material

Project: Part A2247 - piece 1

Report Author: Chad Paulson

Date: 4/19/2022

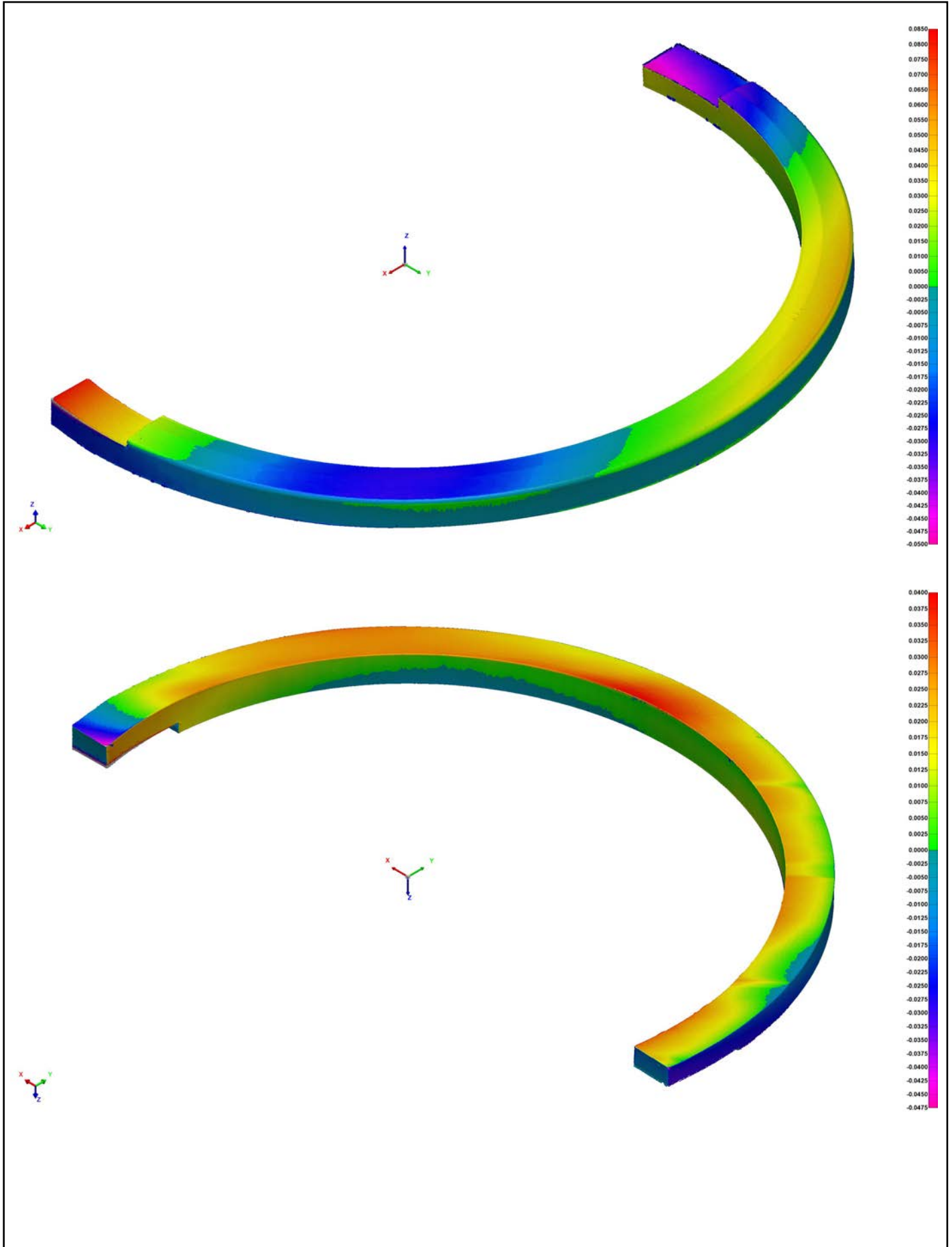


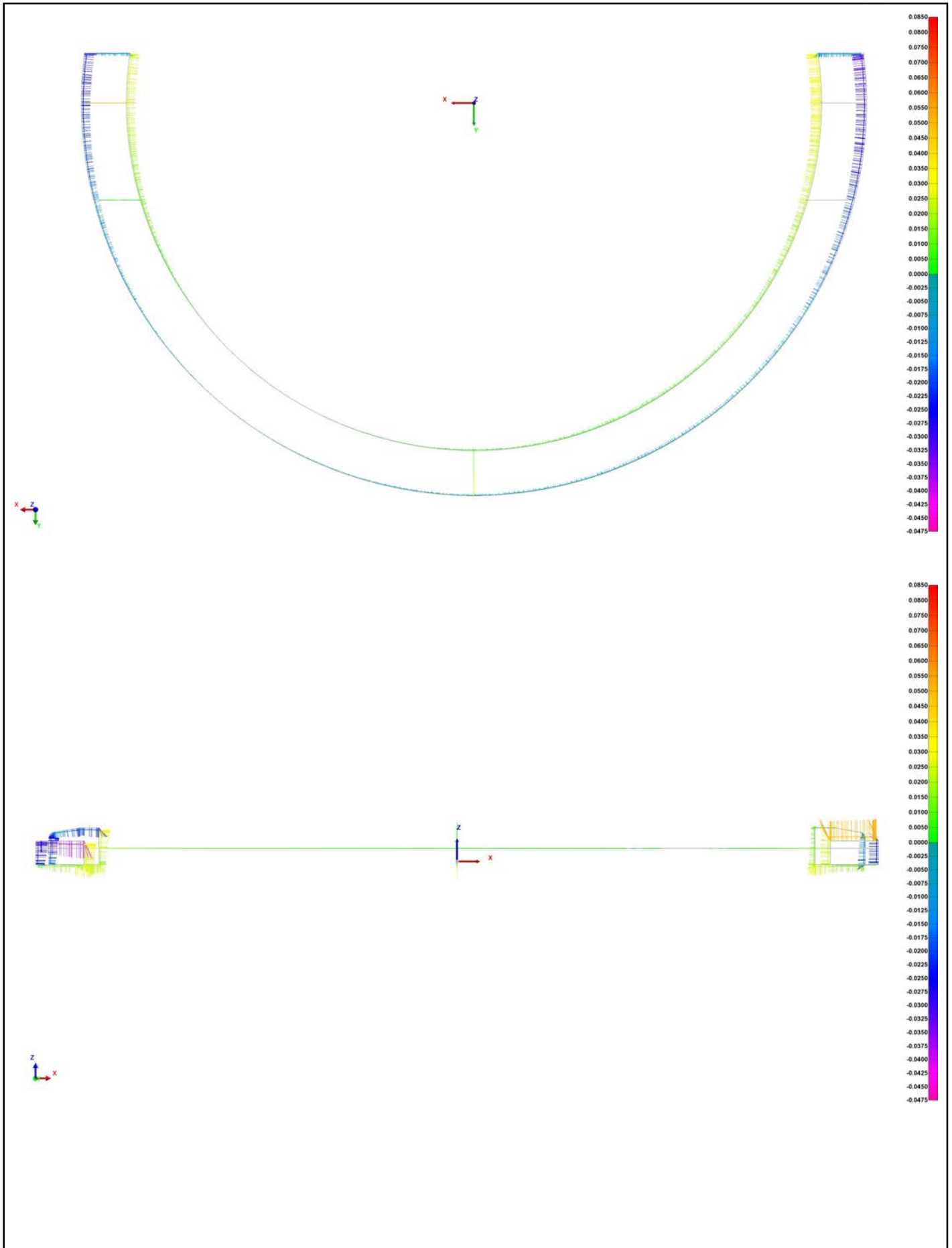


Control View

Control View Name Diameter Comparison
 Units Inches
 Coordinate Systems world
 Data Alignments best-fit to ref 1 (alignment group 1), best-fit to ref 1 (alignment group 2), best-fit to ref 1 (alignment group 3)
 All Statistics Total: 3, Measured: 3 (100.0000%), Pass: 1 (33.3333%), Fail: 2 (66.6667%), Warning: 0 (0.0000%)

Char No.	Object Name	Control	Nom	Meas	Tol	Dev	Test	Out Tol
	Inside Cylinder	Diameter	9.2500	9.2001	±0.0394	-0.0499	Fail	-0.0105
	Outside Cylinder	Diameter	10.4500	10.4009	±0.0394	-0.0491	Fail	-0.0097
	Thickness	3D Distance	0.4550	0.4699	±0.0394	0.0149	Pass	







3D Printed Part A2527

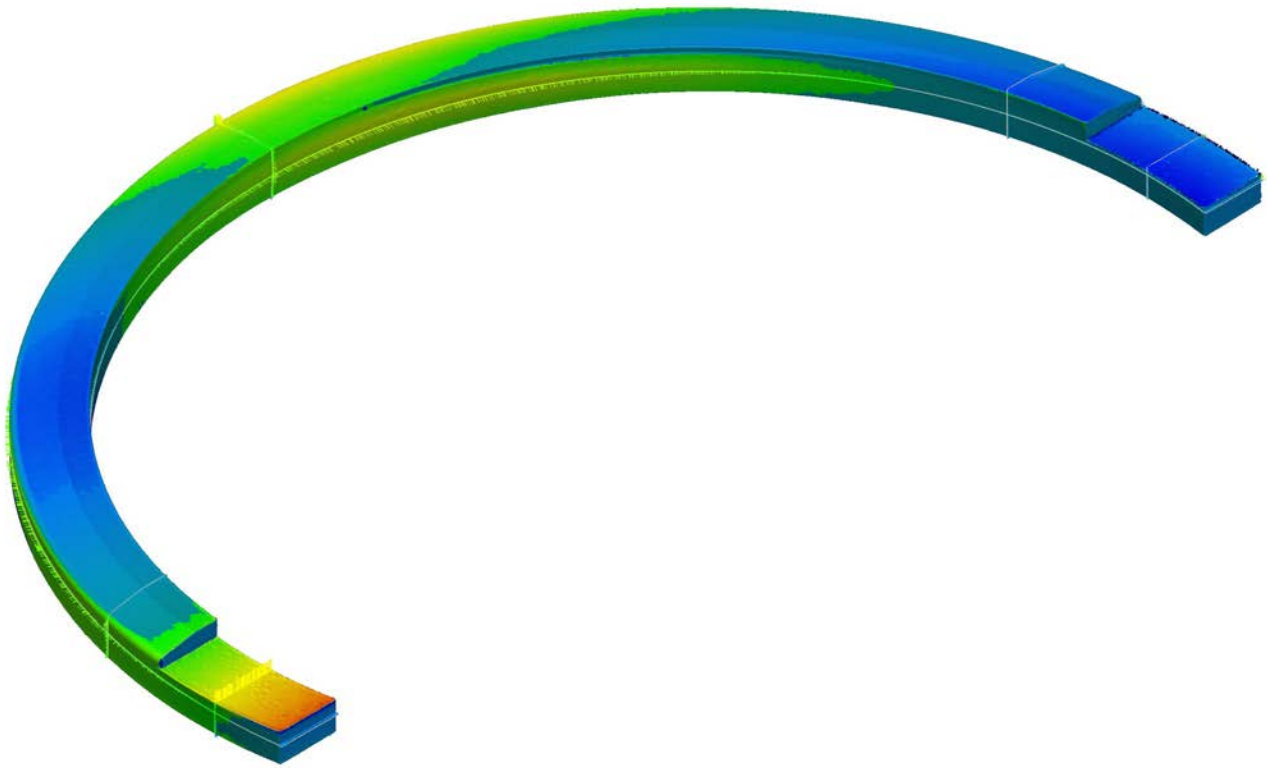
Part number: Slinger Ring A2527

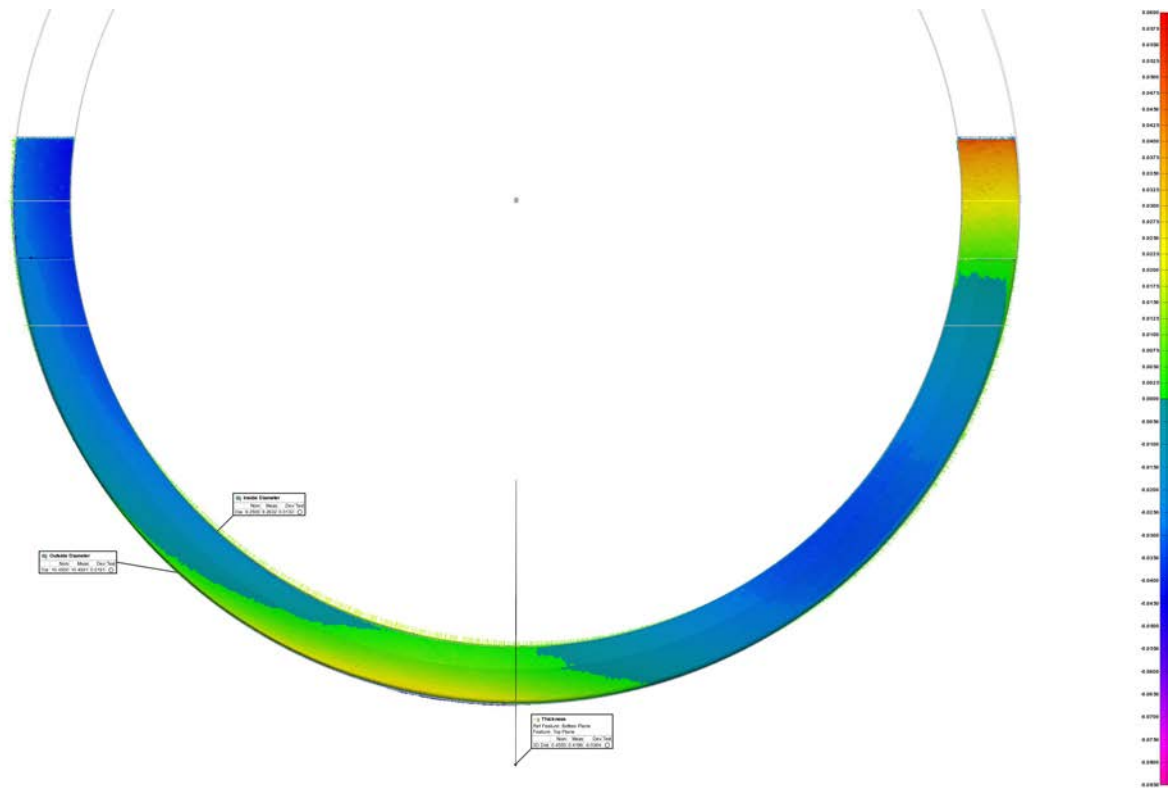
Workspace: Jermyn 3D Printed Material

Project: Part A2527 - piece 1

Report Author: Chad Paulson

Date: 4/11/2022

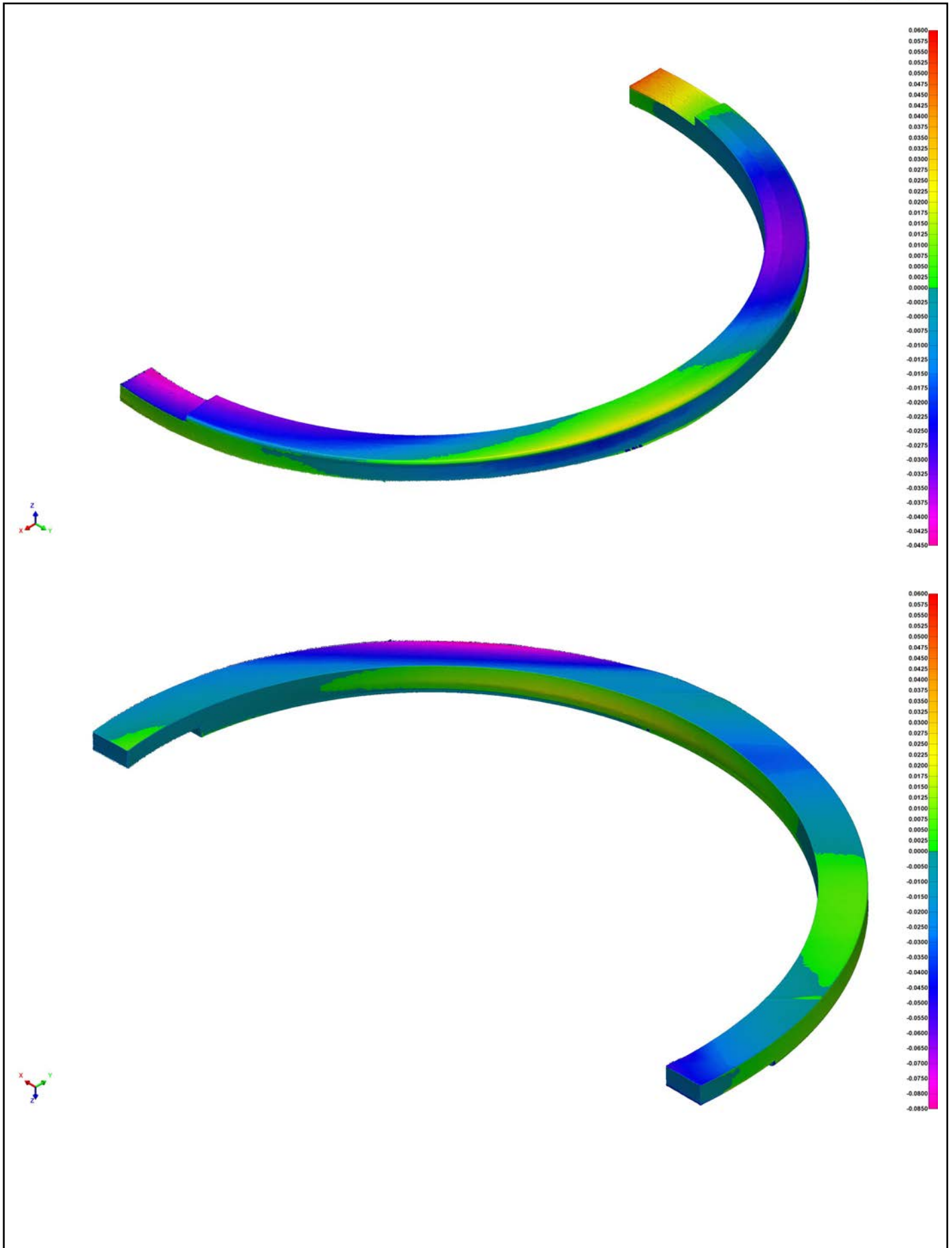


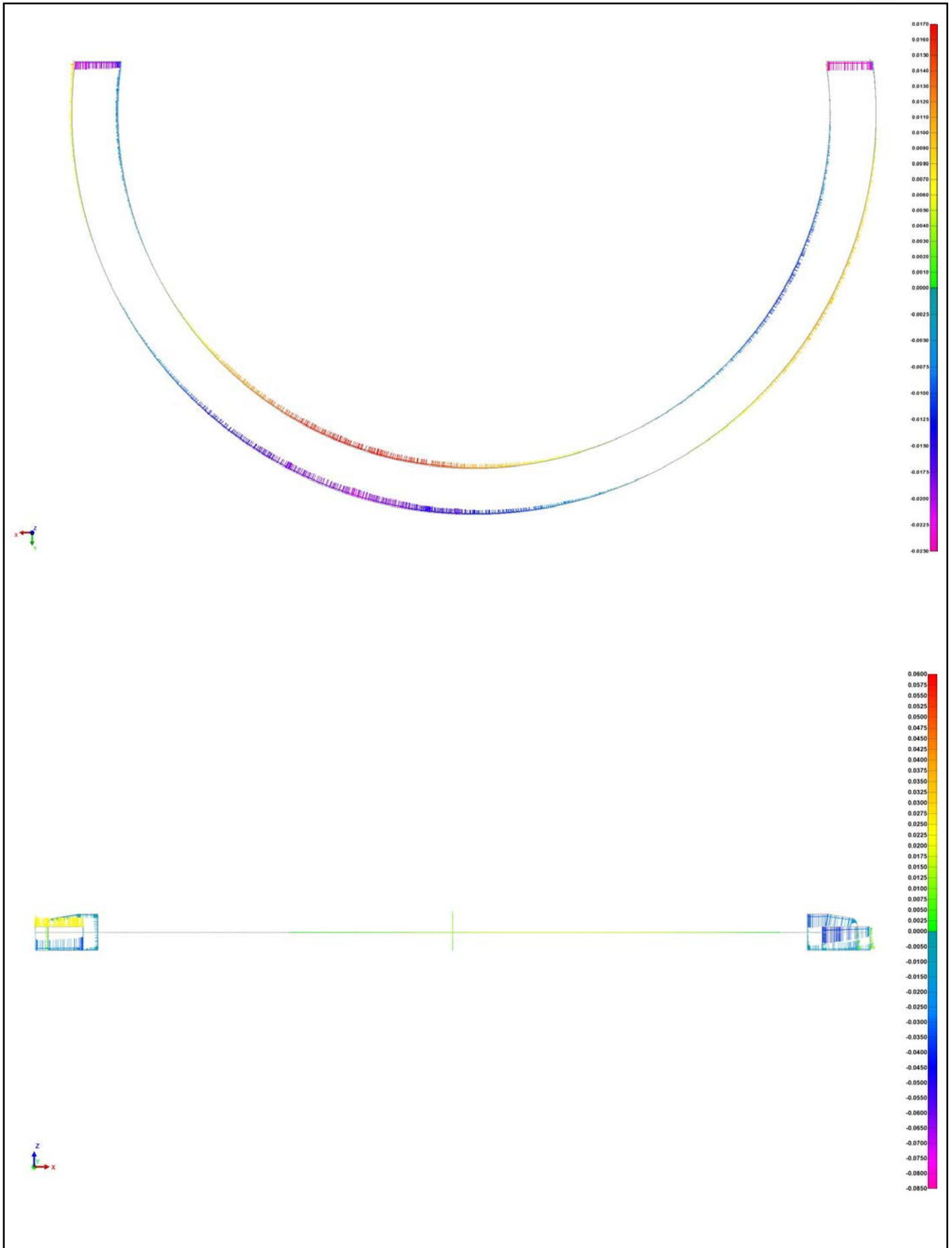


Control View

Control View Name control view 1
 Units Inches
 Coordinate Systems world
 Data Alignments best-fit to ref 2 (alignment group 1), best-fit to ref 2 (alignment group 2), best-fit to ref 2 (alignment group 3)
 All Statistics Total: 3, Measured: 3 (100.0000%), Pass: 3 (100.0000%), Fail: 0 (0.0000%), Warning: 0 (0.0000%)

Char No.	Object Name	Control	Nom	Meas	Tol	Dev	Test	Out Tol
	Inside Diameter	Diameter	9.2500	9.2632	±0.0394	0.0132	Pass	
	Outside Diameter	Diameter	10.4500	10.4691	±0.0394	0.0191	Pass	
	Thickness	3D Distance	0.4550	0.4186	±0.0394	-0.0364	Pass	







3D Printed Part A 2902

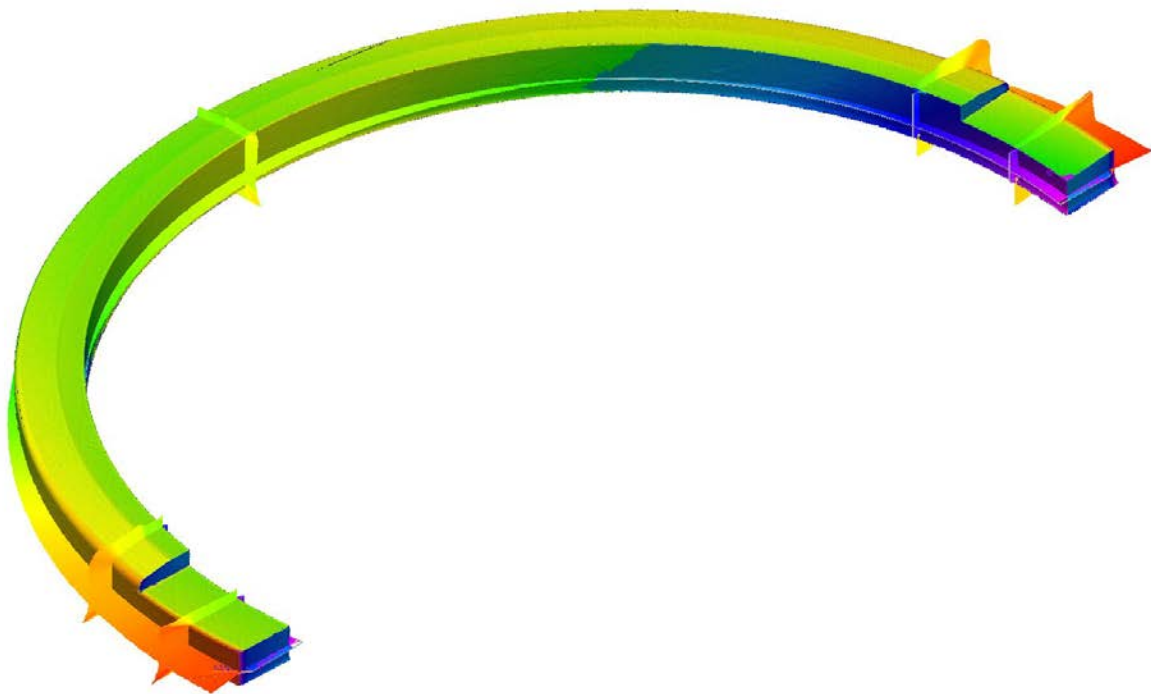
Part number: Slinger Ring A2902

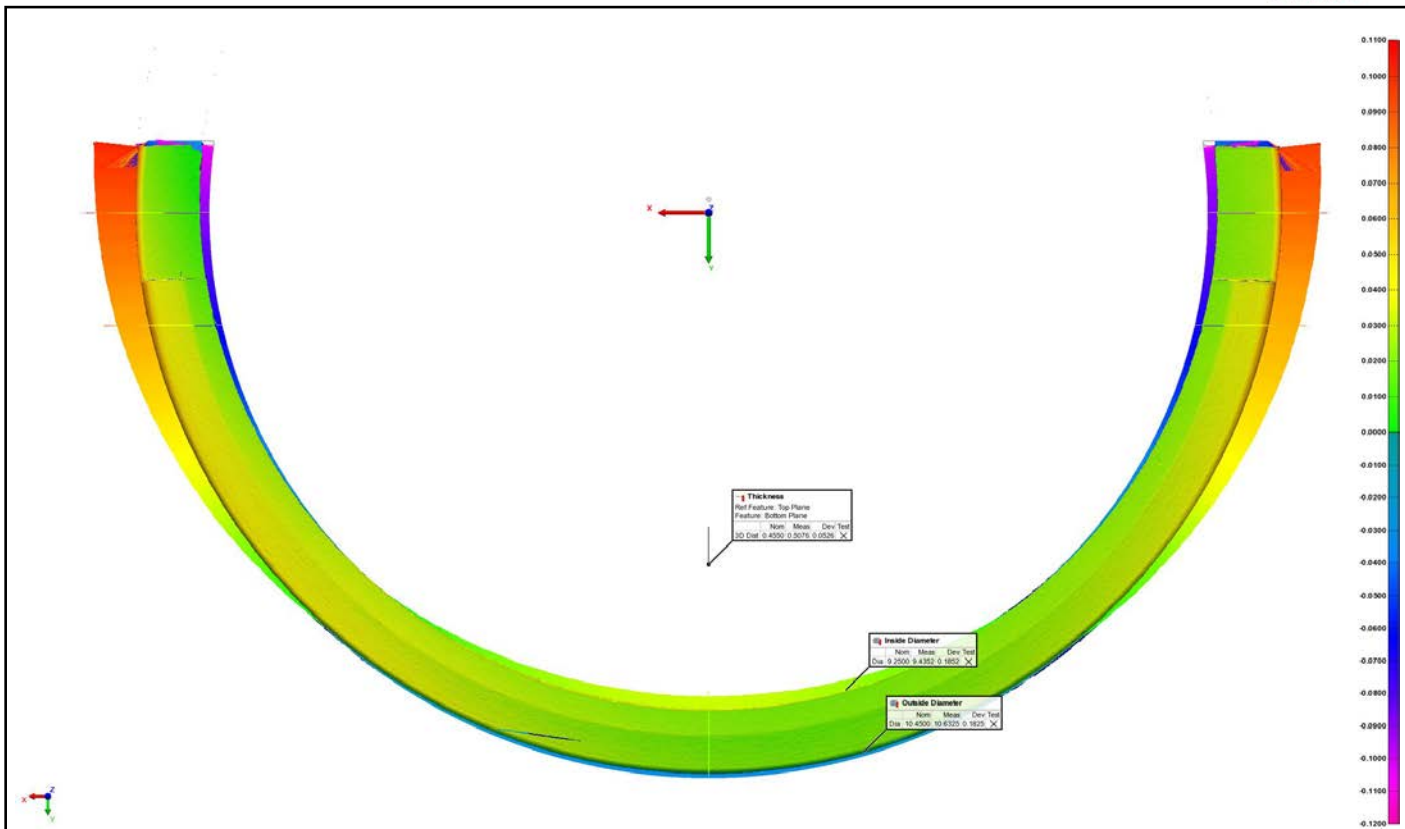
Workspace: Jermyn 3D Printed Material

Project: Part A2902 - piece 1

Report Author: Marcel Sorel

Date: 8/15/2022

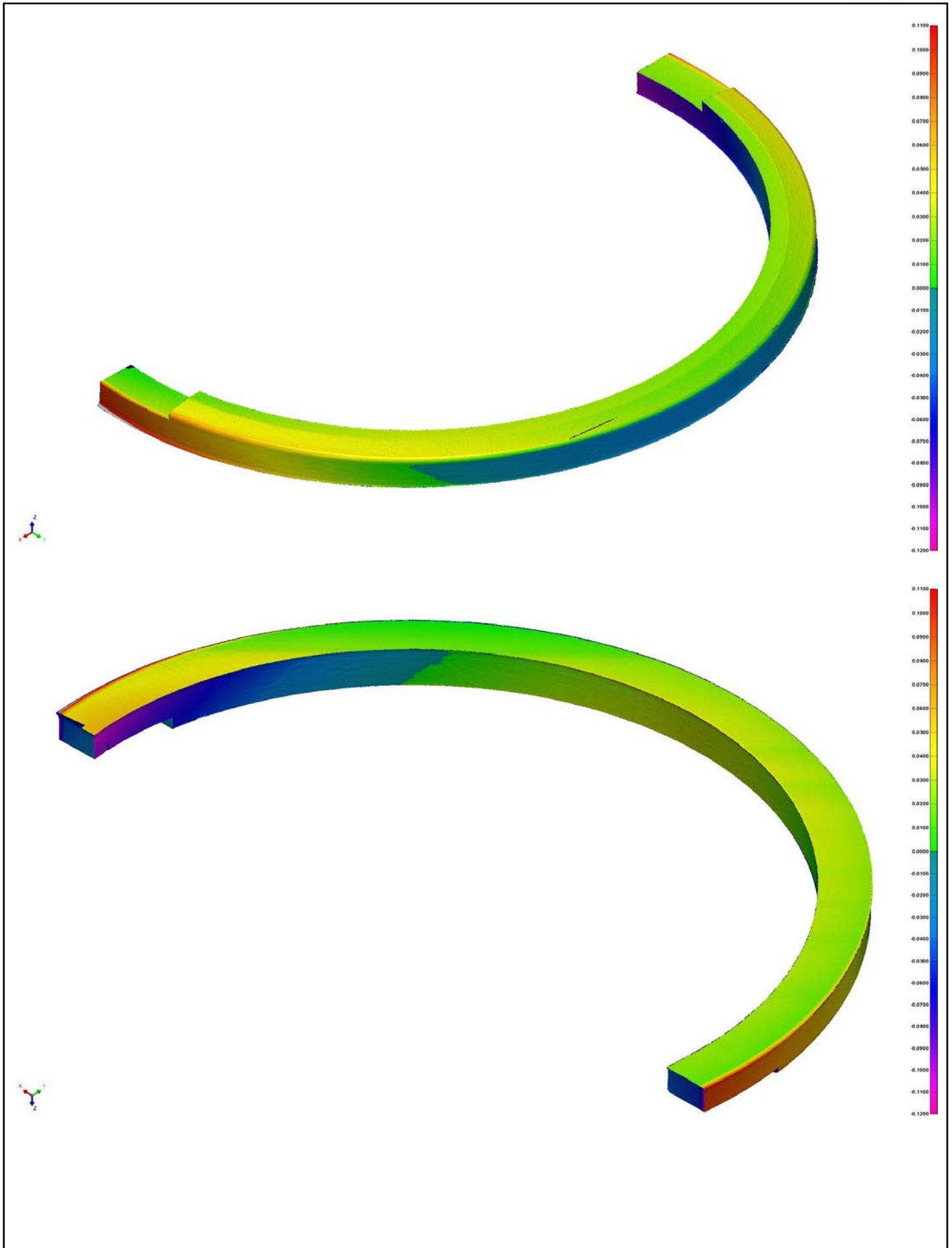


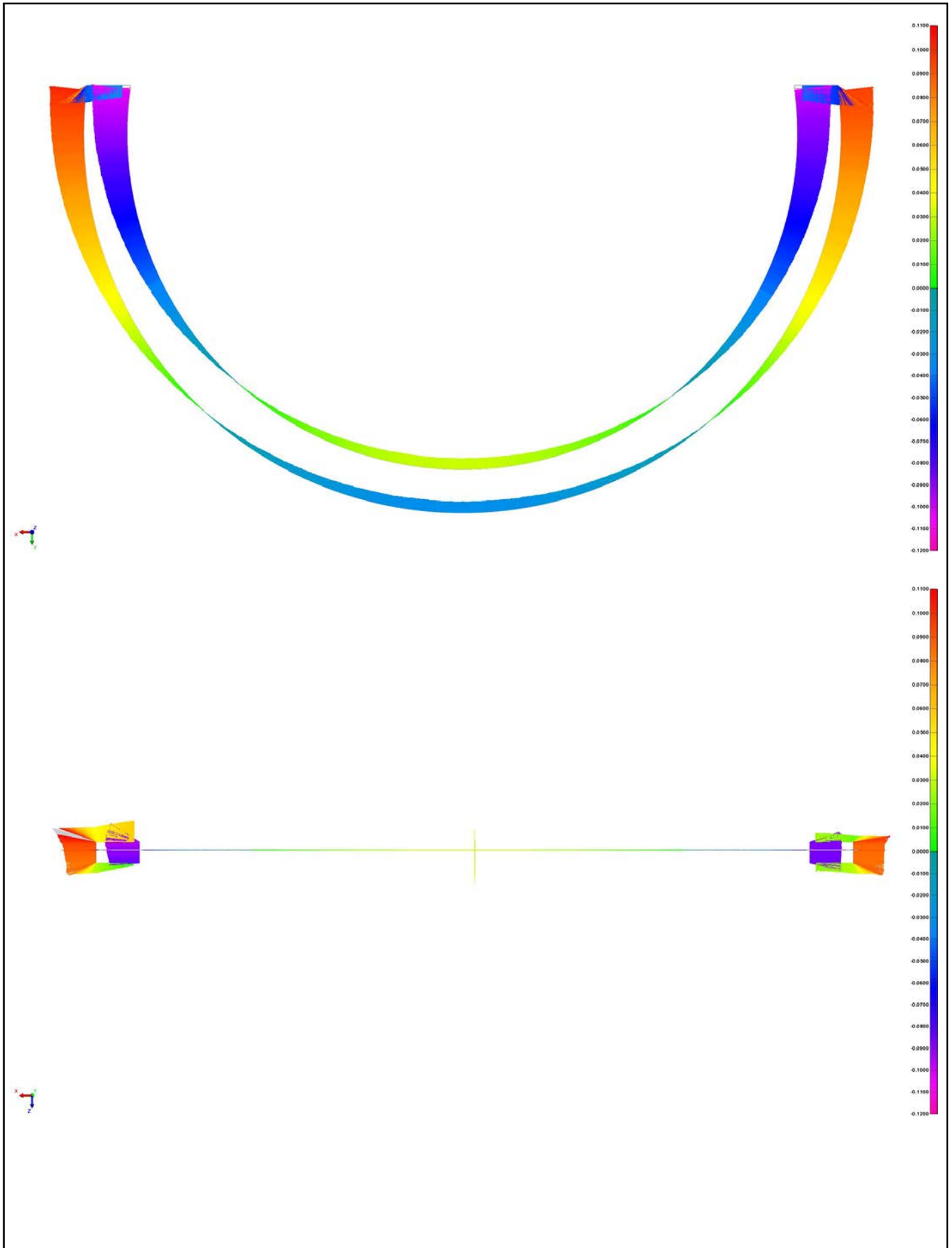


Control View

Control View Name Diameter Comparison
 Units Inches
 Coordinate Systems world
 Data Alignments best-fit to ref 1 (alignment group 2), best-fit to ref 1 (alignment group 3), best-fit to ref 1 (alignment group 4)
 All Statistics Total: 3, Measured: 3 (100.0000%), Pass: 0 (0.0000%), Fail: 3 (100.0000%), Warning: 0 (0.0000%)

Object Name	Control	Nom	Meas	Tol	Dev	Test	Out Tol
Inside Diameter	Diameter	9.2500	9.4352	±0.0394	0.1852	Fail	0.1458
Outside Diameter	Diameter	10.4500	10.6325	±0.0394	0.1825	Fail	0.1431
Thickness	3D Distance	0.4550	0.5076	±0.0394	0.0526	Fail	0.0132





Appendix M

Screenshots of Polylactic Acid Setup

Process Name: Select Profile:

Auto-Configure for Material



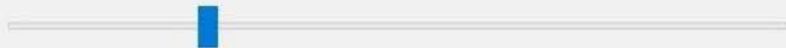
Auto-Configure for Print Quality



Auto-Configure Extruders

General Settings

Infill Percentage:



25%



Include Raft



Generate Support

Extruder

Layer

Additions

Infill

Support

Temperature

Cooling

G-Code

Scripts

Speeds

Other

Advanced

 Use Skirt/Brim

Skirt Extruder

Skirt Layers

Skirt Offset from Part

 mm

Skirt Outlines

 Use Prime Pillar

Prime Pillar Extruder

Pillar Width

 mm

Pillar Location

Speed Multiplier

 % Use Raft

Raft Extruder

Raft Top Layers

Raft Base Layers

Raft Offset from Part

 mm

Separation Distance

 mm

Raft Top Infill

 %

Above Raft Speed

 % Use Ooze Shield

Ooze Shield Extruder

Offset from Part

 mm

Ooze Shield Outlines

Sidewall Shape

Sidewall Angle Change

 deg

Speed Multiplier

 %

Process Name:

Select Profile:

Auto-Configure for Material

Auto-Configure for Print Quality

Auto-Configure Extruders

General Settings
Infill Percentage: 100% Include Raft Generate Support

- Extruder
- Layer
- Additions
- Infill
- Support
- Temperature
- Cooling
- G-Code
- Scripts
- Speeds
- Other
- Advanced

Layer Modifications

Start printing at height mm

Stop printing at height mm

Thin Wall Behavior

External Thin Wall Type

Internal Thin Wall Type

Allowed perimeter overlap %

Single Extrusions

Minimum Extrusion Length mm

Minimum Printing Width %

Maximum Printing Width %

Endpoint Extension Distance mm

Ooze Control Behavior

Only retract when crossing open spaces

Force retraction between layers

Minimum travel for retraction mm

Perform retraction during wipe movement

Only wipe extruder for outer-most perimeters

Movement Behavior

Avoid crossing outline for travel movements

Maximum allowed detour factor

Slicing Behavior

Non-manifold segments: Discard Heal

Merge all outlines into a single solid model

Process Name:

Select Profile:

Auto-Configure for Material

Auto-Configure for Print Quality

Auto-Configure Extruders

General Settings

Infill Percentage: 100% Include Raft Generate Support

- Extruder
- Layer
- Additions
- Infill
- Support
- Temperature
- Cooling
- G-Code
- Scripts
- Speeds
- Other
- Advanced

Per-Layer Fan Controls

Layer	Fan Speed
1	0
3	100

Layer Number

Fan Speed %

Fan Options

Blip fan to full power when increasing from idle

Fan Overrides

Increase fan speed for layers below sec

Maximum cooling fan speed %

Bridging fan speed override %

Process Name:

Select Profile:

Auto-Configure for Material

Auto-Configure for Print Quality

Auto-Configure Extruders

General Settings

Infill Percentage: 25% Include Raft Generate Support

- Extruder
- Layer
- Additions
- Infill
- Support
- Temperature
- Cooling
- G-Code
- Scripts
- Speeds
- Other
- Advanced

Extruder List
(click item to edit settings)

- Left Extruder (T0)
- Right Extruder (T1)**

Right Extruder (T1) Toolhead

Overview

Extruder Toolhead Index:

Nozzle Diameter: mm

Extrusion Multiplier:

Extrusion Width: Auto Manual mm

Ooze Control

Retraction

- Retraction Distance: mm
- Extra Restart Distance: mm
- Retraction Vertical Lift: mm
- Retraction Speed: mm/s

Coast at End

- Coasting Distance: mm

Wipe Nozzle

- Wipe Distance: mm

Process Name:

Select Profile:

Auto-Configure for Material

Auto-Configure for Print Quality

Auto-Configure Extruders

General Settings

Infill Percentage: 100% Include Raft Generate Support

- Extruder
- Layer
- Additions
- Infill
- Support
- Temperature
- Cooling
- G-Code
- Scripts
- Speeds
- Other
- Advanced

G-Code Options

- 5D firmware (include E-dimension)
- Relative extrusion distances
- Allow zeroing of extrusion distances (i.e. G92 E0)
- Use independent extruder axes
- Include M101/M102/M103 commands
- Firmware supports "sticky" parameters
- Apply toolhead offsets to G-Code coordinates

Global G-Code Offsets

	X-Axis	Y-Axis	Z-Axis	
Offset	<input type="text" value="0.00"/>	<input type="text" value="0.00"/>	<input type="text" value="0.00"/>	mm

Update Machine Definition

Machine type

	X-Axis	Y-Axis	Z-Axis	
Build volume	<input type="text" value="406.0"/>	<input type="text" value="355.0"/>	<input type="text" value="350.0"/>	mm
Origin offset	<input type="text" value="0.0"/>	<input type="text" value="0.0"/>	<input type="text" value="0.0"/>	mm
Homing dir	<input type="text" value="Min"/>	<input type="text" value="Min"/>	<input type="text" value="Min"/>	
Flip build table axis	<input type="checkbox"/> X	<input checked="" type="checkbox"/> Y	<input type="checkbox"/> Z	
Toolhead offsets	<input type="text" value="Tool 0"/>	X <input type="text" value="0.00"/>	Y <input type="text" value="0.00"/>	

Update Firmware Configuration

Firmware type

GPX profile

Baud rate bits/sec

Process Name:

Select Profile:

Auto-Configure for Material

Auto-Configure for Print Quality

Auto-Configure Extruders

General Settings
Infill Percentage: 25% Include Raft Generate Support

- Extruder
- Layer
- Additions
- Infill**
- Support
- Temperature
- Cooling
- G-Code
- Scripts
- Speeds
- Other
- Advanced

General
Infill Extruder
Internal Fill Pattern
External Fill Pattern
Interior Fill Percentage %
Outline Overlap %
Infill Extrusion Width %
Minimum Infill Length mm
Combine Infill Every layers
 Include solid diaphragm every layers

Internal Infill Angle Offsets
 deg

 Print every infill angle on each layer

External Infill Angle Offsets
 deg

Process Name:

Select Profile:

Auto-Configure for Material

Auto-Configure for Print Quality

Auto-Configure Extruders

General Settings
Infill Percentage: 25% Include Raft Generate Support

- Extruder
- Layer
- Additions
- Infill
- Support
- Temperature
- Cooling
- G-Code
- Scripts
- Speeds
- Other
- Advanced

Layer Settings

Primary Extruder

Primary Layer Height mm

Top Solid Layers

Bottom Solid Layers

Outline/Perimeter Shells

Outline Direction: Inside-Out Outside-In

Print islands sequentially without optimization

Single outline corkscrew printing mode (vase mode)

First Layer Settings

First Layer Height %

First Layer Width %

First Layer Speed %

Start Points

Use random start points for all perimeters

Optimize start points for fastest printing speed

Choose start point closest to specific location

X: Y: mm

Process Name: Process1

Select Profile: U1 Rev0 Single Extruder PLA v0.9(2) (modified)

Update Profile

Save as New

Remove

Auto-Configure for Material

PLA



Auto-Configure for Print Quality

Default



Auto-Configure Extruders

Single Mode - Left Extruder (T0)

General Settings

Infill Percentage:

100%

Include Raft

Generate Support

Extruder Layer Additions Infill Support Temperature Cooling G-Code Scripts Speeds Other Advanced

Bridging

Unsupported area threshold 5.0 sq mm

Extra inflation distance 5.00 mm

Bridging extrusion multiplier 100 %

Bridging speed multiplier 100 %

Use fixed bridging infill angle 0 deg

Apply bridging settings to perimeters

Dimensional Adjustments

Horizontal size compensation 0.00 mm

Filament Properties

Filament Toolhead Index Tool 0

Filament diameter 1.7500 mm

Filament price 35.00 price/kg

Filament density 1.25 grams/cm³

Tool Change Retraction

Tool change retraction distance 24.50 mm

Tool change extra restart distance -0.25 mm

Tool change retraction speed 166.7 mm/s

Process Name:

Select Profile:

Auto-Configure for Material

Auto-Configure for Print Quality

Auto-Configure Extruders

General Settings

Infill Percentage: 100% Include Raft Generate Support

- Extruder
- Layer
- Additions
- Infill
- Support
- Temperature
- Cooling
- G-Code
- Scripts
- Speeds
- Other
- Advanced

- Starting Script
- Layer Change Script
- Retraction Script
- Tool Change Script
- Ending Script

```
;U1 Left Extruder(T0) Only Startup Script  
  
M203 X18000.00 Y18000.00 Z1200.00 U18000.00 E1800.00 ; U1 max feedrate mm/minute  
M201 X1200 Y1200 Z10 U1200 E2000 ; U1 Maximum Acceleration axes mm/s^2  
M204 P2000 T2000 ; U1 Maximum Acceleration printing / travel mm/s^2  
M566 X300 Y300 Z60 U300 E600 ; U1 instantenous speed change 'jerk' in mm/minute  
M593 F0 ;make sure dynamix acceleration is off  
  
; turn off T0 hot end to reduce ooze on the bed during startup. NOTE: this does not explicitly wait for the hotends to totally cool down  
M104 T0 S0
```

Post Processing

Export file format

Add celebration at end of build (for .x3g files only)

Additional terminal commands for post processing

Process Name:

Select Profile:

Auto-Configure for Material

Auto-Configure for Print Quality

Auto-Configure Extruders

General Settings
Infill Percentage: 100% Include Raft Generate Support

- Extruder
- Layer
- Additions
- Infill
- Support
- Temperature
- Cooling
- G-Code
- Scripts
- Speeds
- Other
- Advanced

Speeds

Default Printing Speed	<input type="text" value="43.3"/>	mm/s
Outline Underspeed	<input type="text" value="60"/>	%
Solid Infill Underspeed	<input type="text" value="80"/>	%
Support Structure Underspeed	<input type="text" value="80"/>	%
X/Y Axis Movement Speed	<input type="text" value="100.0"/>	mm/s
Z Axis Movement Speed	<input type="text" value="20.0"/>	mm/s

Speed Overrides

Adjust printing speed for layers below sec

Allow speed reductions down to %

Process Name:

Select Profile:

Auto-Configure for Material

Auto-Configure for Print Quality

Auto-Configure Extruders

General Settings
Infill Percentage: 25% Include Raft Generate Support

Support Material Generation
 Generate Support Material
Support Extruder
Support Infill Percentage %
Extra Inflation Distance mm
Support Base Layers
Combine Support Every layers

Dense Support
Dense Support Extruder
Dense Support Layers
Dense Infill Percentage %

Automatic Placement
Only used if manual support is not defined
Support Type
Support Pillar Resolution mm
Max Overhang Angle deg

Separation From Part
Horizontal Offset From Part mm
Upper Vertical Separation Layers
Lower Vertical Separation Layers

Support Infill Angles
 deg

Process Name:

Select Profile:

Auto-Configure for Material

Auto-Configure for Print Quality

Auto-Configure Extruders

General Settings

Infill Percentage: 100% Include Raft Generate Support

- Extruder
- Layer
- Additions
- Infill
- Support
- Temperature
- Cooling
- G-Code
- Scripts
- Speeds
- Other
- Advanced

Temperature Controller List
(click item to edit settings)

- Left Extruder (T0)
- Right Extruder (T1)
- Heated Bed**

Heated Bed Temperature

Overview

Temperature Identifier:

Temperature Controller Type: Extruder Heated build platform

Wait for temperature controller to stabilize before beginning build

Per-Layer Temperature Setpoints

Layer	Temperature
1	60
3	0

Layer Number:

Temperature: °C